UNIVERSITY OF CAMBRIDGE

Transcriptional profiling of *Drosophila* larval ventral nervous system hemilineages

JACK N. ETHEREDGE
Christ's College, Cambridge

This dissertation is submitted for the degree of
Doctor of Philosophy

Department of Physiology,
Development and Neuroscience

December 2016

Abstract

Over 90% of neurons in the adult CNS of Drosophila are born from neuronal stem cells (neuroblasts) during the post-embryonic phase of neurogenesis. Most of the post-embryonic neurons derive from type I neuroblasts, which undergo repeated asymmetric divisions to produce a series of ganglion mother cells (GMCs). Each GMC then divides once resulting in two neurons, the "A" (Notch-on) and "B" (Notch-off) daughters. The respective daughter neurons of each type then constitute the A and B hemilineages for that neuroblast. 33 postembryonic hemilineages contribute neurons to each thoracic hemisegment, and these immature neurons arrest their development at a similar stage until metamorphosis. These arrested neuroblast lineages are uniquely identifiable by morphology. Access to a large pool of clonally-related and morphologically similar neurons makes this system tractable to RNA-seq analysis, since one can genetically label and isolate many cells per animal, which are predicted to share similar gene expression profiles. Our primary focus is to examine hemilineages with similar targets (e.g. leg neuropil) to identify genes that are required to establish and maintain hemilineage identity early in development.

Given that activating these hemilineage neurons as a group drives distinct behaviors and that they form morphologically coherent structural units during development, we hypothesized that these hemilineages should express patterns of genes that are: 1) distinct from other hemilineages and 2) characteristic of individual hemilineages.

I employed a transcriptomics approach for characterizing the neuronal diversification processes that occur in the larval-born hemilineages in the *Drosophila* VNS. Neurons from these hemilineages were profiled using fluorescence assisted cell sorting (FACS) and deep sequencing. Differentially expressed genes were determined for individual hemilineages and for neurons with different birth orders. Transcription factors were the primary initial gene class that I targeted experimentally when comparing hemilineages to one another in the larva, since the primary questions are how different the hemilineage expression profiles are and how their identities are encoded. Targeted knock-down and misexpression studies were performed subsequently for differentially expressed transcripts.

After identifying various pitfalls associated with existing methods for cell isolation, I conceived a novel experimental approach that compartmentalized multiple reporters in different cytological domains using transcriptional modifiers that specify localization to the cell membrane using a myristylation tag (myr), or to the nucleus using a nuclear localization signal motif (nls). This labeling scheme gave up to 98% cell purity and facilitated sorting dissociated cell populations by FACS for RNA-Seq analysis.

I have used hemilineage-specific GAL4 lines to isolate hemilineages for RNA-seq analysis, ultimately gathering data for 11 of the 33 hemilineages as well as for some larger populations of neurons. We found that, in addition to combinatorial patterns of genes specifying the hemilineage neurons, there are some genes that are expressed by only a single hemilineage within the ventral nervous system (VNS). Most hemilineages display unique expression of certain transcription factors (TFs) and axon guidance genes. We collected data for two pairs of sibling hemilineages (lineage 1 and lineage 12) in order to identify differences between the A and B hemilineages derived from a common neuroblast. Comparing the gene expression between immature and mature larval neurons revealed that mature neurons express many genes not expressed in immature neurons, such as neuropeptide signaling genes and many neurotransmitter and ion channel genes associated with mature neuron function. Birth order also appears to dictate many differences in expression profile. Younger immature neurons are typified by a period of transient Notch-related gene expression that is absent from older neurons. We are characterizing the function of many differentially expressed genes in particular hemilineages.

Additionally, to determine potential causes for an axonal degeneration and ectopic arborization phenotype observed in hemilineage 12A neurons lacking ecdysone signaling, I performed RNA-seq on these neurons at different points through the progression of this phenotype in genetically induced extended third instar larvae. Data from the wildtype hemilineage 12A neurons allowed me to develop a hypothesis for the cause of this phenotype.

Table of content

List of Figures

List of Abbreviations

AEL – after egg laying

BP – gene ontology biological process

CA – corpora allata

CNS – central nervous system

ETI – extended third instar

FPKM – fragments per kilobase of transcript per million mapped reads

GFP – green fluorescent protein

GSEA – gene set enrichment analysis

IPSC – induced pluripotent stem cells

KEGG - Kyoto Encyclopedia of Genes and Genomes

KG – KEGG pathway

MARCM – mosaic analysis with a repressible cell marker

MF – gene ontology molecular function

Myr – myristoylation

NLS – Nuclear localization signal

NT – neurotransmitter

PBS – phosphate buffered saline

PBSTx - phosphate buffered saline with Triton-X

PC – principal component

PCA – principal component analysis

PG – prothoracic gland

RNAi – ribonucleic acid interference

tdT – tandem dimer tomato red fluorescent protein

TF – transcription factor

VNS – ventral nervous system

WL3 – wandering third instar larvae

WT – wildtype

Declaration

I hereby declare that this dissertation entitled "Transcriptional profiling of Drosophila larval ventral nervous system hemilineages" is the result of my own work and has neither been previously nor concurrently submitted for any other degree or qualification.

This dissertation is the result of my own work and includes nothing which is the outcome of work done in collaboration except where explicit reference is made to the work of others.

This dissertation does not exceed the 60,000-word limit specified by the Degree Committee for the Faculty of Biology.

Date:

Signed:

Jack N. Etheredge
Christ's College
Cambridge
December 2016

Acknowledgements

I'd like to thank Cambridge, HHMI, and Janelia for seeing potential in me and for supporting me and this research. All funding for this research was provided through HHMI. I'd like to thank Jim Truman and Andrea Brand for their mentorship, support, and understanding.

This work could not have been completed without the help of Aaron Baumann, Jenny Ma, Serge Picard, and Jim Truman. Aaron Baumann and Jim Truman assisted with dissections. Without Aaron dedicating large amounts of his time to dissect with me, I would not have been able to do the transcriptomics experiments that are the foundation of this work. Aaron also helped with comments for revising the introduction and methods. Jenny Ma performed all cell sorting using FACS. Serge Picard performed all sequencing of cDNA libraries. Extended third instar experiments could not have been completed without the help of Daniel Miller and Raechel Warner. Daniel Miller assisted with all dissections for extended third instar experiments. Raechel Warner set up the extended third instar crosses and cared for the larvae. Jim was an invaluable resource for experimental design, determining scientific relevance, and revising this thesis.

Haluk Lacin, Michael Texada, Troy Shiranghi, Dave Mellert, Julia Oh, Ella Preger-Ben Noon, Jon Michael Knapp, Carmen Robinett, and Andrew Lemire were all very helpful with comments and teaching me various skills that contributed to this work.

I thank Barret Pfeiffer and Gerald Rubin for providing pJFRC29, pJFRC105, R57C10-GAL80, RLexA, and RGAL4 *Drosophila* stocks and Pamela Mitchell for kindly providing the TfAP-2 antibody used in this study.

Moi Li assisted with stock flipping, read introductory sections for coherence, and helped to keep me sane during my PhD.

Finally, I would like to thank Moi and my family for their love and emotional support.

Chapter 1

Introduction

We each develop from a single cell. The tremendous diversity of adult cell types is generated through successive rounds of division and cellular migration. How this process is coordinated is of paramount importance to human health and has far-reaching implications for regenerative medicine, stem cell therapies, wound healing, and cancer.

The adult *Drosophila* central nervous system (CNS) is composed of an estimated 250,000 neurons. Positional and temporal information are integrated during development in order to generate increasing cellular diversity in the nervous system as in the rest of the organism. The generation of the adult nervous system of Drosophila, though, is complicated because it is produced in two phases due to metamorphosis. An initial set of neurons are generated during embryogenesis to provide the functional neurons for the larval stage. During larval growth there is then an extended phase of "postembryonic" neurogenesis of "adult-specific neurons", but the new neurons do not immediately mature and are stockpiled in an immature state until the end of larval growth. At metamorphosis, the functional larval neurons (those born during embryogenesis) are either remodeled or die and combine with the arrested, postembryonic adult-specific neurons that mature to form the CNS of the adult.

Our best understanding of the relationship of neuronal stem cells to neuronal identities come from studies on the ventral nervous system (VNS) of the fly. This region of the CNS is segmentally organized with the neurons in each segmental unit (called a neuromere) arising from a set of neuronal stem cells, called neuroblasts. In the embryonic nervous system, the neuroblasts are patterned in a row-column grid where each neuroblast expresses a different combination of transcription factors that lead to the development of morphologically distinct neuronal lineages (Reviewed in Skeath, 1999). This pattern is repeated hemisegmentally, generating sets of laterally mirrored pairs of neuroblasts. The segmental structure of the nervous systems of both vertebrates and arthropods also allows for regional specializations with the segmental

units appearing similar during early development but then acquiring distinct morphologies and expression patterns as development progresses.
In the insect CNS, neuronal identity is established based on four different factors: (1) the identity of the neuroblast (NB), (2) the birth-order of the ganglion mother cells (GMCs) produced by that NB, (3) the state of Notch signaling ($Notch^{on}$ or $Notch^{off}$) for the two daughters that arise from the terminal division of the GMC, and, (4) in the context of the whole VNS, the state of HOX gene expression, providing segmental specializations along the body axis. Much of what we know about these various processes comes from the embryonic development of the CNS.

In order to generate neuronal diversity, NBs must first acquire distinct identities. NB identity in the embryonic central nervous system is positionally determined within a segment, with neuroblasts organized in a row-column pattern. Neuroblasts are formed from the ventral neuroectoderm, the gene expression patterning of which determines the fate of the neuroblast before it is born (Udolph et al., 1995). Expression of the segment polarity genes (e.g., wingless (wg) and gooseberry (gbs)) along the anterior-posterior axis specify the identity of the rows while expression of the column genes (e.g., ventral nervous system defective (vnd) and intermediate neuroblasts defective (ind)) along the dorsal-ventral axis specify the columns (Chu-LaGraff and Doe, 1993; Skeath et al., 1995; Mellerick and Nirenberg, 1995; Jiménez et al., 1995; Bhat, 1996; McDonald et al., 1998). This grid-like patterning of the neuroectoderm by combinatorial expression of genes (most of which are transcription factors) by column and row has been extensively studied (reviewed in Skeath, 1999).

Another mechanism by which neuronal diversity is generated in the embryonic CNS is through temporal specification, with neurons born at different times from the same neuroblast acquiring different fates. Temporal specification of fate through birth order within a lineage is established by a transcriptional cascade that occurs within the NB through time. It sequentially expresses *hunchback* (hb), *seven up* (svp), *Kruppel* (kr), POU domain proteins 1 and 2 (pdm1 (nubbin) and pdm2), *castor* (cas), and *grainy head* (grh). The transcription factor that is expressed at the time of the birth of a GMC is the stably expressed in that GMC and results in different neuronal types depending on the transcription factor being expressed. This yields a diverse population of neurons that comprises the larval nervous system (Grosskortenhaus et

al., 2006; Isshiki et al., 2001; Kambadur et al., 1998; Kanai et al., 2005; Novotny et al., 2002; Pearson and Doe, 2003).

The transcription factor cascade produces a highly diverse set of neurons through the first few divisons of the NB. As divisions progress, through the last part of the embryonic phase and then through an extended postembryonic period, the transcription factors expression in the NB does not change from division to division and the NB starts to produce extended cell classes. Early in their larval phase the NBs may continue to express *cas* and *svp* (Tsuji et al., 2008; Maurange, Cheng, and Gould, 2008; Lacin and Truman, 2016), but additional factors come into play. Temporal gradients of the transcription factor (TF) *chinmo* determine what types of neurons a lineage will make (Zhu et al., 2006). An early gene in the ecdysone transcriptional cascade, the BTB-POZ family member *Broad* (*br*), encodes a subset of alternatively-spliced zinc-finger transcription factors designated Z1, Z2, Z3, and Z4. *Broad* is well known as a pupal specifier in holometabolous insects (Zhou and Riddiford, 2002). Each of the four *broad* isoforms has unique temporal and tissue specificity (Spokony and Restifo, 2007; Spokony and Restifo, 2009; Zhou Williams Altman Riddiford Truman, 2009). Work from Tzumin Lee's lab has shown that *imp* and *syp* are expressed at opposing levels during successive rounds of division of the mushroom body and antennal lobe NBs (Liu et al., 2015). *chinmo* and *br* expression interact with Imp and Syp gradients to generate neuronal diversity within the hemilineages. Imp and Syp regulate chinmo translation, which temporally controls mushroom body neuronal lineage fate (Liu et al., 2015).

Although the early studies on cell production in the mushroom bodies showed that both daughters arising from the division of the GMC were indistinguishable, this turns out to be a unique situation. In all other cases that are known, the two daughters that arise from the division of the GMC are quite different. The differences between the two daughters come from Notch signaling. The role for Notch was originally established for the embryonic phase of the neurogenesis. During NB division, localization of the transcription factor *prospero* to the GMC is necessary to establish the different fates of the NB and GMC (Spana and Doe, 1995). During GMC division, differential Notch activity is established in the daughter neurons through asymmetric inheritance of the Notch signaling repressor Numb (Skeath and Doe, 1998). The role

for Notch in determining the fates of the daughter neurons continues into the postembryonic phase of neurogenesis.

Most of the adult nervous system originates from postembryonic neurons: during the third instar, a GMC is generated every hour, thus pairs of new neurons are added to each lineage each hour (Truman and Bate, 1988). Each thoracic segment contains a subset of 26 hemisegmentally-repeating and identifiable postembryonic neuronal lineages (Truman et al., 2004; Lacin and Truman, 2016). Each lineage can be divided into two hemilineages - 'A' (Notch on) and 'B' (Notch off) (Truman et al., 2010). The two hemilineages develop into two distinct groups of neurons with many differences indicating distinct fates including axon morphology and (after maturation through metamorphosis) type of neurotransmitter released. Some hemilineages undergo apoptosis, generating a monotypic lineage with only the A or B hemilineage surviving (Truman et al., 2010). The overall result of the pattern of postembryonic proliferation is a compact cluster of cells associated with each NB that is comprised of both the A and the B daughters.

These lineages and hemilineages can be identified unambiguously by their neurite tracts and by transcription factor immunostaining (Truman et al., 2004; Truman et al., 2010; Lacin et al., 2014). The neurons within a postembryonic hemilineage were all born from the same NB and have the same Notch activity. Before metamorphosis, they are all arrested in an early developmental state soon after their birth and fate acquisition and have nearly identical immature morphology. They differ only by birth order, which plays a much less prominent role in neuronal fate specification in the postembryonic neuroblasts, since these neurons are born during a period when their neuroblasts are expressing the same temporal neuroblast cascade TFs, cas and svp, as previously described. Therefore, especially during larval stages, when the postembryonic neurons exist in this arrested, immature state, the expression pattern of these neurons should be very similar within a hemilineage and it is reasonable to treat them as a single cell class.

There are at least two discrete phases of axonogenesis in early development. The first is characterized by axon pathfinding, while the second phase includes initial target interactions. After Notch is used in sibling neuron determination, Notch is prominent

on cell surfaces during pathfinding, and is required in neurons to establish longitudinal axon connections between successive segments in the VNS through non-canonical Notch/Abl signaling (Kuzina, Song, and Giniger 2011). Expression of *Broad-Z3* is repressed during pathfinding, but then it is expressed once cells reach their arborization target (Scott, Williams, and Truman, 2011). After the postembryonic neurons have undergone axon outgrowth and navigation to their initial target, they then form possible interactions with the target. This is reflected in changes of the gene expression of the neurons. Some cell signaling systems, such as nitric oxide (NO)-guanylate cyclase, are functional only after pathfinding is completed. NO acts on guanylate cyclase to increase cyclic GMP. In the grasshopper *Locusta migratoria*, some motor neurons are NO insensitive during development and only become NO responsive during the transition from growth cone elongation to synapse formation at the neuromuscular junction (Ball and Truman, 1998). There are TFs that are expressed during pathfinding but then disappear after the target is reached – gooseberry appears to be such a TF (JW Truman, unpublished observation). The immature, arrested, postembryonic neurons have passed through both of these developmental phases (pathfinding and initial target interaction) before metamorphosis.

Metamorphosis in insects is analogous to human puberty; each case represents the hormonally controlled development of a sexually mature adult. In contrast to the embryonic-born neurons, postembryonic neurons remain developmentally arrested in an immature state and do not synapse until metamorphosis. As such, postembryonic neurons function only in adults and contribute no function in the larval nervous system (Booker and Truman, 1986; Truman and Booker, 1986). The cells of a postembryonic hemilineage appear similar at this early, arrested phase, but then diversify to some extend during metamorphosis (Harris et al., 2015). During metamorphosis, the postembryonic neurons prune their immature arbors, undergo diversification, generate adult arbors through outgrowth of both terminal and interstitial arbors, and undergo synaptogenesis. The rest of the adult nervous system is composed of the subset of embryonic-born larval neurons that are retained and remodeled. That is, some larval neurons die, while others persist through metamorphosis to become functional adult neurons (Williams and Shepherd,

1999). Larval neurons that persist into adulthood are pruned and then undergo dendritic reorganization (Truman and Reiss, 1976).

Genetic access to a large pool of clonally related and morphologically similar neurons is granted through a library of annotated GAL4 driver lines, each with unique neuronal expression (Brand and Perrimon, 1993; Pfeiffer et al., 2008). Thus, the hemilineages in larval VNS represent a tractable system for RNA-seq analysis; we can genetically label and isolate many cells per animal, and these cells should share molecular identity in terms of gene expression. Our primary focus is to examine hemilineages with similar targets (e.g. leg neuropil) to determine which genes are important for establishing and maintaining hemilineage identity early in development.

An outstanding question in developmental biology is how cellular identity is specified in populations of stem cells and their progeny. With respect to larval hemilineages, a number of key questions remain unanswered: 1) How different are immature neurons from different lineages? 2) How different are immature neuron hemilineages from the same lineage? 3) How different are immature neurons from mature neurons? 4) What genes downstream of notch establish hemilineage identity? 5) Are individual, key transcription factors necessary to establish hemilineage identity? 6) Are there also individual transcription factors that are sufficient to establish hemilineage identity? 7) How does the hemilineage transcriptome change according to birth order? 8) Is there a single transcription factor that controls birth-order dependent diversification of hemilineages?

The A and B hemilineages can be genetically labeled and manipulated individually and independently. I elected to address the above questions using RNA-Seq analyses. The resulting dataset(s) provide an easily mineable, robust resource for future research. Consider that, if experimental interest was restricted to a single gene class, then a large immunohistochemistry or RT-PCR experiment (provided the cell type under study could be adequately isolated to purity) could provide differential expression data. In contrast, RNA-Seq can be used in the future to observe differences in expression for all genes in a given tissue or cell type, under a particular treatment, including potentially novel transcripts (both unannotated genes and unique splice variants). The sequences were generated as paired-end reads, yielding splice

isoform expression data to inform future work. For instance, some genes may show roughly equivalent expression levels across hemilineages, but diverge in isoform expression profiles, potentially generating differences in the developmental behavior of these neurons.

The primary aims of these experiments were: 1) to determine genes that are responsible for establishing and maintaining the identity of postembryonic hemilineages and 2) to determine the extent of transcriptional overlap between hemilineages.

Using the unbiased approach of RNA-seq to get whole transcriptome data on subsets of neurons, I was able to address multiple hypotheses using the same datasets.

Notch signaling and a consistent Notch program - genes downstream of Notch

Notch signaling is used in many locations, times, and pathways throughout development. In this way, the function of Notch is highly context-dependent. Differential Notch signaling is responsible for the generation of two distinct populations of neurons from each neuroblast (Skeath and Doe, 1998). A and B neurons are distinguished by Notch. Mechanistically, Notch differential signaling in A and B daughters is controlled by Numb, which acts as a suppressor of Notch signaling (Spana and Doe, 1996; Skeath and Doe, 1998; Buescher et al., 1998; Berdnik et al., 2002). Numb is asymmetrically localized to the B daughter neuron during GMC division. In the GMC and B neuron, Numb links Notch to α-adaptin and causes it to be endocytosed (Berdnik et al., 2002). CyclinA mutant GMCs cannot divide and thus become B daughters due to the presence of Numb protein. CyclinA, Numb double mutants become A daughters (Beuscher et al., 1998). One of the primary motivations for performing these experiments using individual hemilineages was to ask whether Notch is consistently causing expression of the same downstream genes in each hemilineage where it is active. I hypothesized that Notch signaling would cause downstream expression of a set of genes that was consistent across A hemilineages. I attempted to determine the identity of a number of Notch-dependent genes downstream of the well-characterized Hey and E(spl) complex genes by

comparing the gene expression of multiple A and B hemilineages. I considered both activating and repressing roles downstream of Notch signaling, so I attempted to find genes with transcript abundance consistently over- or under-represented when comparing the B hemilineages to the A hemilineages. I also performed RNA-seq on a sample that included A hemilineages from every neuroblast (at least those that do not normally undergo apoptosis). I chose to add these samples in order to rule out hemilineage-to-hemilineage variability, since I performed RNA-seq on a subset of hemilineages. Additionally, this sample was included to increase confidence in the generalizability of any genes found by these individual hemilineage comparisons.

Type I vs Type II neuroblasts and their relation to vertebrate neurogenesis

Type I neuroblasts are the type of neuroblast from which the neurons studied in this thesis are born. Neurogenesis in vertebrates is more like that seen from type II neuroblasts than type I neuroblasts. Type II neuroblasts generate intermediate neural progenitors (INPs) instead of GMCs, which then generate several types of neurons by acting as a transit amplifying cell. Each of these INPs then generates several GMCs with different temporal identities. Thus the INPs function in a capacity similar to a short-lived neuroblast in their own right. In this way, type II neuroblasts generate a disproportionately large number of cells with a greater degree of diversity than type I neuroblasts. The greater diversity is due to the combination of NB-level temporal diversity and INP-level temporal diversity.

Current models of vertebrate neurogenesis are moving toward a stochastic model in which there is both chance and deterministic bias. The proportional contribution of determinism and stochasticity is still being debated (Losick and Desplan, 2008; Slater et al., 2009; Zernicka-Goetz and Huang, 2010; Gomes et al., 2011). The hemilineage mechanism may have few or no direct parallels in vertebrate neurogenesis, according to current understanding in the field. In the retina, for example, Notch activity does bias the fate of the neurons, but it is not complete and binary as is the case for type I neuroblasts in the Drosophila VNS. Typically, retinal progenitor cells in vertebrates produce rod photoreceptors, bipolar, and Müller glial cells. In early postnatal Notch1 knockout mice, almost all newborn cells became rod photoreceptors, but this fate

transformation was incomplete, with some cells still becoming bipolar cells and Muller glia, the other two cell types observed being generated in early postnatal wildtype mice (Mizeracka, Demaso, and Cepko 2013). There is still debate, however, whether this incomplete determinism observed in the retina is due to lineages that generate subtypes of retinal neurons (Hafler et al., 2012). This would be similar to GMCs in Drosophila, with each NB generating different GMCs that then generate different cells, such that within a lineage, there are two cell types generated, but between lineages, these cells may vary greatly. For example, retinal progenitors expressing Olig2 have been shown to behave somewhat like *Drosophila* GMCs. These Olig2-expressing retinal progenitors produce predominantly either two rod photoreceptors or a rod photoreceptor and an amacrine cell (Hafler et al., 2012), but this seems to be Notch-independent (Mizeracka, Demaso, and Cepko 2013), and they also produce a small number of additional cell types. It seems more likely to me that in the future, as more experiments can be achieved that resolve differences between progenitors and birth orders, that vertebrate neurogenesis will be understood as completely deterministic.

The birth order of retinal cell types in vertebrates is stereotyped (Cepko et al., 1996; Livesey and Cepko, 2001). Studies in mice (Sidman, 1961; Young, 1985a) and Xenopus (Wong and Rapaport, 2009) show that they are born in the following order: retinal ganglion cells, horizontal cells, cone photoreceptors, rod photoreceptors, amacrine cells, bipolar cells, and Müller glia. Retinal progenitor cells pass through successive competence windows (Cepko et al., 1996). During each competence window, the progenitor can generate a subset of differentiated cell types or progress to the next competence window with a different potential for which cell types can be generated. This competence model in vertebrates is similar to the temporal cascade in *Drosophila*, with progenitors remaining competent to generate certain cell types if manipulated to express certain TFs for a shorter or longer period of time than wildtype progenitors, but ultimately still being restricted in their multipotency by the current competence window of the progenitor (Reviewed in Kohwi and Doe, 2013). Clonal analysis of zebrafish retinal development has shown that while the birth order of individual retinal progenitor cells is deterministically biased, the birth order is not as strictly determined as expected from the competence model (He et al., 2012).

Temporal differences in immature neurons – comparing younger (late-born) and older (early-born) neurons

During embryonic neuronal development, differential cell fate specification occurs at many levels to generate the cell type complexity required for a functioning larval nervous system. A Cartesian pattern of gene expression in each segment of the neuroectoderm generates a row-column grid that specifies the segmentally repeating pattern of neuroblasts through the row and column genes (Reviewed in Skeath, 1999). As in vertebrates, segmental specification is determined through expression of different Hox genes to refine the repeating pattern of NBs for different roles along the A-P axis (reviewed in Pearson, Lemons, and Mcginnis, 2005; Wellik, 2007). Finally, during embryonic neurogenesis, expression of a TF cascade by each NB is responsible for the temporal identity of the neurons born. As mentioned earlier, each neuroblast creates a diversity of neurons through sequential divisions, which is achieved by progression through this temporal cascade, with each NB sequentially expressing the same TFs in order: *Hb*, *Kr*, *Pdm*, *cas*, and *grh* (Grosskortenhaus et al., 2006; Isshiki et al., 2001; Kambadur et al., 1998; Kanai et al., 2005; Novotny et al., 2002; Pearson and Doe, 2003). Most NBs create a mix of all interneurons, motor neurons, and glia during embryonic neurogenesis (Schmid et al., 1999). This is achieved by switching what type of cell is being generated as a function of the temporal identity of the neuroblast. In vertebrates, this is paralleled by a switch during development from neurogenesis to gliogenesis (Bayer and Altman, 1991).

Larval neurogenesis creates a comparatively simpler repertoire of neurons with immature neuronal arbors that appear identical at the arrested immature state before metamorphosis. Despite the morphological homogeneity of immature larval-born neurons within each hemilineage, there is eventually further cell type diversification evident after metamorphosis. This cell fate specification is most likely controlled by temporal differences according to the birth order of the neurons, and is therefore likely encoded at the birth of the neurons, but not phenotypically obvious until their maturation. One example of this in the immature neurons is seen in the two morphologically distinct subpopulations of hemilineage 12A, which are divided into the early born and late born neurons from the hemilineage (Mellert et al., 2016). We hoped to identify a gene or set of genes that controlled the temporal diversification

process in the postembryonic neurons. Are there substantial differences between the gene expression profiles of younger and older immature neurons that are consistent across hemilineages? If so, which genes are affected? Can we identify a molecular "switch" that controls temporal cell fate diversification from the gene expression differences between the younger and older immature neurons?

There is a temporal cascade observed during mammalian neurogenesis as well, with progenitor cells progressing through a stereotyped order of competence windows, during which one or more cell types can be generated (Cepko et al., 1996). Mammalian neurogenesis has been particularly well studied in cerebral cortex and retina (reviewed in Lodato and Arlotta, 2015; Centanin and Wittbrodt, 2014). There is a switch in many developing mammalian CNS structures between neurogenesis and gliogenesis (reviewed in Rowitch and Kriegstein, 2010). In the cortex, proliferation is followed by neurogenesis, astrocyte formation, and oligodendrocyte formation. The basic helix-loop-helix (bHLH) proteins Mash1, Neurogenin1, and Neurogenin2 are important in the cortex for promoting neurogenesis after proliferation of progenitors and inhibiting gliogenesis. The inhibition of these factors then promotes astrocyte formation. Finally, the bHLH proteins Olig1 and Olig2 promote oligodendrocyte formation (Ross, Greenberg, and Stiles, 2003). Sox9 has been shown to promote gliogenesis in the spinal cord (Stolt et al., 2003).

Neuronal maturation

The larval nervous system contains both immature and mature neurons, born during larval and embryonic neurogenesis, respectively. Unlike vertebrate neurons, which begin an often lengthy maturation process immediately after their birth (Caviness, Takahashi, and Nowakowski, 1995; Gage and Temple, 2013), Drosophila neurons are pooled during larval neurogenesis in an immature state.

Adult neurogenesis in mammals does have parallels to the immature larval neurogenesis in Drosophila, since the full neuronal maturation and integration into the pre-existing circuitry is delayed (Zhao et al., 2006). The immature mammalian neurons, however, are responsive to local neurotransmitters despite not having formed synapses yet, as shown in a rat model (Song et al., 2002). It takes 6 months for

newborn neurons generated through adult neurogenesis to fully mature in macaque dentate gyrus (Kohler et al., 2011), while the entirety of embryonic neurogenesis in monkeys lasts about 2 months (Caviness, Takahashi, and Nowakowski, 1995). By comparison, it takes about 2 months for newborn neurons to acquire their mature morphology during human development (Gage and Temple, 2013), and human embryonic neurogenesis lasts for about 100 days (Caviness, Takahashi, and Nowakowski, 1995).

Progenitor cells from different regions of the CNS in vertebrates appear to progress through a similar gene expression program over the course of development. Retinal, cortical, and cerebellar cells show similar gene expression progression relative to adult brain gene expression, without roughly 600 transcripts being commonly enriched in progenitors from all three regions relative to adult brain (Livesey et al., 2004).

Immature and mature neurons differ significantly with respect to morphology, connectivity, and other important features of neuronal identity. These immature neurons have not completed pathfinding and have not formed synapses. By comparing the mature and immature larval neurons, I hoped to address how gene expression changes through neuronal maturation in Drosophila. There are likely two general categories of TFs in the context of the development of these neurons: TFs that are expressed only transiently for identity establishment, and TFs that are expressed constitutively that are required for maintenance of neuronal identity. For this reason, I hypothesized that there might be fewer TFs that are highly expressed in mature neurons, because those with transient expression required only for identity establishment should no longer be detectable several days after becoming functional neurons. If there are genes involved in pathfinding that are not required maintenance of the stable, mature morphology of the neurons, such as certain cell adhesion molecules or cell surface receptors necessary for guidance of the growth cone, similarly, these genes might be expressed in developing neurons, but not mature neurons. The arrested immature larval neurons are not actively undergoing pathfinding to their final targets, but have either begun or completed the pathfinding to their immature, local targets and will soon, during metamorphosis, perform much more elaborate pathfinding. Since the immature larval neurons in Drosophila are

arrested in a state where they are not forming synapses, I hypothesized that I would observe more genes associated with neurotransmission and synaptic function in the mature neurons.

Cell fate switching and competence windows and determinism

As previously discussed, the development of *Drosophila* neurons is understood to be completely or nearly completely deterministic, but it is currently unknown to what degree the pre-metamorphic immature neurons express their mature transcriptional patterns. The proteins for Gad1, VGlut, and Cha are believed to be absent in immature neurons in the *Drosophila* VNS because they are negative for immunohistochemistry (Haluk Lacin, personal communication). In mammals, neurotransmitters are present in immature CA1 pyramidal neurons prior to synapse formation, where they have been found to use a vesicle-independent mechanism for signaling between cells (Demarque et al., 2002). As an initial assessment of how early important aspects of the mature transcriptional profile of the neurons are expressed, I assessed the expression of transcripts for neurotransmitter biosynthetic and shuttling proteins.

Combinatorial control of cell fate and a TF code map of the VNS hemilineages

Central to our understanding of molecular genetics and the deterministic model of lineage fate during development is combinatorial control of gene expression. Transcription factors in the form of both activators and repressors act combinatorially on enhancers to cause or prevent expression of each gene. Different cell types are generated in multicellular organisms through this very mechanism to effect combinatorial control of cell fate. Different amounts of TFs are inherited by cells (including progenitor cells) at their birth. The combination of TFs, microRNAs, and other inherited factors restricts cells to a particular fate or set of fates. A number of TF identity maps are being made that help us understand the “code” that specifies each type of cell, including neurons (Lein et al., 2007; Hawrylycz et al., 2012; Shen et al., 2012; Del barrio et al., 2013; Thompson et al., 2014; Bakken et al., 2016; Allen Institute for Brain Science, 2008).

It is difficult to imagine a scenario wherein neurons that are obviously different with respect to their lineage and morphology have identical gene expression. Immature neurons in the larval VNS express a combination of TFs that can be used to uniquely identify each hemilineage (Lacin et al. 2014). We hoped to confirm the previous immunohistochemistry results and to contribute new information to the TF "code" in a more exhaustive and unbiased manner. Where immunohistochemistry had the advantage of assaying all hemilineages for a single protein at a time, RNA-seq afforded the opposite advantage: assaying every gene in a single hemilineage at a time. The TF code responsible for identity establishment in these neurons is combinatorial by nature. This is a logical necessity, since there are more cell types in the animal than there are TFs in its genome. We hypothesized that we would nonetheless find at least one instance of a TF that was important for the identity establishment of one and only one hemilineage in the VNS.

This type of cell fate specification mapping with respect to TF expression has important implications when applied to human health. Medical technologies including stem cell therapies and genetically targeted therapies are two cases in which it is important to be able to distinguish between extremely similar cell types and uniquely identify a population of cells. Hypothetically, an expression code, particularly for TFs controlling identity establishment, would allow one to target specific populations of cells for gene therapies and generate those cells from induced pluripotent stem cells (iPSCs) using the same TF expression code.

Understanding the expression patterns and the control of cell fate in *Drosophila* has implications for human health due to evolutionary conservation and homology between distantly related organisms. There are substantial similarities between the neuronal stem cell development of the *Drosophila* and mammalian CNSs, even the cerebral cortex. *Platynereis dumerilii* mushroom bodies and the developing mammalian cortex share expression patterns and even have similar morphology at earlier parts of development (Tomer et al., 2010), showing that there is remarkable developmental and structural homology between brain regions from species as diverse as humans, flies, and worms. Even when the structural homology disappears at later stages of development, it is the same molecular players that compartmentalize and guide cell fates into distinct neuronal populations.

Chapter 2

Methods, Experimental Design, and Optimization of Flow Cytometric Cell Enrichment for RNA-Seq

Hemilineages are the unit of generating diversity in the nervous system. We focused on the hemilineages in the wandering larval stage when the hemilineage clusters had a large number of neurons but the neurons in the hemilineage unit were fairly similar and most were in an arrested state. The arrested state of the neurons allowed access to a large number of neurons that were all in a state of identity establishment rather than a diverse population of neurons with both mature and immature neurons. This also allowed the treatment of the neurons in a hemilineage as a fairly homogenous group of cells with respect to their developmental timing and cellular identity such that a large amount of RNA could be extracted from the animals and treated as a single cell class. We devised ways to collect the RNA from the clusters of these cells to determine (1) what characterizes these cells in their immature state and (2) how do they differ from each other. Several different labeling, dissociation, and cell sorting methods were attempted before arriving at a good solution that allowed me to isolate only the cells of interest to sufficient purity, as outlined in this chapter.

Fly Rearing

All flies were reared on cornmeal and molasses food in vials or bottles provided by the Janelia Fly Core. Stocks were kept at room temperature and most crosses were performed in humidified incubators with constant light at 25°C unless otherwise specified. In this thesis I used two different binary expression systems in *Drosophila*: GAL4>UAS and LexA>LexAOp (Brand and Perrimon, 1993; Lai and Lee, 2006). A reporter stock consisting of pJFRC105-10XUAS-IVS-nlstdTomato in VK00040 (gift of Barret D. Pfeiffer, Rubin Lab, Janelia Research Campus) and pJFRC29-10XUAS-IVS-myr::GFP-p10 in attP-40 (Pfeiffer et al 2012) was crossed into the various modified GAL4 driver lines to allow the sorting of neurons by Fluorescence Activated Cell Sorting (FACS).

GAL4 lines chosen

The GAL4 lines that provided drivers that were specific for specific hemilineages were from two large collections of GAL4 enhancer lines: one at HHMI Janelia Research Campus (JRC) and one at the Research Institute of Molecular Pathology (IMP) in Vienna. Larval images of the Janelia lines were available through the website from Li et al., (2014) and those from the Vienna line were imaged by the FlyLight project and available through an internal JRC website. Using the approach of Harris et al. (2015), I selected GAL4 lines that showed expression in a particular thoracic hemilineage and then included nSyb-GAL80 to block expression by the mature, larval neurons. An example of this is shown for R15D11 in Figure 2.1. One disadvantage of this strategy is that some of the lines also showed expression in the brain. Consequently, we manually cut the brains from the samples before subjecting the VNSs to dissociation.

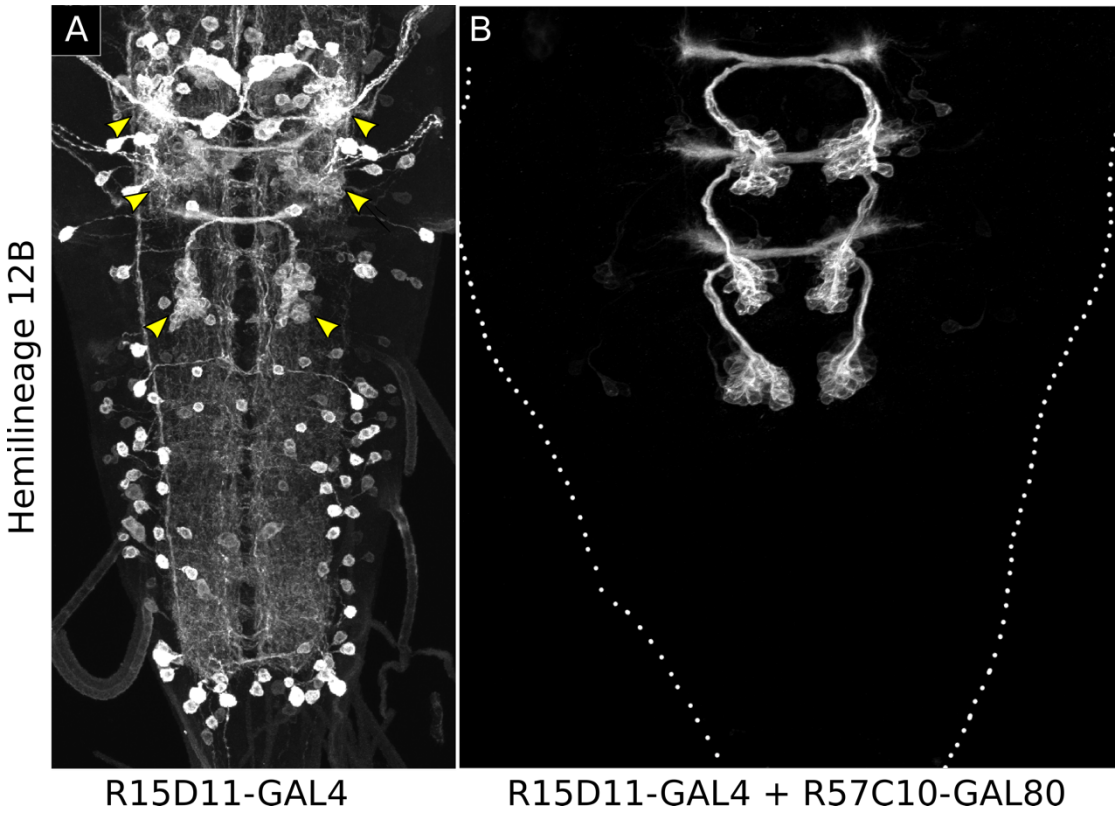

Figure 2.1 | nSyb-GAL80 effectively removes mature neuron GAL4 expression. Confocal Z-projections of the ventral nervous system showing that the R57C10-GAL80 derived from the nSyb enhancer removes expression of GAL4 patterns from mature neurons. A: R15D11-GAL4 driving UAS-GFP expression labels both mature neurons and the segmental clusters of immature hemilineage 12B neurons (Yellow arrowheads) , B: R57C10-GAL80 added to the genotype blocks expression in the mature neurons, without effecting the expression in the immature 12B neurons, thereby generating a far cleaner sample for RNA-seq. Dotted lines in (B) show the outline of the VNS. Image in (A) from Li et al., 2014.

A pilot round of experiments was performed using the R20B05-GAL4 line, which shows expression in all of the postembryonic-born neurons. R20B05-GAL4 was later replaced with R71C09-GAL4 because the latter does not include neuroblast and GMC expression, whereas the former does. This is an important refinement because *Drosophila* neuroblasts have an average cell diameter of 7 um and a GMC is approximately half the size of a neuroblast (Chell et al., 2010; Homem et al., 2013), thus a 10 um filter should still allow both neuroblasts and GMCs through. Drosophila neurons have soma that are typically 2-6 um in diameter (Tuthill, 2009). Most of the hemilineage-specific GAL4 drivers did not include neuroblast or GMC expression because the A or B identity (and hence GFP expression) is acquired after the GMC divides. However, some lineages are monotypic, with the sibling hemilineage undergoing apoptosis, which means that the neuroblasts and/or GMCs could express GAL4 in these otherwise hemilineage-specific drivers.

MARCM Experiments

Mosaic analysis with a repressible cell marker (MARCM; Lee and Luo, 2001) experiments were completed by heat-shocking larvae for 1hr at 39°C, resting at room temperature for 1hr, and then providing a second round of heats-hock for 1hr at 39°C. All animals were dissected and CNSs with GFP expression were stained. Those samples with GFP expression in relevant lineages were imaged. The two genotypes used for TfAP-2 MARCM clones were: (1) hsFLP, elav-GAL4, UAS-mcD8::GFP; +; TfAP-2^{2}, FRT80B/tub-GAL80, FRT80B for *TfAP-*2^{2} and (2) hsFLP, elav-GAL4, UAS-mcD8::GFP; +; TfAP-2^{15}, FRT80B/tub-GAL80, FRT80B for *TfAP-*2^{15}.

Methods for isolation of labeled cells or nuclei

A major problem is generating sufficient numbers of the appropriate number of cells or nuclei for RNA-seq analysis. Isolation of Nuclei Tagged in Specific Cell Types (INTACT; Henry et al., 2012), has been to tag nuclei of the desired cells and then use anti-GFP-coated Protein G-conjugated Dynabeads (Invitrogen) to harvest the labeled nuclei. Another method is "Translating Ribosome Affinity Purification (TRAP)" (Thomas et al., 2012). I tested both TRAP and INTACT as GAL4- and GAL4/LexA-inducible methods, respectively, for generating cDNA for subsequent RNA-Seq.

TRAP (UAS-GFP::RPL10a) and INTACT (13xLexAop-UNC-84::2xGFP) flies have been crossed to a driver specific to hemilineage 12A, and GFP can be detected in the same cells as when this GAL4 driver is crossed to a membrane-localized GFP reporter. Beyond this point, however, INTACT experiments yielded less-than-desirable results. Harvesting of the immature neurons of the lineage clusters was problematic, because expression of low to moderate levels of the nuclear tag was insufficient for effective binding to the Dynabeads. Unfortunately, the boosting of expression levels resulted in cell or organismal death. While INTACT is well suited for questions regarding adult neuronal expression, we were unable to isolate sufficient numbers of labeled nuclei in larval *Drosophila* for the experiments to be viable. Immunoprecipitation of dissociated neurons expressing UAS-mcD8::GFP with anti-mcD8 beads, both directly conjugated and with protein G beads, was unsuccessful despite successful use of this method in the literature (Iyer et al., 2009). I did not try translating ribosomal affinity purification (TRAP) because this method also relies on immunoprecipitation for RNA isolation and was also not optimized for larval samples (Thomas et al., 2012). The other approaches I contemplated was the manual sorting of labeled cells or the use of Fluorescence Activated Cell Sorting (FACS). The latter proved to be the best option for generating large numbers of cells of the appropriate purity for this study.

Artificial hemolymph saline

Samples for RNA-Seq were dissected in, protease treated in, and FACS sorted into artificial hemolymph saline. The artificial hemolymph saline had 2% glucose and 2% trehalose for all steps except dissection. 2% glucose and 2% trehalose mass/volume was used in the dissociation and sorting artificial hemolymph saline to match Schneider's growth media.

Ion / Sugar	Concentration (mM unless otherwise stated)	Previously reported ion concentrations in larval hemolymph
Na	54.7	~60 mM Na
Cl	111	~40 mM Cl
K	45	~45 mM K
Mg	30	~30 mM Mg
PO4	8	~8 mM PO4
Glucose	2% w/v	-
Trehalose	2% w/v	-

Table 2.1 | Artificial hemolymph saline composition. Concentrations in mM unless otherwise stated. pH to 7.4. 2% glucose and trehalose weight/volume.

This saline composition was based roughly on previous publications summarized in Ashburner, "*Drosophila*, A Laboratory Manual", Cold spring Harbor Press, p207, Table 8.5.

Dissociation of VNS neurons for FACS

Manual sorting or FACS of the neurons necessitates first dissociating the neurons. I tried a number of techniques for dissociating the neurons in my dissected VNS samples. I found that *S. griseus* protease significantly disrupted cellular integrity and thus did not use it further. I finally found that treatment with a mixture of dispase and collagenase (2:1 as 1 mg/mL dispase and 0.5 mg/mL collagenase IV) was sufficient to loosen up connections amongst the cells prior to mechanical separation. I then dissociated the treated nervous systems into component neurons using dounce homogenizers. Loose pestle was insufficient to dissociate the brains and loose pestle dounce tractions before tight pestle dounce tractions showed no obvious advantage over just doing tight pestle dounce tractions alone. Tight pestle douncing of the VNSs after protease digestion yielded single cells and some undissociated clumps of tissue. It is possible that the more standard trituration is a gentler method of dissociation that may retain more processes from the neuron soma, but this method was relatively rapid and provided adequate numbers of labeled cells for isorting. I have not compared the two personally, but two comparisons of the methods in collaboration with Carl Wu as well as Pavan Agrawal in the lab of Ulrike Heberlein both slightly favored trituration for decreased number of un-dissociated cells as well as retention of some neuronal processes. In the future, it would be worth considering a switch to trituration if starting a new dataset.

Optimization of FACS sorting

Due to the low purity of the samples in initial pilot datasets, experiments were performed to improve sample purity by optimizing available reporter combinations for FACS. After identifying various pitfalls associated with existing methods, I conceived a novel experimental approach. My method compartmentalizes reporter expression in unique cytological domains using transcriptional modifiers that specify

localization to either the cell membrane using a myristylation tag (myr), or to the nucleus using a nuclear localization signal motif (nls). These transgenes, which have apparently negligible consequences on cell physiology (Pfeiffer, Truman, and Rubin, 2012), are driven in tandem from a single GAL4 driver, generating cells expressing both green fluorescent protein (GFP; Shimomura, Johnson, and Saiga, 1962; Prasher et al., 1992) and tandem dimer tomato (tdTomato; Shaner et al., 2004). This labeling scheme facilitates sorting dissociated cell populations by FACS for RNA-Seq analysis. I arrived at this reporter combination empirically; of the available combinations of nuclear, cytoplasmic, membrane tagged tdTomato and GFP reporters on the basis of contamination rate with unlabeled cells, this reporter combination gives up to 98% cell purity according to DAPI counterstaining.

R24B02-GAL4 virgins were used for all crosses for optimizing reporter combinations for FACS purity. I tried a variety of membrane, cytoplasmic and nuclear reporters to maximize the purity of the FACS isolated cells. As shown in Figure 2.2, a two-color nuclear and membrane reporter combination performed best of all combinations for FACS purity. Of single-color sorting options, membrane reporters performed better than cytoplasmic or nuclear reporters. Membrane reporters reliably gave high purity while cytoplasmic reporters gave poor and variable purity. Having a nuclear reporter in a different emission spectrum is also beneficial for manual sorting, because it allows one to easily distinguish cell bodies from processes in dissociated cells. Once dissociating the central nervous system into a mostly single-cell suspension was optimized, I was able to FACS-sort neurons labeled with myristoylated GFP and nuclear tdTomato using size and fluorescence-intensity gating parameters. These FACS parameters yielded sufficient numbers of cells at high purity (>3000 cells at >95% labeled neurons).

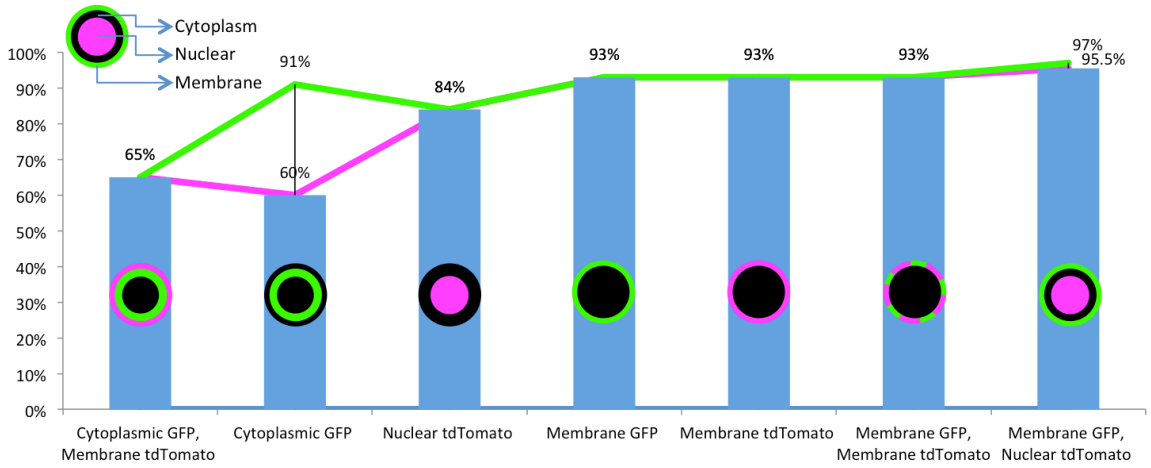

Figure 2.2 | Sorting efficiency by reporter. The two-color nuclear and membrane reporter combination is the best for FACS purity. Membrane reporters perform the best for single-color sorting. Membrane reporters reliably gave high purity while cytoplasmic reporters gave poor and variable purity. Having a nuclear reporter in a different emission spectrum is beneficial for manual sorting, because it allows one to easily distinguish cell bodies from processes in dissociated cells.

Larval-born neuroblast hemilineages in the VNS were profiled using fluorescence assisted cell sorting (FACS) and deep sequencing. Typically, manually sorting fluorescent labeled cells exposes dissociated cell populations to room temperature conditions for several hours, potentially influencing gene expression. In contrast, all of the samples in this study were held either on ice or at 4°C for the duration of dissection followed by only 30 minutes at room temperature for protease digestion. In *Drosophila*, some heat shock genes are upregulated in response to cold stress, but not until recovery from cold (Colinet et al., 2010).

Sample preparation for RNA-Seq

Sample preparation for RNA-seq is summarized in Figure 2.3. Larval CNSs were dissected in artificial hemolymph saline (Table 2.1), the brain lobes removed and the VNSs and pipetted into an Eppendorf Protein Lo-Bind tube with artificial hemolymph saline with 2% glucose and 2% trehalose on ice. VNSs were centrifuged briefly (about 5 seconds in a small tabletop centrifuge) and buffer was replaced with 500 uL protease solution: 1 mg/mL dispase and 0.5 mg/mL collagenase IV in artificial hemolymph saline with 2% glucose and 2% trehalose. The addition of buffer resuspended the VNSs. VNSs were incubated in this protease solution for 30 minutes at room temperature in the dark. A tight pestle dounce homogenizer (Chemglass Life Sciences CLS-5003-01) was chilled on ice after having been coated in 1% BSA.

VNSs were briefly centrifuged again and the protease solution was replaced with 500 uL ice-cold artificial hemolymph saline with 2% glucose and 2% trehalose. The protease-treated VNSs were dissociated using 50 slow tractions with the tight pestle dounce. The cells were pipetted into a 10-um filter (Partec) seated in a 1%-BSA-coated tube used for sorting (Falcon 352058) on ice. The fluid flow through was collected in the sorting tube. The remaining cells were washed from the filter with an additional 500 uL ice-cold artificial hemolymph saline with 2% glucose and 2% trehalose into the same tube.

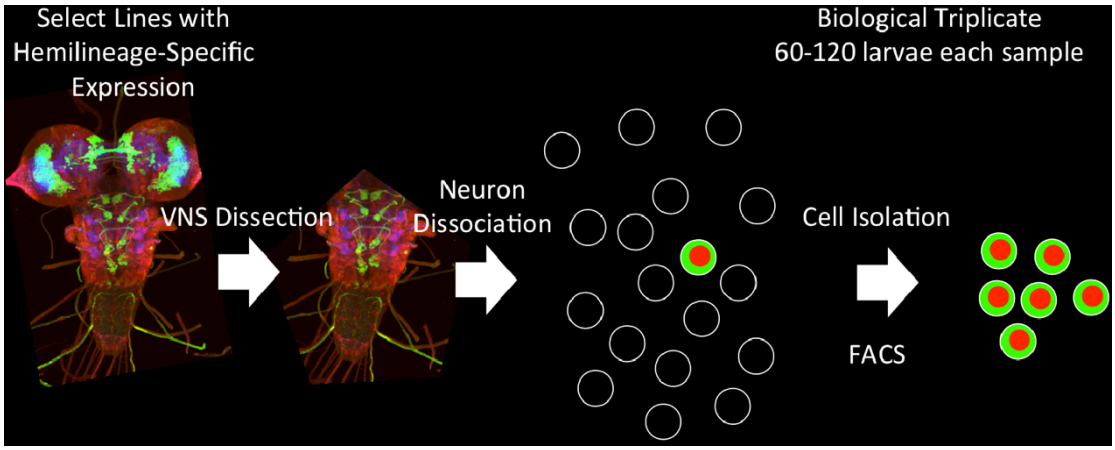

Figure 2.3 | Summary of the steps in preparing the cell samples for RNA-seq. Hemilineage-specific GAL4 lines were selected based on morphology. Contaminating embryonic neuron expression was removed using an nSyb-GAL80 construct. Brain lobes were removed by dissection. Cells were dissociated by dounce homogenization after treatment with collagenase/dispase. FACS sorting was used to enrich cells expressing nuclear tdTomato and myristoilated GFP under the control of GAL4.

All pipette tips were coated with 1% BSA in artificial hemolymph saline before transferring VNSs or cells to keep them from sticking to the tip. Centrifugation steps were used to make buffer replacement easier. Centrifuging for too long generated a tight pellet that was undesirable. A larger (20 or 30 um) filter will be better for larger cells. Because the filters start fairly hydrophobic, I pipetted 500uL of buffer onto both sides of the filter and then gently shook the excess buffer off gently after the buffer observed flowing through the filter. This made the cell filtering much simpler. Some small clumps visible under a microscope remained after filtration.

Cells were sorted on both red and green channels using a BD FACSAria machine at a flow rate of 3.0 and laser intensity of 336 V for GFP and 390 V for PE directly into an Eppendorf Protein Lo-Bind tube with 350 uL of artificial hemolymph saline with 2%

glucose and 2% trehalose at 4°C. The sorted cells were placed on ice and roughly 10% of the sorted sample was placed on a chambered culture slide for purity assessment. The remained of the cells were centrifuged at 3000 rpm for 10 minutes at 4C in a tabletop centrifuge. The buffer was then replaced with 75uL buffer RLT with 1:100 Beta-mercaptoethanol. The cells were then vortexed for 10 seconds and immediately frozen at -80C.

Lysate was thawed at 37°C for 5min and then total RNA was purified from the lysate using the Qiagen RNEasy Micro kit. cDNA libraries were generated using the NuGEN Ovation v2 and Ovation Rapid DR Multiplex System 1-8 and 9-16 kits. Sonication of the cDNA to approximately 200bp was performed using a Covaris S220 before adapter ligation was performed. I used 1uL External RNA Controls Consortium (ERCCs) spike-in ratio mixtures at 1:100,000 dilution after diluting the total RNA to 4000 cells per 13uL and then used a speed-vac to reduce the RNA total volume to 5uL. The RNA and ERCCs were amplified using the NuGEN Ovation v2 kit. The cDNA was then barcoded using the NuGEN Ovation Rapid DR Multiplex System 1-8 and 9-16 kits. Sequencing was performed on an Illumina HiSeq. For each round of sequencing, 16 samples were loaded equally onto 4 lanes for sequencing. All experiments were performed in biological triplicate except for four samples that were performed in quadruplicate.

Analysis Pipeline

Using these cells obtained through FACS, I used the NuGEN Ovation v2 kits (NuGEN) for cDNA synthesis that was then analyzed on the Janelia core facility Illumina Hi-Seq deep sequencer. These transcriptome sequence reads were aligned to a reference transcriptome based on release 5 of the genome (Hoskins et al., 2015) and compared bioinformatically using the "Tuxedo suite" programs Tophat and Cuffdiff (Langmead et al., 2009; Trapnell et al., 2009; Trapnell et al., 2010). Graphs and further analysis was mostly performed using packages for the statistical programming language R.

I performed alignment with TopHat2. I did not trim reads for this pipeline, since there is no appreciable benefit derived from trimming RNA-Seq reads; TopHat2 has

demonstrated an ability to compensate for poor read quality at the extreme ends of each read (Del Fabbro et al., 2013). I used Cuffdiff2 to perform differential expression analysis. The R package CummeRbund was used to organize Cuffdiff2 data into an sqlite database and to graph differential expression of splice isoforms. These software packages were run under standard user settings. Excel and the R package ggplot2 were used to generate differential expression scatterplots. The R package prcomp function was used to perform PCA analysis on the datasets based on FPKM. DAVID (Huang, Sherman, and Lempicki 2009a; Huang, Sherman, and Lempicki 2009b), STRING (Szklarczyk et al., 2015), and PANTHER.db (Mi et al., 2005) were used to determine gene classifications and perform gene set enrichment analysis (GSEA). Information from FlyTF.org was used to estimate what percentage of genes were putative and experimentally confirmed transcription factors. Pearson and Spearman correlations were calculated in R using graphs made in ggplot2 for pairwise expression vs expression plots for replicates of the same sample genotype. The R package heatmap2 was used for hierarchical clustering.

Inter-replicate correlations

Systematic, pairwise, inter-replicate correlations indicate that most of my datasets are >95% correlated, demonstrating high reproducibility of the datasets. Since all of the datasets were run in triplicate (quadruplicate for a small number), in cases where one of the replicates was substantially different from the other two, the odd replicate was omitted from further downstream analyses. One sample, hemilineage 13B, had to be removed entirely from analyses. This decision was based on low inter-replicate correlations and because it adversely affected principal component analyses and hierarchical clustering of other samples to the point of making them impossible to interpret by behaving as an extreme outlier.

Statistics

Statistics were performed by cuffdiff for pairwise ANOVA between RNA-seq samples to generate q values for fold changes used for thresholding downstream. The Benjamini-Hochberg q value is an FDR-adjusted p value used to correct for multiple testing (Benjamini and Hochberg, 1995). Since it is very strict, typically $q<0.1$ is used in place of $p<0.05$. All other statistics were performed with the programming

language R. Many packages were used, including ggplot2 and heatmap2 for various plots.

Chapter 3

Hemilineage-Specific RNA-Seq

Introduction

The *Drosophila* nervous system is composed of an enormous diversity of neurons, the stereotyped development of which is necessary for a healthy adult animal capable of performing many essential behaviors. These diverse neurons are generated from distinct neuronal stem cells called neuroblasts. In the central nervous system (CNS), neurons are formed into developmental and anatomical clusters called lineages, with each lineage being composed of the progeny from an individual neuroblast. The *Drosophila* nervous system provides an important model for studying neuronal development. The clonal arrangement and formation of the nervous system allows for genetic manipulation for studying developmental processes, circuit formation, and behavior.

Neuroblasts each produce two populations of neurons called the A and B hemilineages (Truman et al., 2010). This is achieved through multiple rounds of asymmetric and self-renewing division that each produces a ganglion mother cell (GMC) that terminally and asymmetrically divides into an A and a B neuron. A hemilineage neurons have *Notch* activity while the B hemilineage neurons do not (Skeath and Doe, 1998; Truman et al., 2010).

Neuroblasts undergo two periods of neurogenesis with an intervening phase. The larval nervous system is generated during the embryonic phase of neurogenesis. These neurons function to control the larva. During the post-embryonic phase of neurogenesis, the adult nervous system is generated. Most of these neurons are generated during larval life, but some are generated early in metamorphosis.

The period of neuroblast quiescence that separates embryonic and larval neurogenesis is controlled by the temporal transcription factor cascade, Hox genes *abd-A* and *Antp*, as well as the transcriptional co-factor *Nab* (Tsuji et al., 2008). Not all neuroblasts

reactivate after quiescence. The thoracic segments experience far more neuronal proliferation in the post-embryonic phase neurogenesis. In the abdominal segments, *Abd-A* expression induces apoptosis in many neuroblasts (Bello et al., 2003). Eventually, neuroblasts either terminally differentiate or undergo apoptosis (Pompeiano et al., 2000; Honarpour et al., 2000; Kaun et al., 2000; Maurange, Cheng, and Gould, 2008).

Neurons born during post-embryonic neurogenesis account for about 90% of the neurons in the adult fly (Truman & Bate 1988). Of the 31 neuroblasts per hemisegment in the embryonic nervous system, 26 of these neuroblasts reactivate during larval neurogenesis in some segments (Truman et al., 2004; Lacin and Truman, 2016). Each hemilineage in uniquely identifiable by morphology and combinatorial expression of transcription factors (Truman et al., 2010; Lacin and Truman, 2016). Each hemilineage is a developmental and behavioral subunit, and activation of an entire postembryonic hemilineage elicits characteristic behaviors in the adult (Harris et al., 2015).

During embryogenesis, the neuroblasts each exhibit a transcriptional cascade, consisting of sequential hunchback (hb), seven up (svp), kruppel (kr), POU domain proteins 1 and 2 (pdm1 (nubbin) and pdm2), and castor (cas) transcription factor expression. This yields a diverse population of neurons that comprises the larval nervous system (Grosskortenhaus et al., 2006; Isshiki et al., 2001; Kambadur et al., 1998; Kanai et al., 2005; Novotny et al., 2002; Pearson and Doe, 2003). The ganglion mother cell (GMC) inherits the temporal transcription factor expression of the neuroblast and generates different neuronal types depending on the transcription factor being expressed. Larval neuroblasts express *cas* and *svp* after reactivation (Tsuji et al., 2008; Maurange, Cheng, and Gould, 2008; Lacin and Truman, 2016). In addition to being less diverse with respect to temporal transcription factor expression, these post-embryonic neurons are also far less morphologically diverse than the embryonic-born neurons (Truman et al., 2004).

After their birth, the young, postembryonic neurons undergo two distinctive phases during axon outgrowth. The first is characterized by axon pathfinding, while the second phase involves interactions with the neuron's initial target. These immature

neurons then arrest until metamorphosis, when the cells finally begin to sprout interstitial (dendritic) and terminal (axonal) arbors. Therefore, late in larval life the neurons in a lineage cluster range from the youngest cells that are in the initial phases of growth into the neuropil (most apically in the cluster) to the oldest cells (most basal near the neuropil) that have finished target interactions and are fully arrested.

In contrast to the embryonic-born neurons, postembryonic-born neurons do not form synapses during larval life. They remain non-functional in the larval nervous system and are only functional in the adult stage (Booker and Truman, 1987; Truman and Booker, 1986). During metamorphosis, they then grow their adult arbors and undergo synaptogenesis. During this process, the neurons in the hemilineages display morphological diversification, generating multiple types of neurons (Harris et al., 2015). Thus, despite neurons of the same hemilineage having nearly identical morphology in their immature, arrested state, they do not represent a completely homogeneous group of neurons. This diversity is likely birth-order dependent. For example, there is a shift from neuroblasts generating Chinmo-positive neurons to Broad-positive neurons during the post-embryonic neuroblast divisions (Maurange, Cheng, and Gould, 2008).

We hypothesized that Notch signaling would cause downstream expression of a consistent set of genes in each hemilineage with Notch activity. Thus, in comparing the gene expression of multiple A and B hemilineages, we expected to determine this battery of Notch-dependent genes. In this chapter, I attempt to address the following questions: 1) What transcriptional differences allow different neuronal stem cells to generate diverse adult-specific neurons? 2) How different are the hemilineages? 3) What are the major classes of genes that are differentially expressed between hemilineages? 4) Are sibling hemilineages more alike than non-sibling hemilineages? 5) How does gene expression in the younger and older neurons of a hemilineage differ? 6) How does Notch activity determine the gene expression pattern in the hemilineages?

Which genes are consistently expressed downstream of Notch signaling?

Is Notch consistently causing expression of the same downstream genes in each hemilineage where it is active? We hypothesized that Notch signaling would cause downstream expression of a consistent set of genes in each hemilineage with Notch activity. Thus, in comparing the gene expression of multiple A and B hemilineages, we expected to determine this battery of Notch-dependent genes.

How does neuronal maturation affect gene expression?

How does gene expression change through neuronal maturation? We hypothesized that immature neurons would express more TFs and genes associated with neuronal pathfinding than mature neurons and conversely that the mature neurons would express fewer TFs and more genes associated with neurotransmission and synaptic function. Concerning TF expression, some TFs are likely expressed only transiently for identity establishment, while others are likely required for maintenance of neuronal identity. We hoped to determine which TFs fell into each category, if this assumption held true.

Does immature neuron expression predict mature neuron expression?

Does immature neuron expression predict mature neuron expression? The fate programming in invertebrate neurons is considered to be deterministic. Can this deterministic fate programming be detected in the immature developmentally arrested neurons? If so, how broad are the gene pathways affected by this deterministic fate programming in immature neurons? To answer this question, we asked of the data, more pointedly, which genes and gene classes are expressed in the immature larval neurons in the arrested state that are indicative of their mature neuronal state?

How is temporal diversity reflected within immature neuron gene expression?

Differential cell fate specification occurs many ways during neuronal development. There is the row-column grid that specifies the segmentally repeating pattern of neuroblasts through the row and column genes. Segmental specification occurs through Hox genes. Finally, a TF cascade in each NB is responsible for the temporal identity, allowing each NB to generate a diversity of neurons through sequential

divisions. Within each hemilineage, there is further cell type diversification evident after metamorphosis. Presumably, this cell fate specification is controlled by temporal differences according to the birth order of the neurons. I compared younger and older subsets of immature neurons to determine whether there are substantial differences between the gene expression profiles of younger and older immature neurons that are consistent across hemilineages. I hypothesize that the genes that are affected are similar to the genes that I expected to see differ between immature and mature neurons. I expected to see a larger number of TFs highly expressed in the younger neurons. In the older neurons, I expected to see a greater number of cell adhesion molecules and genes associated with pathfinding and target recognition expressed, since these older immature neurons have completed their initial pathfinding. I hypothesized that there is a gene or set of genes that controls the temporal diversification process in the postembryonic neurons that would be detectable through transcription differences between the younger and older populations of immature neurons.

Combinatorial control of cell fate: refinement of the TF expression map for a subset of VNS hemilineages

Based on previous work (Lacin et al. 2014), we hypothesized that immature neurons would express a combination of TFs that could be used to uniquely identify each hemilineage. We hoped to contribute a higher degree of dimensionality to the TF "code" provided through immunohistochemistry data. We also hypothesized that, while the TF code responsible for identity establishment in these neurons is combinatorial by nature, we might find at least one instance of a TF that was important for the identity establishment of one and only one hemilineage in the VNS.

Methods

Taking advantage of the unique opportunity presented by the arrested adult-specific neurons before metamorphosis to look at many similar lineally-related neurons, I generated RNA-seq transcriptomes for eleven different postembryonic hemilineages from the wandering third instar larvae using the techniques described in Chapter 2.

GAL4 lines used

Table 3.1 shows which GAL4 lines were used to drive expression in the hemilineages. R57C10-GAL80 was used to block GAL4 expression in mature neurons for all hemilineage-specific samples, but was not included in any of the combined neuron samples that express in more diverse neuron populations. This table also shows which gene the cis-regulatory module (CRM) used in constructing the GAL4 was derived from (Pfeiffer et al., 2008; Kvon et al., 2014). In addition to the GAL4 lines that express in an individual hemilieange, a number of combined lineage GAL4 driver lines were used as well (Li et al., 2014).

Hemilineage	Neuropil	CRM Gene	GAL4
12A	flight	*TfAP-2*	R24B02
12B	leg	*trh*	R15D11
1A	leg	*fru*	R22G11
1B	leg	*nub*	R13G06
13B	leg	*TrpA1*	R21E09
19A	leg	*CG42390*	VT045584
4B	leg	*tll*	VT050157
16B	leg	*CG32547*	R24C10
21A	leg	*VGlut*	R51H05
20/22A	leg	*klg*	R52C05
15B	leg	*CG42784*	VT006878
Mature (embryonic-born)	combined	*nSyb*	R57C10
Immature (larval-born without NB)	combined	*cas*	R71C09
Immature A neurons (larval-born)	combined	*Hey*	R12A07
Younger immature neurons + NB + GMC	combined	*B-H1*	R81C10
Older immature neurons	combined	*stg*	R31H08

Table 3.1 | Summary of RNA-Seq Samples. These are the hemilineages and combined lineage samples for which transcriptome analysis was performed. The GAL4 is shown along with the cis-regulatory module (CRM) from which the GAL4 enhancer was cloned.

Immunohistochemistry

Previously published antibody staining patterns for many transcription factors (TFs) were used to validate the expression patterns (Lacin et al. 2014). I used immunostaining with an antibody against TfAP-2 (Monge et al., 2001) to examine the expression pattern of this TF in the larval CNS.

Samples were fixed in 4% formaldehyde in PBS for 1hour at room temperature. PBSTx 0.3% was used for blocking, antibody staining, and washes between primary and secondary antibodies as well as between secondary antibodies and mounting.

Samples were washed with ten volume changes for at least 2 hours total and then blocked for 4 hours at room temperature in 20% normal donkey serum (NDS) or normal goat serum (NGS) depending on the secondary antibody species. Primary antibody solutions included 20% NDS or NGS depending on the secondary antibody species. Secondary antibody solutions included 10% NDS or NGS depending on the secondary antibody species. Samples were stained in primary and secondary antibody solutions for at least 24 hours each at 4°C. Mouse anti-neuroglian (BP104) antibody was used at 1:40 concentration (Hortsch et al., 1990). BP 104 anti-Neuroglian was deposited to the DSHB by Goodman, C. (DSHB Hybridoma Product BP 104 anti-Neuroglian). Rabbit polyclonal TfAP-2 antibody was used at 1:1000 concentration (Monge et al., 2001). Chicken GFP antibody was used 1:1000 (Life Technologies A10262). Sodium azide was used in antibody solutions at 0.02% final concentration. All secondary antibodies were used at a concentration of 1:500 (Jackson ImmunoResearch).

Mounting was performed in Vectashield (Vector laboratories, H-1000) on glass slides using polylysine-coated coverslips with double sided tape as spacers. Slides were sealed with nail polish.

Confocal microscopy

Images were collected on a Zeiss LSM 510 confocal microscope and processed using the Fiji distribution of ImageJ (https://fiji.sc/).

GO term enrichments

For GO term enrichments throughout the chapter, the analyses were performed using either DAVID (https://david.ncifcrf.gov/) or STRING (http://string-db.org/) with dm5 official gene symbols. The two programs produce nearly identical output in virtually all cases where they were compared. Unidentified gene names were replaced from FlyBase synonyms (flybase.org; Atrill et al., 2016).

Results

General patterns in combined lineage samples

I generated RNA-seq data for five samples that comprise many hemilineages to address questions of what happens to all lineages as they develop. These were: (1) combined A hemilineage immature neurons, (2) combined younger immature neurons, (3) combined older immature neurons, (4) combined mature larval neurons, and (5) combined immature neurons (both A and B hemilineages). Figure 3.1 shows a 3D Principal Component Analysis (PCA) of these combined lineage samples.

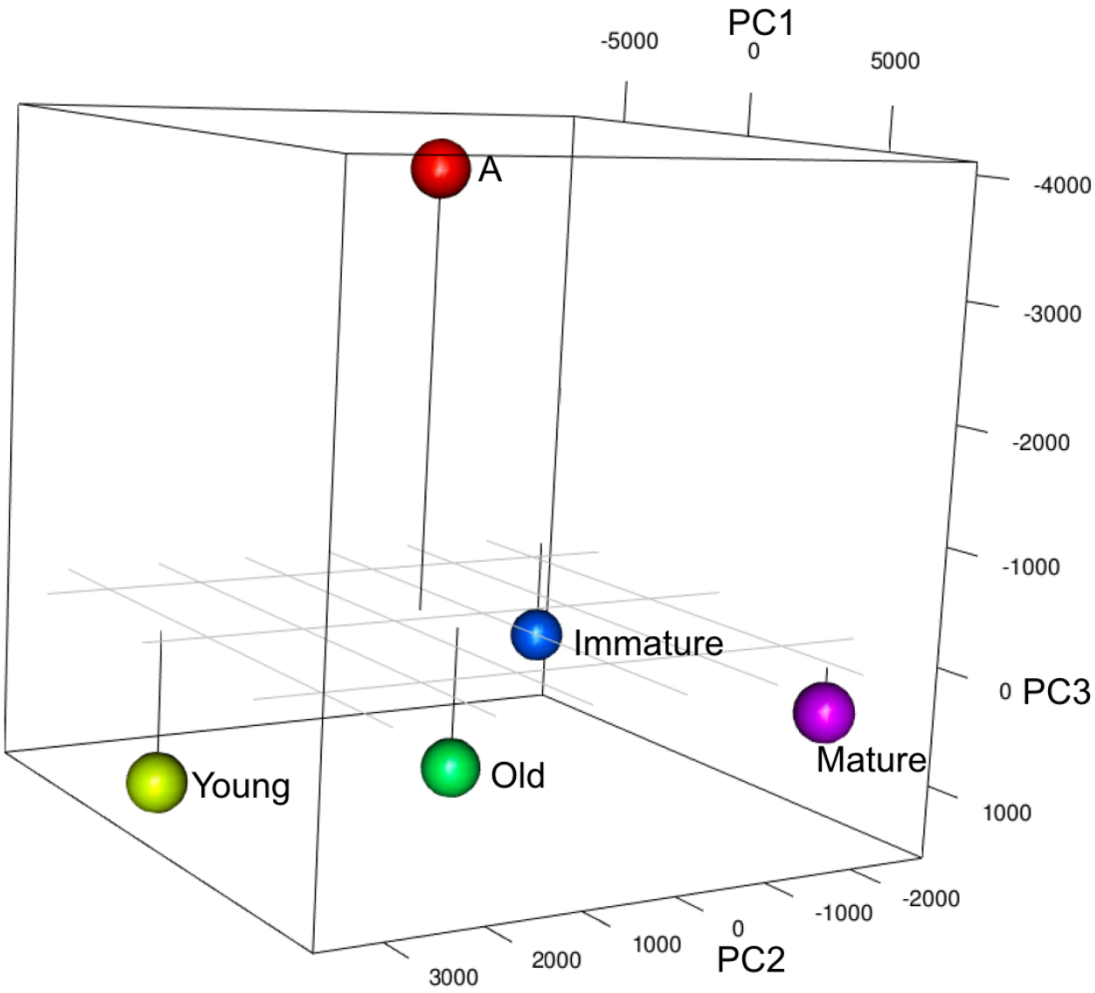

Figure 3.1 | 3D PCA of Combined lineage Samples. Expression values in FPKM for all genes were used to generate the PCA. Each sample has a unique color.

Immature neurons and mature neurons are at the two extreme ends of principal component one. These two samples are the most dissimilar. Immature A neurons, and

both older and younger immature neurons are between the immature neurons and mature neurons in the first principal component. Immature A neurons are closest in expression pattern to the older immature neurons in the first two principal components. The third principal component mainly separates the A hemilineage neurons from the other samples that contain both A and B hemilineage neurons.

The first three principal components describe 93% of the variance between the samples, with PC1 describing 65%, PC2 describing 15%, and PC3 describing 13% (Table 3.S17). The relative contribution of the top 20 positive contributions to each of these components as well as the top 20 negative contributions to each of these components is shown in Table 3.S18.

Comparison of mature versus immature neurons in the larval VNS

The VNS of the late last instar larva contains a set of embryonic-born, functional neurons that mediate larval behavior, and also clusters of arrested, immature adult-specific neurons that are typically generated during larval growth and then arrest after they have navigated to their initial targets, but before they start establishing terminal (axonal) or interstitial (dendritic) arbors.

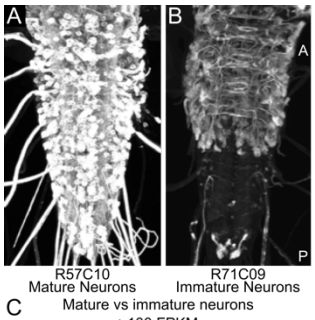

C

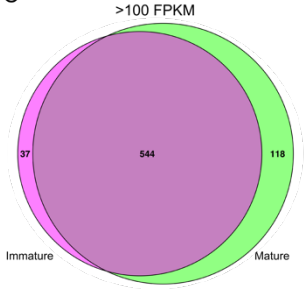

D

Top 20 genes by fold change
>100 FPKM, q<0.1

Mature neurons

	Immature	Mature	fold change
CG4577	8	172	22.6
TM45F	12	250	21.1
Pglym78	11	192	17.9
ia2	54	810	15.1
CG10186	7	109	14.6
CG14509	8	111	14.3
kcc	9	126	13.8
CG8861	11	142	13.6
Cbp53E	17	182	11.0
Sox14	22	246	10.9
Eip74EF	34	368	10.9
CG8216	12	103	8.5
CG31221	47	388	8.2
CG12858	13	106	7.9
Pal	67	491	7.3
zfh2	18	131	7.1
CG34360	28	193	7.0
Imp	17	113	6.7
vri	38	253	6.6
PyK	29	191	6.5

118 total

Top 10 GO terms by biological process and molecular function

Category	Term	Benjamini	Genes
			CG31030, VHA13, VHA26, VHA44, VHAPPA1-1, VHA55, ATPALPHA,
GO Biological Process	ATP hydrolysis coupled proton transport	3.55E-07	VHAM8.9, VHA68-1
GO Biological Process	glycolytic process	2.07E-07	ENO, PGLYM78, HEX-A, TPI, GAPDH2, PYK, GAPDH1, ALD
			SYT1, SYN, CANB, FRQ1, AP-2SIGMA, ENDOA, SYX1A, RAB3,
GO Biological Process	neurotransmitter secretion	1.02E-05	TOMOSYN, SNAP25
GO Biological Process	chemical synaptic transmission	7.15E-05	SYT1, KCC, ATPALPHA, FRQ1, SYX1A, SHI, SNAP25, SAP47
	proton-transporting ATPase activity,		
GO Molecular Function	rotational mechanism	1.97E-03	CG31030, VHA26, VHA44, VHAPPA1-1, VHA55, VHA68-1
	regulation of short-term neuronal		
GO Biological Process	synaptic plasticity	1.30E-03	SHI, RAB3, SNAP25, SAP47
GO Biological Process	response to mechanical stimulus	1.27E-03	RDL, KCC, TPI, ATPALPHA, GAD1
GO Biological Process	proton transport	6.92E-03	VHA13, VHA26, VHA44, VHA55, VHA68-1
GO Biological Process	olfactory learning	7.38E-03	SYN, KLG, FUTSCH, SHI, SRC64B, GAD1
	hydrolase activity, acting on acid		
	anhydrides, catalyzing transmembrane		
GO Molecular Function	movement of substances	1.37E-02	VHA13, VHA44, VHA55

Immature neurons

	Immature	Mature	fold change
pros	4419	324	13.6
pncr002:3R	135	17	7.9
CG2052	559	76	7.3
jim	1521	240	6.3
br	551	115	4.8
CG11030	247	61	4.1
nerfin-1	138	35	3.9
Nrt	221	68	3.2
cenG1A	119	37	3.2
chinmo	235	75	3.1
fne	797	267	3.0
stan	113	38	3.0
noe	8152	2834	2.9
pdm3	156	57	2.8
hdc	1088	394	2.8
Jupiter	820	298	2.8
chn	232	90	2.6
CG6854	193	76	2.5
jing	159	64	2.5
ppa	161	66	2.4

Category	Term	Benjamini	Genes
GO Biological Process	axon guidance	1.11E-06	BIF, SBB, PDM3, NERFIN-1, STAN, LOLA, JING, PROS, NRT, BRAT
	transcription factor activity, sequence-		L(3)NEO38, SBB, PDM3, BR, HTH, CHINMO, CHN, LOLA, JING, PROS,
GO Molecular Function	specific DNA binding	1.22E-06	JIM, ANTP
			L(3)NEO38, SBB, DATI, BR, NERFIN-1, CENG1A, CHINMO, JIM,
GO Molecular Function	metal ion binding	4.51E-06	CG12071, JUPITER, CHN, LOLA, JING
GO Biological Process	dendrite morphogenesis	1.59E-04	BR, NERFIN-1, CHINMO, STAN, CHN, LOLA, PROS, JIM
			L(3)NEO38, CG12071, DATI, JUPITER, NERFIN-1, HANG, CHN, JING,
GO Molecular Function	nucleic acid binding	4.36E-04	JIM
GO Biological Process	axonogenesis	3.37E-03	PDM3, STAN, LOLA, PROS, NRT
	imaginal disc-derived wing		
GO Biological Process	morphogenesis	2.90E-03	BIF, L(3)NEO38, SBB, HDC, HTH, CHINMO, JING
	positive regulation of transcription from		
GO Biological Process	RNA polymerase II promoter	3.20E-03	BR, HTH, CHN, JING, PROS, ANTP, TET
	regulation of transcription from RNA		
GO Biological Process	polymerase II promoter	1.72E-02	BR, HTH, NERFIN-1, CHINMO, LOLA, ANTP
GO Biological Process	transcription, DNA-templated	3.31E-02	L(3)NEO38, PDM3, CHN, LOLA, JING, PROS, SU(W[A])

Figure 3.2 | Comparison of expression in mature neurons and immature neurons in wandering third instar larval VNS. (A): GAL4 driver expression (R57C10-GAL4>UAS-GFP) in the VNS to label for mature neurons. (B): GAL4 driver expression (R71C09-GAL4>UAS-GFP) in the VNS to label arrested immature neurons. (C): Venn diagram of expression over 100 FPKM for immature and mature neurons. 78% of the expressed genes are common expression. (D): Top 20 genes by fold change for both mature and immature neurons. Only genes >100 FPKM, >2-fold change, and with a q-value < 0.1 for the fold change were considered. Top 10 GO term

enrichments for both GO biological process and GO molecular function. Venn diagram overlap is for genes for which there is less than a 2-fold difference in the two samples.

The R57C10 enhancer is associated with the gene for neuronal synaptobrevin (nSyb), which is part of synaptic vesicles found in functioning neurons, and its driver line was used to label mature neurons (Figure 3.2A). By contrast, the R71C09-GAL4 line is expressed only in the arrested clusters of immature neurons, but not the associated NB and GMCs (Figure 3.2B). It was used to label the clusters of arrested, immature neurons in wandering larvae, just before the start of metamorphosis.

As seen in Figure 3.2C, there were 699 genes that were highly expressed in the two cell types, using expression at a level >100 FPKM as a criterion. The expression values of all highly expressed genes enriched in immature neurons relative to mature neurons are shown in Table 3.S12. The expression values of all highly expressed genes enriched in mature neurons relative to immature neurons are shown in Table 3.S13. 78% of the highly expressed genes were found in both the mature and the immature neuron sets. These commonly expressed genes (Table 3.S14) were highly enriched in categories of genes that are involved in many different "housekeeping" processes. 879 terms were enriched for these commonly expressed genes by GO biological process, GO molecular function, GO cellular component, KEGG pathway, and InterPro protein domain. This table was not included due to its large size. Many of these terms are for ribosomes and ribosomal subunits. Many terms are also for metabolic processes and cytoskeletal components. Many pathways are enriched, including Wnt signaling, Hippo signaling, Hedgehog signaling, TGF-beta signaling, etc. Some enriched terms were also specific to neurons.

In general, the genes that were enriched in the two classes of neurons are ones that would be expected in immature versus mature neurons (Figure 3.2D). Using Gene Ontology (GO) categories, expression in mature neurons was dominated by genes associated with neuronal transmission in GO categories including neurotransmitter secretion and chemical synaptic transmission. These include genes involved in recharging synaptic vesicles with neurotransmitters: ATP hydrolysis coupled proton transport, glycolytic process, proton-transporting ATPase activity, rotational mechanism, proton transport, and hydrolase activity (Figure 3.2). Loading synaptic

vesicles with neurotransmitters typically involves H+ ion gradients and proton co-transporters. This requires acidification of vesicles by vacuolar H+ ATPases, which have many subunits encoded in the genome. For example, *Vacuolar H+ ATPase 100kD subunit 1* (Vha100-1) is required for synaptic vesicle exocytosis and removal of this gene results in nearly complete loss of neurotransmission (Hiesinger et al., 2005).

Genes known to be involved in development and transcription factors are the most enriched classes in immature neurons relative to mature neurons. These categories include genes needed for pathfinding and neurite growth, such as those involved in axon guidance, axonogenesis, and dendrite morphogenesis. The other general group of enriched terms is for transcription factors. These include transcription factor activity, and other terms that can be collectively considered transcriptional regulation (Figure 3.2). C2H2 Zinc finger TFs make up 15 of the 73 genes that are enriched in immature neurons over mature neurons when these datasets are compared at a 2-fold enrichment, >10 FPKM, $q<0.1$, making them a significantly enriched gene class relative to the genome (FDR 9.81E-09).

Both Chronologically inappropriate morphogenesis (*chinmo*; Zhu et al., 2006) and broad are expressed highly in immature neurons. Chinmo and broad are markers of neuronal birth order. During postembryonic neuroblast divisions, there is a shift from neuroblasts generating Chinmo-positive neurons to Broad-positive neurons (Maurange, Cheng, and Gould, 2008). Expression of both genes is known to be lost as they begin to mature.

Many genes associated with roles in neuronal transmission and the formation and remodeling of axons and dendrites are enriched in mature neurons. Kazachoc (*kcc*) is a K^+/Cl^- co-transporter that appears to be necessary for proper intracellular Cl^- gradient maintenance for GABAergic inhibition of neuronal activity (Hekmat-Scafe et al., 2010). Hig-anchoring scaffold protein (*Hasp*, CG10186) is a secreted protein accumulated in the extracellular matrix of the synaptic cleft of acetylcholinergic neurons required for nAChR accumulation (Nakayama et al., 2016). Calbindin 53E (*Cbp53E*) is a 6 EF-hand domain containing protein that likely acts as a calcium buffer and calcium sensor. Loss of Cbp53E causes overgrowth of axonal branches

(Hagel, Beriont, and Tessier, 2015). Zn finger homeodomain 2 (*zfh2*) is a TF that is expressed in the late embryonic CNS and is suspected to be involved in neurogenesis (Lai, Fortini, and Rubin, 1991). It is required for cell fate specification of Capaergic neurons in the abdominal segments (Gabilondo et al., 2011).

Some genes enriched in mature neurons are involved in the response to ecdysone signaling. Eip74EF is a TF that responds to ecdysone concentration (Thummel, Burtis, and Hogness, 1990; Burtis et al, 1990). Sox box protein 14 (*Sox14*) is a TF required for expression of ecdysone-regulated genes during metamorphosis (Ritter and Beckstead, 2010). *Sox14* is also required for dendrite pruning in response to ecdysone signaling (Kirilly et al., 2009; Loncle and Williams, 2012; Wong et al., 2013).

Two recently named genes from a screen for thermal nociception are enriched in mature neurons: space blanket (*spab*, CG8216) and jet fuel (*jef*, CG12858). *Spab* loss of function causes heat insensitivity while *jef* loss of function causes heat hypersensitivity (Honjo et al., 2016). Some genes enriched in mature neurons appear to be involved in metabolism, such as phosphoglyceromutase (*Pglym78*) and pyruvate kinase (*Pyk*). IA-2 protein tyrosine phosphatase (*IA-2*) *IA-2* protein is related to transmembrane protein tyrosine phosphatase, but lacks phosphatase activity (Cai et al., 2001). The function of this and similar 'pseudophosphatases' is currently unknown (Hatzihristidis et al., 2015). Several enriched genes in mature neurons have unknown function and could prove to be good targets for future study of neuronal maturation: CG4577, CG8861, and CG31221 are among the top 20 by fold change.

Transmembrane 4 superfamily (*TM4SF*) is expressed at very high levels in mature neurons relative to immature neurons. *TM4SF* is the founding member of the tetraspanin family, which, as their name implies, are a family of proteins with four transmembrane domains. They are found in all multicellular eukaryotes and have many different roles in cellular biology (Huang et al., 2005). Each tetraspanin interacts with different proteins, including other tetraspanins (Reviewed in Hemler, 2005). It is also expressed at much higher levels in older immature neurons relative to younger immature neurons (Figure 3.3). It seems that expression of this tetraspanin is associated with neuronal maturation.

Although the enrichment of transcripts in the two groups would generally be considered to distinguish genes that were characteristic of mature versus immature neurons, this may not be that case on all samples. For example, the mature neurons are highly enriched for the RNA-binding protein *Imp*, while the immature neurons have low levels of this RNA but are enriched for *Syp*. As recently shown by Liu et al., 2015 these two proteins are reciprocally expressed in new-born neurons, with *Imp* expression dominating early in a lineage while *Syp* eventually dominates late. As shown below, the *Imp*/*Syp* expression is related to the time when the cell was born, rather than to whether the cell is mature or immature.

Comparison of young and old cells in the clusters of postembryonic neurons.

In the VNS, neurogenesis resumes during the late first instar and continues until the start of metamorphosis. Consequently, at the end of larval growth each NB is associated with an elongated cluster of about a hundred cells with the NB, GMC's, and recently-born daughter neurons at the apical tip of the cluster and the oldest neurons situated at the base, closest to neuropil. The oldest cells have arrived at an initial target and are arrested prior sprouting terminal or interstitial arbors, whereas the younger cells are involved with fate determination, survival and navigating their axon to their initial target. The GAL4 lines R31H08 and R81C10 express in these groups of old and young postembryonic neurons, respectively (Figure 3.3A; Figure 3.3B; Li et al., 2014; Fig 1A, B) and have been used to examine the patterns of gene expression in these two sets of cells.

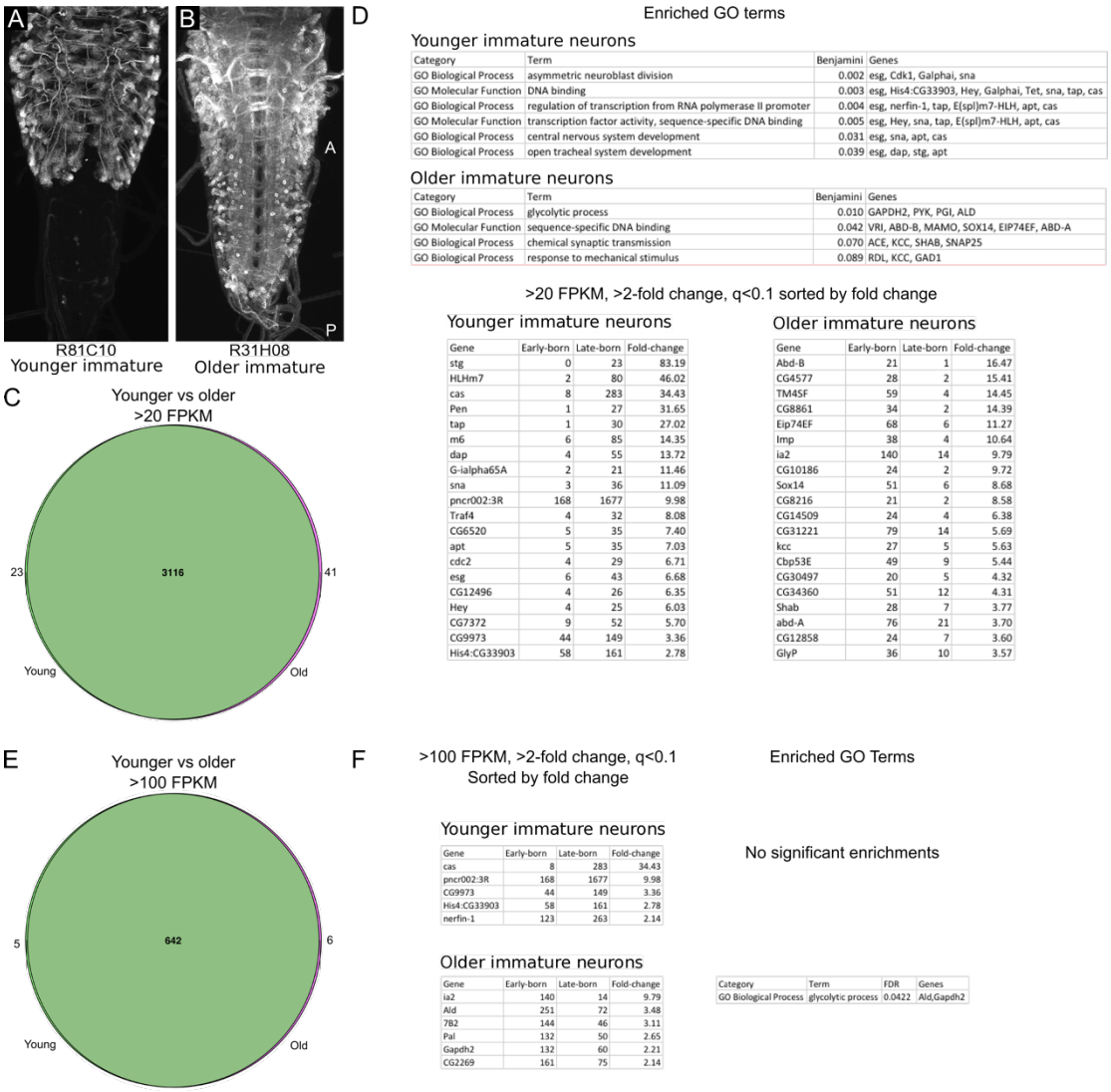

Figure 3.3 | Comparison of expression in older immature neurons and younger immature neurons in wandering third instar larval VNS. (A) GAL4 driver expression (R81C10-GAL4>UAS-GFP) labels young immature neurons in the VNS, and (B) R31H08-GAL4>UAS-GFP labels the older immature neurons. CNSs imaged by FlyLight, HHMI JRC. (C): Venn diagram of expression >100 FPKM for older and younger immature neurons. (D): Top 20 genes by fold change for both older and younger immature neurons. Only genes >20 FPKM, >2-fold change, and with a q-value < 0.1 for the fold change were considered. Significant (q<0.1) GO term enrichments for both GO biological process and GO molecular function. (E): Venn diagram of expression >20 FPKM for older and younger immature neurons. (F): Genes >100 FPKM, >2-fold change, and with a q-value < 0.1 for the fold change. Significant (q<0.1) GO term enrichments for both GO biological process and GO molecular function. Venn diagram overlap is for genes for which there is less than a 2-fold difference in the two samples.

The R81C10-based sample of young immature neurons also potentially includes the NB and the GMC's. Although the R81C10 sample expresses in NBs and GMCs, these cells account for a small percentage of the total cell number and genes that are markers for NBs are not expressed at high levels. For example, *Deadpan*, a gene that is characteristic of NBs, was found at extremely low levels in all samples (3 FPKM in the younger neuron data). Additionally, size selection during FACS purification of

the cells did not favor the recovery of a cell as large as the NB, since size gating was used to remove anything that appeared larger than a single neuron. Consequently, we assume that most of the expression pattern observed from this sample is from the young neurons and possibly GMCs, but not from the NBs.

As seen in Figure 3.3E the samples of young and old immature neurons showed 809 highly expressed genes (defined as >100 FPKM) but only 11 of these were differentially expressed based on a >2 fold difference as a threshold. For the much larger number of moderately expressed genes (> 20 FPKM) there was still only about 1.5% of the genes that were differentially expressed between the two samples (Figure 3.3D). The expression values of the highly expressed genes in both younger immature and older immature neurons are shown in Table 3.S15.

There are a number of interesting genes that are enriched in the collection of young immature neurons. *Hairy/E(spl)-related with YRPW motif* (*Hey*) and *Enhancer of split m7, helix-loop-helix* (*E(spl)m7-HLH*) are both downstream targets of the *Notch* signaling pathway (Knust, Tietze, and Campos-Ortega, 1987; Bailey and Posakony, 1995; Kokubo, Lun, and Johnson, 1999; Monastirioti et al., 2010) and *Notch* is involved in establishing the "A" versus the "B" fate in the daughter neurons that arise from the division of the GMC (Skeath and Doe, 1998; Buescher et al., 1998). Other genes that are associated with asymmetric neuroblast division and CNS development are also enriched in the young immature neurons (Figure 3.3D). Programmed cell death is a prominent feature in some of the clusters since about a third of the neurons that are born die prior to extending their initial axon (Truman et al., 2010). Interestingly, the pro-apoptotic gene *Grim* is expressed in younger neurons at higher levels than older neurons. *Grim* induces apoptosis in the immature neurons of the CNS during metamorphosis (Chen et al., 1996; Kumar, Bello, Reichert 2009). Thus, it is likely involved in killing the sibling neurons that do not survive in the monotypic lineages.

Transcription factors are a significantly enriched class of genes in the young immature neurons relative to the old immature neurons (Figure 3.3D). These transcription factors appear to be involved in axon guidance and neurite development or commitment of cell fate after stem cell division. *Castor* (*cas*) and *apontic* (*apt*) are

transcription factors that are involved in cell fate specification and neuronal differentiation (Mellerick et al., 1992; Gellon et al., 1997; Su et al., 1999). *Target of Poxn* (*Tap*) is a transcription factor that is implicated in negative regulation of axon extension involved in axon guidance in the developing mushroom body by tap inhibiting excessive axonal growth through regulation of the levels of the planar cell polarity non-canonical *Wnt* signaling protein *Dishevelled* (Yuan et al., 2016). *Escargot* (*esg*) is involved in neuroblast differentiation and stem cell maintenance (Whiteley et al., 1992; Ashraf et al., 1999). *Snail* (*sna*) contributes to many developmental processes including asymmetric cell division and neurogenesis (Nusslein-Volhard, Wieschaus, and Kluding, 1984; Ashraf et al., 1999; Ashraf and Ip, 2001). *Sna*, *esg*, and *wor* are all expressed at higher levels in younger neurons and together constitute the Snail family of transcription factors that work antagonistically with Notch to regulate neural commitment (Ramat et al., 2016). Sna, esg, and wor are necessary for asymmetric cell division in neuroblasts, ensuring the proper segregation of cell fate determinants to the NB and GMC (Ashraf and Ip, 2001; Cai, Chia, and Yang, 2001). These genes are critical for proper neurogenesis, with mutations for these genes producing incompletely developed embryonic CNSs (Ashraf et al., 1999; Ashraf and Ip, 2001; Cai, Chia, and Yang, 2001). *Nervous fingers 1* (*nerfin-1*) is involved in axon guidance, dendrite morphogenesis, and neuron development by controlling expression of *robo2*, *wnt5*, *derailed*, and other genes required for early axon guidance decisions (Kuzin et al., 2005; Parrish et al., 2006).

Genes enriched in older neurons relative to younger neurons include *Synaptosomal-associated protein 25kDa* (*Snap25*), *Acetylcholine esterase* (*Ace*), *Shaker cognate b* (*Shab*), and *kazachoc* (*kcc*), which are associated with "chemical synaptic transmission" (Figure 3.3D), suggesting that the immature neurons express more genes involved in synaptic transmission as they begin to mature. *Snap25* is necessary for synaptic transmission. It is a component of SNARE protein complexes involved in neurotransmitter release (Oyler et al., 1989; Söllner et al., 1993). *Ace* is a gene for an enzyme responsible for degrading acetylcholine, and its protein is localized on the membrane of the post-synaptic neuron at the synapse. *Shab* is a subunit of a K^+ channel that regulates neurotransmitter release and neuron excitability (Littleton and Ganetzky, 2000; Vähäsöyrinki et al., 2006). *kcc* is a K^+/Cl^- co-transporter that appears

to be necessary for proper intracellular Cl^- gradient maintenance for GABAergic inhibition of neuronal activity (Hekmat-Scafe et al., 2010).

Two other genes enriched in older neurons, *CG14762* and *Down syndrome cell adhesion molecule 2* (*Dscam2*), are included in the neuron projection morphogenesis GO category. Especially interesting is Dscam2 which is extensively alternatively spliced to mediate homophilic binding of proteins between two neurons for synaptic partner recognition (Yamakawa et al., 1998; Graveley et al., 2004; Schmucker et al., 2000).

Abdominal A (Abd-A) and abdominal-B (Abd-B) are two bithorax complex genes with higher levels of expression in old immature neurons. These transcription factors are used to specify the developmental fate of abdominal segments in the embryo, but appear to be reused by late-stage neural progenitors to time abdominal segment neuroblasts to undergo apoptosis in the case of abd-A (Bello et al., 2003; Cenci and Gould, 2005) and postmitotically to specify neuronal fate in the case of abd-B (Miguel-Aliaga et al., 2008). Expression in the older immature larval neurons of these two transcription factors is likely from the abdominal segments of the VNS, since abd-A and abd-B should not have appreciable expression in the thoracic segments segments and because of differences in timing of birth of immature neurons in these two regions, the older immature neuron sample includes abdominal neurons whereas the younger cell line does not (Figure 3.3A,B). Virtually all of the younger neurons originate from the thoracic segments, due at least in part to abd-A induced neuroblast apoptosis in the abdominal segments (Bello et al., 2003; Cenci and Gould, 2005). R31H08 has substantial abdominal expression, but these abdominal clusters are not evident in the R81C10 sample, most likely because these abdominal lineages stop dividing much earlier. Ubx, the third and final bithorax complex gene is expressed at similar levels in older and younger immature neurons and provides spatial identity to hemilineages that is dependent on the segment and the hemilineage (Marin, et al. 2012).

Differences between the A and B hemilineages

The selection of the "A" versus the "B" fate by the daughter cells from a GMC division is caused by differential Notch signaling from asymmetric inheritance of Numb protein, which suppresses Notch activity (Skeath and Doe, 1998; Buescher et al., 1998.; Truman et al., 2010). Over all of the lineages, there is no consistent phenotype that invariably corresponds to the A or B fate. For the postembryonic lineages survival or death is not associated with either fate, nor is the selection of neurotransmitter. There is a weak bias, though, for the A daughter to be a local interneuron while the B daughter is a projection cell (Truman et al., 2010). Also, all of the postembryonic-born motoneurons come from the B hemilineages (Truman et al., 2010). I used RNA-seq to examine if there were transcripts that might be characteristic of immature A hemilineage neurons. The R12A07-GAL4 line is based on the *Hey* enhancer and labels the immature A neurons in all of the thoracic lineages, while the R71C09-GAL4 line was used to label both the A and the B neurons in these lineages. The R12A07 expression pattern also includes some mature neurons. I found no enhancer that was selective for just the B hemilineages.

As seen in Figure 3.4C, the immature neuron and immature A neuron datasets are extremely similar at all FPKM thresholds. The expression values for common highly expressed genes between the two samples is shown in Table 3.S16. For differentially expressed genes, only some ribosomal subunits in immature neurons are statistically significant as a class. There are four ribosomal genes enriched in immature neurons relative to immature A neurons, suggesting that these ribosomal genes are expressed at higher levels in B-hemilineage neurons than in A-hemilineage neurons. These ribosomal subunits may be important for transcribing genes that are expressed in greater amounts in B-hemilineage neurons. These ribosomal genes are expressed at similar levels in immature neurons, mature neurons, older immature neurons, and younger immature neurons, suggesting that the difference is due to the hemilineage *Notch* activity.

Interestingly, genes that are known to be directly downstream of *Notch* expression, such as *Hey*, did not appear in the A hemilineage sample, although they are present in the sample of young immature neurons, which also includes the GMCs. Likely, these genes are only expressed transiently and I think that they may already be turned off by the time that cells in the R12A07 line begin expressing GFP.

Some genes implicated in post-embryonic development (mostly TFs) are expressed at higher levels in the entire pool of immature neurons relative to the hemilineage A immature cells. These genes may be repressed by *Notch* signaling.

IA-2 protein tyrosine phosphatase (*IA-2*) and Vesicular glutamate transporter (*VGlut*) are the only highly expressed (>100 FPKM) genes that are enriched in immature A neurons relative to immature neurons. IA-2 protein is related to transmembrane protein tyrosine phosphatase, but lacks phosphatase activity (Cai et al., 2001). The function of this and similar 'pseudophosphatases' is currently unknown (Hatzihristidis et al., 2015).

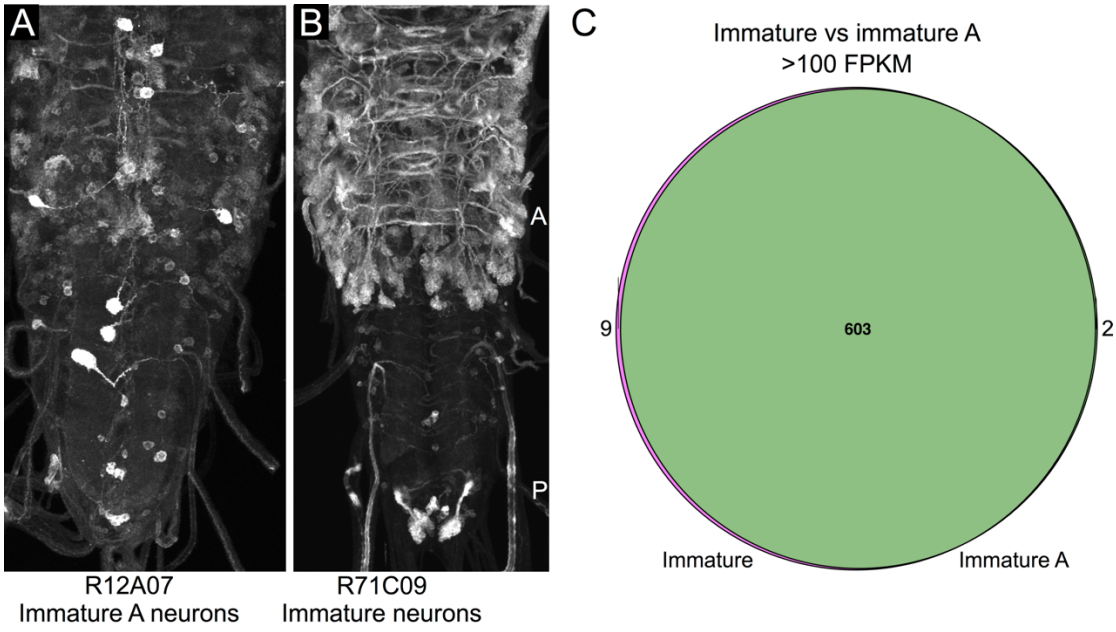

D

Enriched GO terms

Immature A neurons

Category	Term	Benjamini	Genes
GO Biological Process	Cytoplasmic translation	7.99E-04	RPL18, RPS26, RPL23A, RPS8
GO Molecular Function	Structural constituent of ribosome	9.85E-03	RPL18, RPS26, RPL23A, RPS8
GO Biological Process	Translation	9.32E-02	RPL18, RPS26, RPL23A, RPS8

No enriched terms for Immature neurons

>100 FPKM, >2-fold change, q<0.1 sorted by fold change

Immature neurons

	Immature	Immature A	fold change
CG2083	251	107	2.3
CG2865	160	45	3.5
Jupiter	820	361	2.3
RpL18	606	263	2.3
RpL23A	864	394	2.2
RpS26	853	420	2.0
RpS8	949	329	2.9
jing	159	71	2.3
noe	8152	2953	2.8

Immature A neurons

	Immature A	Immature	fold change
VGlut	110	42	2.6
ia2	159	54	3.0

Figure 3.4 | Comparison of combined immature A neurons with all immature neurons. (A): R12A07 was used to label immature A neurons. (B): R71C09 was used to label immature neurons of both the A and B hemilineages. CNSs imaged by FlyLight, HHMI JRC. (C): Extremely few genes are differentially expressed between immature neurons and immature A neurons. (D): Only GO terms associated with four ribosomal subunits enriched in immature neurons were statistically significant. The 9 genes with enriched expression in immature neurons and the 2 genes with enriched expression in immature A neurons are shown. Venn diagram overlap is for genes for which there is less than a 2-fold difference in the two samples.

General patterns in individual hemilineages

Figure 3.6 shows the relationship of 10 individual hemilineages to one another based on PCA. The A hemilineages occupy a larger area of the 2D and 3D PCA than B hemilineages, suggesting a greater transcriptional diversity in A hemilineages than B

hemilineages, although this may be an artifact of sampling only 10 of the 33 thoracic hemilineages.

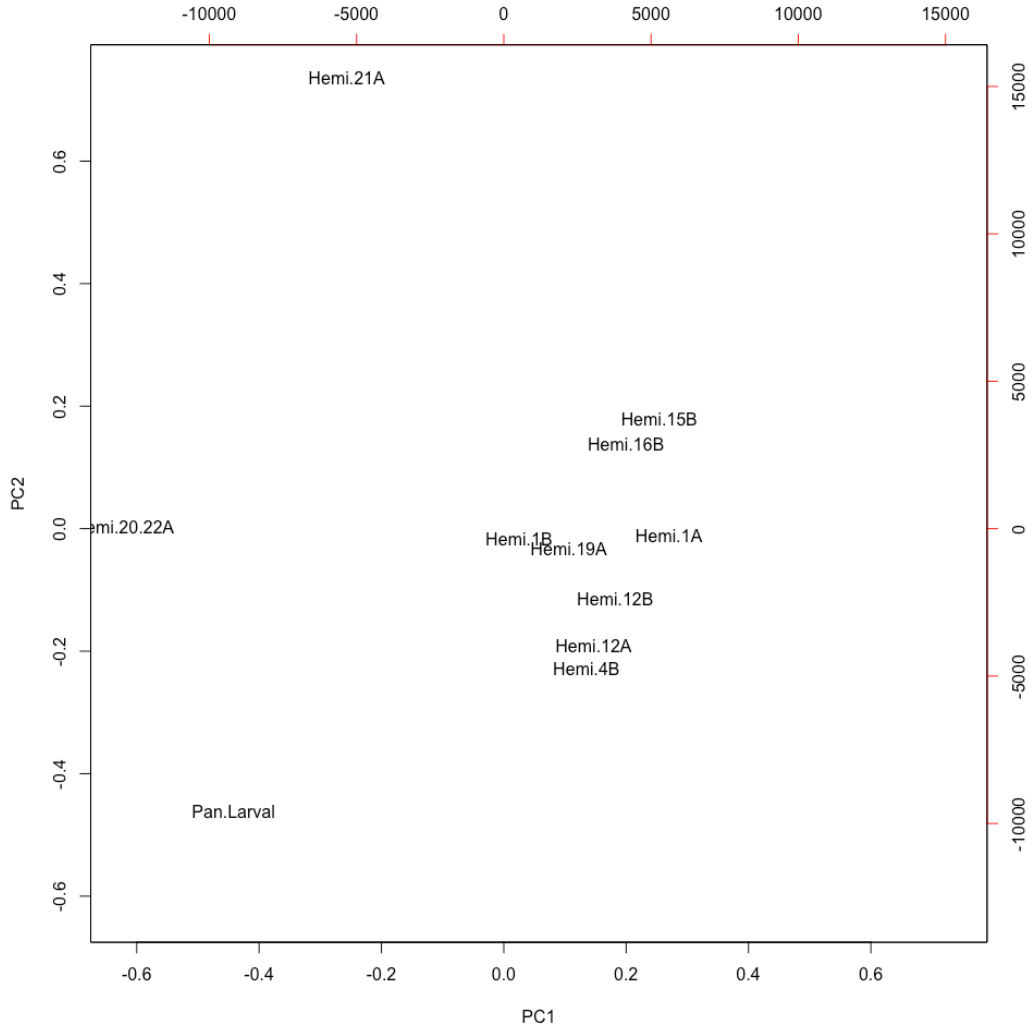

Figure 3.5 | 2D PCA of Hemilineages and Combined Immature Sample. Expression values in FPKM for all genes were used to generate the PCA.

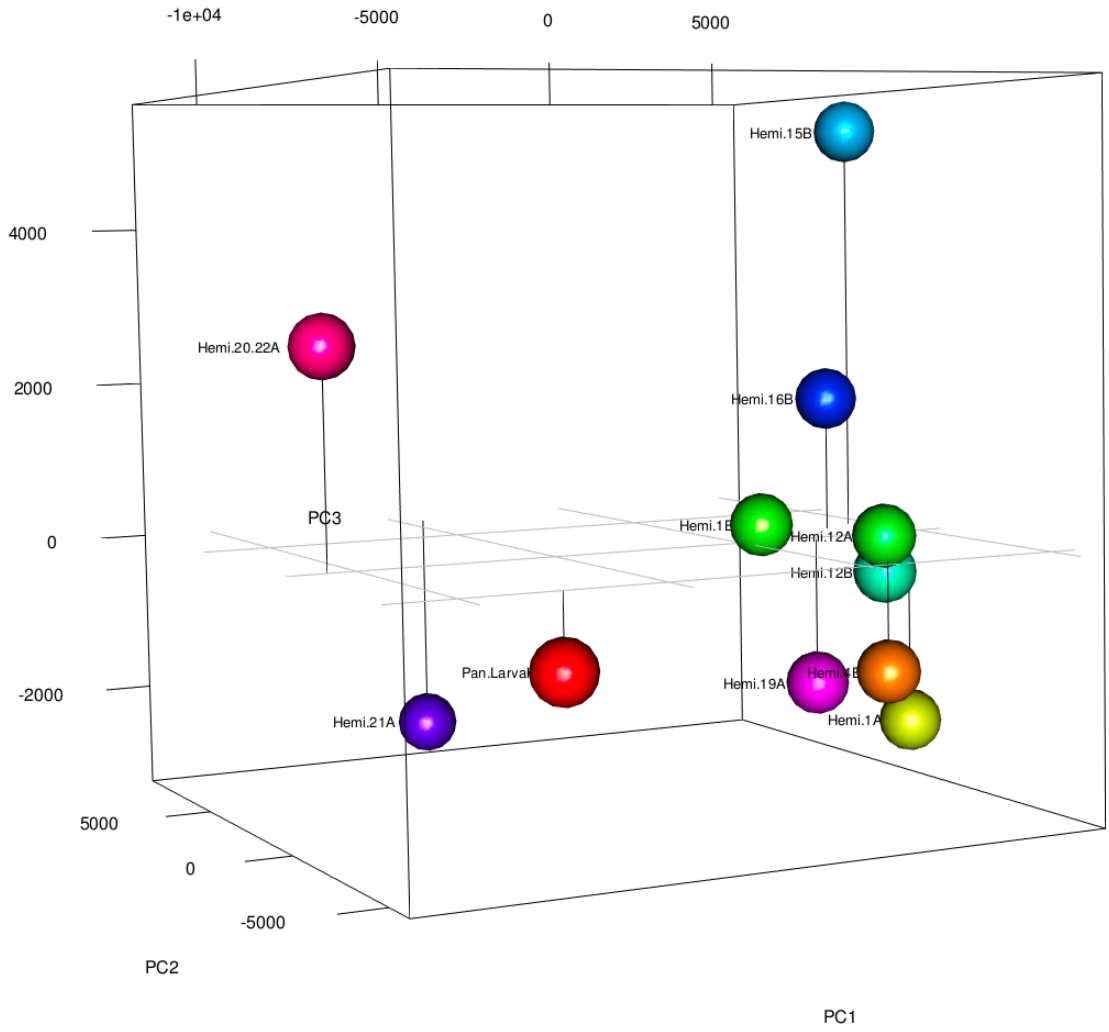

Figure 3.6 | 3D PCA of hemilineages and combined immature neurons sample. Expression values in FPKM for all genes were used to generate the PCA. Each sample has a unique color.

50% of the variance between the hemilineages is accounted for by PC1 (Table 3.S19). The relative contribution of the top 20 positive contributions to each of these components as well as the top 20 negative contributions to each of these components is shown in Table 3.S20. The top 20 positive contributions to PC1 of the hemilineage PCA shows gene set enrichment for genes involved in nervous system development, neuron differentiation, and neurogenesis (Table 3.S21). Hemilineages 20/22A and 21A are outliers relative to the other hemilineages assayed with RNA-seq with respect to their position in PCA (Figure 3.5).

Transcriptional diversity in the immature hemilineages

Each hemilineage has a unique signature of gene expression that is different from other hemilineages. 1A, 1B, 12A, and 12B hemilineage neurons were assayed with

RNA-seq in order to directly compare the contributions of lineage and Notch activity to the genes expressed in the hemilineages.

Based on PCA comparison of all gene expression (Figure 3.1), hemilineages 12A and 12B are more similar to one another than 1A and 1B are to one another. Nonetheless, there are still many genes with common expression in both 1A and 1B hemilineages. By contrast, a comparison of the highly expressed genes (>100 FPKM) in hemilineage 1A, 1B, 12A, and 12B shows little or no relationship between lineage or Notch activity and the percentage of highly expressed genes that are shared in common (Figure 3.7E). Common highly expressed genes in 12A and 12B account for 79% of the highly expressed genes in both samples. Common highly expressed genes in 1A and 1B account for approximately 70% of the highly expressed genes in both samples. Notch activity does not drastically affect the percentage of common highly expressed genes. 71% of genes were common between 12A and 1A and 79% of genes were common between 12B and 1B, while 79% of highly expressed genes were common 12A and 1B and 71% were highly expressed between 12B and 1A. Since the percentage of common highly expressed genes is affected neither by lineage nor *Notch* activity, then it appears that hemilineages have been free to evolve independently of one another.

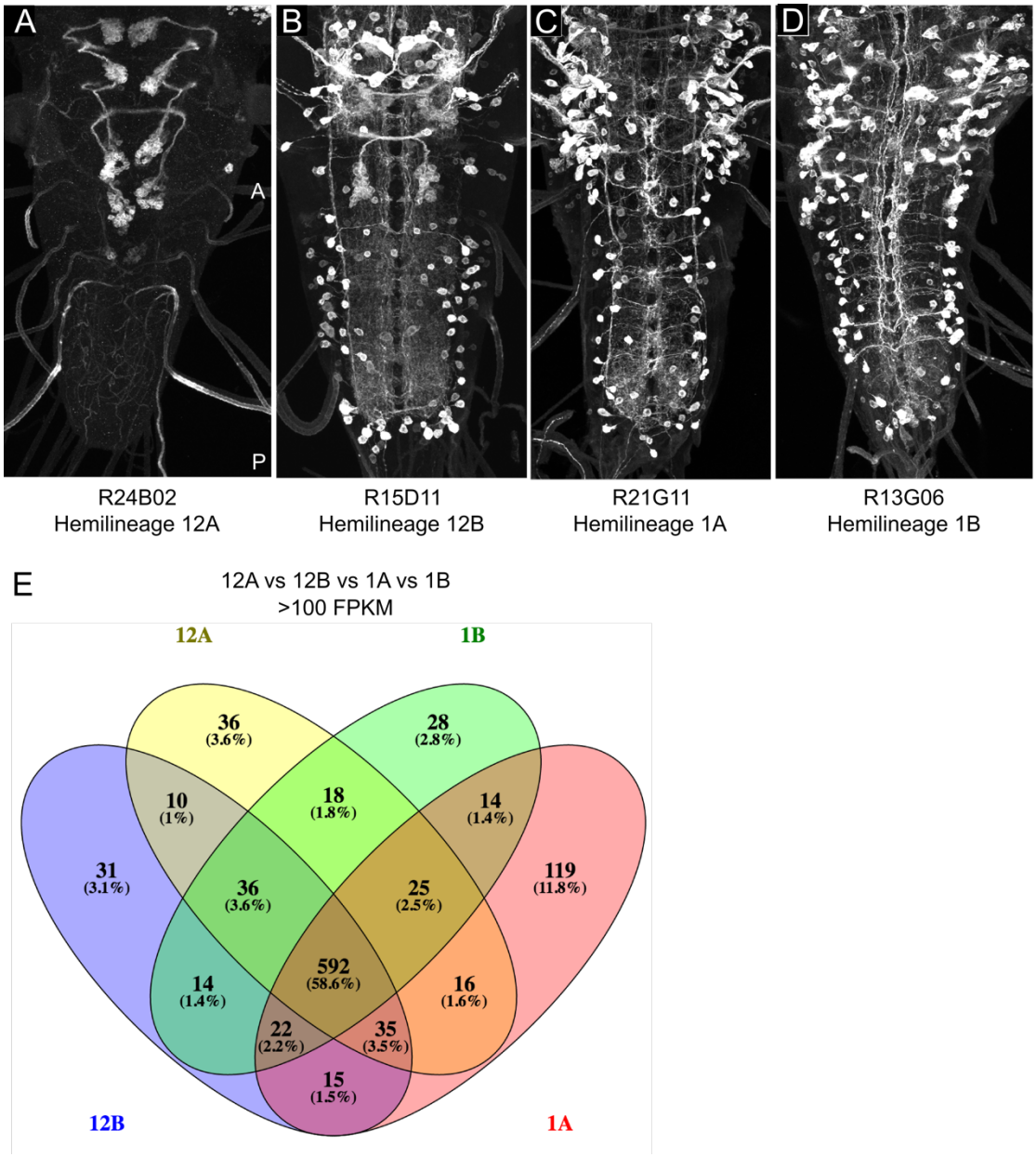

Figure 3.7 | Comparison of expression patterns in the selected hemilineage pairs from the same NB. (A-D): GAL4 lines that provided the basis for collecting neurons that arose in a single hemilineage of immature neurons. These VNS were imaged by FlyLight, JRC (Li et al., 2014) and represent the patterns before R57C10-GAL80 was included in each line to remove mature neuron expression, leaving only the arrested, immature neurons. Target hemilineages were (A): hemilineage 12A, (B): hemilineage 12B, (C): hemilineage 1A; (D): hemilineage 1B . Yellow arrowheads show the segmentally repeating cell clusters. (E): 59% of the highly expressed genes (>100 FPKM) were expressed in common by all four hemilineages. For the two sets of A-B pairs, the neurons from a given hemilineage shares no more genes with its sister hemilineage than it does to a hemilineage from a different NB.

Highly enriched gene expression in individual hemilineages

TFs were the class of genes with the most differential expression between hemilineages (Table 3.S31) and they account for a disproportionate percentage of

highly enriched genes unique to each hemilineage. TFs account for 58% of highly expressed genes (>100) expressed 5-fold relative to other hemilineages and combined immature neurons (Table 3.2) and 33% of moderately expressed genes (>40 FPKM) (Table 3.3). Both of these percentages represent substantial enrichment relative to the genes in the genome, 5% of which represent putative TFs (FlyTF.org).

Gene	Hemilineage	Function
CG32105	1A	TF (Hox)
Ets21C	1A	TF
His2A:CG33814	1A	histone
Ptx1	1A	TF
Vmat	1A	vesicular monamine transporter
nAcRbeta-21C	1A	acetylcholine receptor
opa	1A	TF
ap	4B	TF (Hox)
exex	4B	TF (Hox)
fkh	4B	TF
oc	4B	TF (Hox)
TfAP-2	12A	TF
pb	12B	TF
trh	12B	TF (bHLH-PAS)
CG12842	16B	unknown
beag	16B	mRNA splicing / synaptic transmission
CG34231	16B	nucleotide binding
lbl	19A	TF (Hox)
vg	19A	Transcriptional activator
CG17807	21A	tRNA (uracil) methyltransferase activity
CG8507	21A	unknown / microtubules / endoplasmic reticulum
Rcd4	21A	centriole replication / perception of pain
ey	21A	TF (Hox)
tj	21A	TF

Table 3.2 | Highly enriched genes unique to each hemilineage. 5-fold relative to other hemilineages and combined immature neurons. >100 FPKM. 14/24 (58%) genes were TFs, compared to 5% in the genome (FlyTF.org). Function was manually annotated based on summarized data at flybase.org.

Gene	Hemilineage	Function
CG13330	1A	unknown
CG15308	1A	unknown
CG32105	1A	TF (Hox)
CG33233	1A	transmembrane sugar transporter
CG9272	1A	Endonuclease
Cpr78Ca	1A	cuticular protein
Ets21C	1A	TF
His2A:CG33814	1A	histone
Ptx1	1A	TF
Vmat	1A	vesicular monamine transporter
nAcRbeta-21C	1A	acetylcholine receptor
opa	1A	TF
Hr51	1B	TF
ap	4B	TF (Hox)
exex	4B	TF (Hox)

Gene	Hemilineage	Function
fkh	4B	TF
oc	4B	TF (Hox)
TfAP-2	12A	TF
CG32052	12B	hydrolase
Ilp1	12B	neuropeptide
pb	12B	TF
trh	12B	TF (bHLH-PAS)
AnnIX	15B	annexin
CG12842	16B	unknown
beag	16B	mRNA splicing / synaptic transmission
CG34231	16B	nucleotide binding
CG16989	19A	unknown
lbl	19A	TF (Hox)
vg	19A	Transcriptional activator
CG14543	21A	pre-rRNA-processing / neurogenesis
CG15478	21A	unknown
CG17807	21A	tRNA (uracil) methyltransferase activity
CG31948	21A	ubiquitin domain
CG32267	21A	unknown
CG3546	21A	unknown
CG4709	21A	zinc finger DNA-binding / sleep
CG5245	21A	DNA-binding C2H2 zinc finger protein
CG8021	21A	protein and mRNA binding
CG8507	21A	unknown / microtubules / endoplasmic reticulum
Fdxh	21A	positive regulation, ecdysteroid biosynthesis / iron-sulfur binding
Mst84Dc	21A	spermatogenesis
PGRP-LE	21A	peptidoglycan binding
Prosalpha1	21A	endopeptidase / proteasome complex
Rcd4	21A	centriole replication / perception of pain
ey	21A	TF (Hox)
tj	21A	TF

Table 3.3 | Highly enriched genes unique to each hemilineage. 5-fold relative to other hemilineages and combined immature neurons. >40 FPKM. 15/46 (33%) genes were TFs, compared to 5% in the genome (FlyTF.org). Function was manually annotated based on summarized data at flybase.org.

Commonly and differentially expressed genes in each hemilineage relative to combined immature neurons broken down by molecular function

Transcription factors are the most differentially expressed class of highly expressed genes by molecular function. This was determined by taking highly expressed genes (>100 FPKM) and taking the difference and the intersection of each hemilineage with the combined immature neuron dataset and then running each of those three gene lists through PANTHER.db molecular function. The motivation for doing this was to determine a common set of genes by molecular function that are consistently expressed in most or all immature neurons. The tables associated resulting from this data summarize the commonly expressed genes for TFs (Table 3.S26), translational

regulators (Table 3.S27), receptors (Table 3.S28), transporters (Table 3.S29), and structural proteins (Table 3.S30) and differentially expressed genes for TFs (Table 3.S31), translational regulators (Table 3.S32), receptors (Table 3.S33), transporters (Table 3.S34), and structural proteins (Table 3.S35).

Transcription factor expression

Transcription factors are an important class of genes for development and commitment of cell fate, since they control the expression of many downstream genes. There are 754 putative transcription factors in *Drosophila* (FlyTF.org). I determined the expression level of these genes to determine whether TF expression was similar across all hemilineages and between immature and mature neurons. All 754 putative TFs were considered.

The number of TFs expressed per sample is similar to other samples at both >10 and >100 FPKM (Table 3.4). This suggests that the hemilineages express different compositions of transcription factors, but that the overall number of transcription factors expressed at low and high levels by each hemilineage is largely the same.

Neuronal maturation seems to repress TF expression modestly. Both immature neurons and younger immature neurons express more transcription factors at both thresholds than mature neurons and older immature neurons, suggesting that maturation of the neurons leads to suppression of many transcription factors needed for early development. For highly expressed TFs (>100 FPKM), mature neurons express 20% fewer TFs than immature neurons (Table 3.4). Older immature neurons express 17% fewer TFs highly than younger immature neurons (Table 3.4). Individual immature hemilineages are all fairly similar (52-76 range, average 61, standard deviation 9).

C2H2 zinc fingers are the dominant class of TF (120/383) expressed in immature neurons (>10 FPKM). 173 of the 383 TFs expressed by immature neurons are considered involved in development (GO Biological Process, string-db.org).

The following TFs are highly expressed (>100 FPKM) in all of the hemilineages: Alh, br, cg, CG12071, CG33936, CG8108, CG9705, chinmo, crc, crol, crp, D1, E(bx), Eip75B, hang, HmgD, HmgZ, hth, jim, l(3)neo38, lola, mbf1, MTA1-like, Pep, pros, scrt, seq, Su(var)205. These genes are enriched for enriched for "neurogenesis" and many related terms (Table 3.S37).

	TFs expressed >10 FPKM	TFs expressed >100 FPKM
Immature neurons	383	56
Mature neurons	356	45
Older immature neurons	376	49
Younger immature neurons	401	59
1A	350	75
1B	369	56
12A	336	61
12B	336	65
20/22A	369	52
21A	344	76
15B	359	59
19A	347	69
16B	364	70
4B	360	60

Table 3.4 | Summary of putative transcription factor expression. Number of putative transcription factors (FlyTF.org) per sample expressed at >10 or >100 FPKM.

There are several TFs that are highly expressed (>100 FPKM) in all hemilineages for which data was collected except 15B. Lower expression for these TFs is likely reflective of the hemilineage 15B neurons being embryonic-born. For the genes expressed above 100 FPKM in all hemilineages except 15B, these genes are also expressed at lower levels in mature neurons relative to the immature neurons (Table 3.5). A summary of highly expressed TFs in individual hemilineages is shown in Table 3.S36.

	Immature	Mature	1A	1B	4B	12A	12B	15B	16B	19A	20A	21A
CG2052	559	76	361	388	565	485	547	83	146	442	469	586
Dsp1	153	90	108	145	148	144	145	89	116	154	149	147
Su(var)2-10	126	77	122	103	123	119	143	95	117	115	140	158

	Immature	Mature	1A	1B	4B	12A	12B	15B	16B	19A	20A	21A
chn	232	90	306	166	259	223	264	93	188	213	171	241
onecut	116	88	123	111	117	112	119	84	144	126	132	132
pdm3	156	57	358	207	134	195	307	29	217	158	145	192
sbb	158	71	240	134	151	136	193	99	131	153	114	144

Table 3.5 | TF expression in 15B is reflective of these neurons being embryonic-born. 20A refers to hemilineage 20/22A. Numbers are gene expression values in FPKM. Mature neuron expression and hemilineage 15B expression are highlighted in yellow.

Comparison of TF expression to published TF immunohistochemistry

To confirm the expression patterns for transcription factors, I compared my data to published transcription factor staining in the larval-born neurons (Lacin et al., 2014b) (shown in Table 3.6).

There are a few cases where antibody staining is not observed, but my data indicates that there is moderate mRNA expression. The following are cases for which RNA-seq showed expression where there was no immunocytochemical signal: *unc-4* in hemilineage 16B neurons, *Lim3* in hemilineage 1B neurons, *D* in hemilineage 15B neurons, *vg* in hemilineage 19A neurons. It is possible that in such cases, the mRNA is present, but detectable levels of protein are not translated. Some false positives are also expected in the RNA-seq data.

Harder to explain are examples such as *Lim3* in hemilineage 16B neurons, in which protein apparently exists, but I did not find mRNA. The following are cases for which immunocytochemical signal, but RNA-seq did not show enriched expression: *HGTX* and *tup* in hemilineage 15B neurons, *Lim3* and *exex* in hemilineage 16B neurons, and *H15* in hemilineage 1B neurons.

Overall there was concurrence for 55% of the cases. *B-H1* and *B-H2* are expressed at higher levels in hemilineage 20/22A than other neurons. The antibody for *B-H1* likely recognizes both *B-H1* and *B-H2*, so even though expression is low for both, the protein from both genes would be recognized by immunocytochemistry. *Tup* in hemilineage 1B neurons was not considered enriched despite being 1 standard deviation above the mean, because expression levels were the same as combined immature neurons.

Although D was considered enriched in 15B neurons due to it being expressed 3 standard deviations above the mean, absolute expression in low (6 FPKM).

In addition to these TF expression and immunocytochemical patterns, *Nitric oxide synthase* (*Nos*) is expressed at higher levels in 4B than other samples sequenced, as previously described (Lacin et al., 2014a).

Gene	Imm	4B	1A	1B	12A	12B	15B	16B	21A	19A	20A
apt	4	20**	0	8	3	1	10	4	2	4	1
B-H1	2	0	0	0	0	0	0	0	0	0	5***
B-H2	5	0	1	0	0	0	0	0	0	0	8**
D	1	1	0	1	0	1	6***	2	0	1	2
Dbx	6	0	0	2	1	2	3	5	1	15**	9
Dr	45	15	242**	27	0	1	12	3	159*	3	6
exex	42	335**	1	62	2	8	10	36	0	2	0
H15	12	1	0	41	27	143**	4	3	0	0	14
HGTX	48	160*	1	47	0	150*	1	2	0	1	49
Lim3	17	0	0	32*	1	2	29*	9	0	2	0
tup	13*	1	5	13*	1	1	10	5	0	10	1
unc-4	24	3	0	16	150**	2	23	79*	1	2	14
vg	17	5	1	13	4	5	29	29	7	168**	13

Table 3.6 | Comparison of immunocytochemistry with RNA-seq in determining the presence of transcription factors in specific hemilineages. The sequencing data is largely in agreement with the immunocytochemical data. The two datasets agree in 11 instances. In 5 instances the lineage shows immunocytochemical labeling but lacks significant RNA expression and in 4 instances there is RNA expression data for a given TF but no protein signal. Gray cells indicate TFs that were labeled immunocytochemically in a given hemilineage. Numbers are the level of RNA expression in FPKM; red numbers are below 5 FPKM while black are above this value. * is a value one standard deviation above the mean: ** values > 2 SD, *** values > 3 SD. Imm = combined immature neurons. 20A = Hemilinaege 20/22A. Immunocytochemical data from Lacin et al., 2014b.

PCA of hemilineages based on highly expressed TFs

A 2D (Figure 3.8) and 3D (Figure 3.9) PCA plot of only highly expressed TFs (>100 FPKM in at least one hemilineage) was performed to determine how similar different hemilineages are with respect to their TF expression. The 3 principal components plotted in the 3D PCA represent 92% of the variation observed in the highly expressed TFs in the hemilineages (81%, 7%, 4% for PC1, PC2, PC3 respectively; Table 3.S22). The top positive and negative contributions for the first 3 principal components are show in Table 3.S23.

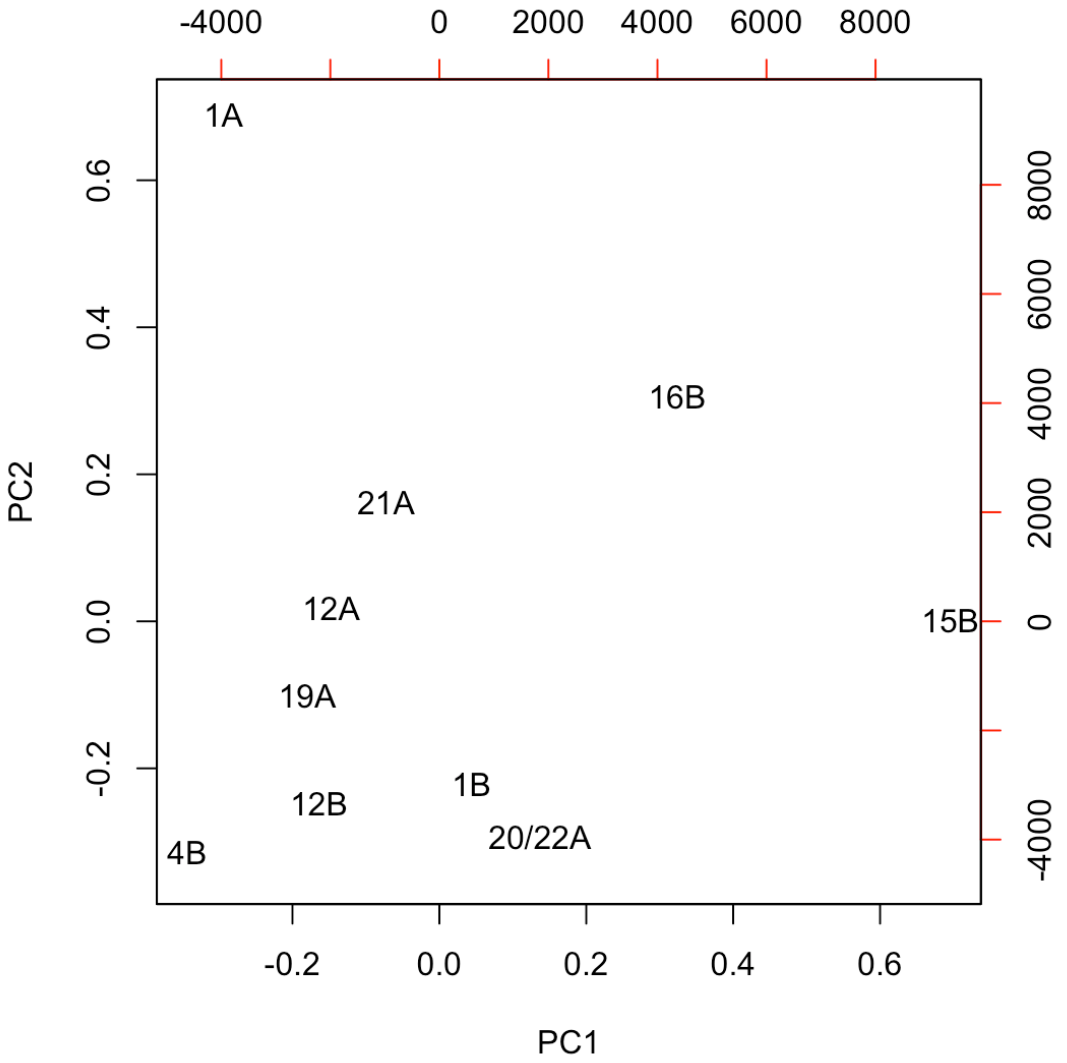

Figure 3.8 | 2D PCA of hemilineages based on highly expressed TFs. Only highly expressed (>100 FPKM) TFs in at least one hemilineage were used for the analysis. All putative TFs from FlyTF.org were considered.

Most hemilineages occupy one quadrant of the 2D PCA. Hemilineage 15B is an outlier for PC1 and hemilineage 1A is an outlier for PC2. 16B is somewhat separated from the other 7 hemilineages in both components PC1 and PC2.

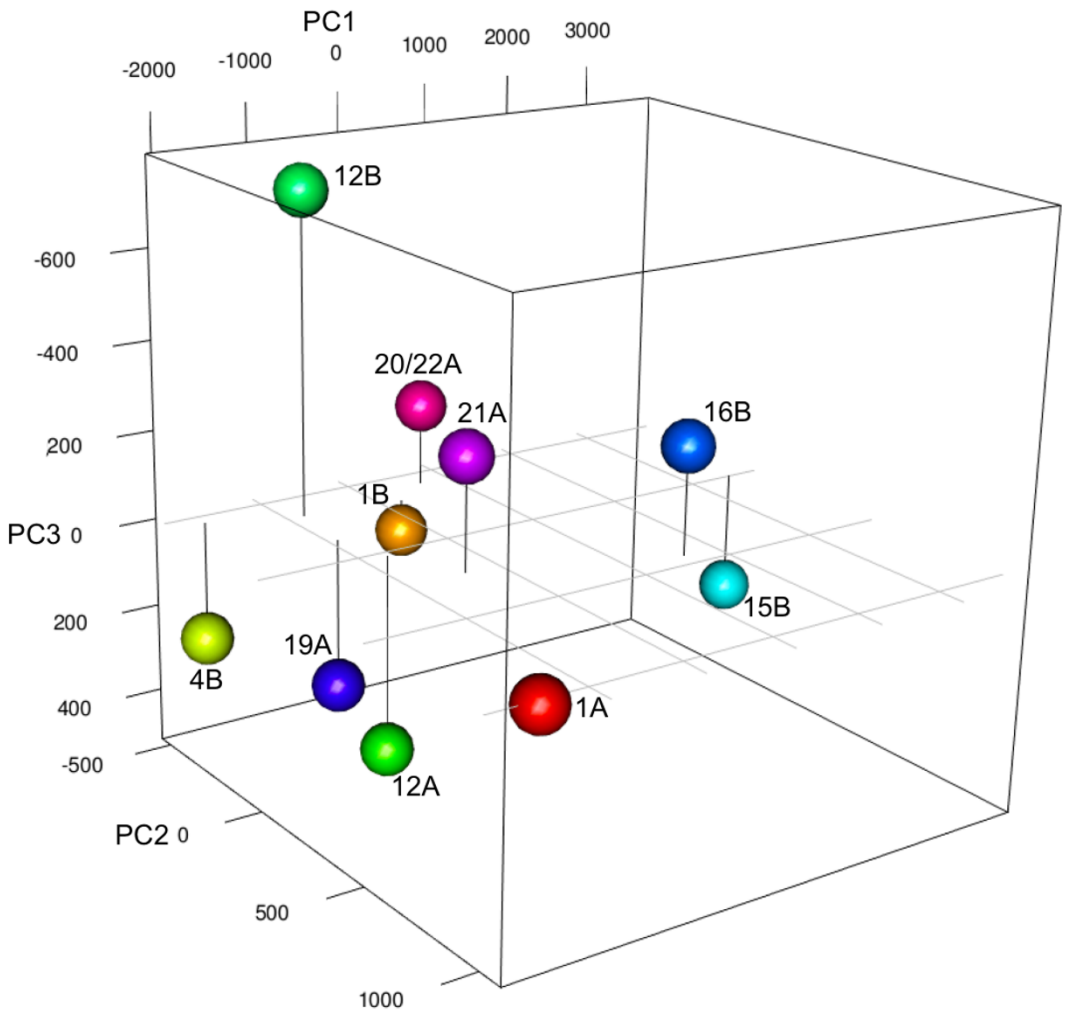

Figure 3.9 | 3D PCA of hemilineages based on highly expressed TFs. Only highly expressed (>100 FPKM) TFs in at least one hemilineage were used for the analysis. All putative TFs from FlyTF.org were considered.

Table 3.7 summarizes the hemilineage expression patterns for the top twenty positive and negative contributions to PC1 in the PCA of highly expressed TFs in the individual hemilineages. *Pros* is the single largest contributor to PC1, with a fold change of 15 between expression in hemilineage 15B and hemilineage 4B. Effectively, this is a ranking of the fold changes between the highest and lowest gene expression value per gene, with the highest fold change being 15 and the lowest fold change making the list being 2 for CG17385 between hemilineage 15B and hemilineages 12A and 16B.

PC1CC	gene	1A	1B	4B	12A	12B	15B	16B	19A	20/22A	21A
-0.9249	*pros*	4664	3320	5256	4293	4205	350	1951	4490	2874	3753
-0.2895	*jim*	2269	1156	1508	1378	1798	197	1295	1407	1103	1731
-0.1341	*br*	1120	480	720	599	655	132	454	516	385	707

PC1CC	gene	1A	1B	4B	12A	12B	15B	16B	19A	20/22A	21A
-0.0883	*CG2052*	361	388	565	485	547	83	146	442	469	586
-0.0614	*Antp*	293	372	241	134	491	31	38	394	318	421
-0.0545	*lola*	819	949	950	758	822	585	635	801	726	581
-0.0527	*l(3)neo38*	904	1091	1003	1041	1035	732	665	834	1105	1084
0.0485	*Scr*	0	22	2	70	4	194	293	13	9	1
-0.0354	*chinmo*	363	209	206	316	353	105	235	214	190	324
0.0352	*Eip74EF*	44	16	36	51	12	223	209	138	6	91
-0.0343	*chn*	306	166	259	223	264	93	188	213	171	241
-0.0341	*pdm3*	358	207	134	195	307	29	217	158	145	192
-0.0330	*hth*	1432	900	802	1239	271	937	764	1028	648	950
-0.0309	*HmgD*	882	1256	966	746	1019	845	520	970	1143	894
-0.0296	*Pep*	380	384	410	394	384	243	224	274	376	278
0.0279	*CG33936*	531	412	390	419	418	629	593	489	273	714
-0.0276	*Ptx1*	442	66	18	4	0	2	15	0	23	0
0.0241	*vri*	13	27	33	40	23	157	121	82	17	60
-0.0238	*Ets21C*	364	3	4	1	3	2	1	0	1	0
-0.0237	*Eip75B*	631	487	530	593	564	476	578	621	416	613
0.0225	*Sox14*	16	13	22	29	4	138	126	65	4	108
-0.0223	*CG6854*	160	187	191	169	231	80	63	158	206	122
-0.0214	*exex*	1	62	335	2	8	10	36	2	0	0
-0.0210	*Su(var)205*	439	558	498	432	469	363	358	380	532	709
0.0199	*HmgZ*	561	590	618	477	524	816	300	496	438	535
0.0199	*CG11071*	41	56	26	44	43	123	167	86	18	69
0.0193	*emc*	175	121	25	210	7	208	166	152	109	175
0.0181	*Atf-2*	86	96	101	111	90	203	142	110	67	118
0.0180	*kn*	6	61	4	48	4	101	59	4	4	0
0.0174	*crc*	189	221	174	148	184	280	191	215	244	213
0.0157	*ct*	16	57	26	20	38	146	79	213	39	44
0.0156	*CG14767*	47	78	78	62	77	117	190	105	90	102
0.0155	*CG15715*	62	73	57	64	54	138	114	92	85	76
0.0144	*mamo*	44	63	31	46	62	107	119	50	18	52
0.0124	*Lim1*	1	59	22	142	3	61	170	65	35	119
0.0119	*pan*	86	71	50	60	42	109	162	129	58	64
0.0116	*salm*	4	32	14	5	0	60	95	101	20	1
0.0104	*Nfl*	77	69	79	84	69	127	146	103	71	127
0.0099	*CG17385*	130	129	107	94	112	188	94	123	105	98

Table 3.7 | Summary of expression for genes contributing most to PC1 in the highly expressed TF hemilineage PCA. Numbers are gene expression values in FPKM. Color coding is per gene: highest expression (green), medium expression (yellow), lowest expression (red). PC1CC column represents the correlation coefficient for PC1. Genes are ordered by absolute value of the correlation coefficient.

I performed GSEA on the top positive and negative contributing genes for PC1 in order to understand which processes they were involved in collectively. Excluding the terms associated with regulation of transcription, the terms associated with the top positive PC1 contributions were largely involved in morphogenesis, including "metamorphosis", "instar larval or pupal development", "post-embryonic appendage morphogenesis", "instar larval or pupal morphogenesis" (43 terms total; Table 3.S24). The top 10 terms associated with the top negative PC1 contributions were all involved

in neurogenesis or some aspect thereof and the rest of the term enrichments were dominated by developmental processes as well (49 terms total; Table 3.S25). Thus, at the two extremes of PC1, 4B is expressing more TFs associated with developmental and neurogenic processes and 15B is expressing more TFs associated with metamorphic process.

Opposing *Imp*/*Syp* expression correlates with neuronal age

Syncrip (*Syp)* and *IGF-II mRNA-binding protein* (*Imp)* are RNA-binding proteins that provide a system to mark the birth order of neurons during the postembryonic phase of neurogenesis (Liu *et al.,* 2015). Early in producing its postembryonic lineage, the NB expresses high levels of *Imp* and very low levels of *Syp* but, through time, these levels in the NB gradually change inversely so that late in the lineage the *Imp* levels are low and *Syp* is now high. The Imp/Syp ratio present at the time of their birth is then maintained in the daughter neurons as a stable indicator of their time of their birth within a lineage.

In the RNA-seq data, the mature larval neurons, that were embryonic born, show similar levels of *Imp* and *Syp* transcripts (Table 3.5). Overall, the clusters of immature, arrested neurons show a strong bias towards Syp transcripts, which is even more pronounced when only the younger cells in the cluster were considered. By contrast, the older cells in the cluster have a reduced Syp/Imp ratio over the cluster as a whole.

The individual hemilineages varied in their overall Syp/Imp ratio. The smallest ratio was seen for the 15B neurons. This hemilineage contains only immature leg motoneurons and these cells in this GAL4 line are born during late embryogenesis (Lacin and Truman, 2016). Their early birth dates would therefore be consistent with a low Syp/Imp ratio. Interestingly, though, a number of the other hemilineages also have rather small Syp/Imp ratios, and produce neurons through most of larval life. Liu et al (2015) showed that the steepness of the Imp-Syp gradient varies amongst the lineages that they examined and was steeper in lineages that generated the more diverse sets of neurons. The differences that we see in the Syp and Imp levels in the

various lineages may likewise reflect differences in the Imp and Syp gradients and, hence, in the diversity of cell types generated in the particular hemilineages.

Cell Type	*Syp*	*Imp*	*Syp/Imp*
Mature	134	113	1.2
Immature	317	17	18.6
Younger Immature	310	4	77.5
Older Immature	261	38	6.9
1A	423	17	24.9
1B	314	40	7.9
4B	406	26	15.6
12A	424	20	21.2
12B	450	21	21.4
15B	218	158	1.4
16B	317	96	3.3
21A	393	57	6.9
19A	328	92	3.6
20/22A	265	14	18.9

Table 3.8 | Levels of Syp and Imp mRNA in different neuron classes at the start of metamorphosis. *Syp* is expressed at high levels and *Imp* is expressed at low levels in immature neurons. Mature neurons have closer to an equal ratio of Syp and Imp with Imp at higher levels and Syp at lower levels than in immature neurons. Numbers are expression values in FPKM.

Axon guidance gene expression in individual hemilineages

Two of the hemilineages assayed for by RNA-seq cross the midline during axon guidance, while the others do not. Expression of genes associated with axon and dendrite guidance was determined to see whether there was a pattern between expression of these genes and whether the neurons crossed the midline (Table 3.9).

	1A	21A	12B	1B	20A	4B	12A	19A	16B	15B
	Ant		Post							
	Contra	Ipsi	Contra	Ipsi	Ipsi	Ipsi	Ipsi	Ipsi	Ipsi	Ipsi
	Int	Int	Int	Int	Int	Int	Int	Int	Int	Motor
NetB	59	19	105	123	85	86	297	119	107	129
NetA	0	0	3	3	4	0	6	2	0	2
fra	95	90	70	90	94	84	118	103	77	102
Snr1	29	73	56	58	60	56	52	53	34	44
Rpd3	65	64	55	83	106	67	60	85	55	42
Bap55	76	82	84	95	172	85	68	94	68	56
Sema-2a	105	86	71	85	123	91	88	83	95	80
kst	1	1	1	1	1	1	0	1	1	0
sli	102	71	99	93	105	90	91	71	75	82
robo3	221	95	195	90	68	122	45	40	151	93
comm	47	19	48	22	25	15	21	36	36	17
CG33960	126	172	355	148	99	35	80	195	115	127
pros	4664	3753	4205	3320	2874	5256	4293	4490	1951	350

	1A	21A	12B	1B	20A	4B	12A	19A	16B	15B
	Ant		Post							
	Contra	Ipsi	Contra	Ipsi	Ipsi	Ipsi	Ipsi	Ipsi	Ipsi	Ipsi
	Int	Int	Int	Int	Int	Int	Int	Int	Int	Motor
brm	63	67	82	73	56	81	77	59	52	54
Chi	82	93	74	81	65	75	65	70	48	56
siz	134	98	117	112	82	104	105	111	80	94
elav	417	412	378	413	277	375	397	375	375	417
dom	117	166	129	107	99	130	121	102	103	93
E(Pc)	70	87	76	71	52	73	68	59	67	54
robo	134	140	144	113	108	117	131	119	122	122
Wnt5	33	56	49	48	42	45	52	47	56	47
unc-5	75	75	57	50	61	55	53	61	63	85
lea	22	21	16	26	24	12	17	10	54	32
Toll-6	53	20	28	36	31	21	31	43	114	37
CG5802	18	14	16	18	31	16	22	24	23	19
ct	16	44	38	57	39	26	20	213	79	146
D	0	0	1	1	2	1	0	1	2	6
drl	81	38	52	91	36	48	43	32	47	71
acj6	0	0	0	24	0	3	1	1	9	5
sqz	10	4	6	7	6	4	7	6	6	3

Table 3.9 | Hemilineage axon guidance gene expression. Expression values in FPKM rounded to the integer. 1 Standard deviation above the mean in green. 2 Standard deviations above the mean in purple. 3 standard deviations above the mean in blue. Gray rows have no sample with expression above 5 FPKM. Row colors correspond to clusters in hierarchical clustering. Column order is determined by hierarchical clustering relatedness. All samples are interneurons (Int) except 15B, which are motoneurons (Motor). 20A = 20/22A. Hemilineages 1A and 12B are contralateral (Contra), but all others are ipsilateral (Ipsi). 1A and 12B cross the commissure anteriorly (Ant) and posteriorly (Post), respectively.

The expression patterns of axon guidance genes suggest that *comm* expression levels are more indicative of midline crossing than *robo1-3*. *Comm* is known to regulate *robo* protein to allow midline crossing, but does not affect *robo* RNA expression (Zou et al., 2000). *Comm* protein is required in the midline crossing neurons, not just in the midline glia (Georgiou & Tear, 2002).

Neurotransmission gene expression in individual hemilineages

Although the arrested postembryonic neurons generally do not express the RNAs for genes that would be expected to be in mature neurons, a notable exception were genes for proteins involved in the biosynthesis and transport of the main small molecule transmitters, acetylcholine, GABA and glutamate. In general, I find that genes involved in neurotransmission are expressed during this arrested developmental state before the neurons form functional synapses (Table 3.10). Many of the transmitter systems for the hemilineages after they are mature are known from immunohistochemical staining. For all instances where antibody staining is known

conclusively for the adult hemilineages, I find that the expression of genes for biosynthesis or transport of that neutoransmitter accurately predicts the neutransmitter released by the adult neurons (Table 3.10). While many of the hemilineages seem to be cleanly specified for a single small molecule transmitter, a few of them, such as 15B and 16B seem ambiguous in that they have molecular signatures for more than one system. It could be that different subsets of cells in the hemilineage express different transmitters or a given neuron might express more than one small molecule transmitter. I found that neurotransmitter receptors are not specific and each neuron expresses receptors for many different types of neurotransmitter (Table 3.S38).

	Imm	4B	1A	1B	12A	12B	15B	16B	21A	19A	20/22A
Cha	19	31	52**	20	42*	6	24	18	2	14	18
VAChT	47	95	120	47	116	7	64	112	5	16	42
Gat	11	8	9	6	11	12*	3	5	6	10	10
Gad1	52	11	2	63	3	188*	92	74	1	248*	55
VGAT	46	32	38	40	44	48	49	83*	43	115**	51
VGlut	42	51	6	27	1	8	159	45	464**	17	30
Type	-	ACh	ACh	?	ACh	GABA	Glut	ACh	Glut	GABA	?
Ab	-	ACh	?	?	ACh	GABA	Glut	Ach	Glut	GABA	?

Table 3.10 | Expression of biosynthesis and transport genes predicts neurotransmitter type in arrested hemilineage neurons. These are the expression levels for the genes responsible for the biosynthesis and transport of the primary three neurotransmitters in Drosophila: acetylcholine, GABA, and glutamate. 8 of the 10 hemilineage neurotransmitter types can be predicted based on expression of these genes. 2 of the 10 hemilineages do not express high levels of any of these genes at this stage. At the bottom of the chart, the type indicates which neurotransmitter the hemilineage is predicted to release based on expression data (Type). 6 hemilineages have known neurotransmitter types from immunohistochemistry that are in complete agreement with the predictions from RNA-Seq (Ab). Green cells are 2-fold or above the sum of immature neurons; yellow are between 1- and 2-fold. Numbers are the level of RNA expression in FPKM. * is a value one standard deviation above the mean: ** values > 2 SD.

TfAP-2 is necessary for development of wildtype 12A morphology

My analysis of TF expression in the various hemilineages identified *TfAP-2* is a transcription factor specific to the neurons of the 12A hemilineage. As seen in Figure 3.8C, an antibody raised against Drosophila *TfAP-2* (Monge et al., 2001) shows nuclear staining only in hemilineage 12A neurons, confirming that these neurons do indeed make *TfAP-2* and that they are the only hemilineage to do so.

The function of *TfAP-2* in the development of the 12A neurons was examined using two null mutants, *TfAP-2*^{2} and *TfAP-2*^{15} (Monge et al., 2001). During wildtype development of hemilineage 12A neurons, the early-born cells extend an axon along an extreme dorsal route while later-born siblings take an intermediate route (Mellert et al., 2016). This axon guidance is disrupted in larvae that are null for the function of *TfAP-2* (Figure 3.10).

I used the MARCM technique to determine the effect of removal of *TfAP-2* from the lineage 12 cells in an otherwise wildtype background. *TfAP-2* MARCM experiments with both null mutants TfAP-2^{2} and TfAP-2^{15} showed a morphologically wildtype 12B, but the 12A neurons stalled their axons at the early-late choice point and produced neither a dorsal nor an intermediate bundle (Figure 3.8F). One clone showed a few 12A axons that escaped and took a novel route to finally end up on the contralateral side of the neuropil near the region where the 12B neurons terminate (Figure 3.8G). Removal of TfAP-2 from lineages other than lineage 12 has no effect on clone morphology. Table 3.11 shows a summary of clone phenotypes per mutant allele.

Flies that were trans-heterozygote mutant for *TfAP-2* (*TfAP-2*^{2}/*TfAP-2*^{15}) produced 12A neurons that only took the intermediate route (Figure 3.8E). *TfAP-2* trans-heterozygote experiments showed 12A with a missing dorsal branch and a morphologically wildtype 12B. As with the MARCM experiments, other lineages in the *TfAP-2* mutants look morphologically wildtype.

TfAP-2 has a characterized binding site (Bauer, 1998). Most genes did not appear to have more binding sites in their 5' and intronic sequences than would be predicted by chance, with the exception of Tiwaz (*twz*), which is known to be co-regulated with *TfAP-2* (Williams et al., 2014). *TfAP-2* and *twz* are also known to form heterodimers.

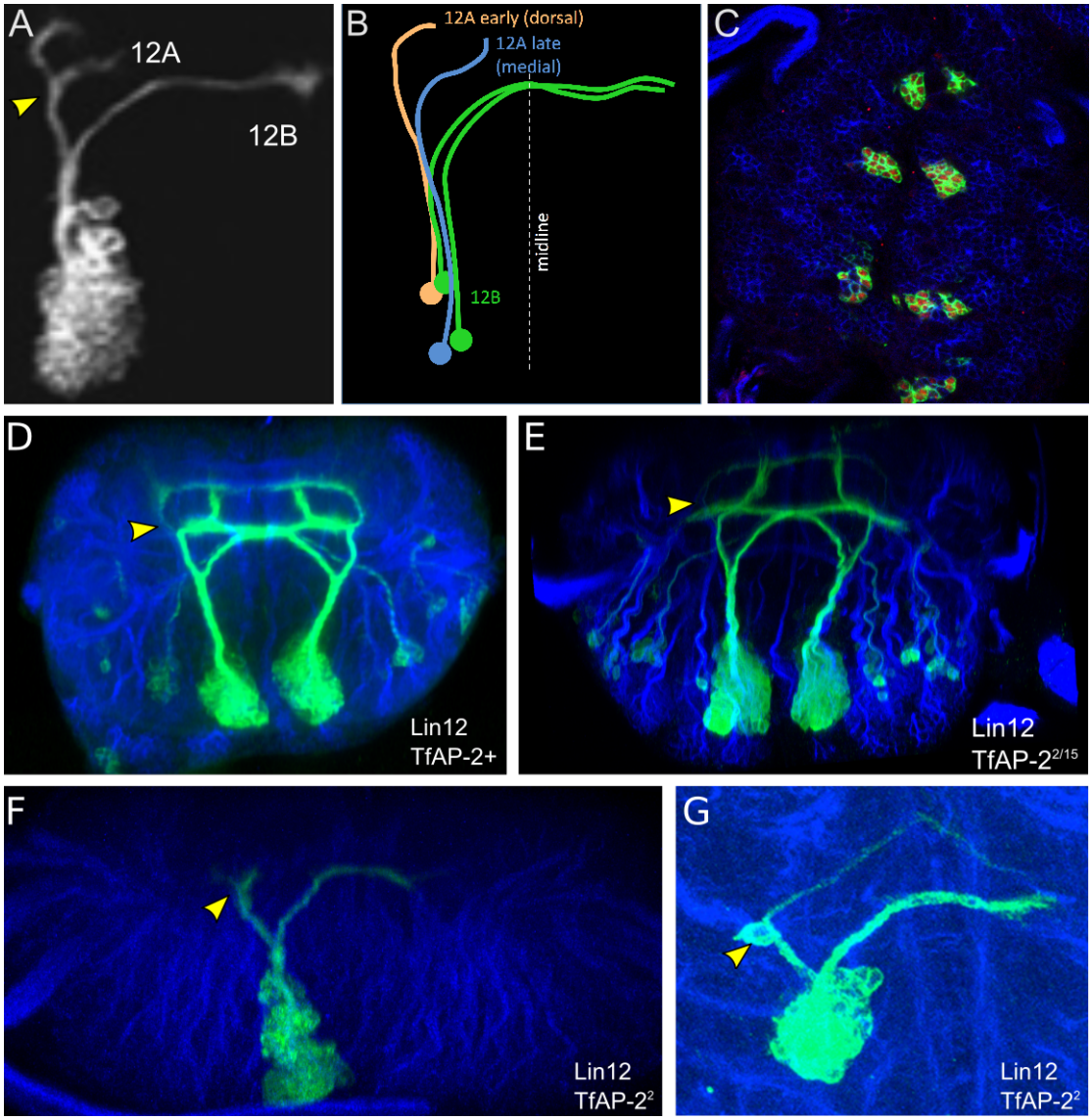

Figure 3.10 | *TfAP-2* is required for proper anatomy of the immature 12A hemilineage. (A): MARCM clone of an immature lineage 12 showing the ventral axon bundle of the 12B siblings and the split bundle carrying the axons of the 12A siblings (from Truman et al., 2010). (B): Schematic drawing showing that the dorsal branch of the 12A bundle carries the axons from the early-born daughters, whereas the late-born daughters have their axons in the intermediate branch (based on Mellert et al., 2016). Hemilineage 12B neurons cross the midline. (C): *TfAP-2* immunohistochemistry shows that *TfAP-2* is expressed in hemilineage 12A neurons, labeled with GFP by R24B02-GAL4. Single Z-slice through subesophogeal and thoracic segments of VNS. *TfAP-2* antibody staining (red) is specific to the nuclei of GFP-labeled hemilineage 12A neurons (green). (D, E): Compared to wildtype 12A neurons (D), *TfAP-2* trans-heterozygote larvae (E) are missing the early-born, dorsal bundle of hemilineage 12A. (F): In *TfAP-2* null MARCM clones of lineage 12, the 12A neurons stall axon outgrowth at the point (yellow arrowhead) where they would decide to take the dorsal or the medial route. Hemilineage 12B is morphologically wildtype in *TfAP-2* MARCM clones. (G): An example of the MARCM clone in which a 12A axon escaped its arrest and took an ectopic pathway to end near the termination of the 12B siblings. Yellow arrowheads show the point where hemilineage 12A axons take the dorsal or medial paths. Genotypes for TfAP-2 MARCM clones: *TfAP-2*^{2}: hsFLP, elav-GAL4, UAS-mcD8::GFP; +; TfAP-2^{2}, FRT80B/tub-GAL80, FRT80B. *TfAP-2*^{15}: hsFLP, elav-GAL4, UAS-mcD8::GFP; +; TfAP-2^{15}, FRT80B/tub-GAL80, FRT80B.

Mutant allele	Arrested axon	Misrouted axon
TfAP-2^{2}	4	1
TfAP-2^{15}	3	0

Table 3.11 | TfAP-2 MARCM clone summary. MARCM clones were induced at the same time and using the same conditions. Genotypes used: *TfAP-2*^{2}: hsFLP, elav-GAL4, UAS-mcD8::GFP; +; TfAP-2^{2}, FRT80B/tub-GAL80, FRT80B. *TfAP-2*^{15}: hsFLP, elav-GAL4, UAS-mcD8::GFP; +; TfAP-2^{15}, FRT80B/tub-GAL80, FRT80B.

Discussion

Notch functions in a neuroblast-specific manner to cause expression of different downstream genes in each hemilineage

I hypothesized that Notch signaling would cause downstream expression of a consistent set of genes in each hemilineage with Notch activity. Thus, in comparing the gene expression of multiple A and B hemilineages, I expected to determine this battery of Notch-dependent genes. Additionally, I compared the expression of the combined A hemilineage neurons from all lineages to the combined immature neurons (both and A and B). One potential way to achieve a more direct comparison between A and B hemilineages would have been to subtract the A hemilineage expression from the immature neurons labeled with R71C09-GAL4 using R12A07-GAL80. While comparing A hemilineages labeled with R12A07-GAL4 to B hemilineages labeled with R71C09-GAL4 and R12A07-GAL80 would have been more direct, an R12A07-GAL80 construct currently does not exist. Since bulk RNA-seq has high read depth and sensitivity, it seemed reasonable to assume that large and consistent differences in expression owing to A vs B hemilineage identity should still be detectable by comparing all A hemilineage neurons to all A and B hemilineage neurons.

We expected to see expression of the known immediate downstream targets of Notch signaling expressed much more abundantly in A hemilineages than B hemilineages, if these genes were expressed at detectable levels in B hemilineages at all. We did not observe this, however. Hey and E(spl) complex genes were detected at significant levels only in the subset of younger immature neurons. This suggests that the expression of the genes immediately downstream of Notch signaling is quite transient, as has been previously reported (Monastirioti et al., 2010). While the known immediate downstream targets of Notch including Hey and E(spl) complex genes are expressed transiently, there was no consistent downstream expression observed.

Hemilineages do not seem to be constrained by their Notch activity or lineage identity with respect to gene expression pattern. Notch activity does not seem to contribute significantly and consistently to the pattern of highly expressed genes. Not only do

combined A hemilineage neurons have a nearly identical expression pattern to combined A and B hemilineage neurons, but the percentage of common highly expressed genes between individual hemilineages is not affected by Notch activity. Lineage/neuroblast identity also does not seem to contribute significantly to the pattern of highly expressed genes, with sibling hemilineages showing no greater overlap between highly expressed genes than with non-siblings. These patterns are observed both for the overlap of highly expressed TFs and for the total of highly expressed genes belonging to all gene classes. Thus, it appears that the function of Notch signaling in A neurons is not a simple "and" operation adding the Notch gene expression pattern to the NB gene expression pattern. Notch is performing a more complicated context-specific role that causes different downstream gene expression dependent upon the NB identity.

Notch signaling caused context-specific downstream gene expression. The presence or absence of Notch did not consistently cause expression of the same genes in every hemilineage. The sibling hemilineages 12A and 12B have significant gene expression differences, including TfAP-2 expression in 12A, but these differences were not consistent across hemilineages derived from other stem cells. Thus, Notch signaling is integrated with the neuroblast identity of the hemilineage in order to cause differential gene expression that is different for each stem cell lineage. One possibility for how this may occur is that the inherited transcription factors and microRNAs that differ between stem cells cooperate with Notch signaling to activate or repress different enhancers through combinatorial control. Additionally, chromatin architecture may differ between stem cells such that Notch signaling has a different group of enhancers in an open chromatin state upon which to act depending on the stem cell. It seems likely that the combination of these two mechanisms integrates Notch signaling with neuroblast identity to cause downstream expression of a different set of genes in each "A" (Notch-"on") hemilineage.

Temporal specification of neurons through birth order: comparing older (early-born) and younger (late-born) immature neurons

The arrested, immature larval VNS neurons born during larval neurogenesis are accumulated in a non-synapsing state with simple arbors that are nearly identical

within each hemilineage. These neurons mature during metamorphosis, when they undergo their final pathfinding and synapse formation. There is cell type diversity within each larval-born lineage evident after metamorphosis despite identical morphology in their arrested immature form preceding it. Presumably, this cell fate specification is controlled by temporal differences according to the birth order of the neurons, as has been shown to be the case for the dorsal and intermediate branches of hemilineage 12A larval-born neurons (Mellert et al., 2016). I used two different GAL4 lines to label the older and younger subpopulations of immature neurons separately. By virtue of the fact that there are enhancers that label each temporally distinct subpopulation of every hemilineage, it seems that these younger and older neuronal subpopulations are molecularly distinct from one another in a way that is generalized across all hemilineages long before metamorphosis.

In collecting and analyzing these datasets, I wanted to address whether there are substantial differences between the gene expression profiles of younger and older immature neurons that are consistent across hemilineages. Younger immature neurons are more like immature neurons while older immature neurons are more like mature neurons according to PCA of expression values for all genes. The chinmo-broad transition (Emery, Bedian, and Guild, 1994; Zhu et al., 2006; Maurange, Cheng, and Gould, 2008; Zhou et al., 2009; Syed, Mark, and Doe, 2017) is observed in the younger vs older immature neurons, with younger immature neurons showing higher chinmo and lower broad expression. The complexity of TF expression appears to become somewhat simplified as the immature neurons move into arrest, as RNA for a greater number of TFs are detected at high levels in younger immature neurons than older immature neurons.

In addition to identifying what gene expression changes occur during the early maturation and local pathfinding of the immature neurons, I hoped to identify a gene or set of genes that controlled the temporal diversification process in the postembryonic (larval-born) neurons. By comparing gene expression between the younger and older immature neurons in the larval VNS, I hoped to identify a molecular “switch” that controls temporal cell fate diversification from the differentially expressed genes. There are no obvious novel candidates for genes that control the temporal diversification process among the differentially expressed genes

detected between the older and younger immature neurons. It is likely that the chinmo to broad transition and Imp/Syp gradients that have already been described in literature are primary controllers of this temporal identity progression. It is also possible that additional molecular "switch(es)" exist, but that they were transiently expressed and thus not abundant enough to meet thresholds for high abundance and a high degree of differential expression in the bulk neuron sample.

The genes immediately downstream of *Notch*, including *Hey* are transiently expressed. RNA for these genes is detectable in younger immature neurons but not in the older immature neurons. Interestingly, genes that are known to be directly downstream of *Notch* expression, such as *Hey*, did not appear in the A hemilineage sample, even though they are present in the sample of young immature neurons, displaying that they are detectable in these datasets. A likely explanation is that these genes are only expressed transiently and may already be turned off by the time that cells in the R12A07 line begin expressing GFP. The young immature neuron sample includes GMCs. Assuming that some of these GMCs made it through the FACS purification process to become part of the bulk RNA pool that was amplified, this should not be the source of any RNA for genes dependent on Notch for expression. This is because Numb protein in the GMC suppresses Notch activity (Spana and Doe, 1996; Skeath and Doe, 1998; Buescher et al., 1998; Berdnik et al., 2002). In this way, the cells are primed for differential Notch signaling after GMC division through asymmetric inheritance of Numb protein.

It would be surprising in light of the results of the work presented in this thesis if a new mechanism was discovered beyond the previously published chinmo-broad transition and the Imp/Syp gradient. It is possible that an additional pathway exists, but that the two populations of neurons I studied did not give me sufficient granularity to detect it. A binary expression switch would be easily detectable, but a gradient might not appear as highly differentially expressed, because a large percentage of both populations might have an intermediate level of expression for such a transcript. Advances in single-cell RNA-seq technology during this thesis work would be particularly appropriate to leverage for refining our understanding of temporal diversity in the larval and adult nervous systems. Since we can label and isolate the neurons at the hemilineage population level for nearly all of the hemilineages in the

VNS, we could use single cell RNA-seq in the future to determine the degree of temporal diversity that exists in these hemilineages, and possibly determine an additional mechanism of temporal diversification in the form of an additional transcriptional gradient of some regulatory gene. Furthermore, it is possible that an additional mechanism exists that is controlled post-transcriptionally and thus would not be detected by either bulk or single cell RNA-seq technology.

Expression differences between immature and mature larval neurons reflects the lack of functional synapses in immature neurons

Unlike vertebrate neurons, which begin an often lengthy maturation process immediately after their birth, Drosophila neurons are pooled during larval neurogenesis in an immature state. Immature and mature neurons differ significantly with respect to morphology, connectivity, and other important features of neuronal identity. These immature neurons have not completed pathfinding and have not formed synapses. What gene expression differences are observed between immature and mature neurons? Comparing the same population of larval-born neurons before and after metamorphosis would have been a more direct way to assay the effects of neuronal maturation on the transcriptome. However, there were multiple problems with this approach. I did not have access to sufficient dissecting resources to make adult VNS dissection feasible on the same scale that I performed the larval VNS experiments. Furthermore, due to temporal changes in GAL4 expression patterns, I would have had to either accept a mixed population of embryonic-born and larval-born neurons in the adult VNS or I would have had to introduce additional transgenes in order to immortalize the larval-born neuron pattern with R71C09-GAL4. The introduction of additional transgenes was avoided because this would confound the interpretation of the results and would have made the initial stock building process lengthier. In order to address the question of how maturation affects neurons more generally, I instead compared immature larval-born neurons and mature embryonic-born neurons both from the larval VNS. I hypothesized that immature neurons would express a greater number of TFs and genes associated with neuronal pathfinding as highly abundant transcripts than mature neurons. I expected a greater number of highly expressed TFs to be observed in immature neurons because some TFs are likely expressed only transiently for identity establishment, while others are likely

required for maintenance of neuronal identity. I did observe a greater number of highly abundant TF transcripts in the immature neurons. In the future, I plan to determine which TFs fell into each category of identity establishment and identity maintenance, since this assumption held true.

I expected that the mature neurons would express more genes associated with neurotransmission and synaptic function. RNA expressed in immature, arrested neuron reflects their lack of synaptic connectivity. Arrested immature neurons do not express genes required for synaptic transmission. Mature neurons express much higher levels of the genes for the vacuolar H+ ATP-ases that are responsible for acidifying synaptic vesicles in order to load them with neurotransmitters. Neurotransmitter transport genes, neurotransmitter receptors, neuropeptides, and neuropeptide receptors are not expressed abundantly in arrested neurons, but are expressed in mature neurons. Mature neurons also show enriched expression for some ecdysone-responsive genes including *Eip74EF* and *Sox14*. It seems that expression of the *TM4SF* tetraspanin is associated with neuronal maturation, as it is expressed at much higher levels in mature neurons relative to immature neurons as well as older immature neurons relative to younger immature neurons.

Adult neurotransmitter type is predicted by expression of biosynthetic and transport genes in arrested neurons

Does immature neuron expression predict mature neuron expression? The fate programming in invertebrate neurons is understood to be deterministic (Doe, 1992; Skeath et al., 1995). The cells are fated to mature into a particular type from the moment they are born. I hypothesized that some genes associated with the mature identity of the neurons may be expressed by the immature neurons. I started with genes associated with neurotransmitter type, since this is a core feature of a neuron's mature identity and function, and for most of these hemilineages, we had pre-existing immunohistochemistry data for the neurotransmitters synthesized by the mature neurons.

I found that the neurotransmitter type for each hemilineage is already determined in the immature neurons before they have formed synapses. Most of the arrested neurons

(8 of 10 hemilineages assayed) express either the gene for the major small molecule neurotransmitter (acetylcholine, GABA, or glutamate) biosynthetic enzyme, the neurotransmitter transporter, or both. For all known patterns in the adult, the transporter or biosynthetic enzyme gene expression accurately predicts the adult neurotransmitter type. Based on this pattern, I predict that 1A is cholinergic, which is currently uncharacterized in the adult. This is an interesting finding counter to our assumptions, since the immature neurons have not formed synapses yet and do not express many of the genes necessary for synaptic transmission, such as vacuolar H+ ATPases. Since the immature neurons have yet to form synapses, I expected them to have little or no expression of genes for neurotransmitter biosynthesis enzymes and neurotransmitter transporters. In each hemilineage, neurotransmitter synthesis and release is restricted to a single type, but the neurotransmitter receptor expression is diverse. This earlier-than-expected expression of neurotransmitter genes suggests that the neurons have committed to a neurotransmitter type long before they are active as part of the neuronal circuitry of the animal.

Diverse receptor expression is what I expected to find. It suggests one or both of two things: The neurons may be diverse with respect to receptor expression, presumably determined by birth order differences. This is likely true to some extent. Each neuron may express a diversity of receptors in order to respond to multiple neurotransmitter types from presynaptic neurons. This is generally accepted to be the case with many neurons (Clendening and Hume, 1990; Genzen, Van cleve, and Mcgehee, 2001; Borgmann-winter et al., 2009).

Combinatorial control of identity and a TF "code"

The "TF code" of expressed TFs responsible for identity establishment in the VNS hemilineage neurons is necessarily combinatorial. Previous work has shown that immature neurons express a combination of TFs that can be used to uniquely identify each hemilineage by immunohistochemistry (Lacin et al. 2014). Through an unbiased RNA-seq approach, we hoped to recapitulate and refine the TF "code" provided through immunohistochemistry data by finding additional TFs that were not assayed by antibody staining. We also hypothesized that there may be examples of TFs that are important for the identity establishment of one and only one hemilineage in the

VNS. There was reasonable concordance between published antibody staining patterns of TF expression and my RNA-seq data. Disparities could be due to false negatives and false positives with either technique, but in some cases may be real differences between the existence of RNA and protein in the cells. At any given point in time, not all transcripts are translated. Conversely, inherited proteins or those translated from transiently expressed transcripts would not have abundant RNAs to match the protein in the cell. In this thesis, I have added to a pre-existing combinatorial TF code that can be used to uniquely identify the hemilineage neurons.

Future directions for this code are to confirm the expression patterns and to perform necessity and sufficiency experiments in the neurons. Many of these TFs have RNAi and cDNA constructs that can be used for knockdown and overexpression experiments to test for necessity in the same hemilineage and sufficiency in a different hemilineage, respectively. Some of these TFs are likely involved in establishing the wildtype morphology of the neurons that express them. Other cases will be more difficult to probe rapidly without performing a substantial number of experiments, because their perturbation will not cause morphological changes in the neurons. In these cases where no morphological phenotype is observed, it will be less straightforward to determine whether the reagents are working as expected in the neurons, therefore necessitating a disentangling of experimental reagent effectiveness and meaningful biological phenomena. Thus, I will focus efforts on genes with obvious morphological phenotypes in the immature neurons that can be induced with available reagents, since this is the simplest phenotype to look for in the labeled hemilienage populations. I performed preliminary experiments on a TF that proved to have a role in establishing the wildtype morphology of the neurons from a particular hemilineage.

TfAP-2 is necessary for hemilineage 12A development

TfAP-2 expression is specific to hemilineage 12A in the VNC and its expression is necessary for wildtype development of the dorsal arbors. Using RNA-seq, I identified *TfAP-2* as a potentially interesting gene associated with a single hemilineage: hemilineage 12A. I found that manipulation of this gene shows it is involved in the early development of the hemilineage. I showed that *TfAP-2* is expressed specifically

in hemilineage 12A neurons, where it is necessary for wildtype morphological development. The dorsal branches of hemilineage 12A require *TfAP-2* expression. To test the sufficiency of TfAP-2 in generating 12A neuron identity distinct from 12B neuron identity, I attempted to change the morphology of 12B neurons with expression of TfAP-2, but saw no obvious difference from wildtype morphology. There are multiple reasons why I would see no morphological difference with this manipulation. This could be due to poor expression of the TF, which could be assayed through antibody staining of the genetically manipulated neurons. TfAP-2 may not be a master-regulator or "terminal selector" gene. It may simply be one of many TFs that combinatorially control 12A vs 12B identity. It is possible that TfAP-2 causes expression of genes associated with other aspects of 12B neuron identity, but not immature neuron morphology. Next steps in elucidating the role of TfAP-2 in this lineage are to 1) repeat the experiment with TfAP-2 antibody staining to compare levels of detectable TfAP-2 protein between 12A and 12B neurons, 2) determine which genes are affected by TfAP-2 removal in 12A and/or addition in 12B, including genes such as those responsible for neurotransmitter type.

Supplemental tables

Differentially and commonly expressed genes in immature neurons compared to mature neurons

Gene	Immature	Mature	Immature/Mature
Antp	242	110	2.2
CG11030	247	61	4.1
CG12071	178	85	2.1
CG17838	317	134	2.4
CG2052	559	76	7.3
CG2083	251	105	2.4
CG32676	150	72	2.1
CG3408	195	93	2.1
CG42251	142	58	2.4
CG6854	193	76	2.5
CG7971	244	103	2.4
Jupiter	820	298	2.8
Nrt	221	68	3.2
bif	116	53	2.2
br	551	115	4.8
brat	634	313	2.0
cenG1A	119	37	3.2
chinmo	235	75	3.1
chn	232	90	2.6
fne	797	267	3.0
hang	247	119	2.1
hdc	1088	394	2.8
hth	846	358	2.4
jim	1521	240	6.3
jing	159	64	2.5
l(3)neo38	901	392	2.3
lola	983	442	2.2
nerfin-1	138	35	3.9
noe	8152	2834	2.9
pdm3	156	57	2.8
pncr002:3R	135	17	7.9
ppa	161	66	2.4
pros	4419	324	13.6
sbb	158	71	2.2
spri	135	62	2.2
stan	113	38	3.0
su(w[a])	186	82	2.3

Table 3.S12 | Highly expressed genes enriched in immature neurons relative to mature neurons (2-fold, q<0.1, >100 FPKM). Numbers are genes expression values in FPKM.

Gene	Immature	Mature	Mature/Immature
7B2	91	516	5.7
AP-2sigma	50	191	3.8
Ald	143	841	5.9
Atpalpha	246	703	2.9
CG10186	7	109	14.6

Gene	Immature	Mature	Mature/Immature
CG10830	37	121	3.3
CG11071	26	148	5.6
CG11317	37	210	5.7
CG12858	13	106	7.9
CG13253	25	103	4.0
CG13830	214	490	2.3
CG14509	8	111	14.3
CG14762	56	223	4.0
CG14989	926	2218	2.4
CG1600	77	168	2.2
CG17124	233	676	2.9
CG2269	136	276	2.0
CG31030	65	142	2.2
CG31221	47	388	8.2
CG31665	35	113	3.2
CG34360	28	193	7.0
CG3662	104	375	3.6
CG42540	29	168	5.8
CG4577	8	172	22.6
CG6767	48	132	2.7
CG6770	101	259	2.6
CG7433	37	106	2.9
CG7781	96	273	2.8
CG8029	38	102	2.7
CG8216	12	103	8.5
CG8861	11	142	13.6
CG9003	32	100	3.2
CG9368	102	210	2.1
CG9413	38	141	3.7
CR18854	69	149	2.2
Cam	1275	3999	3.1
CanB	338	692	2.0
Cbp53E	17	182	11.0
DopEcR	67	178	2.7
Drep-1	27	100	3.8
Drep-2	65	148	2.3
Drep-3	40	216	5.4
EcR	65	230	3.6
Eip74EF	34	368	10.9
Eno	86	288	3.4
Fas1	240	586	2.4
Frq1	66	182	2.7
G-oalpha47A	453	967	2.1
Gad1	52	158	3.0
Gapdh1	49	247	5.1
Gapdh2	79	435	5.5
Ggamma1	372	1094	2.9
GlyP	20	120	6.1
Hex-A	44	121	2.8
Hsp67Bc	87	429	4.9
Imp	17	113	6.7
Nckx30C	84	203	2.4
Nplp1	18	100	5.7
Obp44a	102	417	4.1
Pal	67	491	7.3
Pde1c	43	105	2.5
Pglym78	11	192	17.9

Gene	Immature	Mature	Mature/Immature
Pk61C	63	177	2.8
Pka-R2	82	225	2.7
PyK	29	191	6.5
Rab3	92	305	3.3
Rdl	23	122	5.3
Ric	51	265	5.2
Sap47	162	452	2.8
Snap	54	190	3.5
Snap25	44	147	3.4
Sox14	22	246	10.9
Src64B	114	326	2.9
Syn	57	137	2.4
Syt1	144	316	2.2
Syx1A	146	321	2.2
TM4SF	12	250	21.1
Tpi	30	168	5.6
Tsp66E	75	219	2.9
Ubi-p5E	102	225	2.2
VGlut	42	162	3.9
Vha13	70	237	3.4
Vha16	464	1061	2.3
Vha26	175	413	2.4
Vha44	88	255	2.9
Vha55	66	251	3.8
Vha68-1	59	183	3.1
VhaAC39	35	131	3.7
VhaM8.9	58	162	2.8
VhaPPA1-1	60	147	2.4
Wnt4	70	151	2.2
abd-A	46	242	5.3
amon	26	116	4.5
beat-Ia	37	101	2.8
bru-3	63	157	2.5
desat1	30	107	3.6
dpr12	49	105	2.1
dpr8	40	108	2.7
endoA	59	125	2.1
futsch	22	116	5.3
ia2	54	810	15.1
igl	53	140	2.6
kcc	9	126	13.8
klg	122	281	2.3
l(1)G0156	92	254	2.8
l(3)82Fd	102	250	2.4
mp	50	142	2.8
n-syb	209	546	2.6
nAcRbeta-64B	61	168	2.8
nrv3	518	1247	2.4
shi	91	226	2.5
skap	52	128	2.5
svr	82	184	2.3
synaptogyrin	51	185	3.6
tomosyn	42	108	2.5
unc-104	93	237	2.5
vri	38	253	6.6
zfh2	18	131	7.1

Table 3.S13 | Highly expressed genes enriched in mature neurons relative to immature neurons (2-fold, q<0.1, >100 FPKM). Numbers are genes expression values in FPKM.

Gene	Immature	Mature	Immature/Mature
14-3-3epsilon	3330	3006	1.1
14-3-3zeta	1939	3837	0.5
AGO1	194	155	1.3
ATPsyn-b	100	149	0.7
ATPsyn-beta	628	996	0.6
ATPsyn-d	238	284	0.8
Aac11	280	155	1.8
Act42A	788	796	1.0
Act5C	4364	3448	1.3
Akap200	877	764	1.1
Akt1	183	143	1.3
Alh	205	132	1.6
Amun	277	242	1.1
Ank2	351	273	1.3
Appl	823	903	0.9
Aps	196	173	1.1
Arf79F	721	959	0.8
Argk	818	446	1.8
Asator	127	113	1.1
Atf-2	103	182	0.6
Atg8a	138	220	0.6
B52	358	258	1.4
CG10077	305	249	1.2
CG10098	117	137	0.9
CG10326	196	148	1.3
CG10417	162	139	1.2
CG10641	222	148	1.5
CG10664	124	183	0.7
CG10713	107	138	0.8
CG10990	207	216	1.0
CG11148	112	104	1.1
CG11155	138	156	0.9
CG11267	235	343	0.7
CG11360	215	147	1.5
CG1142	130	157	0.8
CG11873	139	105	1.3
CG1240	464	252	1.8
CG12643	122	105	1.2
CG13298	763	928	0.8
CG13364	184	201	0.9
CG13551	230	243	0.9
CG13908	120	135	0.9
CG13928	1651	1389	1.2
CG13993	108	115	0.9
CG14235	228	236	1.0
CG14478	175	127	1.4
CG14715	115	155	0.7
CG15012	142	171	0.8
CG15628	143	141	1.0
CG15765	140	216	0.6
CG16791	193	125	1.5
CG16817	451	571	0.8

Gene	Immature	Mature	Immature/Mature
CG17385	134	146	0.9
CG1746	1114	1301	0.9
CG17471	139	167	0.8
CG17737	301	432	0.7
CG18811	146	130	1.1
CG1943	282	343	0.8
CG2249	333	360	0.9
CG2852	225	269	0.8
CG2862	279	210	1.3
CG2865	160	120	1.3
CG2924	154	139	1.1
CG2993	142	214	0.7
CG30172	537	706	0.8
CG30415	123	167	0.7
CG30423	221	211	1.1
CG3056	124	113	1.1
CG31051	104	103	1.0
CG31140	346	299	1.2
CG31715	165	163	1.0
CG31998	150	108	1.4
CG32230	222	353	0.6
CG32264	142	109	1.3
CG32458	129	114	1.1
CG33199	146	152	1.0
CG3321	227	245	0.9
CG33229	453	316	1.4
CG33558	203	138	1.5
CG33936	342	436	0.8
CG33960	132	109	1.2
CG34362	125	146	0.9
CG3689	155	101	1.5
CG3800	1012	916	1.1
CG40045	295	330	0.9
CG40451	344	395	0.9
CG40498	113	155	0.7
CG4068	207	138	1.5
CG41518	122	320	0.4
CG42492	540	505	1.1
CG42574	165	131	1.3
CG42575	167	328	0.5
CG42621	106	129	0.8
CG42622	1148	3326	0.3
CG42724	218	109	2.0
CG4300	133	172	0.8
CG4502	120	110	1.1
CG4612	146	148	1.0
CG4692	230	227	1.0
CG5151	155	159	1.0
CG5525	144	221	0.7
CG5676	311	363	0.9
CG5830	147	197	0.7
CG6024	255	289	0.9
CG6115	150	120	1.2
CG6180	116	115	1.0
CG6719	109	116	0.9
CG6783	983	989	1.0
CG6982	178	194	0.9

Gene	Immature	Mature	Immature/Mature
CG7033	134	156	0.9
CG7048	200	210	0.9
CG7484	109	108	1.0
CG7630	133	261	0.5
CG7646	158	250	0.6
CG7911	174	184	0.9
CG8108	224	158	1.4
CG8188	144	135	1.1
CG8223	154	132	1.2
CG8258	116	158	0.7
CG8709	105	139	0.8
CG8860	194	149	1.3
CG8963	198	213	0.9
CG9099	148	177	0.8
CG9135	138	100	1.4
CG9363	466	539	0.9
CG9548	167	134	1.2
CG9603	199	288	0.7
CG9636	167	132	1.3
CG9705	233	191	1.2
CG9821	666	629	1.1
CG9894	1488	1040	1.4
CG9919	256	259	1.0
CHKov1	135	154	0.9
CR32028	488	292	1.7
CR33987	171	110	1.6
CR42862	1286	931	1.4
CaMKI	183	204	0.9
CaMKII	275	388	0.7
CadN	227	169	1.3
Caki	148	224	0.7
Caps	223	228	1.0
Cbp20	155	178	0.9
Cct5	109	161	0.7
Cdc42	146	164	0.9
Cdk5alpha	203	227	0.9
Cip4	142	103	1.4
Cirl	171	129	1.3
CkIIalpha	198	216	0.9
CkIIbeta	322	363	0.9
CkIalpha	149	216	0.7
CoVa	300	360	0.8
Crc	240	254	0.9
Crk	124	164	0.8
Csp	185	352	0.5
CtBP	185	110	1.7
CycG	265	228	1.2
Cyp1	1010	1299	0.8
D1	375	314	1.2
DIP1	254	175	1.5
DIP2	109	118	0.9
Dcp2	161	111	1.5
Dek	172	104	1.7
Df31	3686	2762	1.3
Dg	270	152	1.8
Dlc90F	115	165	0.7
DnaJ-1	207	278	0.7

Gene	Immature	Mature	Immature/Mature
Dpy-30L1	163	104	1.6
Droj2	229	321	0.7
Dscam	233	178	1.3
E(bx)	202	129	1.6
ERp60	223	189	1.2
Eaat2	105	104	1.0
Ef1alpha100E	1926	2137	0.9
Ef1alpha48D	944	1652	0.6
Ef1beta	348	470	0.7
Ef1gamma	261	340	0.8
Ef2b	369	570	0.6
Eip75B	517	445	1.2
Elongin-C	154	180	0.9
Eph	120	129	0.9
FK506-bp2	388	612	0.6
FKBP59	157	147	1.1
Fer1HCH	219	425	0.5
Fer2LCH	359	672	0.5
Fim	129	103	1.3
Fis1	105	220	0.5
Fmr1	146	139	1.1
G-salpha60A	100	147	0.7
Gbeta13F	503	536	0.9
Gdi	260	373	0.7
Ggamma30A	1296	1381	0.9
Gp93	106	117	0.9
HP4	138	121	1.1
His2A:CG33820	233	361	0.6
His2A:CG33835	756	1028	0.7
His2Av	423	283	1.5
His3.3B	2376	1701	1.4
His4r	5780	5479	1.1
HmgD	955	735	1.3
HmgZ	399	518	0.8
Hop	167	153	1.1
Hrb27C	471	361	1.3
Hrb87F	279	300	0.9
Hrb98DE	977	739	1.3
Hsc70-3	356	390	0.9
Hsc70-4	825	903	0.9
Hsp22	114	189	0.6
Hsp23	3442	3021	1.1
Hsp26	290	295	1.0
Hsp27	2457	1844	1.3
Hsp67Ba	442	311	1.4
Hsp68	205	243	0.8
Hsp83	676	652	1.0
Hsromega	626	358	1.8
Jafrac1	224	250	0.9
KdelR	127	132	1.0
Lis-1	159	220	0.7
Lk6	248	149	1.7
MED21	119	129	0.9
MESK2	116	116	1.0
Map205	164	148	1.1
Mapmodulin	532	520	1.0
Mgstl	103	202	0.5

Gene	Immature	Mature	Immature/Mature
Mlf	150	176	0.9
Mob4	198	233	0.8
Mpcp	170	337	0.5
Msp-300	176	237	0.7
NAT1	189	275	0.7
Nacalpha	572	542	1.1
Nap1	208	280	0.7
Neb-cGP	275	326	0.8
Nlp	971	722	1.3
Ntf-2	201	182	1.1
Oda	180	250	0.7
Oscp	172	209	0.8
PDCD-5	122	194	0.6
PHGPx	128	128	1.0
PMCA	290	331	0.9
PP2A-B'	163	147	1.1
PPP4R2r	242	169	1.4
PRL-1	181	222	0.8
Pabp2	102	113	0.9
Paip2	123	137	0.9
Pdi	368	393	0.9
Pep	395	240	1.6
Pka-C1	306	293	1.0
Pka-R1	136	215	0.6
Pp1-87B	221	234	0.9
Pp2A-29B	175	183	1.0
Pros25	312	347	0.9
Pros35	113	144	0.8
Prosalpha5	114	155	0.7
Prosalpha7	149	207	0.7
Prosbeta1	159	221	0.7
Ptp99A	147	108	1.4
Qm	2157	2703	0.8
RYBP	124	168	0.7
Rab1	173	201	0.9
Rab11	178	244	0.7
Rab2	151	179	0.8
Rab35	246	220	1.1
Rab5	154	172	0.9
Rab6	124	153	0.8
Rack1	357	431	0.8
Rbp1-like	280	142	2.0
Rbp2	173	175	1.0
Rbp6	244	178	1.4
Rho1	558	583	1.0
RhoGAPp190	115	109	1.1
RhoGDI	269	303	0.9
Rm62	837	496	1.7
Roc1a	135	132	1.0
RpL10Ab	843	953	0.9
RpL11	969	1079	0.9
RpL12	993	1088	0.9
RpL13	1055	1106	1.0
RpL13A	914	944	1.0
RpL14	1015	998	1.0
RpL15	1109	1683	0.7
RpL17	370	488	0.8

Gene	Immature	Mature	Immature/Mature
RpL18	606	759	0.8
RpL18A	996	1097	0.9
RpL19	1000	1173	0.9
RpL21	910	1258	0.7
RpL22	249	318	0.8
RpL23	984	1353	0.7
RpL23A	864	1001	0.9
RpL24	988	871	1.1
RpL26	730	1065	0.7
RpL27	808	875	0.9
RpL27A	977	1102	0.9
RpL28	1022	931	1.1
RpL29	1979	2221	0.9
RpL3	400	472	0.8
RpL30	991	992	1.0
RpL31	1656	1790	0.9
RpL32	906	1182	0.8
RpL34a	202	244	0.8
RpL34b	153	160	1.0
RpL35	993	1075	0.9
RpL35A	464	639	0.7
RpL36	1279	1603	0.8
RpL36A	914	1093	0.8
RpL37A	603	603	1.0
RpL37a	441	538	0.8
RpL38	660	532	1.2
RpL39	2095	1797	1.2
RpL4	401	430	0.9
RpL40	2245	1900	1.2
RpL41	8466	8461	1.0
RpL5	826	1092	0.8
RpL6	562	676	0.8
RpL7	715	1006	0.7
RpL7A	694	726	1.0
RpL8	694	753	0.9
RpL9	826	984	0.8
RpLP0	372	367	1.0
RpLP1	1068	1213	0.9
RpLP2	759	855	0.9
RpS10b	743	851	0.9
RpS11	1605	1465	1.1
RpS12	1137	1086	1.0
RpS13	1360	1473	0.9
RpS14a	1034	1044	1.0
RpS14b	651	586	1.1
RpS15	2570	2663	1.0
RpS15Aa	882	1176	0.8
RpS16	1244	1388	0.9
RpS17	1056	1162	0.9
RpS18	1654	1752	0.9
RpS19a	1313	1345	1.0
RpS20	1008	1034	1.0
RpS23	1647	1434	1.1
RpS24	575	589	1.0
RpS25	939	1089	0.9
RpS26	853	880	1.0
RpS27	1499	1340	1.1

Gene	Immature	Mature	Immature/Mature
RpS27A	1892	2280	0.8
RpS28b	1019	1237	0.8
RpS29	1073	1051	1.0
RpS3	2269	3017	0.8
RpS30	1116	1163	1.0
RpS3A	1115	1281	0.9
RpS4	570	637	0.9
RpS5a	591	610	1.0
RpS6	954	1034	0.9
RpS7	2591	2780	0.9
RpS8	949	1180	0.8
RpS9	1117	1210	0.9
Rpn11	143	219	0.7
Rpn6	105	149	0.7
Rsf1	436	237	1.8
Rtnl1	102	135	0.8
SF2	244	163	1.5
SKIP	170	120	1.4
Sam-S	186	149	1.3
Sdc	202	380	0.5
Sec61alpha	131	128	1.0
Sec61beta	122	114	1.1
Sec61gamma	111	117	0.9
Sema-1a	155	109	1.4
Set	256	143	1.8
Sh	116	132	0.9
Sh3beta	150	219	0.7
SmD2	143	129	1.1
SmE	143	126	1.1
SmG	264	169	1.6
Sod	295	274	1.1
Spase12	111	113	1.0
Su(var)205	535	389	1.4
Suv4-20	134	102	1.3
Sxl	171	120	1.4
Syt4	164	190	0.9
T-cp1	139	135	1.0
TER94	189	253	0.7
Tao-1	198	147	1.3
Tapdelta	103	101	1.0
Tctp	1938	3297	0.6
Ten-m	237	202	1.2
TfIIA-S	297	293	1.0
Thd1	245	188	1.3
Tm1	161	114	1.4
Tom7	180	309	0.6
Top1	159	161	1.0
Tsp97E	268	326	0.8
Txl	124	135	0.9
Uba1	208	187	1.1
UbcD6	103	142	0.7
Ubi-p63E	113	137	0.8
Uch	248	319	0.8
Ucrh	295	289	1.0
Uev1A	262	305	0.9
Unr	197	122	1.6
Vap-33-1	165	210	0.8

Gene	Immature	Mature	Immature/Mature
Yeti	175	195	0.9
Zyx102EF	145	142	1.0
akirin	168	177	1.0
alphaTub84B	991	1377	0.7
alphaTub84D	102	150	0.7
arm	174	209	0.8
awd	651	571	1.1
bel	101	105	1.0
ben	346	385	0.9
beta-Spec	117	100	1.2
betaTub56D	838	1051	0.8
bic	637	755	0.8
bip2	139	125	1.1
bl	219	196	1.1
blw	307	433	0.7
bun	303	349	0.9
cals	143	258	0.6
casp	119	177	0.7
caz	131	106	1.2
cg	180	113	1.6
chic	1690	1498	1.1
chrb	205	315	0.6
cib	1831	1050	1.7
cl	372	356	1.0
cpx	420	611	0.7
crc	180	263	0.7
crp	244	149	1.6
ctp	982	832	1.2
cype	157	232	0.7
dco	140	113	1.2
dpr7	145	220	0.7
drk	199	152	1.3
e(r)	169	179	0.9
eEF1delta	155	122	1.3
eIF-1A	259	406	0.6
eIF-3p40	163	183	0.9
eIF-4B	168	134	1.3
eIF-4E	336	359	0.9
eIF-4a	495	710	0.7
eIF-5A	981	994	1.0
eIF3-S9	120	181	0.7
eIF4G	158	194	0.8
eIF5	188	232	0.8
eff	432	424	1.0
elav	394	240	1.6
emc	164	195	0.8
endos	251	247	1.0
exba	342	480	0.7
fas	100	131	0.8
fax	1496	1589	0.9
flfl	168	134	1.3
flower	161	341	0.5
gfA	183	127	1.4
gish	136	124	1.1
glec	135	156	0.9
glo	375	278	1.3
gpp	175	125	1.4

Gene	Immature	Mature	Immature/Mature
growl	155	136	1.1
gw	194	158	1.2
hkl	295	211	1.4
hts	216	182	1.2
janA	134	103	1.3
kis	423	301	1.4
kuk	137	109	1.3
l(1)G0230	256	300	0.9
l(1)G0320	311	308	1.0
l(2)06225	101	120	0.8
l(2)NC136	135	127	1.1
l(2)k16918	233	143	1.6
l(3)01239	280	259	1.1
lark	136	122	1.1
larp	136	141	1.0
levy	411	523	0.8
lig	152	124	1.2
lolal	314	375	0.8
lwr	107	112	1.0
mam	203	139	1.5
mask	129	115	1.1
mbf1	153	171	0.9
mbl	215	178	1.2
miple	1638	1709	1.0
mmd	116	122	1.0
mnb	186	109	1.7
mod(mdg4)	607	361	1.7
msn	132	152	0.9
mtacp1	136	165	0.8
mts	296	288	1.0
mub	160	130	1.2
mura	148	120	1.2
nAcRalpha-34E	116	103	1.1
nmo	237	312	0.8
nocte	184	120	1.5
nonA	171	118	1.4
oho23B	602	565	1.1
p130CAS	107	109	1.0
pAbp	968	868	1.1
par-1	172	153	1.1
plexA	215	211	1.0
plexB	139	102	1.4
pnut	165	159	1.0
pod1	287	164	1.7
porin	265	454	0.6
prominin-like	165	327	0.5
qkr58E-3	149	108	1.4
qvr	132	170	0.8
ran	473	506	0.9
rin	229	256	0.9
rl	150	134	1.1
roX1	1001	1055	0.9
roX2	476	213	2.2
rump	243	204	1.2
sar1	191	220	0.9
scrt	183	134	1.4
scyl	238	281	0.8

Gene	Immature	Mature	Immature/Mature
sesB	426	662	0.6
sgg	138	166	0.8
shep	607	506	1.2
skpA	600	550	1.1
sm	533	275	1.9
smt3	1630	1213	1.3
sn	438	269	1.6
snf	138	151	0.9
snmRNA:158	473	679	0.7
snmRNA:331	12657	3592	3.5
snmRNA:641	148	113	1.3
snoRNA:Psi18S-1377c	221	523	0.4
snoRNA:Psi18S-1389a	233	202	1.2
snoRNA:Psi28S-1060	399	524	0.8
snoRNA:Psi28S-1192a	190	236	0.8
snoRNA:Psi28S-3436a	491	759	0.6
sop	1128	1181	1.0
spen	281	172	1.6
spi	167	104	1.6
sqd	447	274	1.6
sta	598	533	1.1
stai	154	181	0.8
stau	114	136	0.8
tacc	179	180	1.0
tau	106	146	0.7
th	234	160	1.5
tinc	143	112	1.3
tral	167	120	1.4
tsh	152	112	1.4
tsr	1709	1676	1.0
tsu	167	160	1.0
unc-13	394	353	1.1
vig	239	252	0.9
vsg	108	172	0.6
wdb	201	182	1.1
yps	413	263	1.6

Table 3.S14 | Intersection of highly expressed genes (100 FPKM) in mature and immature neurons. Numbers are gene expression values in FPKM.

Differentially and commonly expressed genes in young immature neurons compared to old immature neurons

Gene	Young	Old	Young/Old
14-3-3epsilon	3149	3321	0.9
14-3-3zeta	1862	2493	0.7
AGO1	191	158	1.2
ATPsyn-b	114	106	1.1
ATPsyn-beta	597	755	0.8
ATPsyn-d	192	254	0.8
Aac11	277	243	1.1
Act42A	715	766	0.9
Act5C	4102	4154	1.0
Akap200	922	848	1.1
Akt1	197	172	1.1
Alh	237	192	1.2
Amun	368	263	1.4
Ank2	352	301	1.2
Antp	339	241	1.4
Appl	766	872	0.9
Aps	149	146	1.0
Arf79F	900	838	1.1
Argk	741	702	1.1
Art4	147	137	1.1
Asator	116	121	1.0
Atg8a	173	162	1.1
Atpalpha	272	347	0.8
B52	448	330	1.4
Bap55	107	107	1.0
Bap60	136	123	1.1
Bsg	103	105	1.0
Bx	135	108	1.3
CG10077	313	283	1.1
CG10098	109	125	0.9
CG10326	216	183	1.2
CG10417	218	182	1.2
CG10508	137	140	1.0
CG10641	185	166	1.1
CG10777	134	112	1.2
CG10990	235	216	1.1
CG11030	223	190	1.2
CG11148	120	115	1.0
CG11155	133	155	0.9
CG11267	199	359	0.6
CG11360	200	185	1.1
CG1142	168	157	1.1
CG11873	132	112	1.2
CG12054	137	114	1.2
CG12071	181	174	1.0
CG1240	476	413	1.2
CG13298	733	956	0.8
CG13364	193	214	0.9
CG1354	105	103	1.0
CG13551	203	258	0.8
CG13830	168	230	0.7
CG13928	1486	1492	1.0

Gene	Young	Old	Young/Old
CG14213	110	102	1.1
CG14235	235	230	1.0
CG14478	198	186	1.1
CG14715	122	157	0.8
CG14989	852	1106	0.8
CG15012	110	174	0.6
CG15628	149	148	1.0
CG15735	140	125	1.1
CG16791	193	169	1.1
CG16817	418	447	0.9
CG17124	213	259	0.8
CG17202	138	103	1.3
CG17385	116	144	0.8
CG1746	980	1205	0.8
CG17471	136	155	0.9
CG17737	303	364	0.8
CG17838	310	261	1.2
CG18811	141	123	1.1
CG1890	128	107	1.2
CG1910	238	137	1.7
CG1943	240	284	0.8
CG2052	502	371	1.4
CG2083	258	195	1.3
CG2249	242	309	0.8
CG2852	206	217	0.9
CG2862	254	272	0.9
CG2865	138	101	1.4
CG2924	148	133	1.1
CG30172	396	595	0.7
CG30389	130	122	1.1
CG30415	105	126	0.8
CG30423	203	192	1.1
CG3056	131	123	1.1
CG31140	269	294	0.9
CG31715	183	177	1.0
CG31998	148	130	1.1
CG32016	118	123	1.0
CG32230	299	327	0.9
CG32264	121	134	0.9
CG32676	145	127	1.1
CG32810	119	110	1.1
CG33199	122	147	0.8
CG3321	179	235	0.8
CG33229	400	358	1.1
CG33558	211	177	1.2
CG33691	145	113	1.3
CG33936	374	371	1.0
CG33960	126	130	1.0
CG3408	200	200	1.0
CG34362	108	133	0.8
CG3662	105	149	0.7
CG3689	171	146	1.2
CG3800	1297	993	1.3
CG40045	291	339	0.9
CG40451	330	381	0.9
CG4068	184	175	1.1
CG42251	120	126	1.0

Gene	Young	Old	Young/Old
CG42492	506	507	1.0
CG42574	167	148	1.1
CG42575	182	193	0.9
CG42622	824	864	1.0
CG42724	227	177	1.3
CG4300	123	146	0.8
CG4502	116	107	1.1
CG4612	152	140	1.1
CG4692	203	260	0.8
CG4747	118	103	1.2
CG5151	126	135	0.9
CG5525	137	167	0.8
CG5642	116	111	1.1
CG5676	307	335	0.9
CG5746	150	111	1.4
CG5830	152	159	1.0
CG6024	329	278	1.2
CG6084	122	100	1.2
CG6115	136	157	0.9
CG6422	111	106	1.0
CG6719	106	115	0.9
CG6783	933	1095	0.9
CG6854	154	157	1.0
CG6982	176	197	0.9
CG7033	148	128	1.2
CG7048	242	230	1.1
CG7484	107	124	0.9
CG7630	171	183	0.9
CG7646	178	211	0.8
CG7911	201	186	1.1
CG7971	260	225	1.2
CG8108	206	196	1.1
CG8188	143	135	1.1
CG8223	122	142	0.9
CG8258	123	125	1.0
CG8860	248	216	1.1
CG8963	225	210	1.1
CG9099	139	175	0.8
CG9135	198	121	1.6
CG9344	122	116	1.1
CG9363	576	421	1.4
CG9548	185	152	1.2
CG9603	216	214	1.0
CG9636	132	134	1.0
CG9705	218	242	0.9
CG9821	534	590	0.9
CG9894	2314	1373	1.7
CG9919	219	250	0.9
CHKov1	107	120	0.9
CR32028	487	421	1.2
CR33328	173	139	1.2
CR33987	102	127	0.8
CR42862	1193	1065	1.1
CaMKI	214	196	1.1
CaMKII	261	292	0.9
CadN	184	204	0.9
Caki	129	153	0.8

Gene	Young	Old	Young/Old
Cam	1122	1721	0.7
CanB	340	433	0.8
Caps	208	220	0.9
Cbp20	211	169	1.2
Cct5	116	127	0.9
Cdc42	153	153	1.0
Cdk5alpha	191	203	0.9
Cip4	127	131	1.0
Cirl	168	163	1.0
CkIIalpha	254	245	1.0
CkIIbeta	377	335	1.1
CkIalpha	157	159	1.0
CoVa	281	315	0.9
Crc	242	217	1.1
Crk	136	148	0.9
Csp	194	215	0.9
CtBP	177	171	1.0
CycG	226	243	0.9
Cyp1	953	1021	0.9
D1	473	374	1.3
DIP1	228	210	1.1
DIP2	129	130	1.0
Dcp2	166	161	1.0
Dek	210	157	1.3
Df31	3835	3570	1.1
Dg	261	271	1.0
Dlc90F	130	132	1.0
DnaJ-1	127	161	0.8
Droj2	206	212	1.0
Dscam	214	197	1.1
Dsp1	176	146	1.2
E(bx)	266	190	1.4
E2f	105	104	1.0
ERp60	234	207	1.1
Ef1alpha100E	1629	2097	0.8
Ef1alpha48D	1956	1128	1.7
Ef1beta	416	449	0.9
Ef1gamma	329	290	1.1
Ef2b	436	373	1.2
Eip75B	421	407	1.0
Elongin-C	165	135	1.2
Eph	128	125	1.0
FK506-bp2	368	439	0.8
FKBP59	126	150	0.8
Fas1	222	255	0.9
Fer1HCH	206	249	0.8
Fer2LCH	301	401	0.7
Fim	110	112	1.0
Flo	156	157	1.0
Fmr1	166	147	1.1
G-oalpha47A	493	590	0.8
Gbeta13F	516	504	1.0
Gdi	288	320	0.9
Ggamma1	395	545	0.7
Ggamma30A	902	1342	0.7
Gprk1	119	113	1.1
HIP-R	130	102	1.3

Gene	Young	Old	Young/Old
HP4	169	173	1.0
Hel25E	196	151	1.3
His2A:CG33820	436	266	1.6
His2A:CG33835	1352	750	1.8
His2Av	688	498	1.4
His3.3A	143	121	1.2
His3.3B	2189	2168	1.0
His4r	4378	5980	0.7
HmgD	1768	1135	1.6
HmgZ	623	550	1.1
Hop	161	156	1.0
Hrb27C	577	418	1.4
Hrb87F	432	315	1.4
Hrb98DE	1086	873	1.2
Hsc70-3	367	361	1.0
Hsc70-4	823	778	1.1
Hsp23	2564	3218	0.8
Hsp26	137	208	0.7
Hsp27	2249	2349	1.0
Hsp67Ba	308	388	0.8
Hsp83	485	482	1.0
Hsromega	775	507	1.5
Jafrac1	240	242	1.0
Jupiter	800	670	1.2
KdelR	108	114	0.9
Klc	112	125	0.9
Lam	177	119	1.5
Lis-1	156	157	1.0
Lk6	230	181	1.3
MED21	160	153	1.0
MESK2	117	106	1.1
MTA1-like	145	116	1.3
Map205	180	140	1.3
Mapmodulin	510	536	1.0
Mlf	134	138	1.0
Mob4	191	202	0.9
Mpcp	178	215	0.8
Msp-300	144	169	0.9
NAT1	178	165	1.1
NKAIN	121	108	1.1
Nacalpha	593	609	1.0
Nap1	194	240	0.8
Neb-cGP	222	291	0.8
Nedd8	148	139	1.1
Nlp	983	925	1.1
Nrt	326	194	1.7
Nrx-IV	117	105	1.1
Ntf-2	220	230	1.0
Obp44a	131	102	1.3
Oda	190	210	0.9
Oscp	152	185	0.8
PDCD-5	152	162	0.9
PHGPx	117	164	0.7
PMCA	294	303	1.0
PP2A-B'	147	157	0.9
PPP4R2r	220	212	1.0
PRL-1	165	187	0.9

Gene	Young	Old	Young/Old
Pabp2	161	143	1.1
Pcf11	164	160	1.0
Pdi	365	400	0.9
Pep	439	343	1.3
Pka-C1	300	291	1.0
Pka-R1	142	156	0.9
Pp1-87B	269	249	1.1
Pp2A-29B	167	189	0.9
Pros25	255	278	0.9
Pros35	107	141	0.8
Prosalpha5	122	108	1.1
Prosalpha7	156	147	1.1
Prosbeta1	148	186	0.8
Prp8	126	106	1.2
Ptp61F	104	106	1.0
Ptp69D	132	113	1.2
Ptp99A	162	143	1.1
Qm	2220	2407	0.9
Rab1	134	131	1.0
Rab11	162	197	0.8
Rab2	143	151	1.0
Rab35	237	216	1.1
Rab5	136	136	1.0
Rab6	127	112	1.1
Rack1	401	372	1.1
Rbp1-like	275	218	1.3
Rbp2	180	212	0.8
Rbp6	169	216	0.8
Rho1	581	578	1.0
RhoGDI	302	286	1.1
Rm62	803	701	1.1
Roc1a	131	128	1.0
RpII18	112	141	0.8
RpL10Ab	941	1055	0.9
RpL11	983	1139	0.9
RpL12	1056	1239	0.9
RpL13	995	1109	0.9
RpL13A	927	996	0.9
RpL14	1008	1115	0.9
RpL15	1442	1434	1.0
RpL17	414	456	0.9
RpL18	613	737	0.8
RpL18A	1095	1228	0.9
RpL19	1113	1183	0.9
RpL21	1087	1206	0.9
RpL22	304	289	1.1
RpL23	1072	1375	0.8
RpL23A	886	889	1.0
RpL24	980	1042	0.9
RpL26	842	957	0.9
RpL27	783	915	0.9
RpL27A	853	1099	0.8
RpL28	1096	1106	1.0
RpL29	1880	2231	0.8
RpL3	469	381	1.2
RpL30	943	1134	0.8
RpL31	1842	2021	0.9

Gene	Young	Old	Young/Old
RpL32	978	1141	0.9
RpL34a	219	240	0.9
RpL34b	138	151	0.9
RpL35	1034	988	1.0
RpL35A	490	568	0.9
RpL36	1228	1568	0.8
RpL36A	1066	1107	1.0
RpL37A	624	718	0.9
RpL37a	485	543	0.9
RpL38	532	700	0.8
RpL39	2195	2599	0.8
RpL4	451	429	1.1
RpL40	1901	2118	0.9
RpL41	8491	10522	0.8
RpL5	1098	998	1.1
RpL6	591	601	1.0
RpL7	846	915	0.9
RpL7A	593	791	0.8
RpL8	659	738	0.9
RpL9	933	1005	0.9
RpLP0	334	333	1.0
RpLP1	1444	1251	1.2
RpLP2	723	937	0.8
RpS10b	710	812	0.9
RpS11	1459	1791	0.8
RpS12	1024	1118	0.9
RpS13	1286	1414	0.9
RpS14a	901	1200	0.8
RpS14b	616	652	0.9
RpS15	2534	3115	0.8
RpS15Aa	1069	1228	0.9
RpS16	1308	1454	0.9
RpS17	1162	1241	0.9
RpS18	1782	2026	0.9
RpS19a	1257	1491	0.8
RpS20	1013	1200	0.8
RpS23	1441	1678	0.9
RpS24	607	659	0.9
RpS25	1019	1119	0.9
RpS26	794	928	0.9
RpS27	1578	1706	0.9
RpS27A	1895	2335	0.8
RpS28b	1108	1458	0.8
RpS29	1214	1371	0.9
RpS3	2666	2868	0.9
RpS30	1152	1319	0.9
RpS3A	1307	1303	1.0
RpS4	614	637	1.0
RpS5a	661	644	1.0
RpS6	1026	1097	0.9
RpS7	2854	2775	1.0
RpS8	986	1098	0.9
RpS9	1128	1193	0.9
Rpn11	157	169	0.9
Rpn6	108	116	0.9
Rsf1	436	396	1.1
SC35	165	150	1.1

Gene	Young	Old	Young/Old
SF2	293	245	1.2
SKIP	174	159	1.1
Sam-S	151	171	0.9
Sap47	112	191	0.6
Sdc	162	219	0.7
Sec61alpha	131	113	1.2
Sec61beta	115	134	0.9
Sema-1a	178	135	1.3
Set	322	203	1.6
Sh3beta	146	167	0.9
SmD2	169	164	1.0
SmE	135	174	0.8
SmG	320	267	1.2
Smox	121	118	1.0
Sod	199	285	0.7
Spase12	101	110	0.9
Spase22-23	127	122	1.0
Src64B	135	121	1.1
Su(var)2-10	127	105	1.2
Su(var)205	470	499	0.9
Suv4-20	135	131	1.0
Sxl	213	169	1.3
Syt1	105	175	0.6
Syt4	160	170	0.9
Syx1A	139	160	0.9
T-cp1	144	139	1.0
TER94	219	196	1.1
Tao-1	190	167	1.1
Tapdelta	141	118	1.2
Tctp	2453	2370	1.0
Ten-m	240	225	1.1
TfIIA-S	310	313	1.0
Thd1	258	234	1.1
Tm1	199	146	1.4
Tom7	174	201	0.9
Top1	166	154	1.1
Tsp97E	273	282	1.0
Uba1	232	212	1.1
UbcD6	100	103	1.0
Ubi-p63E	101	109	0.9
Uch	190	246	0.8
Ucrh	255	366	0.7
Uev1A	251	287	0.9
Ulp1	152	130	1.2
Unr	197	152	1.3
Utx	136	108	1.3
Vap-33-1	162	167	1.0
Vha16	432	586	0.7
Vha26	128	186	0.7
Yeti	167	187	0.9
Zyx102EF	156	158	1.0
akirin	183	195	0.9
alph	137	112	1.2
alphaTub84B	1056	1084	1.0
alt	137	108	1.3
arm	187	199	0.9
awd	517	645	0.8

Gene	Young	Old	Young/Old
ben	321	318	1.0
beta-Spec	138	108	1.3
betaTub56D	821	911	0.9
bic	703	692	1.0
bif	124	107	1.2
bip2	146	147	1.0
bl	250	223	1.1
blw	350	357	1.0
br	488	444	1.1
brat	571	475	1.2
bun	296	305	1.0
cals	158	164	1.0
casp	128	138	0.9
caz	165	128	1.3
cg	176	167	1.1
chic	2088	1789	1.2
chinmo	227	187	1.2
chn	178	182	1.0
chrb	194	209	0.9
cib	2111	1900	1.1
cl	343	372	0.9
cpx	233	407	0.6
crc	202	182	1.1
crol	199	160	1.2
crp	217	193	1.1
ctp	1009	942	1.1
cype	181	213	0.9
d4	133	116	1.1
dco	136	140	1.0
dock	144	129	1.1
dom	141	110	1.3
dpr7	124	169	0.7
drk	224	197	1.1
e(r)	194	169	1.1
eEF1delta	139	157	0.9
eIF-1A	314	321	1.0
eIF-3p40	192	190	1.0
eIF-4B	189	158	1.2
eIF-4E	307	350	0.9
eIF-4a	604	612	1.0
eIF-5A	1052	1045	1.0
eIF3-S9	152	140	1.1
eIF4G	187	164	1.1
eIF4G2	164	125	1.3
eIF5	182	207	0.9
eff	430	408	1.1
elav	559	344	1.6
emc	195	157	1.2
endos	253	263	1.0
exba	388	393	1.0
fax	1551	1483	1.0
fd68A	130	120	1.1
flfl	186	148	1.3
flower	124	217	0.6
fne	894	757	1.2
fz2	116	114	1.0
gfA	115	146	0.8

Gene	Young	Old	Young/Old
gish	181	148	1.2
glec	198	155	1.3
glo	464	360	1.3
gpp	161	143	1.1
growl	156	170	0.9
gus	107	102	1.0
gw	196	189	1.0
hang	200	194	1.0
hdc	983	804	1.2
hkl	306	284	1.1
hth	928	692	1.3
hts	212	192	1.1
icln	127	122	1.0
janA	135	120	1.1
jim	1181	1139	1.0
jing	183	110	1.7
kis	493	376	1.3
klg	162	170	1.0
kuk	176	154	1.1
l(1)G0156	114	138	0.8
l(1)G0230	226	266	0.9
l(1)G0289	144	117	1.2
l(1)G0320	289	270	1.1
l(2)06225	102	120	0.9
l(2)NC136	165	146	1.1
l(2)k16918	209	204	1.0
l(3)01239	286	248	1.2
l(3)L1231	116	101	1.2
l(3)neo38	1345	914	1.5
lark	164	137	1.2
larp	121	122	1.0
levy	320	467	0.7
lig	152	125	1.2
lola	1463	845	1.7
lolal	390	347	1.1
lwr	107	123	0.9
mam	193	167	1.2
mask	131	117	1.1
mbf1	162	153	1.1
mbl	211	217	1.0
me31B	133	122	1.1
miple	1375	1569	0.9
miple2	102	102	1.0
mnb	190	162	1.2
mod(mdg4)	635	558	1.1
msi	137	119	1.1
msn	130	120	1.1
mtacp1	132	146	0.9
mts	290	273	1.1
mub	183	176	1.0
n-syb	147	253	0.6
nmo	248	219	1.1
nocte	172	156	1.1
noe	3735	4115	0.9
nonA	153	133	1.2
nrv3	426	618	0.7
oho23B	581	631	0.9

Gene	Young	Old	Young/Old
onecut	137	108	1.3
p120ctn	109	113	1.0
p130CAS	111	114	1.0
pAbp	831	827	1.0
par-1	188	178	1.1
pdm3	131	177	0.7
pho	115	118	1.0
plexA	215	225	1.0
plexB	168	133	1.3
pnut	136	153	0.9
pod1	287	253	1.1
porin	291	313	0.9
ppa	167	121	1.4
prominin-like	122	173	0.7
pros	3382	2945	1.1
pum	130	115	1.1
qkr54B	121	107	1.1
qkr58E-3	147	153	1.0
ran	496	437	1.1
rin	236	208	1.1
rl	154	168	0.9
roX1	1040	968	1.1
roX2	338	342	1.0
robo	101	106	1.0
rump	243	245	1.0
sar1	186	177	1.1
sbb	128	120	1.1
scrt	186	161	1.2
scyl	327	275	1.2
seq	180	124	1.5
sesB	393	486	0.8
sgg	138	132	1.0
shep	499	500	1.0
sick	134	117	1.1
simj	140	130	1.1
siz	109	106	1.0
skpA	491	544	0.9
sm	647	550	1.2
smt3	1915	1692	1.1
sn	398	424	0.9
snf	117	144	0.8
snmRNA:158	379	340	1.1
snmRNA:331	7658	6046	1.3
snmRNA:641	138	119	1.2
snoRNA:MeU5-C46	109	149	0.7
snoRNA:Psi18S-1377d	120	259	0.5
snoRNA:Psi18S-1389a	164	211	0.8
snoRNA:Psi28S-1060	308	350	0.9
snoRNA:Psi28S-3305c	104	186	0.6
snoRNA:Psi28S-3436a	193	195	1.0
sop	1012	1235	0.8
spen	285	228	1.2
spi	163	153	1.1
spri	105	106	1.0
sqd	542	414	1.3
sta	554	530	1.0
stai	148	168	0.9

Gene	Young	Old	Young/Old
stau	107	101	1.1
su(w[a])	159	168	0.9
tacc	178	205	0.9
th	205	188	1.1
tinc	109	116	0.9
tmod	120	109	1.1
tou	191	135	1.4
tral	160	142	1.1
tsh	167	128	1.3
tsr	1651	1969	0.8
tsu	214	185	1.2
tud	110	110	1.0
unc-13	368	385	1.0
vig	187	226	0.8
vih	110	109	1.0
vsg	112	129	0.9
vtd	129	110	1.2
wdb	193	187	1.0
xl6	112	113	1.0
yps	446	373	1.2

Table 3.S15 | Intersection of highly expressed genes (100 FPKM) in younger immature and older immature neurons. Numbers are gene expression values in FPKM.

Differentially and commonly expressed genes in combined immature A and B neurons compared to immature A neurons

Gene	Immature	A	Immature/A
14-3-3epsilon	3330	2444	1.4
14-3-3zeta	1939	2433	0.8
26-29-p	103	106	1.0
AGO1	194	150	1.3
ATPsyn-beta	628	1115	0.6
ATPsyn-d	238	235	1.0
Aac11	280	224	1.2
Act42A	788	986	0.8
Act5C	4364	4103	1.1
Akap200	877	441	2.0
Akt1	183	163	1.1
Ald	143	258	0.6
Alh	205	124	1.6
Amun	277	150	1.8
Ank2	351	305	1.1
Antp	242	231	1.0
Appl	823	615	1.3
Aps	196	140	1.4
Arf79F	721	753	1.0
Argk	818	877	0.9
Art4	160	111	1.4
Asator	127	162	0.8
Atg8a	138	136	1.0
Atpalpha	246	334	0.7
B52	358	356	1.0
Bap60	133	118	1.1
Bx	145	126	1.2
CG10077	305	269	1.1
CG10098	117	154	0.8
CG10326	196	138	1.4
CG10417	162	198	0.8
CG10508	157	113	1.4
CG10641	222	171	1.3
CG10713	107	100	1.1
CG10990	207	222	0.9
CG11030	247	124	2.0
CG11148	112	111	1.0
CG11155	138	269	0.5
CG11267	235	269	0.9
CG11360	215	233	0.9
CG1142	130	144	0.9
CG12071	178	116	1.5
CG1240	464	307	1.5
CG12643	122	105	1.2
CG13298	763	796	1.0
CG13364	184	207	0.9
CG13551	230	193	1.2
CG13830	214	215	1.0
CG13928	1651	1405	1.2
CG14235	228	180	1.3
CG14459	102	141	0.7
CG14478	175	130	1.3

Gene	Immature	A	Immature/A
CG14715	115	187	0.6
CG14989	926	734	1.3
CG15012	142	127	1.1
CG15628	143	136	1.1
CG15735	153	142	1.1
CG16791	193	208	0.9
CG16817	451	294	1.5
CG17124	233	161	1.5
CG1746	1114	1067	1.0
CG17471	139	189	0.7
CG17698	102	111	0.9
CG17737	301	344	0.9
CG17838	317	287	1.1
CG18811	146	100	1.5
CG1890	129	131	1.0
CG1943	282	160	1.8
CG2052	559	372	1.5
CG2249	333	327	1.0
CG2269	136	118	1.2
CG2852	225	215	1.0
CG2862	279	281	1.0
CG2924	154	116	1.3
CG2993	142	137	1.0
CG30172	537	529	1.0
CG30389	135	105	1.3
CG30415	123	114	1.1
CG30423	221	202	1.1
CG31051	104	148	0.7
CG31140	346	336	1.0
CG31715	165	230	0.7
CG31998	150	146	1.0
CG32230	222	402	0.6
CG32264	142	113	1.3
CG32458	129	101	1.3
CG32676	150	129	1.2
CG33199	146	109	1.3
CG3321	227	224	1.0
CG33229	453	516	0.9
CG33558	203	146	1.4
CG33936	342	262	1.3
CG33960	132	102	1.3
CG3408	195	171	1.1
CG34362	125	115	1.1
CG3662	104	110	0.9
CG3689	155	131	1.2
CG3800	1012	735	1.4
CG40045	295	375	0.8
CG40451	344	418	0.8
CG40498	113	143	0.8
CG4068	207	188	1.1
CG41518	122	158	0.8
CG42251	142	109	1.3
CG42492	540	541	1.0
CG42574	165	130	1.3
CG42575	167	222	0.8
CG42621	106	127	0.8
CG42622	1148	1405	0.8

Gene	Immature	A	Immature/A
CG42724	218	158	1.4
CG4300	133	123	1.1
CG4612	146	142	1.0
CG4692	230	221	1.0
CG5525	144	179	0.8
CG5676	311	455	0.7
CG5830	147	173	0.9
CG6024	255	248	1.0
CG6180	116	100	1.2
CG6422	105	119	0.9
CG6783	983	822	1.2
CG6854	193	170	1.1
CG6982	178	180	1.0
CG7033	134	128	1.0
CG7048	200	226	0.9
CG7484	109	102	1.1
CG7630	133	135	1.0
CG7646	158	275	0.6
CG7911	174	135	1.3
CG7971	244	143	1.7
CG8108	224	131	1.7
CG8188	144	114	1.3
CG8223	154	119	1.3
CG8258	116	159	0.7
CG8300	138	131	1.1
CG8709	105	108	1.0
CG8860	194	255	0.8
CG8963	198	219	0.9
CG9099	148	152	1.0
CG9135	138	117	1.2
CG9363	466	322	1.4
CG9368	102	107	1.0
CG9548	167	149	1.1
CG9603	199	168	1.2
CG9636	167	145	1.1
CG9705	233	135	1.7
CG9821	666	474	1.4
CG9894	1488	1256	1.2
CG9919	256	288	0.9
CHKov1	135	139	1.0
CR32028	488	326	1.5
CR33328	134	135	1.0
CR42862	1286	1631	0.8
CaMKI	183	298	0.6
CaMKII	275	338	0.8
CadN	227	230	1.0
Caki	148	149	1.0
Cam	1275	1406	0.9
CanB	338	549	0.6
Caps	223	297	0.8
Cbp20	155	291	0.5
Cct5	109	153	0.7
Cdc42	146	131	1.1
Cdk5alpha	203	187	1.1
Cirl	171	169	1.0
CkIIalpha	198	286	0.7
CkIIbeta	322	323	1.0

Gene	Immature	A	Immature/A
CkIalpha	149	144	1.0
CoVa	300	284	1.1
Crc	240	194	1.2
Crk	124	209	0.6
Csp	185	211	0.9
CtBP	185	134	1.4
CycG	265	291	0.9
Cyp1	1010	1295	0.8
D1	375	283	1.3
DIP1	254	203	1.3
DIP2	109	146	0.7
Dcp2	161	130	1.2
Dek	172	107	1.6
Df31	3686	2864	1.3
Dg	270	239	1.1
DnaJ-1	207	165	1.3
Droj2	229	248	0.9
Dscam	233	193	1.2
Dsp1	153	129	1.2
E(bx)	202	178	1.1
ERp60	223	250	0.9
Eaat2	105	118	0.9
Ef1alpha100E	1926	1736	1.1
Ef1alpha48D	944	961	1.0
Ef1beta	348	264	1.3
Ef1gamma	261	210	1.2
Ef2b	369	438	0.8
Eip75B	517	377	1.4
Elongin-C	154	228	0.7
Eph	120	160	0.8
FK506-bp2	388	364	1.1
FKBP59	157	190	0.8
Fas1	240	206	1.2
Fer1HCH	219	198	1.1
Fer2LCH	359	284	1.3
Fim	129	111	1.2
Fis1	105	149	0.7
Flo	156	137	1.1
Fmr1	146	133	1.1
G-oalpha47A	453	471	1.0
G-salpha60A	100	124	0.8
Gbeta13F	503	451	1.1
Gdi	260	266	1.0
Ggamma1	372	519	0.7
Ggamma30A	1296	1048	1.2
Gprk1	106	147	0.7
HP4	138	150	0.9
Hel25E	163	155	1.0
His2A:CG33820	233	394	0.6
His2A:CG33835	756	865	0.9
His2Av	423	297	1.4
His3.3B	2376	2097	1.1
His4r	5780	6207	0.9
HmgD	955	844	1.1
HmgZ	399	425	0.9
Hop	167	136	1.2
Hrb27C	471	386	1.2

Gene	Immature	A	Immature/A
Hrb87F	279	232	1.2
Hrb98DE	977	588	1.7
Hsc70-3	356	259	1.4
Hsc70-4	825	889	0.9
Hsp23	3442	3237	1.1
Hsp26	290	161	1.8
Hsp27	2457	1874	1.3
Hsp67Ba	442	315	1.4
Hsp68	205	127	1.6
Hsp83	676	425	1.6
Hsromega	626	653	1.0
Idh	129	123	1.0
Jafrac1	224	194	1.2
KdelR	127	112	1.1
Lam	137	110	1.2
Lis-1	159	142	1.1
Lk6	248	143	1.7
MED21	119	127	0.9
MESK2	116	127	0.9
MTA1-like	132	104	1.3
Map205	164	126	1.3
Mapmodulin	532	561	0.9
Mgstl	103	125	0.8
Mlf	150	144	1.0
Mob4	198	174	1.1
Mpcp	170	181	0.9
Msp-300	176	172	1.0
NAT1	189	114	1.7
NKAIN	110	105	1.0
Nacalpha	572	463	1.2
Nap1	208	262	0.8
Neb-cGP	275	272	1.0
NetB	110	106	1.0
Nlp	971	889	1.1
Nrt	221	158	1.4
Nrx-IV	111	120	0.9
Ntf-2	201	199	1.0
Oda	180	217	0.8
Oscp	172	247	0.7
PDCD-5	122	176	0.7
PHGPx	128	168	0.8
PMCA	290	372	0.8
PP2A-B'	163	182	0.9
PPP4R2r	242	180	1.3
PRL-1	181	175	1.0
Pabp2	102	169	0.6
Pcf11	164	149	1.1
Pdi	368	381	1.0
Pep	395	318	1.2
Pka-C1	306	264	1.2
Pka-R1	136	174	0.8
Pp1-87B	221	170	1.3
Pp2A-29B	175	211	0.8
Pros25	312	208	1.5
Prosalpha7	149	121	1.2
Prosbeta1	159	185	0.9
Prp8	111	122	0.9

Gene	Immature	A	Immature/A
Ptp69D	122	110	1.1
Ptp99A	147	110	1.3
Qm	2157	2620	0.8
RYBP	124	109	1.1
Rab1	173	148	1.2
Rab11	178	132	1.3
Rab2	151	133	1.1
Rab35	246	205	1.2
Rab6	124	135	0.9
Rack1	357	292	1.2
Rbp1-like	280	170	1.6
Rbp2	173	129	1.3
Rbp6	244	231	1.1
Rho1	558	376	1.5
RhoBTB	108	146	0.7
RhoGAPp190	115	108	1.1
RhoGDI	269	372	0.7
Rm62	837	599	1.4
Roc1a	135	139	1.0
RpII18	113	127	0.9
RpL10Ab	843	719	1.2
RpL11	969	635	1.5
RpL12	993	665	1.5
RpL13	1055	987	1.1
RpL13A	914	738	1.2
RpL14	1015	641	1.6
RpL15	1109	1247	0.9
RpL17	370	296	1.2
RpL18A	996	790	1.3
RpL19	1000	805	1.2
RpL21	910	742	1.2
RpL22	249	166	1.5
RpL23	984	808	1.2
RpL24	988	616	1.6
RpL26	730	586	1.2
RpL27	808	662	1.2
RpL27A	977	827	1.2
RpL28	1022	798	1.3
RpL29	1979	1058	1.9
RpL3	400	370	1.1
RpL30	991	759	1.3
RpL31	1656	1326	1.2
RpL32	906	746	1.2
RpL34a	202	217	0.9
RpL35	993	942	1.1
RpL35A	464	346	1.3
RpL36	1279	1241	1.0
RpL36A	914	765	1.2
RpL37A	603	486	1.2
RpL37a	441	418	1.1
RpL38	660	728	0.9
RpL39	2095	1673	1.3
RpL4	401	270	1.5
RpL40	2245	1868	1.2
RpL41	8466	9499	0.9
RpL5	826	885	0.9
RpL6	562	460	1.2

Gene	Immature	A	Immature/A
RpL7	715	429	1.7
RpL7A	694	376	1.8
RpL8	694	472	1.5
RpL9	826	614	1.3
RpLP0	372	260	1.4
RpLP1	1068	1197	0.9
RpLP2	759	727	1.0
RpS10b	743	522	1.4
RpS11	1605	1277	1.3
RpS12	1137	926	1.2
RpS13	1360	994	1.4
RpS14a	1034	1057	1.0
RpS14b	651	646	1.0
RpS15	2570	1963	1.3
RpS15Aa	882	797	1.1
RpS16	1244	886	1.4
RpS17	1056	754	1.4
RpS18	1654	1526	1.1
RpS19a	1313	1132	1.2
RpS20	1008	703	1.4
RpS23	1647	1134	1.5
RpS24	575	414	1.4
RpS25	939	596	1.6
RpS27	1499	1397	1.1
RpS27A	1892	1532	1.2
RpS28b	1019	864	1.2
RpS29	1073	1231	0.9
RpS3	2269	1983	1.1
RpS30	1116	701	1.6
RpS3A	1115	1397	0.8
RpS4	570	365	1.6
RpS5a	591	431	1.4
RpS6	954	773	1.2
RpS7	2591	1754	1.5
RpS9	1117	667	1.7
Rpn11	143	140	1.0
Rpn6	105	129	0.8
Rsf1	436	327	1.3
SC35	130	151	0.9
SF2	244	172	1.4
SKIP	170	158	1.1
Sam-S	186	163	1.1
Sap47	162	220	0.7
Sdc	202	170	1.2
Sec61alpha	131	152	0.9
Sema-1a	155	141	1.1
Set	256	209	1.2
Sh	116	104	1.1
Sh3beta	150	134	1.1
SmD2	143	199	0.7
SmE	143	159	0.9
SmG	264	185	1.4
Smox	121	122	1.0
Sod	295	206	1.4
Src64B	114	112	1.0
Su(var)2-10	126	124	1.0
Su(var)205	535	441	1.2

Gene	Immature	A	Immature/A
Sxl	171	163	1.0
Syt1	144	174	0.8
Syt4	164	166	1.0
Syx1A	146	179	0.8
T-cp1	139	163	0.9
TER94	189	194	1.0
Tao-1	198	136	1.5
Tctp	1938	1748	1.1
Ten-m	237	243	1.0
TfIIA-S	297	254	1.2
Thd1	245	282	0.9
Tl	109	133	0.8
Tm1	161	147	1.1
Tom7	180	209	0.9
Top1	159	112	1.4
Tsp97E	268	286	0.9
Uba1	208	235	0.9
UbcD6	103	106	1.0
Ubi-p5E	102	102	1.0
Uch	248	216	1.1
Ucrh	295	403	0.7
Uev1A	262	269	1.0
Ulp1	133	108	1.2
Unr	197	177	1.1
Utx	116	104	1.1
Vap-33-1	165	116	1.4
Vha16	464	421	1.1
Vha26	175	218	0.8
Yeti	175	180	1.0
Zyx102EF	145	177	0.8
akirin	168	125	1.3
alphaTub84B	991	1006	1.0
arm	174	182	1.0
awd	651	453	1.4
ben	346	251	1.4
beta-Spec	117	112	1.1
betaTub56D	838	782	1.1
bic	637	458	1.4
bip2	139	124	1.1
bl	219	232	0.9
blw	307	318	1.0
br	551	390	1.4
brat	634	497	1.3
bun	303	266	1.1
cals	143	197	0.7
casp	119	112	1.1
caz	131	120	1.1
cg	180	159	1.1
chic	1690	1311	1.3
chinmo	235	208	1.1
chn	232	138	1.7
chrb	205	176	1.2
cib	1831	1522	1.2
cl	372	258	1.4
cpx	420	316	1.3
crc	180	255	0.7
crol	177	130	1.4

Gene	Immature	A	Immature/A
crp	244	170	1.4
ctp	982	756	1.3
cype	157	131	1.2
dco	140	122	1.1
dj-1beta	105	105	1.0
dock	140	127	1.1
dpr7	145	225	0.6
drk	199	217	0.9
e(r)	169	130	1.3
eEF1delta	155	169	0.9
eIF-1A	259	207	1.2
eIF-3p40	163	118	1.4
eIF-4B	168	167	1.0
eIF-4E	336	301	1.1
eIF-4a	495	586	0.8
eIF-5A	981	1015	1.0
eIF3-S9	120	126	1.0
eIF4G	158	166	1.0
eIF4G2	153	123	1.2
eIF5	188	195	1.0
eff	432	281	1.5
elav	394	261	1.5
emc	164	138	1.2
endos	251	169	1.5
exba	342	417	0.8
fas	100	144	0.7
fax	1496	1265	1.2
flfl	168	169	1.0
flower	161	151	1.1
fne	797	695	1.1
fz2	128	120	1.1
gfA	183	223	0.8
gish	136	157	0.9
glec	135	113	1.2
glo	375	363	1.0
gpp	175	138	1.3
growl	155	170	0.9
gw	194	181	1.1
hang	247	176	1.4
hdc	1088	862	1.3
hkl	295	220	1.3
hth	846	742	1.1
hts	216	172	1.3
icln	114	120	0.9
jim	1521	1221	1.2
kis	423	382	1.1
klg	122	157	0.8
kuk	137	127	1.1
l(1)G0230	256	198	1.3
l(1)G0289	132	103	1.3
l(1)G0320	311	264	1.2
l(2)NC136	135	113	1.2
l(2)k16918	233	171	1.4
l(3)01239	280	170	1.6
l(3)82Fd	102	126	0.8
l(3)neo38	901	908	1.0
lark	136	133	1.0

Gene	Immature	A	Immature/A
levy	411	370	1.1
lola	983	695	1.4
lolal	314	273	1.1
lwr	107	102	1.1
mam	203	139	1.5
mask	129	110	1.2
mbf1	153	161	0.9
mbl	215	158	1.4
me31B	118	160	0.7
mei-P26	121	118	1.0
miple	1638	1598	1.0
mmd	116	127	0.9
mnb	186	168	1.1
mod(mdg4)	607	462	1.3
msi	139	101	1.4
msn	132	119	1.1
mtacp1	136	116	1.2
mts	296	197	1.5
mub	160	142	1.1
n-syb	209	164	1.3
nAcRalpha-34E	116	114	1.0
nerfin-1	138	102	1.4
nmo	237	145	1.6
nocte	184	118	1.6
nonA	171	109	1.6
nrv3	518	629	0.8
oho23B	602	341	1.8
onecut	116	131	0.9
pAbp	968	827	1.2
par-1	172	172	1.0
pdm3	156	153	1.0
pho	103	146	0.7
plexA	215	303	0.7
plexB	139	157	0.9
pnut	165	102	1.6
pod1	287	202	1.4
porin	265	236	1.1
prominin-like	165	158	1.0
pros	4419	2614	1.7
pum	125	127	1.0
qkr58E-3	149	126	1.2
qvr	132	138	1.0
ran	473	394	1.2
rin	229	148	1.5
rl	150	173	0.9
roX1	1001	1359	0.7
roX2	476	621	0.8
robo	108	110	1.0
rump	243	216	1.1
sar1	191	128	1.5
sbb	158	111	1.4
scrt	183	107	1.7
scyl	238	202	1.2
sesB	426	343	1.2
sgg	138	126	1.1
shep	607	423	1.4
simj	148	124	1.2

Gene	Immature	A	Immature/A
skpA	600	795	0.8
sm	533	451	1.2
smt3	1630	1308	1.2
sn	438	395	1.1
snf	138	121	1.1
snmRNA:158	473	462	1.0
snmRNA:331	12657	8777	1.4
snmRNA:641	148	135	1.1
snoRNA:MeU5-C46	201	149	1.3
snoRNA:Psi18S-1377c	221	142	1.6
snoRNA:Psi18S-1389a	233	172	1.4
snoRNA:Psi28S-1060	399	305	1.3
snoRNA:Psi28S-1192a	190	167	1.1
snoRNA:Psi28S-291	126	103	1.2
snoRNA:Psi28S-3305c	138	113	1.2
snoRNA:Psi28S-3436a	491	359	1.4
sop	1128	1074	1.0
spen	281	208	1.3
spi	167	134	1.2
sqd	447	389	1.2
sta	598	404	1.5
stai	154	133	1.2
su(w[a])	186	151	1.2
tacc	179	198	0.9
th	234	179	1.3
tinc	143	104	1.4
tou	161	125	1.3
tral	167	116	1.4
tsh	152	117	1.3
tsr	1709	1706	1.0
tsu	167	169	1.0
tud	112	117	1.0
unc-13	394	472	0.8
vig	239	183	1.3
vsg	108	114	0.9
vtd	114	144	0.8
wdb	201	189	1.1
yps	413	277	1.5

Table 3.S16 | Intersection of highly expressed genes (100 FPKM) in immature neurons and immature A neurons. Numbers are gene expression values in FPKM.

Supplemental tables: Combined neuronal samples PCA

Pan-Line PCA Component Summary.

Components	PC1	PC2	PC3	PC4	PC5
Standard deviation	4753	2296	2136	1594	0
Proportion of Variance	65%	15%	13%	7%	0%
Cumulative Proportion	65%	80%	93%	100%	100%

Table 3.S17 | Combined lineage PCA Component Summary. The 3 principal components plotted in the 3D PCA represent 93% of the variation observed in the hemilineages. 5 principal components are necessary to explain 100% of the variation.

Top 20 positive PC1	Correlation coefficient
Cam	0.215
CG42644	0.170
CG42622	0.165
14-3-3zeta	0.148
Tctp	0.106
CG14989	0.104
RpS3	0.063
snRNA:U6:96Aa	0.059
ia2	0.058
nrv3	0.057
Ggamma1	0.056
Ald	0.054
Vha16	0.048
Ef1alpha48D	0.046
RpL15	0.043
G-oalpha47A	0.040
Qm	0.040
RpS27A	0.038
Atpalpha	0.035
CG17124	0.035

Top 20 negative PC1	Correlation coefficient
snmRNA:331	-0.689
noe	-0.366
pros	-0.305
jim	-0.097
Act5C	-0.068
Df31	-0.067
cib	-0.059
hdc	-0.054
His3.3B	-0.050
lola	-0.045
l(3)neo38	-0.043
CG9894	-0.042
Hsp27	-0.041
fne	-0.041
hth	-0.039
Jupiter	-0.038
CG2052	-0.037
br	-0.033
CR42862	-0.032
smt3	-0.031

Top 20 positive PC2	Correlation coefficient
snoRNA:Me28S-A2589a	0.264
pncr002:3R	0.249
snRNA:U6:96Aa	0.168
CG9894	0.160
HmgD	0.148
pros	0.119
l(3)neo38	0.115
lola	0.112
cib	0.107
Ef1alpha48D	0.100
RpL41	0.085
Df31	0.082
smt3	0.075
chic	0.072
His2A:CG33835	0.071
fne	0.059
RpLP1	0.054
His2Av	0.053
hth	0.050
CG3800	0.046

Top 20 negative PC2	Correlation coefficient
noe	-0.450
Cam	-0.251
CG42622	-0.245
snmRNA:331	-0.245
His4r	-0.176
CG42644	-0.175
14-3-3zeta	-0.154
CG14989	-0.126
Hsp23	-0.110
snoRNA:Psi28S-3436a	-0.081
nrv3	-0.074
Ggamma30A	-0.074
ia2	-0.068
Ald	-0.067
Ef1alpha100E	-0.065
Vha16	-0.056
RpL29	-0.053
snoRNA:Psi18S-1377c	-0.052
Ggamma1	-0.052
miple	-0.050

Top 20 positive PC3	Correlation coefficient
His4r	0.180
snmRNA:331	0.176
CR42862	0.100
ATPsyn-beta	0.087
RpL41	0.075
snRNA:U6:96Aa	0.074
roX1	0.072
Qm	0.063
Cyp1	0.056
roX2	0.054
skpA	0.053
CG42622	0.049
Act42A	0.047
Hsp23	0.043
Argk	0.033

14-3-3zeta	0.031
CanB	0.030
RpS3A	0.029
snRNA:U5:63BC	0.029
CG5676	0.027

Top 20 negative PC3	Correlation coefficient
noe	-0.386
RpS7	-0.207
RpL29	-0.205
14-3-3epsilon	-0.163
RpS15	-0.161
Df31	-0.153
RpS8	-0.145
RpS3	-0.142
Tctp	-0.132
pncr002:3R	-0.128
RpL39	-0.121
snoRNA:Me28S-A2589a	-0.119
pros	-0.117
RpS27A	-0.112
chic	-0.109
RpL31	-0.108
RpL23A	-0.103
RpS30	-0.103
RpS9	-0.101
RpS16	-0.095

Table 3.S18 | Combined lineage PCA Top Gene Correlation Coefficients. For the first 3 principal components for the combined lineage PCA, the top positive and negative contributions to each component.

Supplemental tables: Hemilineage PCA

Hemilineage PCA Component Summary.											
Component	PC1	PC2	PC3	PC4	PC5	PC6	PC7	PC8	PC9	PC10	PC11
Standard deviation	5190	3327	2361	1939	1630	1286	1064	710	633	593	0
Proportion of Variance	50%	20%	10%	7%	5%	3%	2%	1%	1%	1%	0%
Cumulative Proportion	50%	70%	81%	88%	93%	96%	98%	99%	99%	100%	100%

Table 3.S19 | Hemilineage PCA Component Summary. The 3 principal components plotted in the 3D PCA represent 81% of the variation observed in the hemilineages. 11 principal components are necessary to explain 100% of the variation.

Top 20 positive PC1	Correlation coefficient
fax	0.096
Cam	0.077
14-3-3zeta	0.051
snoRNA:Me28S-A2589a	0.038
Ggamma30A	0.029
CG13928	0.025
Ef1alpha100E	0.023
snoRNA:Me28S-A2589c	0.022
nrv3	0.022
Appl	0.019
snmRNA:158	0.019
cpx	0.019
chic	0.018
ia2	0.018
CG42622	0.017
G-oalpha47A	0.017
shep	0.015
hth	0.015
Frq1	0.015
CG14989	0.013

Top 20 negative PC1	Correlation coefficient
snmRNA:331	-0.750
RpL41	-0.495
His4r	-0.151
RpL39	-0.123
noe	-0.100
RpS27A	-0.081
Qm	-0.076
RpS15	-0.070
RpS27	-0.067
tsr	-0.063
RpL40	-0.063
Hsp23	-0.056
RpL29	-0.055
RpS18	-0.054
RpL31	-0.052
RpS11	-0.051
RpL30	-0.049
snoRNA:Or-CD1	-0.046
RpS16	-0.045

RpS12	-0.044

Top 20 positive PC2	Correlation coefficient
RpL41	0.563
Hsp23	0.250
RpL39	0.211
RpS27A	0.139
14-3-3zeta	0.133
Cam	0.116
snRNA:U6:96Aa	0.111
CG42644	0.110
RpS7	0.108
His4r	0.100
Ggamma30A	0.099
RpS3	0.095
smt3	0.083
RpL29	0.078
RpS28b	0.068
RpS15	0.065
RpS13	0.064
CG1746	0.058
RpS11	0.055
RpL32	0.053

Top 20 negative PC2	Correlation coefficient
snmRNA:331	-0.500
pros	-0.169
noe	-0.134
CG14989	-0.038
lola	-0.034
snoRNA:Me28S-A2589c	-0.030
snoRNA:Psi28S-3436a	-0.030
hdc	-0.025
His2A:CG33835	-0.025
Jupiter	-0.020
Hsp27	-0.018
Hsp83	-0.018
CG11030	-0.017
Akap200	-0.017
CG42342	-0.016
snoRNA:Or-CD1	-0.016
Argk	-0.014
Pep	-0.013
RpL27	-0.013
sn	-0.013

Top 20 positive PC3	Correlation coefficient
snmRNA:331	0.231
CG42622	0.210
Cam	0.177
14-3-3zeta	0.142
Act5C	0.130
Hsp23	0.107
Ef1alpha100E	0.092
Tctp	0.080
snoRNA:Or-CD1	0.072
alphaTub84B	0.072
snRNA:U6:96Aa	0.070
nrv3	0.066
Ef1alpha48D	0.064

CanB	0.060
chic	0.053
ia2	0.052
CG13928	0.048
Hsc70-4	0.047
betaTub56D	0.047
His2A:CG33835	0.047

Top 20 negative PC3	Correlation coefficient
pros	-0.526
noe	-0.476
jim	-0.190
CG42644	-0.145
snoRNA:Me28S-A2589a	-0.097
RpS27A	-0.086
br	-0.086
CR42862	-0.079
His3.3B	-0.076
RpL39	-0.071
RpL29	-0.068
smt3	-0.062
RpL27A	-0.061
RpL41	-0.061
RpS19a	-0.061
RpS11	-0.057
fne	-0.050
CG2052	-0.050
RpS16	-0.048
RpL11	-0.047

Table 3.S20 | Hemilineage and combined immature PCA gene contributions. For the first 3 principal components for the hemilineages, the top positive and negative contributions to each component.

Pathway description	Gene Number	FDR
nervous system development	10	0.00632
neuron differentiation	8	0.00632
generation of neurons	8	0.00632
central nervous system development	5	0.00753
system development	11	0.00753
neurogenesis	9	0.0106
brain development	4	0.0111
regulation of secretion	3	0.0202
head development	4	0.0202
single-multicellular organism process	12	0.0214
multicellular organismal development	11	0.0296
response to abiotic stimulus	5	0.0296
haltere development	2	0.0325
cell projection organization	6	0.0325
haltere disc development	2	0.0325

Pathway description	Gene Number	FDR
neurological system process	5	0.0483
regulation of transport	4	0.0495

Table 3.S21 | STRING GO Biological Process top 20 gene contributions hemilineages PCA PC1. Significant (<0.05 FDR) gene set enrichments.

Supplemental tables: Hemilineage highly expressed TFs PCA contributions

	PC1	PC2	PC3	PC4	PC5	PC6	PC7	PC8	PC9	PC10
Standard deviation	1581	455	355	283	250	201	184	145	101	0
Proportion of Variance	81%	7%	4%	3%	2%	1%	1%	1%	0%	0%
Cumulative Proportion	81%	88%	92%	95%	97%	98%	99%	100%	100%	100%

Table 3.S22 | Summary of PCA component contribution percentages of hemilineages based on highly expressed TFs. The 3 principal components plotted in the 3D PCA represent 92% of the variation observed in the highly expressed TFs in the hemilineages. 10 principal components are necessary to explain 100% of the variation.

Top 20 positive contritutions to PC1	
Gene	Correlation Coefficient
Scr	0.048451052
Eip74EF	0.035249901
CG33936	0.027884236
vri	0.024096214
Sox14	0.022467865
HmgZ	0.019921467
CG11071	0.019917578
emc	0.019281192
Atf-2	0.018083688
kn	0.018004046
crc	0.017354114
ct	0.015684928
CG14767	0.015601777
CG15715	0.01546925
mamo	0.014433152
Lim1	0.012369738
pan	0.011850086
salm	0.011612736
NfI	0.010424362
CG17385	0.009949736
Top 20 negative contritutions to PC1	
Gene	Correlation Coefficient
pros	-0.924850119
jim	-0.289459778
br	-0.13408731
CG2052	-0.088303496
Antp	-0.061371142
lola	-0.054511793
l(3)neo38	-0.05270508
chinmo	-0.035406694
chn	-0.034286152
pdm3	-0.034095764
hth	-0.033007214
HmgD	-0.030863382
Pep	-0.029602115
Ptx1	-0.027646972
Ets21C	-0.023822268

Eip75B	-0.023674026
CG6854	-0.022310349
exex	-0.021362838
Su(var)205	-0.020977105
Top 20 positive contritutions to PC2	
Gene	Correlation Coefficient
jim	0.483370868
hth	0.452634217
br	0.291239958
Ptx1	0.217692176
Ets21C	0.191450141
CG33936	0.173583171
Dr	0.139152497
SoxN	0.126458481
mirr	0.123179368
pdm3	0.09661617
Eip75B	0.095512065
emc	0.092742106
rn	0.08424957
chinmo	0.08100385
CG32105	0.071398426
opa	0.068337084
tna	0.063966504
Scr	0.062139024
Eip74EF	0.059623157
tio	0.049496527
Top 20 negative contritutions to PC2	
Gene	Correlation Coefficient
HmgD	-0.262131258
pros	-0.173470564
l(3)neo38	-0.15322696
CG2052	-0.141304643
lola	-0.106611896
Antp	-0.098707389
HGTX	-0.085695747
exex	-0.085066463
CG6854	-0.063933502
oc	-0.059290124
trh	-0.049410472
Pep	-0.049246993
HmgZ	-0.044470347
ap	-0.043519099
Su(var)205	-0.042523058
Fer2	-0.039259344
Fer3	-0.038770168
mid	-0.037334082
H15	-0.036345332
nerfin-1	-0.034213891
Top 20 positive contritutions to PC3	
Gene	Correlation Coefficient
hth	0.62103969
pros	0.207645852
HmgZ	0.128228891
emc	0.094986703
grn	0.077405917
exex	0.074216742
CG11317	0.069915498

AP-2	0.062233658
lbl	0.061816051
lola	0.059949934
ct	0.057693533
tsh	0.055845929
toy	0.054540915
Eip74EF	0.049880855
Fer2	0.048471052
unc-4	0.045959138
oc	0.045957309
scro	0.040401823
nerfin-1	0.039934745
ap	0.036368754
Top 20 negative contritutions to PC3	
Gene	Correlation Coefficient
jim	-0.525484381
Antp	-0.205304428
trh	-0.146747597
pdm3	-0.128698397
pb	-0.121998679
vvl	-0.1028756
Fer3	-0.101374762
br	-0.101342752
chinmo	-0.099514767
Su(var)205	-0.093586719
CG2052	-0.082564506
H15	-0.079604113
l(3)neo38	-0.076769999
HGTX	-0.062230518
CG18619	-0.05693529
mid	-0.056437675
ey	-0.049225995
HmgD	-0.047483417
Alh	-0.046939462
Rpb4	-0.044816654

Table 3.S23 | Top gene correlation coefficients for PCA of highly expressed TFs in hemilineages. Top 20 positive and negative contributions to the first 3 principal components for highly expressed TFs.

Term	Gene #	FDR	Genes
regulation of transcription, DNA-templated	12	2.32E-07	Atf-2, Eip74EF, Lim1, Scr, Sox14, crc, ct, emc, kn, pan, salm, vri
regulation of transcription from RNA polymerase II promoter	10	2.98E-07	Atf-2, Eip74EF, Scr, Sox14, crc, ct, emc, kn, pan, vri
metamorphosis	9	4.53E-06	Lim1, Sox14, crc, ct, emc, kn, pan, salm, vri
negative regulation of transcription, DNA-templated	7	3.07E-05	Lim1, crc, ct, emc, pan, salm, vri
positive regulation of transcription, DNA-templated	7	3.30E-05	Atf-2, Eip74EF, Lim1, Scr, crc, kn, pan
positive regulation of transcription from RNA polymerase II promoter	6	8.70E-05	Atf-2, Eip74EF, Scr, crc, kn, pan
instar larval or pupal development	8	9.92E-05	Lim1, crc, ct, emc, kn, pan, salm, vri

post-embryonic appendage morphogenesis	7	0.000109	Lim1, ct, emc, kn, pan, salm, vri
imaginal disc-derived appendage morphogenesis	7	0.00012	Lim1, ct, emc, kn, pan, salm, vri
imaginal disc-derived appendage development	7	0.000122	Lim1, ct, emc, kn, pan, salm, vri
imaginal disc morphogenesis	7	0.000253	Lim1, ct, emc, kn, pan, salm, vri
regionalization	7	0.000291	Lim1, Scr, ct, emc, kn, pan, salm
instar larval or pupal morphogenesis	7	0.000298	Lim1, ct, emc, kn, pan, salm, vri
organ morphogenesis	8	0.0005	Lim1, Scr, ct, emc, kn, pan, salm, vri
post-embryonic organ development	7	0.0005	Lim1, ct, emc, kn, pan, salm, vri
tube development	8	0.000529	Lim1, Scr, ct, emc, kn, pan, salm, vri
spiracle morphogenesis, open tracheal system	3	0.000561	ct, pan, salm
imaginal disc-derived wing morphogenesis	6	0.000622	ct, emc, kn, pan, salm, vri
wing disc morphogenesis	6	0.000665	ct, emc, kn, pan, salm, vri
imaginal disc development	7	0.0016	Lim1, ct, emc, kn, pan, salm, vri
antennal joint development	2	0.00183	ct, salm
anatomical structure morphogenesis	10	0.00212	Lim1, Scr, Sox14, crc, ct, emc, kn, pan, salm, vri
segment specification	3	0.00234	Scr, kn, salm
sensory organ development	6	0.00246	Lim1, Scr, ct, emc, salm, vri
wing disc development	6	0.00285	ct, emc, kn, pan, salm, vri
negative regulation of transcription from RNA polymerase II promoter	4	0.00688	crc, ct, emc, vri
positive regulation of biological process	8	0.0114	Atf-2, Eip74EF, Lim1, Scr, crc, kn, pan, vri
organ development	8	0.012	Lim1, Scr, ct, emc, kn, pan, salm, vri
transcription, DNA-templated	4	0.0145	Atf-2, Eip74EF, crc, vri
open tracheal system development	4	0.0153	ct, pan, salm, vri
specification of segmental identity, head	2	0.0216	Scr, kn
segmentation	4	0.0216	Scr, kn, pan, salm
posterior head segmentation	2	0.0216	Scr, kn
R8 cell differentiation	2	0.0262	emc, salm
sex differentiation	3	0.0281	Scr, ct, salm
digestive tract development	3	0.0296	Scr, ct, emc
digestive system development	3	0.0296	Scr, ct, emc
cell fate commitment	5	0.0298	ct, emc, kn, pan, salm
neuron differentiation	6	0.031	Sox14, ct, emc, kn, salm, vri
embryo development	5	0.0346	Scr, ct, emc, kn, pan
antennal development	2	0.0401	ct, salm
segment polarity determination	2	0.0456	kn, pan
regulation of hemocyte differentiation	2	0.0485	kn, pan

Table 3.S24 | GO biological process for top 20 positive contributions to PC1 in hemilineage TF PCA. 43 terms. Terms sorted by FDR.

Term	Gene #	FDR	Genes
generation of neurons	13	2.08E-08	Antp, Ets21C, HmgD, Lin29, Ptx1, chinmo, chn, exex, hth, jim, lola, pdm3, pros
neuron projection development	11	3.81E-08	Ets21C, HmgD, Lin29, Ptx1, chinmo, chn, exex, jim, lola, pdm3, pros
neuron differentiation	12	3.84E-08	Ets21C, HmgD, Lin29, Ptx1, chinmo, chn, exex, hth, jim, lola, pdm3, pros
neurogenesis	14	7.02E-08	Antp, Ets21C, HmgD, Lin29, Ptx1, Su(var)205, chinmo, chn, exex, hth, jim, lola, pdm3, pros
cell morphogenesis involved in neuron differentiation	10	7.02E-08	Ets21C, HmgD, Ptx1, chinmo, chn, exex, jim, lola, pdm3, pros
dendrite development	8	7.13E-08	Ets21C, HmgD, Ptx1, chinmo, chn, jim, lola, pros
neuron development	11	7.13E-08	Ets21C, HmgD, Lin29, Ptx1, chinmo, chn, exex, jim, lola, pdm3, pros
dendrite morphogenesis	8	7.13E-08	Ets21C, HmgD, Ptx1, chinmo, chn, jim, lola, pros
nervous system development	14	1.28E-07	Antp, Ets21C, HmgD, Lin29, Ptx1, Su(var)205, chinmo, chn, exex, hth, jim, lola, pdm3, pros
neuron projection morphogenesis	10	1.55E-07	Ets21C, HmgD, Ptx1, chinmo, chn, exex, jim, lola, pdm3, pros
regulation of gene expression	12	3.64E-07	Antp, Eip75B, Pep, Ptx1, Su(var)205, chinmo, chn, exex, hth, jim, lola, pros
cell development	13	4.84E-07	Antp, Eip75B, Ets21C, HmgD, Lin29, Ptx1, chinmo, chn, exex, jim, lola, pdm3, pros
system development	15	4.84E-07	Antp, Ets21C, HmgD, Lin29, Ptx1, Su(var)205, chinmo, chn, exex, hth, jim, l(3)neo38, lola, pdm3, pros
cell differentiation	15	5.54E-07	Antp, Eip75B, Ets21C, HmgD, Lin29, Ptx1, Su(var)205, chinmo, chn, exex, hth, jim, lola, pdm3, pros
regulation of RNA metabolic process	11	9.13E-07	Antp, Pep, Ptx1, Su(var)205, chinmo, chn, exex, hth, jim, lola, pros
anatomical structure development	16	1.84E-06	Antp, Eip75B, Ets21C, HmgD, Lin29, Ptx1, Su(var)205, chinmo, chn, exex, hth, jim, l(3)neo38, lola, pdm3, pros
regulation of transcription, DNA-templated	10	5.00E-06	Antp, Ptx1, Su(var)205, chinmo, chn, exex, hth, jim, lola, pros
single-multicellular organism process	16	5.00E-06	Antp, Eip75B, Ets21C, HmgD, Lin29, Ptx1, Su(var)205, chinmo, chn, exex, hth, jim, l(3)neo38, lola, pdm3, pros
single-organism developmental process	16	5.71E-06	Antp, Eip75B, Ets21C, HmgD, Lin29, Ptx1, Su(var)205, chinmo, chn, exex, hth, jim, l(3)neo38, lola, pdm3, pros
multicellular organismal development	15	6.31E-06	Antp, Ets21C, HmgD, Lin29, Ptx1, Su(var)205, chinmo, chn, exex, hth, jim, l(3)neo38, lola, pdm3, pros
head development	6	6.31E-06	Antp, Lin29, chinmo, hth, lola, pros
anatomical structure morphogenesis	12	1.93E-05	Ets21C, HmgD, Ptx1, chinmo, chn, exex, hth, jim, l(3)neo38, lola, pdm3, pros
central nervous system development	6	6.04E-05	Lin29, chinmo, exex, hth, lola, pros
brain development	5	7.23E-05	Lin29, chinmo, hth, lola, pros

Term	Gene #	FDR	Genes
positive regulation of gene expression	6	0.000595	Antp, Su(var)205, chn, hth, lola, pros
cellular component organization	12	0.000595	Ets21C, HmgD, Lin29, Ptx1, Su(var)205, chinmo, chn, exex, jim, lola, pdm3, pros
specification of segmental identity, antennal segment	2	0.000701	Antp, hth
organ development	9	0.00134	Antp, HmgD, Lin29, chinmo, chn, hth, l(3)neo38, lola, pros
regulation of cell fate specification	3	0.00143	chn, hth, pros
muscle structure development	5	0.00147	Antp, HmgD, chn, hth, lola
regulation of transcription from RNA polymerase II promoter	6	0.00274	Antp, Ptx1, chn, hth, lola, pros
positive regulation of transcription, DNA-templated	5	0.00446	Antp, Su(var)205, chn, hth, lola
compound eye photoreceptor fate commitment	3	0.00512	hth, lola, pros
anterior head segmentation	2	0.00618	Antp, hth
anterior head development	2	0.00618	Antp, hth
biological regulation	13	0.007	Antp, Eip75B, Lin29, Pep, Ptx1, Su(var)205, chinmo, chn, exex, hth, jim, lola, pros
regulation of chromatin modification	3	0.00982	Su(var)205, jim, l(3)neo38
somatic muscle development	3	0.0127	chn, hth, lola
axon target recognition	2	0.0155	exex, pdm3
peripheral nervous system development	3	0.0213	chn, hth, pros
compound eye morphogenesis	4	0.0237	chn, hth, lola, pros
organ morphogenesis	6	0.0259	chinmo, chn, hth, l(3)neo38, lola, pros
cell fate commitment	5	0.0263	Antp, exex, hth, lola, pros
post-embryonic organ development	5	0.0348	chinmo, chn, hth, l(3)neo38, lola
axonogenesis	4	0.0367	exex, lola, pdm3, pros
axon development	4	0.0404	exex, lola, pdm3, pros
cellular process	15	0.0436	Antp, Ets21C, HmgD, Lin29, Pep, Ptx1, Su(var)205, chinmo, chn, exex, hth, jim, lola, pdm3, pros
larval somatic muscle development	2	0.044	chn, lola
response to external stimulus	6	0.044	Eip75B, Ets21C, chn, lola, pdm3, pros

Table 3.S25 | GO biological process for top 20 negative contributions to PC1 in hemilineage TF PCA. 49 terms. Terms sorted by FDR.

Supplemental tables: commonly expressed genes

Gene	19A	21A	20/22A	1A	1B	12A	12B	4B	15B	16B
bun										
Bx										
CG30122										
d4										
E2f										
Eip75B										
emc										
fd68A										
jumu										
Kr-h1										
MED21										
onecut										
pdm3										
pho										
qkr58E-3										
Rpn11										
Smox										
tsh										
Utx										
dj-1beta										
Alh										
Antp										
bic										
caz										
CG13993										
crp										
e(r)										
eIF-3p40										
l(3)neo38										
mbf1										
pros										
Su(var)205										

Table 3.S26 | Highly expressed TFs - individual hemilineages intersection with combined immature (>100 FPKM in both). Cell color indicates whether genes are expressed at >100 FPKM in a single hemilineage (orange), multiple hemilineages (purple), or all hemilineages (green).

Gene	19A	21A	20/22A	1A	1B	12A	12B	4B	15B	16B
bel										
CG9099										
me31B										

Gene	19A	21A	20/22A	1A	1B	12A	12B	4B	15B	16B
CG10077										
CG10777										
eEF1delta										
Ef1alpha100E										
Ef1alpha48D										
Ef1beta										
Ef1gamma										
eIF-1A										
eIF-4a										
eIF-4B										
eIF-4E										
eIF-5A										
eIF4G										
eIF4G2										
eIF5										
Hel25E										
Rbp2										
Rm62										

Table 3.S27 | Highly expressed translational regulators – individual hemilineages intersection with combined immature (>100 FPKM in both). Cell color indicates whether genes are expressed at >100 FPKM in a single hemilineage (orange), multiple hemilineages (purple), or all hemilineages (green).

Gene	19A	21A	20/22A	1A	1B	12A	12B	4B	15B	16B
CG30423										
fas										
KdelR										
NetB										
Ten-m										
Nrx-IV										
Tl										
ATPsyn-beta										
blw										
Caps										
Cirl										
Eip75B										
fz2										
plexB										
robo										
Tsp97E										

Table 3.S28 | Highly expressed receptors – individual hemilineages intersection with combined immature (>100 FPKM in both). Cell color indicates whether genes are expressed at >100 FPKM in a single hemilineage (orange), multiple hemilineages (purple), or all hemilineages (green).

Gene	19A	21A	20/22A	1A	1B	12A	12B	4B	15B	16B
Eaat2										
icln										
l(1)G0230										
Mpcp										
Nrx-IV										
Sec61alpha										
Sh										
tty										
Atpalpha										
ATPsyn-beta										
blw										
CG1746										
CG4692										
cl										
PMCA										
porin										
scrt										
sesB										

Table 3.S29 | Highly expressed transporters – individual hemilineages intersection with combined immature (>100 FPKM in both). Cell color indicates whether genes are expressed at >100 FPKM in a single hemilineage (orange), multiple hemilineages (purple), or all hemilineages (green).

Gene	19A	21A	20/22A	1A	1B	12A	12B	4B	15B	16B
alphaTub84D										
beta-Spec										
bif										
Bx										
capt										
Dlc90F										
Fim										
Lam										
Moe										
pnut										
RpL34a										
Ubi-p5E										
Act42A										
Act5C										
alphaTub84B										

Gene	19A	21A	20/22A	1A	1B	12A	12B	4B	15B	16B
Ank2										
betaTub56D										
br										
chic										
chinmo										
ctp										
Ef1gamma										
glo										
hts										
lolal										
Mpcp										
RpL10Ab										
RpL11										
RpL12										
RpL13										
RpL13A										
RpL15										
RpL19										
RpL22										
RpL23										
RpL23A										
RpL24										
RpL26										
RpL27										
RpL27A										
RpL28										
RpL29										
RpL3										
RpL30										
RpL31										
RpL34b										
RpL35										
RpL35A										
RpL36										
RpL37A, RpL37a										
RpL38										
RpL39										
RpL40										
RpL5										
RpL6										
RpL7										
RpL7A										
RpL8										
RpL9										

Gene	19A	21A	20/22A	1A	1B	12A	12B	4B	15B	16B
RpLP0										
RpLP2										
RpS10b										
RpS11										
RpS12										
RpS13										
RpS14a										
RpS15										
RpS15Aa										
RpS16										
RpS18										
RpS19a										
RpS20										
RpS23										
RpS26										
RpS27										
RpS27A										
RpS28b										
RpS29										
RpS3										
RpS30										
RpS3A										
RpS4										
RpS5a										
RpS8										
RpS9										
sesB										
sn										
sta										
Tctp										
Tm1										
tsr										

Table 3.S30 | Highly expressed structural genes – individual hemilineages intersection with combined immature (>100 FPKM in both). Cell color indicates whether genes are expressed at >100 FPKM in a single hemilineage (orange), multiple hemilineages (purple), or all hemilineages (green).

Supplemental tables: Differentially expressed genes between hemilineages relative to combined immature neurons

Gene	19A	21A	20/22A	1A	1B	12A	12B	4B	15B	16B
Bx42										
CG32105										
CG5708										
CG8149										
ct										
Dp										
Dr										
Dys										
EcR										
Eip74EF										
gro										
HGTX										
Lim1										
mirr										
Not1										
ph-p										
qkr54B										
qkr58E-1										
rdx										
salm										
Scr										
Sox14										
SoxN										
toy										
Trf2										
Ubx										
vri										
vvl										
abd-A										
scro										
CG31224										
ey										
svp										
TfIIFbeta										
TfIIS										
ush										
Tif-IA										
Ets21C										
phol										
Ptx1										
tio										
TfAP-2										
unc-4										
H15										

Gene	19A	21A	20/22A	1A	1B	12A	12B	4B	15B	16B
mid										
pb										
ap										
exex										
fkh										
oc										

Table 3.S31 | TFs >100 FPKM in individual hemilineages and <100 FPKM in combined immature neurons. Purple cells indicate genes expressed in multiple hemilineages. Orange cells indicate genes expressed in a single hemilineage.

Gene	19A	21A	20/22A	1A	1B	12A	12B	4B	15B	16B
4EHP										
CG9281										
Dbp80										
eIF-2beta										
Elf										

Table 3.S32 | Translational regulator genes >100 FPKM in hemilineages and <100 FPKM in combined immature neurons. Purple cells indicate genes expressed in multiple hemilineages. Orange cells indicate genes expressed in a single hemilineage.

Gene	19A	21A	20/22A	1A	1B	12A	12B	4B	15B	16B
2mit										
babo										
CG14762										
CG17816										
CG6700										
Con										
Dp										
EcR										
Fas2										
fra										
GluClalpha										
kek2										
mge										
robo3										
sli										
SP2353										
TM4SF										
Tsp42Ee										
Tsp66E										

tutl										
unc-119										
Vha55										
Vha68-1										
kek1										
caps										
svp										
beat-Vb										
Toll-7										

Table 3.S33 | Receptor genes >100 FPKM in hemilineages and <100 FPKM in combined immature neurons. Purple cells indicate genes expressed in multiple hemilineages. Orange cells indicate genes expressed in a single hemilineage.

Gene	19A	21A	20/22A	1A	1B	12A	12B	4B	15B	16B
CG10638										
CG12817										
CG31030										
CG32000										
CG3638										
CG40042										
CG6084										
CG6700										
CG9132										
CG9281										
CG9413										
GluClalpha										
Nckx30C										
shakB										
Task6										
Teh2										
Tom20										
VGlut										
Vha100-1										
Vha13										
Vha44										
Vha55										
Vha68-1										
VhaPPA1-1										
vib										
VGAT										
ATPsyn-gamma										
Tim10										
foi										

Gene	19A	21A	20/22A	1A	1B	12A	12B	4B	15B	16B
pog										
CG14654										

Table 3.S34 | Transporter genes >100 FPKM in hemilineages and <100 FPKM in combined immature neurons. Purple cells indicate genes expressed in multiple hemilineages. Orange cells indicate genes expressed in a single hemilineage.

Gene	19A	21A	20/22A	1A	1B	12A	12B	4B	15B	16B
alpha-Cat										
bab2										
Bap55										
CG11242										
CG15207										
CG32276										
CG5708										
CG7637										
Dys										
Eb1										
Klc										
Lim1										
Mlc-c										
msps										
Nedd8										
psq										
rdx										
rhea										
robl										
RpL24-like										
Sep4										
shi										
Syn										
Synd										
zip										
mRpL33										
mRpS18A										
CG32105										

Table 3.S35 | Structural genes >100 FPKM in individual hemilineages and <100 FPKM in combined immature neurons. Purple cells indicate genes expressed in multiple hemilineages. Orange cells indicate genes expressed in a single hemilineage.

Supplemental tables: highly expressed (>100 FPKM) TFs

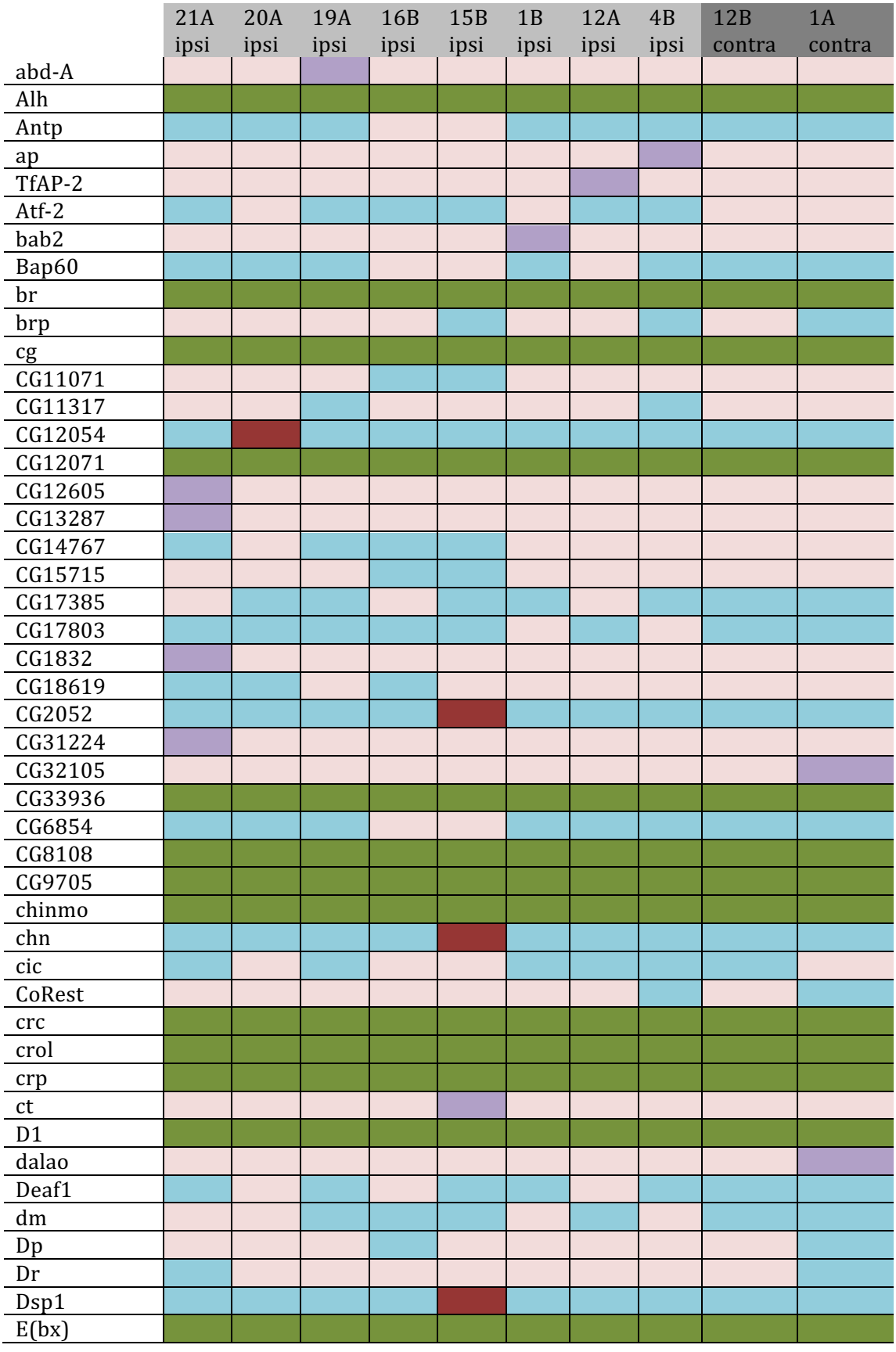

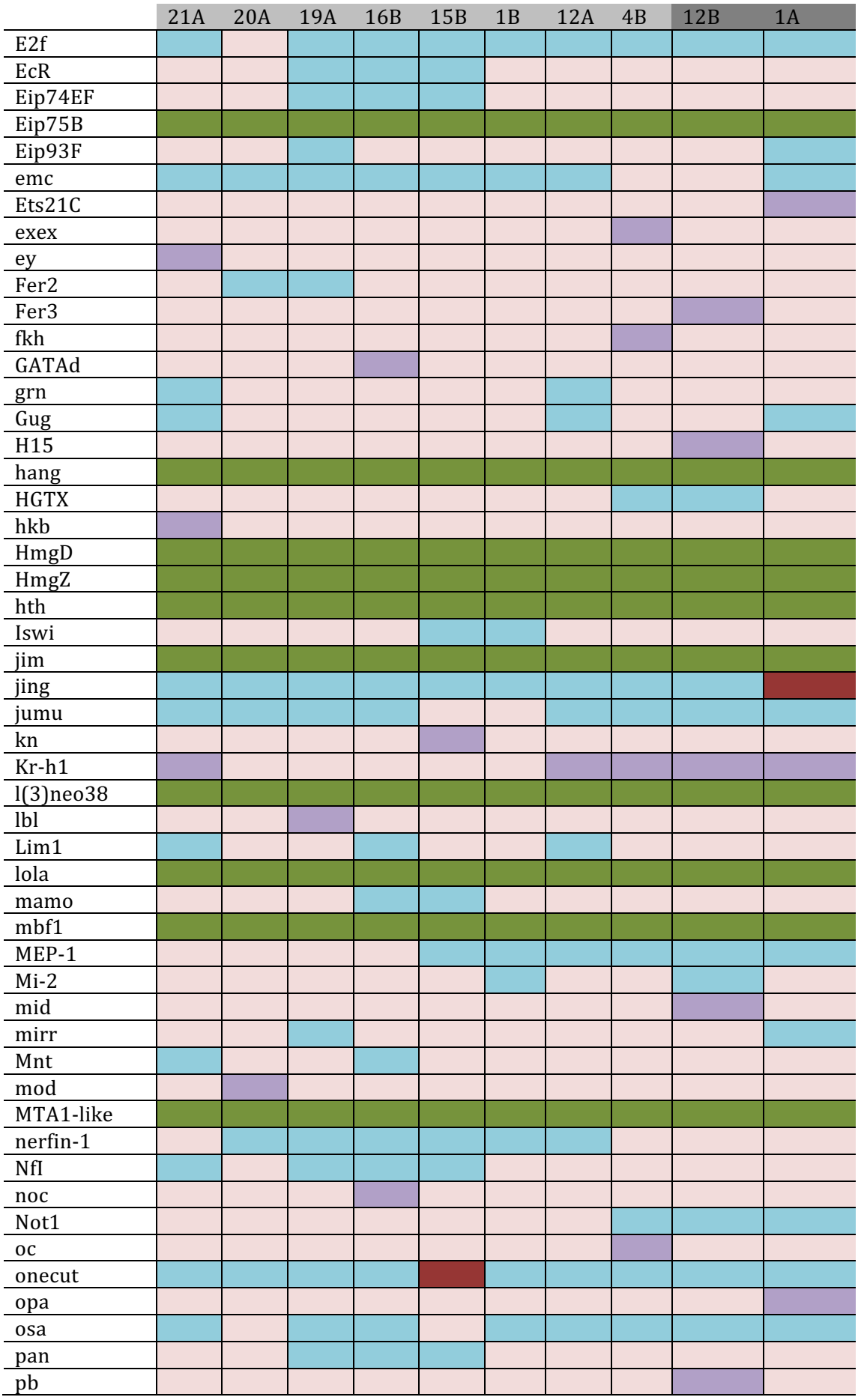
21A
20A
19A
16B
15B
1B
12A
4B
12B
1A
E2f
EcR
Eip74EF
Eip75B
Eip93F
emc
Ets21C
exex
ey
Fer2
Fer3
fkh
GATAd
grn
Gug
H15
hang
HGTX
hkb
HmgD
HmgZ
hth
Iswi
jim
jing
jumu
kn
Kr-h1
l(3)neo38
lbl
Lim1
lola
mamo
mbf1
MEP-1
Mi-2
mid
mirr
Mnt
mod
MTA1-like
nerfin-1
Nfl
noc
Not1
oc
onecut
opa
osa
pan
pb

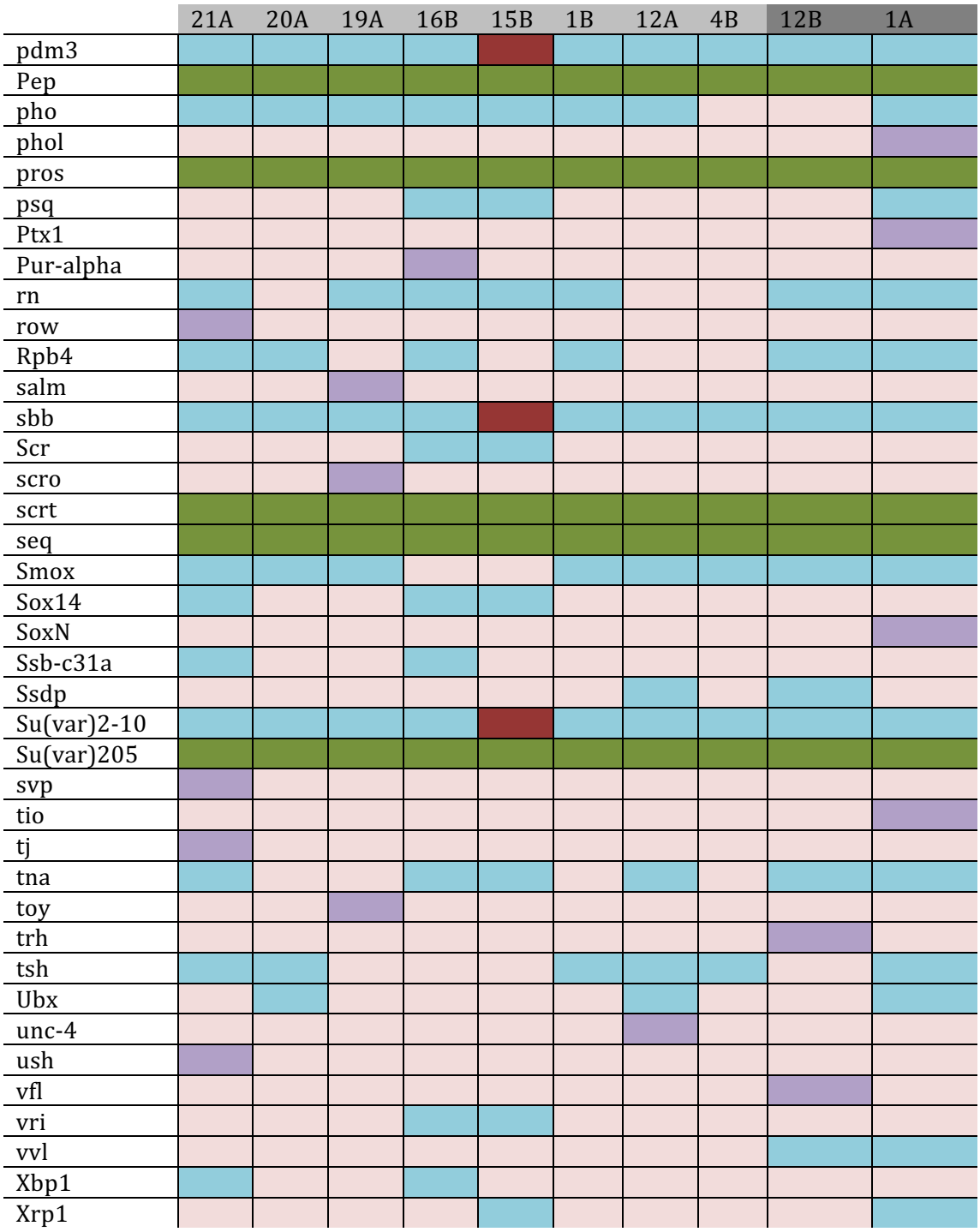

Table 3.S36 | Transcription factor gene expression > 100 FPKM per hemilineage. For each transcription factor, expression is common to all hemilineages (green), unique to a particular hemilineage (purple), expressed in multiple hemilineages (blue), or not expressed in a hemilineage (light red or dark red for instances where only one hemilineage is lacking expression). Ipsilateral projecting hemilineages denoted in light gray and contralateral projecting hemilineages denoted in dark gray.

Term Classification	Term	Gene #	FDR	Genes
Molecular Function	nucleic acid binding	24	3.04E-17	Alh, CG12071, CG9705, D1, E(bx), Eip75B, HmgD, HmgZ, MTA1-like, Pep, Su(var)205, cg, crc, crol, crp, hang, hth, jim, l(3)neo38, lola, mbf1, pros, scrt, seq
Biological Process	regulation of gene expression	18	1.25E-10	Alh, CG9705, E(bx), Eip75B, MTA1-like, Pep, Su(var)205, cg, chinmo, crc, crol, hth, jim, lola, mbf1, pros, scrt, seq
Biological Process	regulation of RNA metabolic process	17	1.25E-10	Alh, CG9705, E(bx), MTA1-like, Pep, Su(var)205, cg, chinmo, crc, crol, hth, jim, lola, mbf1, pros, scrt, seq
Biological Process	regulation of transcription, DNA-templated	16	2.36E-10	Alh, CG9705, E(bx), MTA1-like, Su(var)205, cg, chinmo, crc, crol, hth, jim, lola, mbf1, pros, scrt, seq
Molecular Function	DNA binding	15	1.37E-09	Alh, CG9705, D1, E(bx), Eip75B, HmgD, HmgZ, MTA1-like, Pep, Su(var)205, crc, crp, hth, mbf1, pros
Biological Process	dendrite morphogenesis	10	1.38E-09	CG9705, E(bx), HmgD, chinmo, jim, lola, mbf1, pros, scrt, seq
Biological Process	dendrite development	10	1.54E-09	CG9705, E(bx), HmgD, chinmo, jim, lola, mbf1, pros, scrt, seq
Molecular Function	transcription factor activity, sequence-specific DNA binding	11	6.87E-08	Alh, MTA1-like, cg, chinmo, crc, hth, jim, l(3)neo38, lola, pros, scrt
Protein Domains	Zinc finger, C2H2	10	2.02E-07	MTA1-like, br, cg, chinmo, crol, hang, jim, l(3)neo38, scrt, seq
Protein Domains	Zinc finger, C2H2-like	10	2.05E-07	CG8108, br, cg, chinmo, crol, hang, jim, l(3)neo38, scrt, seq
Molecular Function	metal ion binding	15	3.17E-07	Alh, CG12071, E(bx), Eip75B, MTA1-like, Pep, cg, chinmo, crol, hang, jim, l(3)neo38, lola, scrt, seq
Biological Process	cell morphogenesis involved in neuron differentiation	10	1.74E-06	CG9705, E(bx), HmgD, chinmo, jim, lola, mbf1, pros, scrt, seq
Molecular Function	binding	22	9.50E-06	CG12071, CG9705, D1, E(bx), Eip75B, HmgD, HmgZ, MTA1-like, Pep, Su(var)205, cg, chinmo, crc, crol, crp, hth, jim, l(3)neo38, mbf1, pros, scrt, seq
Biological Process	single-multicellular organism process	20	1.50E-05	Alh, CG9705, E(bx), Eip75B, HmgD, Su(var)205, cg, chinmo, crc, crol, crp, hang, hth, jim, l(3)neo38, lola, mbf1, pros, scrt, seq
Biological Process	system development	17	1.50E-05	Alh, CG9705, E(bx), HmgD, Su(var)205, cg, chinmo, crol, crp, hth, jim, l(3)neo38, lola, mbf1, pros, scrt, seq
Biological Process	anatomical structure morphogenesis	15	1.64E-05	CG9705, E(bx), HmgD, cg, chinmo, crc, crol, hth, jim, l(3)neo38, lola, mbf1, pros, scrt, seq
Molecular Function	sequence-specific DNA binding	8	1.95E-05	D1, Eip75B, HmgD, MTA1-like, Su(var)205, crc, crp, mbf1
Biological Process	neuron differentiation	11	2.12E-05	CG9705, E(bx), HmgD, chinmo, hth, jim, lola, mbf1, pros, scrt, seq
Biological Process	anatomical structure development	19	2.59E-05	Alh, CG9705, E(bx), Eip75B, HmgD, Su(var)205, cg, chinmo, crc, crol, crp, hth, jim, l(3)neo38, lola, mbf1, pros, scrt, seq
Biological	regulation of	9	3.66E-05	E(bx), crc, crol, hth, lola, mbf1, pros, scrt,

Term Classification	Term	Gene #	FDR	Genes
Process	transcription from RNA polymerase II promoter			seq
Biological Process	post-embryonic development	10	4.22E-05	Alh, E(bx), cg, chinmo, crc, crol, crp, hth, l(3)neo38, lola
Biological Process	multicellular organismal development	18	4.72E-05	Alh, CG9705, E(bx), HmgD, Su(var)205, cg, chinmo, crc, crol, crp, hth, jim, l(3)neo38, lola, mbf1, pros, scrt, seq
Biological Process	neuron development	10	5.00E-05	CG9705, E(bx), HmgD, chinmo, jim, lola, mbf1, pros, scrt, seq
Biological Process	generation of neurons	11	6.78E-05	CG9705, E(bx), HmgD, chinmo, hth, jim, lola, mbf1, pros, scrt, seq
Biological Process	single-organism developmental process	19	9.24E-05	Alh, CG9705, E(bx), Eip75B, HmgD, Su(var)205, cg, chinmo, crc, crol, crp, hth, jim, l(3)neo38, lola, mbf1, pros, scrt, seq
Biological Process	regulation of biological process	19	9.69E-05	Alh, CG8108, CG9705, E(bx), Eip75B, MTA1-like, Pep, Su(var)205, cg, chinmo, crc, crol, hth, jim, lola, mbf1, pros, scrt, seq
Protein Domains	Zinc finger C2H2-type/integrase DNA-binding domain	7	0.000152	MTA1-like, cg, crol, jim, l(3)neo38, scrt, seq
Biological Process	instar larval or pupal development	9	0.00016	Alh, E(bx), cg, chinmo, crc, crol, hth, l(3)neo38, lola
Biological Process	regulation of cellular process	18	0.000163	Alh, CG8108, CG9705, E(bx), MTA1-like, Pep, Su(var)205, cg, chinmo, crc, crol, hth, jim, lola, mbf1, pros, scrt, seq
Biological Process	organ development	12	0.000197	Alh, E(bx), HmgD, cg, chinmo, crol, crp, hth, l(3)neo38, lola, pros, seq
Biological Process	post-embryonic organ development	8	0.000671	Alh, cg, chinmo, crol, crp, hth, l(3)neo38, lola
Biological Process	neurogenesis	12	0.000748	CG9705, E(bx), HmgD, Su(var)205, chinmo, hth, jim, lola, mbf1, pros, scrt, seq
Biological Process	imaginal disc-derived appendage development	7	0.0014	Alh, cg, chinmo, crol, hth, l(3)neo38, lola
Biological Process	regulation of chromatin modification	4	0.00142	Su(var)205, crol, jim, l(3)neo38
Biological Process	nervous system development	12	0.00191	CG9705, E(bx), HmgD, Su(var)205, chinmo, hth, jim, lola, mbf1, pros, scrt, seq
Biological Process	negative regulation of transcription, DNA-templated	6	0.00191	Su(var)205, crc, crol, pros, scrt, seq
Biological Process	somatic muscle development	4	0.00192	Alh, crp, hth, lola
Biological Process	cell differentiation	14	0.00252	CG9705, E(bx), Eip75B, HmgD, Su(var)205, chinmo, crol, hth, jim, lola, mbf1, pros, scrt, seq
Biological Process	larval somatic muscle development	3	0.00257	Alh, crp, lola
Biological Process	cell development	11	0.00396	CG9705, E(bx), Eip75B, HmgD, chinmo, jim, lola, mbf1, pros, scrt, seq
Biological Process	metamorphosis	7	0.00406	cg, chinmo, crc, crol, hth, l(3)neo38, lola

Term Classification	Term	Gene #	FDR	Genes
Biological Process	imaginal disc-derived wing morphogenesis	6	0.00465	cg, chinmo, crol, hth, l(3)neo38, lola
Biological Process	wing disc morphogenesis	6	0.0047	cg, chinmo, crol, hth, l(3)neo38, lola
Biological Process	positive regulation of gene expression	6	0.0047	Su(var)205, crc, hth, lola, mbf1, pros
Biological Process	regulation of chromatin silencing	3	0.0047	crol, jim, l(3)neo38
Biological Process	epithelial tube morphogenesis	7	0.0047	cg, chinmo, crol, hth, l(3)neo38, lola, seq
Biological Process	organ morphogenesis	8	0.00625	cg, chinmo, crol, hth, l(3)neo38, lola, pros, seq
Biological Process	tube development	8	0.00655	Alh, cg, chinmo, crol, hth, l(3)neo38, lola, seq
Biological Process	central nervous system development	5	0.00671	chinmo, hth, lola, mbf1, pros
Biological Process	muscle structure development	5	0.00734	Alh, HmgD, crp, hth, lola
Biological Process	brain development	4	0.00784	chinmo, hth, lola, pros
Molecular Function	AT DNA binding	2	0.0082	D1, HmgD
Biological Process	R7 cell differentiation	3	0.00862	lola, pros, seq
Molecular Function	satellite DNA binding	2	0.0113	D1, Su(var)205
Biological Process	compound eye photoreceptor fate commitment	3	0.0118	hth, lola, pros
Biological Process	single-organism process	21	0.0118	Alh, CG12071, CG9705, E(bx), HmgD, MTA1-like, Su(var)205, cg, chinmo, crc, crol, crp, hang, hth, jim, l(3)neo38, lola, mbf1, pros, scrt, seq
Biological Process	compound eye photoreceptor cell differentiation	4	0.0127	hth, lola, pros, seq
Biological Process	imaginal disc development	7	0.013	Alh, cg, chinmo, crol, hth, l(3)neo38, lola
Biological Process	tissue development	9	0.013	Alh, cg, chinmo, crol, hth, l(3)neo38, lola, pros, seq
Biological Process	haltere development	2	0.0139	Alh, hth
Biological Process	haltere disc development	2	0.0139	Alh, hth
Biological Process	head development	4	0.0139	chinmo, hth, lola, pros
Biological Process	wing disc development	6	0.0162	cg, chinmo, crol, hth, l(3)neo38, lola
Biological Process	instar larval or pupal morphogenesis	6	0.017	cg, chinmo, crol, hth, l(3)neo38, lola
Biological Process	cell fate commitment	6	0.0175	E(bx), crol, hth, lola, pros, seq
Biological	positive regulation	5	0.0175	Su(var)205, crc, hth, lola, mbf1

Term Classification	Term	Gene #	FDR	Genes
Process	of transcription, DNA-templated			
Biological Process	molting cycle, chitin-based cuticle	3	0.0177	Alh, Eip75B, crc
Biological Process	negative regulation of transcription from RNA polymerase II promoter	4	0.0183	crc, pros, scrt, seq
Biological Process	positive regulation of biological process	9	0.0203	CG8108, E(bx), Su(var)205, crc, crol, hth, lola, mbf1, pros
Biological Process	positive regulation of cellular process	8	0.0267	CG8108, E(bx), Su(var)205, crc, crol, hth, lola, mbf1
Biological Process	epithelium development	8	0.0274	Alh, cg, chinmo, crol, hth, l(3)neo38, lola, seq
Biological Process	pupariation	2	0.0278	E(bx), crc
Biological Process	prepupal development	2	0.0343	E(bx), crc
Molecular Function	methylated histone binding	2	0.0384	E(bx), Su(var)205
Biological Process	R7 cell development	2	0.0485	lola, seq

Table 3.S37 | GSEA for commonly expressed TFs at >100 FPKM. STRING was used for this analysis. GO Biological process, GO molecular function, and InterPro protein domains were included. Terms are sorted by FDR.

Supplemental table: Expression patterns of genes involved in neurotransmission

	Hemi.1A	Hemi.12A	Hemi.12B	Hemi.4B	Hemi.20.22A	Hemi.1B	Pan.Larval	Hemi.21A	Hemi.15B	Pan.Embryonic	Hemi.16B	Hemi.19A
oa2	2	8	3	13	2	3	3	4	20	39	8	22
Octbeta2R	0	4	1	2	0	2	1	5	3	26	10	19
VGAT	38	44	48	32	51	40	47	43	49	79	83	115
Oamb	4	2	1	2	1	2	2	24	6	26	16	11
5-HT7	6	3	0	7	5	4	3	21	22	37	14	21
DopR2	0	1	4	1	1	1	2	2	1	7	6	3
5-HT1A	5	6	62	14	11	6	15	12	33	42	42	37
nAcRalpha-80B	57	52	41	45	60	53	44	42	53	51	110	66
GABA-B-R1	18	15	16	8	16	11	11	17	18	28	45	24
nAcRbeta-96A	82	77	69	74	79	58	50	45	83	68	116	94
nAcRalpha-96Ab	105	39	48	46	41	47	35	32	65	64	78	85
DopR	21	8	15	3	9	5	10	6	10	23	15	25
nAcRalpha-96Aa	36	45	42	47	19	29	31	37	56	53	70	65
cpx	468	652	472	497	260	332	420	537	737	611	728	621
Eaat2	101	138	127	116	97	98	105	130	133	104	166	109
nAcRbeta-64B	81	83	37	53	44	49	61	59	112	168	141	122
Rdl	49	56	29	25	15	20	23	32	93	122	134	89
DopEcR	147	78	89	94	46	74	67	86	147	178	160	129
Ace	52	39	23	31	17	21	28	19	79	90	80	38
5-HT1B	13	9	6	9	4	9	8	8	17	21	14	6
Octbeta3R	9	9	5	6	5	5	6	2	8	15	13	8
GluClalpha	98	113	58	76	75	71	74	77	84	114	105	97
tup	5	1	1	1	1	13	13	0	10	8	5	10
nAcRalpha-34E	212	152	176	135	81	110	116	211	97	103	154	130
GABA-B-R2	44	39	35	33	40	35	40	46	29	42	32	27
GABA-B-R3	22	18	10	12	11	22	30	81	37	37	102	12
5-HT2	1	2	2	1	1	1	2	10	2	4	7	1
nAcRalpha-30D	118	93	73	111	81	90	87	258	123	122	162	165
CG15438	5	6	10	6	12	8	7	16	5	13	14	7
VGlut	6	1	8	51	30	27	42	464	159	162	45	17
CG9317	2	2	1	1	1	2	1	8	3	1	2	1
TyrR	1	6	4	2	2	2	3	18	7	6	7	4
D2R	4	45	34	14	12	25	26	94	46	51	32	28
CG7918	11	6	2	1	2	5	4	24	10	15	10	4
Vmat	218	1	1	2	2	2	1	0	7	51	1	2
DAT	38	5	3	4	3	5	1	2	4	8	1	2
nAcRbeta-21C	161	1	0	2	0	2	3	7	0	2	0	0
nAcRalpha-7E	36	23	18	21	9	8	14	11	11	10	17	17
bdg	12	6	5	10	9	5	5	2	7	5	5	5
VAChT	120	116	7	95	42	47	46	5	64	87	112	16
Cha	52	42	6	31	18	20	19	2	24	28	18	14
Dat	13	6	6	37	9	26	18	24	31	18	9	14
CG42796	1	22	8	6	4	2	8	2	2	3	4	5
CG1732	9	11	12	8	10	6	11	6	3	3	5	10

Table 3.S38 | Neurotransmission gene expression. These are the expression levels for most of the genes known to be involved in neurotransmission. Hemilineage 21A expresses VGlut, which is confirmed by antibody staining in the adult (David Shepherd, personal communication). Pan-embryonic and Hemilineage 15B expression of VGlut is expected, because 15B is composed of motor neurons and the pan-embryonic set includes functional motorneurons.

Chapter 4

The instability of arrested postembryonic neuronal clusters during an extended last larval instar

Introduction

Holometabolus insects, including *Drosophila*, undergo metamorphosis as they transition between larval and adult stages of life. In *Drosophila*, metamorphosis is initiated by the steroid hormone 20-hydroxyecdysone. There are three checkpoints in larval development, all of which correspond to an ecdysone peak (reviewed in Rewitz, Yamanaka, and O'Connor, 2013). During the early third instar there is ecdysone signaling that is responsible for the transition of gamma neurons to alpha'-beta' neurons in the mushroom body (Zheng et al., 2003). Early induction of EcR-B1 expression is observed in the optic lobe of *Met* JH receptor (Charles et al., 2011; Jindra et al., 2015) mutants and in animals in which the JH biosynthetic organ has been genetically ablated (allatectomy; Riddiford et al, 2010), suggesting that juvenile hormone signaling through *Met* is necessary for proper temporal interpretation of ecdysone signaling.

The neuropeptide neuropeptide prothoracicotropic hormone (PTTH) causes the release of ecdysone from the prothoracic gland (PG) portion of the ring gland (Truman and Riddiford, 1974; reviewed in Gilbert et al., 2002). Ecdysone is the precursor for 20-hydroxyecdysone. Ablation of PTTH-releasing neurons (McBrayer et al., 2007) or knockdown of the PTTH receptor torso in the PG causes a prolongation of the third instar larvae (Rewitz et al. 2009; Miller, Ballard, and Ganetzky 2012). These larvae eventually pupate after about nine days in third instar and eclose as abnormally large adult flies (Rewitz et al., 2009). In contrast to the removal of PTTH, the destruction of the PG cells themselves results in larvae that are

permanently locked in the third instar and will never undergo metamorphosis (Warren et al., 2004).

The difference in phenotype between removing the PG and removing the tropic hormone that drives ecdysone secretion from the PG is due to their being a second peptide hormone, the *Drosophila* insulin-like peptides (dILPs) that can induce ecdysone secretion from the PG. The pathways for PTTH and dILP stimulation in the PG, though, converge at a common step that involves *Smad on X* (smox) (Gibbens et al., 2011). Larvae in which smox is removed by RNAi apparently can release no ecdysone and these remain a permanent third instar larvae for weeks and never initiate metamorphosis. Larvae generated in this way are termed "extended third instar" (ETI) larvae Gibbens et al. 2011). Daniel Miller performed the initial characterization of the neurons of the 12A hemilineage in a timed series of ETI larvae. The 12A neurons were morphologically normal at 120 hrs AEL (After Egg Laying), which is equivalent to wandering stage of wildtype larvae. They continued to appear normal at 240 hr AEL, but by 360 hr the neurons in the 12A clusters showed degeneration if the distal portions of their axons. They subsequently extended their axons into abnormal regions that had no relationship to the normal pattern of growth of these cells (576 hr AEL). In order to determine what might be happening in the 12A neurons as these normally arrested cells showed distal degeneration and sprouting, I generated a RNA-seq time series for these neurons at various times in these permanently arrested third instar larvae.

Methods

Genetic strains

Metamorphosis can be prevented and larvae can be maintained as permanent last stage larvae by blocking the response of the PG cells in the ring gland to PTTH and to the dILPs. This blockade was accomplished using the technique of Gibbens et al., (2011) in which an RNAi against smox is expressed selectively in the PG cells using a phm-GAL4. *Phantom* (phm) expression is specific to the PG (Warren et al., 2004). The following genotype was used so that we could block PG activity in larvae and then recover GFP-labeled hemilineage 12A neurons: R24B02-LexA; phm-GAL4/ UAS-smox-RNAi, JFRC19 LexOp-GFP.

Sample preparation

ETI larvae were raised on standard fly food at 25C and batches dissected at 120hrs, 240hrs, 360hrs, and 576hrs AEL. For each sample, approximately 120 nervous systems were dissected, the, the brain lobes were removed and the VNSs were dissociated as described in Chapter 3. GFP-labeled cells were isolated by FACS and their RNA extracted and subjected to RNA-seq as described in Chapter 3. Each time point was done in triplicate.

Data analysis

The data analysis pipeline was used as described in Chapter 3. Tophat2 and Cuffdiff2 from the tuxedo suite was used for mapping reads to the transcriptome, counting transcripts, and differential expression analysis. R was used for downstream analysis. DAVID (https://david.ncifcrf.gov/), STRING (http://string-db.org/), and PantherDB (http://www.pantherdb.org/) were used for gene set enrichment analysis. The gene background used was the entire *Drosophila* genome.

Immunocytochemistry

VNSs were dissected in phosphate buffered saline (PBS) and then fixed for 1 hour in 4% paraformaldehyde in PBS at room temperature (approximately 22°C). They were then washed in PBS with 0.3% Triton-X (PBSTx), blocked for 4 hours with 20% normal donkey serum in PBSTx, and incubated for at least 24 hours in primary antibody in PBSTx 0.3%. Samples were washed again before incubation for at least 24 hours in secondary antibody solution in PBSTx 0.3%. Samples were washed again in PBSTx 0.3% and then mounted in Vectashield (Vector Laboratories, H-1000) on glass slides for imaging with confocal microscopy with a Zeiss LSM 510. Images were processed with the Fiji version of ImageJ (https://fiji.sc/).

Mouse neuroglian (BP104) antibody was used at 1:40 concentration (Hortsch et al., 1990). BP 104 anti-Neuroglian was deposited to the DSHB by Goodman, C. (DSHB Hybridoma Product BP 104 anti-Neuroglian). Rabbit polyclonal TfAP-2 antibody was used at 1:1000 concentration (Monge et al., 2001). Chicken GFP antibody was used 1:1000 (Life Technologies A10262). Sodium azide was used in antibody solutions at

0.02% final concentration. All secondary antibodies were used at a concentration of 1:500 (Jackson ImmunoResearch).

Results

Changes in hemilineage 12A phenotype as larvae stay permanently in their last instar.

As previously reported (Gibbens et al., 2011), the targeting of smox-RNAi selectively to the PG cells using phm-GAL4 resulted in larvae that remained permanently in the last larval stage for up to a month until they eventually died. Larval structures including neuromuscular junctions remain stable in similarly generated ETI larvae through their extended life-span (Miller, Ballard, and Ganetzky 2012) and the larvae appear to behave normally other than wandering periodically in and out of food. This suggests that although the larvae cannot undergo metamorphosis, the lack of ecdysone signaling does not completely prevent wandering behavior.

At 120 hrs AEL, the neurons of the 12A cluster show a prominent axon bundle that takes the dorsal pathway, which is characteristic of the early-born cells in the lineage (Mellert et al, 2016). This pattern differs from wildtype larvae of the same age (wandering larvae) which show the dorsal-routed bundle and a medially-routed bundle that comes from later born neurons. By 240hrs AEL, both the dorsal and medial bundles are evident and the 12A morphology appears wildtype. By 360hrs AEL, though, the bundles show the degeneration of the distal portion of the axons and some of the bundles are redirected. By 576 hrs AEL, more elaborate ectopic branches have formed.

Removal of ecdysone signaling causes pruning and ectopic arborization in arrested larval-born neuronal hemilineages (Fig 4.1). Hemilineage 12A extended third instar (ETI) birth order is same as wildtype (WT). The dorsal branch of 12A is born first in both ETI and WT (Fig 4.1). The morphology of multiple hemilineages is aberrant after a certain point of extended third instar life despite the initial development being stereotyped (Fig 4.1). This loss of wildtype morphology occurs between 240 and 360 hrs after egg laying in ETI larvae.

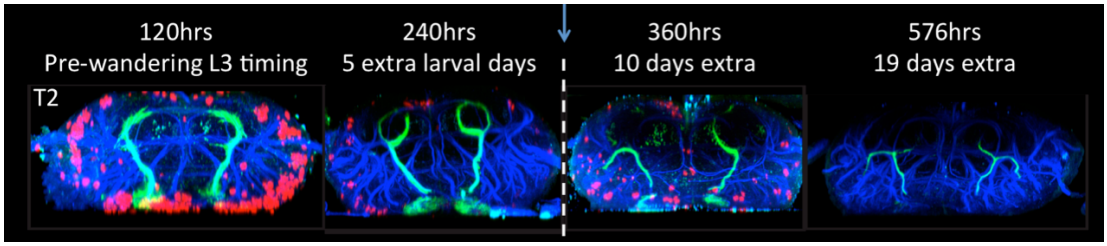

Figure 4.1 | Extended Third Instar Phenotype in 12A neurons. Transverse optical slice through the T2 segment ETI larvae of various ages. 120hrs, 240hrs, 360hrs, and 576hrs AEL. (GFP in green, Neuroglian in blue, BrdU in red). Images from Daniel Miller.

Sequencing quality is similar across the samples in the time series

In order to check the sequencing quality for the samples, the distribution of the FPKM values for all genes was determined. There are not substantial differences in the sequencing quality and overall distribution of expression within the time series, with similar median and mean FPKM values for all samples (Table 4.1). Strongly expressed genes are less variable between the two samples than weakly expressed genes. <10 FPKM is most variable between the two datasets, and >100 FPKM was the least variable between the two datasets. If the more abundantly expressed genes are the genes that are more important for the wildtype function of the neurons, then this would suggest that the neurons mostly differ in gene expression for less important genes.

	120hr ETI	240hr ETI	360hr ETI	576hr ETI
Median FPKMs	3	3	3	3
Mean FPKMs	24	27	21	21
Maximum FPKMs	16517	53426	7020	5518

Table 4.1 | Summary of expression in ETI 12A time series. Numbers are gene expression values in FPKM.

Housekeeping gene expression is largely preserved through the time series

To determine whether the morphological changes observed in the ETI time series were due to changes in general cellular processes, I examined the expression for a small number of "housekeeping" genes (involved in cell growth, cell cycle, or cytoskeletal structure) in the RNA-seq data. There is some variability within with the "housekeeping" genes shown in Table 4.2, but the greatest fold change observed was 3.46 in Gapdh2. The time points do not appear to have gross differences in expression for genes involved in very general cellular processes. However, 120hr ETI has much higher levels of both Act42A and Gapdh2, which may suggest that after this initial time point there is a general repression of genes involved in many basic cellular processes in the ETI neurons.

	120hr ETI	240hr ETI	360hr ETI	576hr ETI
myc (AKA *dm*)	127	194	208	176
Act42A	248	128	92	76
Gapdh1	31	26	15	20
Gapdh2	90	34	32	26
RpL13A	571	374	269	482
cyp33	5	6	10	3

Table 4.2 | Summary of "housekeeping" gene expression. Numbers are gene expression values in FPKM.

Similarity between stages in the ETI time series and WT 120hr 12A determined by PCA

I performed a principle component analysis (PCA) on the data of the ETI series to explore the basis for the variance amongst the various time points. *noe* expression was excluded from the PCA since it disproportionately affected the PCA to the point of completely overshadowing all other expression differences. The PCA shows that WT 120hr 12A neurons are most closely related to those from the 120 hr ETI sample and that the 120 hr ETI is separate from later stages in the ETI time series. PC1 accounts for much (69%) of the variability between ETI time points and WT 120hr 12A neurons (Table 4.3). WT 120hr 12A neurons are closest to ETI 120hr 12A in the first principal component (Figure 4.2). PC1 separates WT 120hr 12A neurons from 120hr ETI neurons and the later ETI time points from both 120hr ETI and WT 120hr

12A neurons. WT 120hr is roughly as similar to ETI 120hr as ETI 120hr is to the later ETI time points. PC2 accounts for 20% of the variability between these samples (Table 4.3). PC2 separates 120hr, 240hr, 360hr, and 576hr time points in chronological order. Interestingly, WT 120hr 12A neurons are considered most similar to 576hr ETI 12A neurons in PC2.

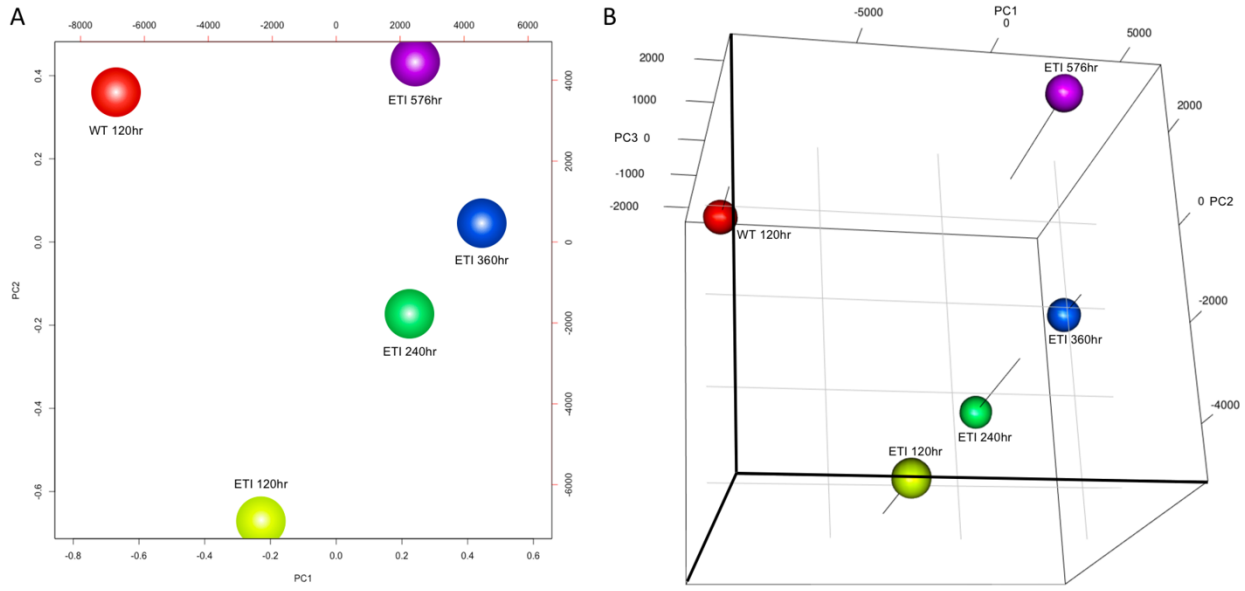

Figure 4.2 | PCA of ETI and WT 120hr 12A. (A): 2D PCA and (B): 3D PCA of ETI 12A time-points and WT 120hr 12A excluding *noe* expression. PCA created using FPKM values for every gene in each sample.

ETI 12A and WT 120hr 12A PCA Component Summary.					
Components	PC1	PC2	PC3	PC4	PC5
Standard deviation	5751	3067	1850	1450	1.04E-11
Proportion of Variance	69%	20%	7%	4%	0%
Cumulative Proportion	69%	88%	96%	100%	100%

Table 4.3 | ETI 12A and WT 120hr 12A PCA component summary. Standard deviation, proportion of variance, and cumulative proportion of variance for the five principal components for the ETI and WT 120hr 12A PCA (Figure 4.2).

The relative contributions of the top 20 genes that contribute positively and the top 20 genes that contribute negatively to each of the three principal components shown in Figure 4.2B are summarized in Table 4.S19.

Expression of the top 20 genes contributing positively and negatively to PC1 are shown in Table 4.4. These genes contribute most to separating WT 120 from the ETI time points and ETI 120hr from the other ETI time points. *Hdc* and *jim* are the two single largest contributors, with much higher expression in the later time points of the time series (after 120hr).

gene	PC1CC	WT 120hr	ETI 120hr	ETI 240hr	ETI 360hr	ETI 576hr
hdc	0.3521	1054	2582	4765	6393	4428
jim	0.3500	1378	2340	5508	6093	4873
CR42862	0.2649	1857	3585	5147	5319	5518
Df31	0.2347	3172	4654	6401	7020	4621
CG9894	0.2263	1248	3391	4144	4785	3871
lola	0.2122	758	2114	3243	3958	3014
His2A:CG33835	0.2081	762	2415	2606	4196	3296
CG9821	0.1910	720	1655	2747	3560	2743
Hsp23	-0.1896	4188	1564	1435	1232	1479
Hsromega	0.1873	658	1526	3300	2897	2996
RpL41	-0.1545	5526	6889	5106	3712	3906
Act5C	-0.1384	3917	3087	2687	1898	2006
Hsp27	-0.1336	2752	832	747	698	781
pAbp	0.1315	814	1896	2699	2840	2042
CG42622	0.1249	1109	3465	3681	3031	2836
14-3-3epsilon	-0.1090	3112	3259	2333	1840	1613
Lk6	0.0984	285	700	1258	1689	1440
miple	-0.0886	1718	941	564	469	518
Ef1alpha100E	-0.0883	1818	1456	883	648	683
snmRNA:331	-0.0850	3410	6150	3871	3214	2313
Qm	-0.0803	1867	1005	753	698	760
CG13928	-0.0771	1956	2613	1713	1089	1085
scyl	0.0759	193	624	1046	1329	999
fax	-0.0746	1913	1267	1069	735	1026
l(3)neo38	0.0745	1041	1466	1384	1837	2892
Rm62	0.0736	615	1669	1927	1885	1242
Cam	-0.0727	1546	1067	628	458	808
His2A:CG33820	0.0697	226	897	949	1458	938
tsr	-0.0662	1534	822	579	544	700
CG33229	0.0626	590	809	1264	1420	1348
roX1	0.0621	1032	1857	1512	1740	2768
snoRNA:Me28S-A2589a	0.0617	0	1871	0	2173	458
RpS27A	-0.0614	1373	944	640	510	582
CG2052	0.0585	485	760	1323	1250	1083
RpS15	-0.0584	1781	1747	956	1234	1003
RpS7	-0.0579	1783	2382	1296	1317	1171
cib	-0.0545	1615	1762	1470	951	761
alphaTub84B	-0.0531	1019	637	372	271	336
pros	-0.0508	4293	4518	5167	3690	2600

gene	PC1CC	WT 120hr	ETI 120hr	ETI 240hr	ETI 360hr	ETI 576hr
RpS11	-0.0490	1166	1003	618	531	576

Table 4.4 | Summary of expression for genes contributing most to PC1 in the PCA of ETI and WT 120hr hemilineage 12A neurons. Numbers are gene expression values in FPKM. Color coding is per gene: highest expression (green), medium expression (yellow), lowest expression (red). PC1CC column represents the correlation coefficient for PC1. Genes are ordered by absolute value of the correlation coefficient.

Expression of the top 20 genes contributing positively and negatively to PC2 are shown in Table 4.5. These genes contribute most to the temporal progression through the time series as shown in the PCA order of the time series, with negative contributions associated with early time points and positive contributions associated with later time points. The genes that contribute most to the variance described by PC2 are all genes expressed most highly in ETI 120hr neurons. The top contributions PC2 have diverse functions. The top contributors are snmRNA:331, a small nuclear RNA with an unknown function, Histone H4 replacement (*His4r*), Ribosomal protein L41 (RpL41), and Myosin 81F (Myo81F, CG42622). One of these genes, *Ef1alpha48D*, encodes a protein that delivers tRNA to the ribosome as part of the translation process, decreased expression of which is associated with subsequent decline in protein synthesis and aging, but the causal relationship for the latter is debated (Shepherd et al., 1989; Shikama, Ackermann, and Brack, 1994). The function of Prospero (*pros*) is described in Chapter 1. Pros acts a TF to repress genes associated with stem cell identity including cell cycle re-entry for proliferation. It also induces the expression of genes associated with neuronal differentiation. Hsp23 and Hsp27, both of which are code for heat shock proteins, respond to ecdysone (Amin, Mestril, and Voellmy, 1991). The other top contributions contain similarly diverse genes from nuclear RNAs, nucleolar RNAs, histone variants, ribosomal subunits, genes involved in alternative splicing, and transcription factors. Interestingly, two genes with highest expression in ETI 120hr neurons, chickadee (*chic*) and ciboulot (*cib*), are involved in remodeling of postembryonic neurons during metamorphosis (Boquet, 2000). Smt3 is the SUMO protein in *Drosophila* and is added to proteins using the SUMOylation enzyme lesswright (*lwr*) (Bhaskar, Valentine, and Courey, 2000).

gene	PC2CC	WT 120hr	ETI 120hr	ETI 240hr	ETI 360hr	ETI 576hr
snmRNA:331	-0.4380	3410	6150	3871	3214	2313
His4r	-0.3553	4309	6935	5840	5267	4375
RpL41	-0.2977	5526	6889	5106	3712	3906
CG42622	-0.2147	1109	3465	3681	3031	2836
Ef1alpha48D	-0.2016	672	2546	1262	1062	1202
pros	-0.1953	4293	4518	5167	3690	2600
snRNA:U6:96Aa	-0.1756	1265	1921	2087	1031	418
snoRNA:Me28S-A2589a	-0.1729	0	1871	0	2173	458
His3.3B	-0.1663	1982	2994	2366	1774	1620
Hsp23	0.1658	4188	1564	1435	1232	1479
CG13928	-0.1494	1956	2613	1713	1089	1085
smt3	-0.1443	1200	2440	2001	1560	1567
Df31	-0.1344	3172	4654	6401	7020	4621
RpS3	-0.1264	1755	3166	1924	2508	2314
14-3-3epsilon	-0.1237	3112	3259	2333	1840	1613
Hsp27	0.1229	2752	832	747	698	781
CG9894	-0.1135	1248	3391	4144	4785	3871
RpS7	-0.1105	1783	2382	1296	1317	1171
Rm62	-0.1092	615	1669	1927	1885	1242
l(3)neo38	0.0917	1041	1466	1384	1837	2892
RpL40	-0.0898	1508	1971	1254	1215	1020
cib	-0.0871	1615	1762	1470	951	761
chic	-0.0862	1734	2381	2212	2219	1780
jim	0.0711	1378	2340	5508	6093	4873
snoRNA:Me28S-A2589c	0.0635	800	0	0	329	105
snoRNA:Or-aca4	0.0457	8	21	33	27	608
tsr	0.0421	1534	822	579	544	700
Qm	0.0421	1867	1005	753	698	760
kis	0.0398	489	482	626	670	1012
14-3-3zeta	0.0377	2117	1531	1469	1670	1484
Obp44a	0.0371	89	154	177	115	686
CG42644	0.0368	424	0	0	0	114
sm	0.0355	635	490	580	535	848
Hsp68	0.0330	457	140	100	153	277
shep	0.0316	775	384	491	369	504
Jupiter	0.0310	391	786	727	929	1458
roX1	0.0286	1032	1857	1512	1740	2768
CG34360	0.0280	40	89	230	421	501
pUf68	0.0279	82	209	422	602	706
betaTub56D	0.0274	883	473	525	442	506

Table 4.5 | **Summary of expression for genes contributing most to PC2 in the PCA of ETI and WT 120hr hemilineage 12A neurons.** Numbers are gene expression values in FPKM. Color coding is per gene: highest expression (green), medium expression (yellow), lowest expression (red). PC2CC column represents the correlation coefficient for PC2. Genes are ordered by absolute value of the correlation coefficient.

Hierarchical clustering ETI time series and WT 120hr 12A determined by Hierarchical clustering

In order to visualize patterns of expression changes in differentially expressed genes, I performed a hierarchical clustering of genes in the ETI time series and WT 120hr 12A neurons that showed 2-fold enrichment between any sample with an associated q-value <0.1 and >100 FPKM expression in at least one sample. Several different patterns of gene expression changes can be seen in the differentially expressed genes when visualized by hierarchical clustering (Figure 4.3). There are genes with expression that's highest in WT 120hr 12A (cluster 3), genes with highest expression in 120hr ETI (clusters 1, 2, and 6), genes with highest expression in 240hr ETI neurons (cluster 7), genes with highest expression in 360hr ETI neurons (cluster 5), genes with highest expression in 576hr ETI neurons (clusters 4 and 9), and genes with increased expression at all time points after 120hrs ETI (cluster 10).

GSEA shows that genes from cluster 3, which represents genes with highest expression in WT 120hr 12A are enriched for terms for ribosomal subunits, but also for many processes involved in development and axonogenesis (Table 4.S16). GSEA shows many term enrichments for cluster 10, genes with expression that increase over the course of the time series. These enriched terms are mostly for very general processes including "gene expression", "metabolic processes", but also "neuron differentiation" (Table 4.S17).

Genes from the 576hr clusters (clusters 4 and 9) are diverse and do not show any significant gene set enrichments. Genes from the ETI 120hr cluster (cluster 6) did not show any significant gene set enrichments. Of the 16 genes in this cluster, several are known to have roles in neuron development. *Wnt4* is involved in many processes including axon guidance (Inaki et al., 2007). *Knot* (*kn*) is a TF involved in dendrite morphogenesis (Jinushi-Nakao et al., 2007), VNS development and cell fate specification for *FMRFamide* producing neurons (Bivik et al., 2015), and other processes. *Smt3* is an enzyme responsible for SUMOylation and nuclear import (Shih et al., 2002; Bhaskar, Valentine, and Courey, 2000) that is also implicated in axonogenesis and dendrite morphogenesis (Berdnik et al., 2012). *High mobility group protein D* (*HmgD*) is a TF involved in chromatin reorganization and promotion of dendrite arborization (Parrish et al., 2006). *Threonyl-tRNA synthetase* (*Aats-thr*) RNAi knockdowns show an underproliferation phenotype in neuronal stem cells (Neumüller et al., 2011). *Phyllopod* (*phyl*) controls the amount of *Notch* and *Wg*

signal by trafficking *Notch* and *Wg* pathway components in endocytic vesicles for degradation (Nagaraj and Banerjee, 2009). *Phyl* is also required for neuronal cell fate and differentiation in both photoreceptor neurons and external sensory organs (Chang et al., 1995; Pi, Wu, and Chien, 2001).

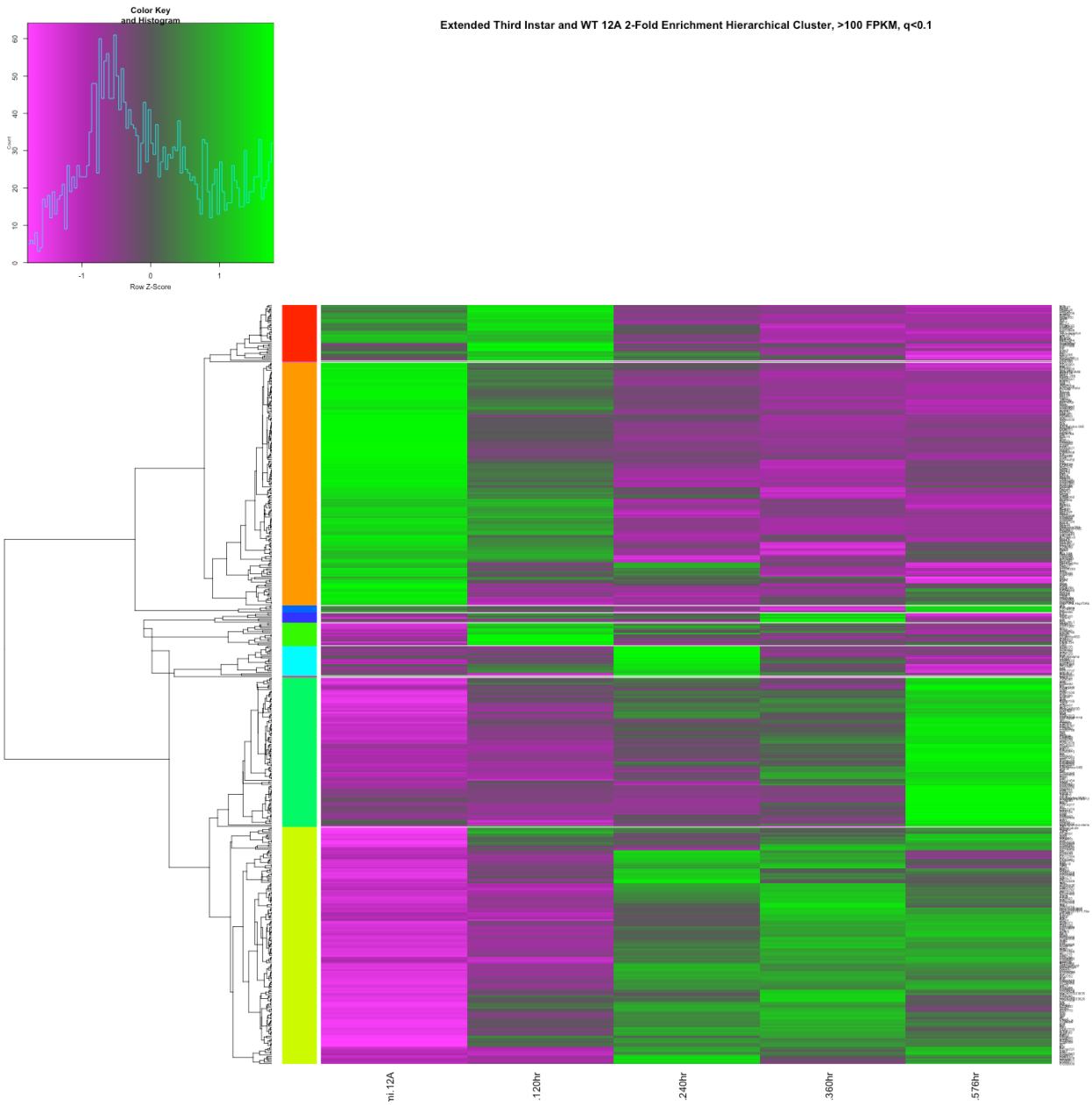

Figure 4.3 | ETI and WT 120hr 12A hierarchical clustering. 2-fold enrichment with an associated q-value <0.1 and >100 FPKM expression in at least one sample.

Comparison of 12A neurons from wildtype wandering larvae with similarly aged 120 hr ETI larvae.

ETI larvae are induced through removing ecdysone synthesis in the animals. The differences in expression between ETI 120hr and WT 120hr 12A neurons, therefore, should be due to the loss of ecdyse signaling. In order to determine which genes are being controlled by ecdysone signaling in these neurons, the two timepoints were compared. A summary of the number of genes expressed at various thresholds in both samples and the overlap in expression between the two samples showed that genes with low expression values were more variable between the two samples than genes with higher expression values (Table 4.S13).

When these two samples were compared, there were 101 genes differentially expressed at >100 FPKM, 2-fold change, q < 0.1 between the 120hr ETI and WT 120hr 12A (Table 4.S18). Genes with greater expression in WT 120hr 12A neurons are enriched for heat shock proteins (GO term "response to heat", 9 genes, FDR 6.8E-9). Some of these heat shock proteins are known to be involved in the response to ecdysone (Table 4.3). Genes with greater expression in ETI 120hr 12A neurons are enriched for transcription factors including *longitudinals lacking* (*lola*), *zelda* (*zld*), *knot* (*kn*), with 16 genes being associated with the GO term "regulation of gene expression" (FDR 0.0396). Charlatan (*chn*) is enriched in WT-120hr neurons relative to ETI-120hr neurons. *Chn* is a C2H2 TF that maintains a chromatin structure associated with proliferation and prevents differentiation in stem cells (Amcheslavsky et al., 2014).

	WT 120hr	120hr ETI	240hr ETI	360hr ETI	576hr ETI
Hsp70Aa	238*	63	87	121	172
Eip63E	46	94*	61	67	90
Eip74EF	51*	7	11	21	17
Hsp68	457*	140	100	153	277
Hsp70Ab	222*	68	85	116	163

Table 4.6 | Expression changes in a subset of genes that respond to ecdysone signaling. Numbers are gene expression values in FPKM. 1 standard deviation above the mean represented by: *.

Differentially expressed genes between WT 120hr and ETI 576hr hemilineage 12A neurons

Since hierarchical clustering of the differentially expressed genes between all samples did not show any significantly enriched gene sets in ETI 576hr, I performed a comparison of ETI 576hr to WT 120hr hemilineage 12A neurons directly in order to determine which genes and processes are disrupted between wildtype this later time point and WT animals. Since the removal of ecdysone is conflated with the progression of the time series in this comparison, I removed the genes that were differentially expressed between ETI 120hr and WT 120hr. These comparisons were performed by looking for genes with 2-fold change between WT 120hr 12A and 576hr ETI and q-value<0.1 and then removing genes that also met these criteria for WT 120hr 12A vs 120hr.

WT 120hr 12A neurons express several ribosomal subunits, expression of which is lost in 576hr ETI 12A neurons (GO term "structural constituent of ribosome", 31 genes, 2.28E-32) (Table 4.S15). WT 120hr 12A neurons also express several genes associated with locomotion that are lost in 576hr ETI 12A neurons (GO term "locomotion", 12 genes, FDR 0.0445). 12A locomotion: CadN, Cdc42, Jafrac1, NetB, Ten-m, dock, fra, lwr, qm, sn, spri, tsr (Table 4.S15).

576hr ETI 12A neurons express many genes associated with the synapse at higher levels than WT 120hr 12A neurons (Table 4.S14) as well as many genes associated with neurogenesis and neuron differentiation (Table 4.S14). Nine genes with increased expression in 576hr ETI compared to WT 120hr 12A are involved in synapse function: CG6490, S6k, brp, cac, dlg1, endoA, futsch, simj, stj (GO term "regulation of synapse structure or activity", FDR 0.0136).

18 genes with increased expression in 576 hr ETI are associated with the term "locomotion": Fas3, FoxP, InR, Mtl, Ptp99A, Ptpmeg, S6k, abd-A, cdm, csw, dlg1, foi, hipk, klar, nudE, seq, shot, spen (Table 4.S14).

Acetylcholinergic identity of 12A is maintained through the ETI time series

Hemilineage 12A neurons are acetylcholinergic in the adult (H Lacin, unpublished) and express the genes for the acetylcholine synthetic enzyme and vesicular transporter *Cha* and *VAChT* in immature larval-born neurons before metamorphosis (Table 3.10). Both *Cha* and *VAChT* expression is maintained at similar or higher levels than WT 120hr 12A neurons during the time series (Table 4.1). Thus, the 12A neurons maintain their cholinergic fate throughout the extended third instar period.

	WT WL3 12A	120hr ETI	240hr ETI	360hr ETI	576hr ETI
Cha	42	65	76	54	49
VAChT	116	177	128	111	117

Table 4.7 | Comparable levels of *Cha* and *VAChT* are expressed in WT WL3 hemilineage neurons and ETI 12A neurons. Numbers are expression values in FPKM.

The expression of beat family genes changes over the course of ETI time series

Beat genes are an immunoglobulin secreted and transmembrane proteins involved in axon guidance, choice of axon growth cone growth direction, and defasciculation of axons (Fambrough and Goodman, 1996; Pipes et al., 2001; Girard et al., 2006). *beat* genes are differentially expressed in ETI throughout the time series (Table 4.8). These changes in *beat* gene expression could partially explain the changes in arborization patterns that occur in the older animals. The other *beat* genes not included in the table did not meet the inclusion criteria for differential expression in the hierarchical clustering (2.5-fold change between any of the four time points, $q<0.1$ on that fold change, and FPKM >10 in at least one sample).

Beat-Ia expressing growth cones interact with the axonal attractant sidestep, in motor neurons (Siebert et al., 2009). Expression of *Sidestep* (*Side*) is also downregulated in the 12A neurons over the course of the ETI time series. If *Side* is downregulated in other VNS neurons as well, this could contribute to the ETI phenotype, since WT 120hr 12A and 120 hr ETI 12A neurons express *beat-Ia* at moderate levels, but then its level drop in later ETI time points.

high -> low

	120hr ETI	240hr ETI	360hr ETI	576hr ETI
beat-IIIa	90	49	30	20
beat-IIIb	74	56	54	29
beat-IV	20	13	2	9
beat-Ia	33	4	3	10
beat-Ic	42	19	23	15
beat-Vb	53	19	33	1

low -> high

	120hr ETI	240hr ETI	360hr ETI	576hr ETI
beat-VII	2	2	2	15

low -> high -> low

	120hr ETI	240hr ETI	360hr ETI	576hr ETI
beat-IIa	15	47	70	19
beat-IIb	14	5	27	5

Table 4.8 | Beat family genes differentially expressed during the ETI period. There are beaten-path genes that decrease in expression, increase in expression, and ones that first increase and then decrease. Numbers are expression values in FPKM.

Syp is expressed at much higher levels than Imp in hemilineage 12A ETI neurons

Syp and *Imp* are genes expressed at different ratios depending on the birth order of the neurons in a lineage and their ratio in individual cells is involved in establishing the temporal identity of individual neurons within the lineage (Liu et al., 2015). *Imp* is expressed at higher levels early into lineage production and *Syp* is expressed at higher levels late into lineage production.

Like other hemilineage clusters of interneurons late in larval life (Chapter 3) the 12A neurons in the 120 hr ETI larvae show high *Syp* and low *Imp* expression (Table 4.3). The ratio becomes a bit more extreme in later samples, likely due an extension of proliferation in the 12A cluster in the ETI larvae. However, the overall maintenance of the *Syp*/*Imp* ratio is consistent with individual neurons in the cluster maintaining their characteristic values despite the extended period of time in the last larval stage.

Sample	*Syp*	*Imp*	*Syp/Imp*
120hr ETI	351	34	10.3
240hr ETI	339	2	169.5
360hr ETI	266	0	∞
576hr ETI	346	8	43.3

Table 4.9 | *Syp* is expressed at much higher levels than *Imp* in all ETI samples. *Syp* is expressed at high levels and *Imp* is expressed at low levels in all ETI immature 12A neurons. Numbers are gene expression values in FPKM.

Mamo and noe expression decline during the ETI series

Maternal gene required for meiosis (mamo) is a C2H2 zinc finger TF and *novel* (noe) is a gene of unknown function expressed specifically in the CNS and it encodes a protein that is not related to any known gene family (Kim et al., 1998). Loss of expression of these two genes might also contribute to the ETI phenotype (Table 4.6). *noe* represent the greatest fold change between the 120hr ETI and 576hr ETI.

	12A	120hr ETI	240hr ETI	360hr ETI	576hr ETI
mamo	46	40	2	4	8
noe	3578	16517	53426	0	0

Table 4.10 | Two genes lose expression after early time points in the 12A ETI time series. Numbers are gene expression values in FPKM.

Transcription factor expression is mostly preserved in hemilineage 12A ETI neurons

Transcription factors are an important class of genes for development and establishing cell fate. *Tiwaz* (*twz*), *unc-4*, and *Transcription factor AP-2* (*TfAP-2*) are all expressed in WT 120hr 12A neurons. Expression *TfAP-2* and *unc-4* remains at high levels (Table 4.4). *TfAP-2* is expressed at higher levels in ETI neurons at all time points relative to WT 120hr 12A neurons. *Unc-4* expression is slightly higher in ETI neurons with the exception of the final 576hr time point and peaks at 240hrs.

	12A	120hr ETI	240hr ETI	360hr ETI	576hr ETI
TfAP-2	163	333*	294	262	283
unc-4	150	189	216*	188	98

Table 4.11 | Transcription factor gene expression in WT WL3 12A neurons and in ETI 12A neurons. Expression values above 1 standard deviation above the mean for each gene indicated by *. Numbers are gene expression values in FPKM.

ETI phenotype correlates with decreased expression of genes required for TfAP-2 function

In contrast to the TFs *TfAP-2* and *unc-4*, expression of the gene for transcription factor interacting protein tiwaz (*twz*) is not maintained (Table 4.5). *Twz* expression decreases throughout the time series and is decreased relative to expression in WT 120hr 12A neurons. Functional twz is required for TfAP-2 function and the mouse homologues of both genes interact molecularly (Williams et al., 2014). Thus, a substantial decrease in *twz* expression could cause a TfAP-2 loss of function phenotype to occur. As shown in Chapter 3, the lack of TfAP-2 function in the 12A neurons results in arbors that abort before making the decision to take a dorsal or medial path. Higher levels of *TfAP-2* expression in the ETI neurons could be an attempt by the neurons to compensate for the loss of the *TfAP-2* pattern *twz*.

Interestingly, in the older ETI larvae, the axons of the 12A neurons degenerate back to the point where the young neurons make the decision to take the dorsal or the medial pathway (Figure 4.1). This appears to be the same point where the *TfAP-2* mutants axons are arrested (Chapter 3; Figure 3.10). *TfAP-2* expression does not decrease during the ETI time series, but two known *TfAP-2* interactors - *twz* and *lwr* - do. Both decline markedly as the larvae age. I think that this compromise in the TfAP-2 pathway may be a major contributor to the instability of the 12A phenotype as the larvae age.

	12A	120hr ETI	240hr ETI	360hr ETI	576hr ETI
TfAP-2	163	333*	294	262	283
twz	110*	66	37	22	22
lwr	107*	92	51	52	30

Table 4.12 | Expression of TfAP-2 and two interacting proteins, twz and lwr. TfAP-2 is maintained at high levels throughout the time series and relative to the WT 120hr 12A neurons. Gene expression for the TfAP-2 interacting proteins twz and lwr are decreased relative to WT 120hr 12A neurons and continue to decrease throughout the time series. Expression values above 1 standard deviation above the mean for each gene indicated by *. Numbers are gene expression values in FPKM.

Discussion

Removal of ecdysone signaling can be achieved by expressing smox-RNAi in the ring gland with phm-GAL4. Removing ecdysone in the larva prevents metamorphosis and causes the animals to remain in an extended third instar until eventually dying. Lack of ecdysone signaling and an extended period of third instar causes changes in axon morphology in hemilineage 12A that become more extreme with time. This breakdown in axon morphology correlates with transcriptional changes, both increases and decreases in genes with diverse functions and belonging to many different classes of protein.

There are two ecdysone-dependent decisions that occur in the third instar. The first occurs at critical weight, about 8-10 hrs into the third instar. Critical weight is the species-specific weight of the larva necessary to initiate metamorphosis through a series of hormonal changes and subsequent behaviors (Nijhout and Williams 1974b). Juvenile hormone is released by the corpora allata (CA) and is needed for larval growth and to suppress metamorphosis before critical weight is achieved (Nijhout and Williams 1974a). After critical weight is reached, larvae are now large enough to undergo metamorphosis and their imaginal discs will subsequently undergo morphogenesis even if the larvae are starved (Mirth et al., 2009). The second is the ecdysone induced changes that cause the larva to stop feeding and leave the food (Nijhout and Williams, 1974b; Dominick and Truman, 1986), the timing of which is at least partially mediated by DHR4, the expression of which is induced by ecdysone (King-Jones et al., 2005). The neurons in the 12A cluster switch their axon path from the dorsal pathway to the intermediate pathway around the time of the critical weight (Mellert et al., 2016). The observation that the neurons in the 120hr ETI group were still showing the dorsal projection suggests that this shift in neuronal phenotypes has not yet occurred in the 120h ETI larvae.

Why do the hemilineage 12A neurons prune and sprout ectopic arbors? A number of different hypotheses about why this may occur can be considered. The neurons could be losing their identity. Alternatively, the neurons could be undergoing some of the

processes of maturation proper ecdysone signaling due to an inability to maintain the arrested neuronal state.

Important transcription factor, neurotransmitter synthesis, and neurotransmitter transport gene expression related to the identity of the hemilineage 12A neurons is not lost, which suggests that the neurons have not lost their identity. Loss of ecdysone does not cause loss of expression for many genes expressed by wildtype 12A that are necessary for the development of wildtype 12A morphology, including unc-4 and TfAP-2. Maintenance of expression of the acetylcholine neurotransmission genes *Cha* and *VAChT* along with the TFs *TfAP-2* and *unc-4* suggests that the morphological phenotype is not caused by a breakdown in identity maintenance.

Early effects of ecdysone abolishment are not very dramatic. Gene expression in 120hr 12A ETI is very similar to wildtype 12A expression. *mamo*, *noe*, and other genes with lost expression may be required for identity maintenance or maintenance of arrested state. Loss of *mamo* and *noe* expression after early ETI time points correlates to the transition from wildtype to pruned arbors. *mamo* and *noe* are highly expressed early in the ETI time series and then expression is completely lost, which makes them seem likely to be important to the development of the ETI ectopic arborization phenotype. They represent the highest fold changes between the early time points and late time points of the ETI time series. This data together with the change in expression from genes associated with developmental to synaptic genes from 120hr to 576hr ETI time points, this suggests that *mamo* and *noe* may be needed to maintain the immature neuron state. Based on the rest of the data, however, if this is the case, it seems to be a process that is occurring alongside other causes for the changes in the axon morphologies of hemilineage 12A neurons over the course of the time series. There are many differentially expressed genes between the wildtype 12A neurons and the extended third instar neurons. Some known ecdysone response genes are differentially expressed as expected. Many genes are differentially expressed over the course of the time series as well, including some genes associated with neuronal maturation, but no obvious pattern emerges from these genes. They are involved in many disparate processes. The neurons do not appear to have lost their neuronal identity nor do they appear to be undergoing general maturation processes. I propose, instead, that the primary cause of this phenotype is due to loss of TfAP-2 function.

The expression of two genes for proteins that have been previously shown to be required for TfAP-2 function are decreased in ETI neurons compared to WT neurons and decreases over the course of the ETI time series: *lwr* and *twz*. Twz is required for TfAP-2 function and based on mouse homologues of these genes, lwr most likely SUMOylates TfAP-2 for it to function normally (Eloranta and Hurst, 2002; Williams et al., 2014). Twz and lwr molecularly interact (Giot et al., 2003). The pruning of hemilineage 12A neuron axons observed at 360hrs into the ETI time series is similar to the TfAP-2 mutant clone phenotype. *TfAP-2* mutant axons are arrested at the choice point between dorsal and medial branches, which is the same point along the axon that the neurons in the ETI animals are pruned to before forming ectopic outgrowths. Notably, ectopic branching was also observed on one occasion in the TfAP-2 mutant clones, suggesting an even greater similarity between the two phenotypes. Thus, I propose that impairment of TfAP-2 function may explain the morphological changes in ETI 12A axons.

Supplemental figures and tables

Supplemental figure: Summary of common/invariant expression in WT 120hr 12A vs 120hr ETI

	Number of genes expressed			Percent of all genes expressed within 1.5-fold in both samples	
FPKM threshold	12A	120hr ETI	Within 1.5-fold between 12A and 120hr ETI	12A	120hr ETI
>1 FPKM	9253	9043	4609	50%	51%
>10 FPKM	5030	5022	3232	64%	64%
>20 FPKM	3372	3429	2332	69%	68%
>100 FPKM	768	804	600	78%	75%
>500 FPKM	142	135	97	68%	72%

Table 4.S13 | Summary of common/invariant expression 12A vs 120hr ETI. Shown are the number of genes expressed at each threshold (1, 10, 20, 100, 500 FPKM) by WT 120hr 12A neurons, 120hr ETI 12A neurons, and the percentage of genes in each sample that are expressed within 1.5-fold between the two samples.

Term Category	Term	gene #	FDR	gene names
Cellular Component	cell	91	0.00215	Aac11, Arc1, CG10077, CG10277, CG11486, CG14977, CG30497, CG3287, CG42258, CG42678, CG42748, CG5554, CG5792, CG6340, CG6490, CG7611, CG8680, CG9003, CycG, DOR, Dcp2, E(var)3-9, FBpp0073155, FBpp0084023, Fas3, FoxP, GATAd, InR, MEP-1, MSBP, Manf, Mtl, Myb, Ncoa6, Pitslre, Prp3, Ptp99A, Ptpmeg, Rbp1-like, Rtnl1, S6k, SNF4Agamma, Sep4, Set1, TSG101, Tango5, Tfb1, Tsp42Ee, abd-A, brp, cac, casp, chrb, cora, crc, csw, dlg1, endoA, foi, futsch, galectin, glec, hipk, inaE, jigr1, jim, klar, l(3)neo38, lack, lolal, lost, maf-S, mtt, nrv2, nudE, or, pk, pog, qvr, seq, shot, shrb, simj, slim, spen, stau, stj, su(w[a]), tws, vsg, wech
Cellular Component	cell part	91	0.00215	Aac11, Arc1, CG10077, CG10277, CG11486, CG14977, CG30497, CG3287, CG42258, CG42678, CG42748, CG5554, CG5792, CG6340, CG6490, CG7611, CG8680, CG9003, CycG, DOR, Dcp2, E(var)3-9, FBpp0073155, FBpp0084023, Fas3, FoxP, GATAd, InR, MEP-1, MSBP, Manf, Mtl, Myb, Ncoa6, Pitslre, Prp3, Ptp99A, Ptpmeg, Rbp1-like, Rtnl1, S6k, SNF4Agamma, Sep4, Set1, TSG101, Tango5, Tfb1, Tsp42Ee, abd-A, brp, cac, casp, chrb, cora, crc, csw, dlg1, endoA, foi, futsch, galectin, glec, hipk, inaE, jigr1, jim, klar, l(3)neo38, lack, lolal, lost, maf-S, mtt, nrv2, nudE, or, pk, pog, qvr, seq, shot, shrb, simj, slim, spen, stau, stj, su(w[a]), tws, vsg, wech
Biological Process	generation of neurons	28	0.00229	CG11448, CG6490, Fas3, InR, Lin29, MEP-1, Manf, Mtl, Ptp99A, Ptpmeg, S6k, abd-A, alph, cora, csw, dlg1, drpr, futsch, galectin, jim, klar, pk, seq, shot, shrb, spen, stau, tws
Biological Process	regulation of growth	14	0.00264	CG6490, InR, S6k, TSG101, cac, chrb, dlg1, drpr, futsch, lack, shot, shrb, simj, stj
Biological Process	biological regulation	66	0.00279	Aac11, Alg-2, CG13624, CG14977, CG40191, CG5315, CG5554, CG6490, CycG, DOR, Dcp2, InR, Lin29, MEP-1, Manf, Myb, NaCP60E, Ncoa6, PNUTS, Pitslre, Prp3, Ptp99A, RhoGAP19D, Rlip, SNF4Agamma, Set1, TSG101, Teh2, abd-A, alph, brp, cac, casp, cdm, cora, crc, csw, dlg1, drpr, endoA, futsch, hipk, inaE, jigr1, jim, klar, lack, lolal, maf-S, mtt, nrv2, or, pk, pog, qvr, seq, shrb, simj, slim, spen, stau, stj, tws, uex, vsg, wech
Biological Process	regulation of biological quality	29	0.00279	CG14977, CG5315, CG5554, CG6490, InR, Lin29, Manf, Mtl, Myb, Pitslre, S6k, SNF4Agamma, brp, cac, cora, dlg1, endoA, futsch, hipk, klar, nrv2, or, pk, qvr, shot, simj, stj, tws, uex
Biological Process	tube morphogenesis	20	0.00377	CG6767, Fas3, Mtl, RhoGAP19D, TSG101, alph, cora, csw, dlg1, foi, hipk, klar, l(3)neo38, lack, lolal, pk, seq, shot, spen, vsg
Biological Process	tube development	24	0.00377	CG6767, Fas3, InR, Mtl, RhoGAP19D, TSG101, abd-A, alph, cora, csw, dlg1, drpr, foi, hipk, klar, l(3)neo38, lack, lolal, pk, seq, shot, spen, tws, vsg
Biological Process	regulation of cellular process	58	0.00492	Aac11, Alg-2, CG13624, CG14977, CG40191, CG5315, CG5554, CG6490, CycG, DOR, Dcp2, InR, MEP-1, Myb, NaCP60E, Ncoa6, PNUTS, Pitslre, Prp3, Ptp99A, RhoGAP19D, Rlip, SNF4Agamma, Set1, TSG101, abd-A, alph, brp, cac, casp, cdm, chrb, crc, csw, dlg1, drpr, futsch, hipk, inaE, jim, klar, lack, lolal, maf-S, mtt, pk, pog, qvr, seq, shrb, simj, slim, spen, stau, stj, tws, vsg, wech
Cellular Component	smooth septate junction	3	0.00734	Fas3, cora, dlg1
Cellular Component	presynaptic active zone	4	0.00734	S6k, brp, cac, stj

Term Category	Term	gene #	FDR	gene names
Cellular Component	neuron part	13	0.00734	CG6490, Ptp99A, Rtnl1, S6k, brp, cac, dlg1, futsch, mtt, nrv2, or, shot, stj
Biological Process	neuron differentiation	23	0.00749	CG11448, CG6490, Fas3, InR, Lin29, MEP-1, Manf, Mtl, Ptp99A, Ptpmeg, S6k, cora, csw, drpr, futsch, galectin, jim, klar, pk, seq, shot, shrb, spen
Biological Process	cell development	34	0.00749	CG11448, CG5315, CG6490, Fas3, InR, Lin29, MEP-1, Manf, Msi, Myb, Ptp99A, Ptpmeg, S6k, TSG101, abd-A, cora, csw, drpr, futsch, galectin, jim, klar, l(3)01239, lack, lost, maf-S, mri, nrv2, nudE, seq, shot, shrb, spen, stau
Biological Process	localization	38	0.00749	CG10277, CG11374, CG14977, CG32000, CG3287, CG6364, FBpp0084023, MFS17, Mtl, NaCP60E, PNUTS, Rlip, S6k, SNF4Agamma, TSG101, Tango5, abd-A, brp, cac, cdm, cora, csw, dlg1, drpr, endoA, foi, futsch, galectin, klar, l(3)01239, lost, nrv2, nudE, pk, qtc, spen, stau, stj
Biological Process	single-organism behavior	16	0.00771	Fas3, FoxP, Lin29, NaCP60E, Ptpmeg, Rtnl1, S6k, brp, cac, dlg1, drpr, futsch, mtt, simj, stau, vsg
Biological Process	anatomical structure development	56	0.00877	Aac11, CG11448, CG17683, CG5315, CG6490, CG6767, CycG, Fas3, InR, Lin29, MEP-1, Manf, Msi, Mtl, Myb, Ptp99A, Ptpmeg, RhoGAP19D, S6k, TSG101, abd-A, alph, chrb, cora, crc, csw, dlg1, drpr, foi, futsch, galectin, glec, hipk, jim, klar, l(3)01239, l(3)neo38, lack, lolal, lost, maf-S, mri, nrv2, nudE, pk, pog, rgn, seq, shot, shrb, simj, spen, stau, tws, vsg, wech
Biological Process	cellular component organization	46	0.0099	CG11448, CG14977, CG17683, CG9836, CycG, E(var)3-9, Fas3, InR, Lin29, MEP-1, Manf, Mtl, Myb, Ncoa6, Ptp99A, Ptpmeg, Rbp1-like, Rtnl1, S6k, Set1, TSG101, Tango5, Tfb1, brp, cora, csw, dlg1, drpr, endoA, futsch, jim, klar, lost, mri, mus210, nrv2, nudE, or, pk, seq, shot, shrb, spen, stau, stj, tws
Cellular Component	basolateral plasma membrane	5	0.01	Fas3, cac, dlg1, foi, stau
Biological Process	single-organism cellular process	78	0.0106	Aac11, Alg-2, CG11374, CG11448, CG14977, CG17683, CG32000, CG5315, CG5554, CG6364, CG6490, CG6767, CycG, DOR, Dcp2, E(var)3-9, FBpp0073155, FBpp0084023, Fas3, InR, Lin29, MEP-1, MFS17, Manf, Msi, Myb, NaCP60E, Ncoa6, Pitslre, Ptp99A, Ptpmeg, RhoGAP19D, SNF4Agamma, Sep4, Set1, TSG101, Tango5, Tfb1, abd-A, alph, brp, cac, cdm, chrb, cora, crc, csw, dlg1, drpr, endoA, foi, futsch, galectin, inaE, jim, klar, l(3)01239, lack, lolal, lost, maf-S, mri, mtt, mus210, nrv2, nudE, or, pk, pog, qtc, seq, shrb, simj, spen, stau, stj, tws, uex
Biological Process	regulation of cellular component organization	20	0.0113	CG6490, Dcp2, InR, Mtl, Myb, Pitslre, Prp3, S6k, cac, dlg1, drpr, futsch, jim, klar, l(3)neo38, shot, simj, stau, stj, tws
Biological Process	behavior	18	0.0123	Fas3, FoxP, InR, Lin29, NaCP60E, Ptpmeg, Rtnl1, S6k, brp, cac, dlg1, drpr, futsch, mtt, qtc, simj, stau, vsg
Biological Process	anatomical structure morphogenesis	36	0.0123	CG11448, CG6767, Fas3, InR, MEP-1, Mtl, Myb, Ptp99A, Ptpmeg, RhoGAP19D, S6k, TSG101, abd-A, alph, chrb, cora, crc, csw, dlg1, foi, futsch, hipk, jim, klar, l(3)neo38, lack, lolal, nrv2, nudE, pk, pog, seq, shot, shrb, spen, vsg
Biological Process	regulation of cell communication	21	0.0123	Alg-2, CG14977, CG5315, Ncoa6, Rlip, S6k, Set1, TSG101, alph, brp, cac, casp, cdm, chrb, hipk, lack, pk, qvr, shrb, slim, spen
Biological	developmental	59	0.0123	Aac11, CG11448, CG17683, CG5315, CG6490, CG6767,

Term Category	Term	gene #	FDR	gene names
Process	process			CycG, Fas3, InR, Lin29, MEP-1, Manf, Msi, Mtl, Myb, PNUTS, Ptp99A, Ptpmeg, RhoGAP19D, S6k, TSG101, abd-A, alph, chrb, cora, crc, csw, dlg1, drpr, foi, futsch, galectin, glec, hipk, jim, klar, l(3)01239, l(3)neo38, lack, lolal, lost, maf-S, mri, nrv2, nudE, or, pk, pog, qtc, rgn, seq, shot, shrb, simj, spen, stau, tws, vsg, wech
Biological Process	single-multicellular organism process	58	0.0123	Aac11, Arc1, CG11448, CG17683, CG5315, CG6490, CG6767, Fas3, FoxP, InR, Lin29, MEP-1, Manf, Mtl, Obp44a, Ptp99A, Ptpmeg, RhoGAP19D, S6k, TSG101, abd-A, alph, brp, cac, chrb, cora, crc, csw, dlg1, drpr, foi, futsch, galectin, glec, hipk, jim, klar, l(3)neo38, lack, lolal, lost, mri, mtt, nrv2, nudE, pk, pog, qvr, seq, shot, shrb, simj, spen, stau, stj, tws, vsg, wech
Biological Process	regulation of developmental growth	10	0.0123	CG6490, InR, S6k, TSG101, cac, dlg1, futsch, shot, simj, stj
Biological Process	regulation of biological process	59	0.0123	Aac11, Alg-2, CG13624, CG14977, CG40191, CG5315, CG5554, CG6490, CycG, DOR, Dcp2, InR, MEP-1, Myb, NaCP60E, Ncoa6, PNUTS, Pitslre, Prp3, Ptp99A, RhoGAP19D, Rlip, SNF4Agamma, Set1, TSG101, Teh2, abd-A, alph, brp, cac, casp, cdm, crc, csw, dlg1, drpr, futsch, hipk, inaE, jigr1, jim, klar, lack, lolal, maf-S, mtt, pk, pog, qvr, seq, shrb, simj, slim, spen, stau, stj, tws, vsg, wech
Biological Process	positive regulation of multicellular organismal process	9	0.0132	InR, S6k, abd-A, alph, cac, dlg1, qvr, shot, simj
Biological Process	neurogenesis	32	0.0134	Aac11, CG11448, CG17683, CG6490, Fas3, InR, Lin29, MEP-1, Manf, Mtl, Ptp99A, Ptpmeg, S6k, abd-A, alph, cora, csw, dlg1, drpr, foi, futsch, galectin, jim, klar, nrv2, pk, seq, shot, shrb, spen, stau, tws
Biological Process	cell differentiation	44	0.0134	Aac11, CG11448, CG17683, CG5315, CG6490, Fas3, InR, Lin29, MEP-1, Manf, Msi, Mtl, Myb, Ptp99A, Ptpmeg, S6k, TSG101, abd-A, alph, cora, csw, dlg1, drpr, foi, futsch, galectin, jim, klar, l(3)01239, lack, lost, maf-S, mri, nrv2, nudE, pk, qtc, seq, shot, shrb, simj, spen, stau, tws
Biological Process	multicellular organismal process	63	0.0134	Aac11, Arc1, CG11448, CG17683, CG3662, CG5315, CG6490, CG6767, Fas3, FoxP, InR, Lin29, MEP-1, Manf, Msi, Mtl, Myb, Obp44a, Ptp99A, Ptpmeg, RhoGAP19D, S6k, TSG101, abd-A, alph, brp, cac, chrb, cora, crc, csw, dlg1, drpr, foi, futsch, galectin, glec, hipk, jim, klar, l(3)01239, l(3)neo38, lack, lolal, lost, mri, mtt, nrv2, nudE, pk, pog, qtc, qvr, seq, shot, shrb, simj, spen, stau, stj, tws, vsg, wech
Biological Process	locomotion	18	0.0134	Fas3, FoxP, InR, Mtl, Ptp99A, Ptpmeg, S6k, abd-A, cdm, csw, dlg1, foi, hipk, klar, nudE, seq, shot, spen
Biological Process	single-organism process	87	0.0134	Aac11, Alg-2, Arc1, CG10277, CG11374, CG11448, CG14977, CG17683, CG32000, CG5315, CG5554, CG6364, CG6490, CG8680, CycG, DOR, Dcp2, E(var)3-9, FBpp0084023, Fas3, FoxP, InR, Lin29, MEP-1, MFS17, Manf, Msi, Myb, NaCP60E, Ncoa6, Obp44a, PNUTS, Pitslre, Ptp99A, Ptpmeg, RhoGAP19D, Rtnl1, SNF4Agamma, Sep4, Set1, TSG101, Tango5, Tfb1, abd-A, alph, brp, cac, cdm, chrb, cora, crc, csw, dlg1, drpr, endoA, foi, futsch, galectin, glec, hipk, jim, klar, l(3)01239, l(3)neo38, lack, lolal, lost, maf-S, mri, mtt, mus210, nrv2, nudE, or, pk, pog, qvr, rgn, seq, simj, spen, stau, stj, tws,

Term Category	Term	gene #	FDR	gene names
				uex, vsg, wech
Biological Process	single-organism developmental process	58	0.0134	Aac11, CG11448, CG17683, CG5315, CG6490, CG6767, Fas3, InR, Lin29, MEP-1, Manf, Msi, Mtl, Myb, PNUTS, Ptp99A, Ptpmeg, RhoGAP19D, S6k, TSG101, abd-A, alph, chrb, cora, crc, csw, dlg1, drpr, foi, futsch, galectin, glec, hipk, jim, klar, l(3)01239, l(3)neo38, lack, lolal, lost, maf-S, mri, nrv2, nudE, or, pk, pog, qtc, rgn, seq, shot, shrb, simj, spen, stau, tws, vsg, wech
Biological Process	positive regulation of developmental growth	6	0.0134	InR, S6k, cac, dlg1, shot, simj
Biological Process	epithelial tube morphogenesis	17	0.0134	CG6767, Fas3, Mtl, RhoGAP19D, TSG101, alph, cora, csw, dlg1, foi, hipk, l(3)neo38, pk, seq, shot, spen, vsg
Biological Process	organ development	29	0.0136	CG6767, Fas3, InR, Lin29, Mtl, Ptpmeg, RhoGAP19D, TSG101, abd-A, alph, cora, csw, dlg1, drpr, foi, futsch, hipk, klar, l(3)neo38, lolal, nrv2, pk, seq, shot, simj, spen, tws, vsg, wech
Biological Process	regulation of synapse structure or activity	9	0.0136	CG6490, S6k, brp, cac, dlg1, endoA, futsch, simj, stj
Biological Process	establishment of localization	31	0.0136	CG10277, CG11374, CG32000, CG3287, CG6364, FBpp0084023, MFS17, NaCP60E, PNUTS, Rlip, S6k, TSG101, Tango5, brp, cac, cdm, cora, csw, dlg1, drpr, endoA, foi, futsch, galectin, klar, l(3)01239, nrv2, nudE, pk, qtc, stj
Biological Process	system development	43	0.0151	Aac11, CG11448, CG17683, CG6490, CG6767, Fas3, InR, Lin29, MEP-1, Manf, Mtl, Ptp99A, Ptpmeg, RhoGAP19D, S6k, TSG101, abd-A, alph, cora, csw, dlg1, drpr, foi, futsch, galectin, glec, hipk, jim, klar, l(3)neo38, lack, lolal, nrv2, pk, seq, shot, shrb, simj, spen, stau, tws, vsg, wech
Cellular Component	synapse	10	0.0153	Arc1, FBpp0073155, FBpp0084023, Fas3, S6k, brp, cac, dlg1, or, stj
Biological Process	regulation of signaling	20	0.0167	Alg-2, CG14977, CG5315, Ncoa6, Rlip, Set1, TSG101, alph, brp, cac, casp, cdm, chrb, hipk, lack, pk, qvr, shrb, slim, spen
Biological Process	tissue morphogenesis	19	0.0187	CG6767, Fas3, InR, Mtl, RhoGAP19D, TSG101, abd-A, alph, cora, csw, dlg1, foi, hipk, l(3)neo38, pk, seq, shot, spen, vsg
Biological Process	neuron development	19	0.0204	CG11448, CG6490, Fas3, InR, Lin29, MEP-1, Manf, Ptp99A, Ptpmeg, S6k, drpr, futsch, galectin, jim, klar, seq, shot, shrb, spen
Cellular Component	synapse part	8	0.0219	FBpp0073155, FBpp0084023, S6k, brp, cac, dlg1, or, stj
Cellular Component	axon	7	0.0235	CG6490, Ptp99A, Rtnl1, dlg1, futsch, nrv2, shot
Biological Process	single-organism localization	30	0.0252	CG10277, CG11374, CG32000, CG6364, FBpp0084023, MFS17, NaCP60E, PNUTS, S6k, TSG101, Tango5, brp, cac, cora, csw, dlg1, drpr, endoA, foi, futsch, galectin, klar, l(3)01239, lost, nrv2, nudE, or, qtc, stau, stj
Biological Process	nervous system development	33	0.0254	Aac11, CG11448, CG17683, CG6490, Fas3, InR, Lin29, MEP-1, Manf, Mtl, Ptp99A, Ptpmeg, S6k, abd-A, alph, cora, csw, dlg1, drpr, foi, futsch, galectin, glec, jim, klar, nrv2, pk, seq, shot, shrb, spen, stau, tws
Biological Process	regulation of multicellular	18	0.0254	CG6490, InR, Mtl, S6k, TSG101, abd-A, alph, cac, csw, dlg1, futsch, klar, qvr, shot, simj, stau, stj, tws

Term Category	Term	gene #	FDR	gene names
	organismal process			
Biological Process	regulation of multicellular organismal development	15	0.0254	CG6490, Mtl, TSG101, abd-A, alph, cac, csw, dlg1, futsch, klar, shot, simj, stau, stj, tws
Biological Process	regulation of cellular component biogenesis	10	0.0259	CG6490, Dcp2, cac, dlg1, futsch, klar, shot, simj, stau, stj
Biological Process	regulation of developmental process	19	0.0263	CG5315, CG6490, InR, Mtl, Pitslre, S6k, TSG101, abd-A, alph, cac, csw, dlg1, futsch, klar, shot, simj, stau, stj, tws
Biological Process	negative regulation of multi-organism process	4	0.0265	TSG101, casp, klar, shrb
Cellular Component	intracellular	75	0.03	Aac11, Arc1, CG10077, CG10277, CG11486, CG14977, CG30497, CG3287, CG42678, CG5792, CG6340, CG7611, CG8680, CG9003, CycG, DOR, Dcp2, E(var)3-9, Fas3, FoxP, GATAd, MEP-1, Manf, Mtl, Myb, Ncoa6, Pitslre, Prp3, Ptpmeg, Rbp1-like, Rtnl1, S6k, SNF4Agamma, Sep4, Set1, TSG101, Tango5, Tfb1, Tsp42Ee, abd-A, brp, casp, chrb, cora, crc, csw, dlg1, endoA, futsch, galectin, glec, hipk, inaE, jigr1, jim, klar, l(3)neo38, lack, lolal, lost, maf-S, nudE, or, pk, seq, shot, shrb, simj, slim, spen, stau, su(w[a]), tws, vsg, wech
Cellular Component	nucleus	39	0.03	Aac11, CG30497, CG3287, CG6340, DOR, E(var)3-9, FBpp0091148, FBpp0091152, Fas3, FoxP, GATAd, MEP-1, Myb, Ncoa6, Pitslre, Prp3, Rbp1-like, S6k, SNF4Agamma, Set1, Tfb1, abd-A, crc, glec, hipk, jigr1, jim, klar, l(3)neo38, lack, lolal, lost, maf-S, nudE, seq, simj, spen, su(w[a]), tws
Cellular Component	lateral plasma membrane	3	0.03	CG42748, Fas3, dlg1
Biological Process	morphogenesis of an epithelium	18	0.0327	CG6767, Fas3, InR, Mtl, RhoGAP19D, TSG101, alph, cora, csw, dlg1, foi, hipk, l(3)neo38, pk, seq, shot, spen, vsg
Biological Process	imaginal disc development	18	0.0327	CG6767, Fas3, InR, Mtl, RhoGAP19D, abd-A, alph, cora, csw, dlg1, drpr, hipk, l(3)neo38, pk, shot, spen, tws, vsg
Biological Process	organ morphogenesis	20	0.0327	CG6767, Fas3, Mtl, RhoGAP19D, TSG101, alph, cora, csw, dlg1, foi, hipk, klar, l(3)neo38, lolal, nrv2, pk, seq, shot, spen, vsg
Biological Process	epithelium development	24	0.0338	CG6767, CycG, Fas3, InR, Mtl, Myb, RhoGAP19D, TSG101, abd-A, alph, cora, csw, dlg1, drpr, foi, hipk, l(3)neo38, nudE, pk, seq, shot, spen, tws, vsg
Biological Process	positive regulation of developmental process	8	0.0354	InR, S6k, abd-A, alph, cac, dlg1, shot, simj
Cellular Component	septate junction	4	0.0362	Fas3, cora, dlg1, nrv2
Biological Process	cellular localization	19	0.0385	CG10277, CG14977, CG3287, PNUTS, TSG101, Tango5, brp, cac, cdm, cora, dlg1, endoA, futsch, klar, lost, nudE, qtc, stau, stj
Biological Process	cell projection organization	18	0.0389	CG11448, Fas3, InR, Lin29, MEP-1, Manf, Mtl, Ptp99A, Ptpmeg, S6k, cora, futsch, jim, pk, seq, shot, shrb, spen

Term Category	Term	gene #	FDR	gene names
Biological Process	branching involved in open tracheal system development	5	0.039	TSG101, csw, foi, seq, shot
Biological Process	maintenance of imaginal disc-derived wing hair orientation	2	0.0402	cora, spen
Biological Process	positive regulation of biological process	27	0.0402	Alg-2, CG14977, CG5315, DOR, InR, Mtl, Myb, Ncoa6, RhoGAP19D, Rlip, S6k, SNF4Agamma, Set1, abd-A, alph, cac, crc, dlg1, drpr, hipk, maf-S, qvr, shot, simj, slim, spen, stau
Biological Process	developmental growth	8	0.0402	InR, Mtl, PNUTS, Ptpmeg, S6k, dlg1, hipk, rgn
Biological Process	regulation of synapse organization	7	0.0441	CG6490, S6k, cac, dlg1, futsch, simj, stj
Cellular Component	fusome	4	0.0445	Rtnl1, Tsp42Ee, shot, shrb
Cellular Component	intracellular part	73	0.0462	Aac11, Arc1, CG10077, CG10277, CG11486, CG14977, CG30497, CG3287, CG42678, CG5792, CG6340, CG7611, CG8680, CG9003, CycG, DOR, Dcp2, E(var)3-9, Fas3, FoxP, GATAd, MEP-1, Manf, Myb, Ncoa6, Pitslre, Prp3, Ptpmeg, Rbp1-like, Rtnl1, S6k, SNF4Agamma, Sep4, Set1, TSG101, Tango5, Tfb1, Tsp42Ee, abd-A, brp, casp, chrb, cora, crc, csw, dlg1, endoA, futsch, galectin, glec, hipk, inaE, jigr1, jim, klar, l(3)neo38, lack, lolal, lost, maf-S, nudE, or, pk, seq, shot, shrb, simj, slim, spen, stau, su(w[a]), tws, vsg
Cellular Component	cell junction	7	0.0472	Fas3, InR, cora, dlg1, nrv2, shot, wech
Biological Process	regulation of synaptic growth at neuromuscular junction	6	0.0499	CG6490, cac, dlg1, futsch, simj, stj
Biological Process	cellular process	84	0.0499	Aac11, Alg-2, CG10277, CG11374, CG11448, CG11486, CG14977, CG17683, CG32000, CG42678, CG5315, CG6364, CG6490, CG6767, CG9003, CG9836, CycG, DOR, Dcp2, E(var)3-9, FBpp0073155, FBpp0084023, Fas3, InR, Lin29, MEP-1, MFS17, Manf, Msi, Myb, NaCP60E, Ncoa6, PNUTS, Prp3, Ptp99A, Ptpmeg, Rbp1-like, RhoGAP19D, Rtnl1, S6k, SNF4Agamma, Sep4, Set1, Tango5, Tfb1, abd-A, alph, brp, cac, cdm, chrb, cora, crc, csw, dlg1, drpr, endoA, foi, futsch, galectin, hipk, inaE, jim, klar, lack, lolal, lost, maf-S, mtt, mus210, nrv2, nudE, or, pk, pog, qtc, seq, shrb, simj, spen, stau, stj, tws, uex

Table 4.S14 | GSEA for genes expressed in 576hr ETI enriched relative to WT 120hr 12A neurons. Cellular component and biological process terms were both enriched. Terms are sorted by FDR.

Term Category	GO Term	Gene #	FDR	Genes
Molecular Function	structural constituent of ribosome	31	2.28E-32	RpL11, RpL12, RpL13, RpL17, RpL19, RpL21, RpL22, RpL26, RpL30, RpL34a, RpL34b, RpL36A, RpL37a, RpL4, RpL7, RpL7A, RpLP0, RpLP2, RpS11, RpS14a, RpS15Aa, RpS16, RpS19a, RpS2, RpS21, RpS25, RpS4, RpS5a, RpS6, RpS8, RpS9
Biological Process	translation	29	6.35E-23	Rack1, Rbp2, RpL12, RpL13, RpL17, RpL19, RpL22, RpL26, RpL30, RpL34b, RpL36A, RpL37a, RpL4, RpL7, RpL7A, RpLP0, RpS11, RpS14a, RpS15Aa, RpS16, RpS19a, RpS2, RpS21, RpS25, RpS4, RpS5a, RpS6, RpS8, RpS9
Biological Process	peptide metabolic process	30	1.75E-22	7B2, Rack1, Rbp2, RpL12, RpL13, RpL17, RpL19, RpL22, RpL26, RpL30, RpL34b, RpL36A, RpL37a, RpL4, RpL7, RpL7A, RpLP0, RpS11, RpS14a, RpS15Aa, RpS16, RpS19a, RpS2, RpS21, RpS25, RpS4, RpS5a, RpS6, RpS8, RpS9
Biological Process	mitotic spindle elongation	19	3.12E-21	RpL11, RpL12, RpL13, RpL17, RpL19, RpL21, RpL22, RpL26, RpL30, RpL36A, RpL7, RpL7A, RpS11, RpS15Aa, RpS16, RpS4, RpS5a, RpS6, RpS9
Biological Process	organonitrogen compound biosynthetic process	33	3.12E-21	ATPsyn-d, FBpp0305828, Rack1, Rbp2, RpL12, RpL13, RpL17, RpL19, RpL22, RpL26, RpL30, RpL34b, RpL36A, RpL37a, RpL4, RpL7, RpL7A, RpLP0, RpS11, RpS14a, RpS15Aa, RpS16, RpS19a, RpS2, RpS21, RpS25, RpS4, RpS5a, RpS6, RpS8, RpS9, blw, l(1)G0230
Molecular Function	structural molecule activity	32	2.47E-19	Prosap, RpL11, RpL12, RpL13, RpL17, RpL19, RpL21, RpL22, RpL26, RpL30, RpL34a, RpL34b, RpL36A, RpL37a, RpL4, RpL7, RpL7A, RpLP0, RpLP2, RpS11, RpS14a, RpS15Aa, RpS16, RpS19a, RpS2, RpS21, RpS25, RpS4, RpS5a, RpS6, RpS8, RpS9
Biological Process	mitotic spindle organization	23	3.64E-18	CG13298, Cct5, FBpp0081153, Pp2A-29B, RpL11, RpL12, RpL13, RpL17, RpL19, RpL21, RpL22, RpL26, RpL30, RpL36A, RpL7, RpL7A, RpS11, RpS15Aa, RpS16, RpS4, RpS5a, RpS6, RpS9
Biological Process	cellular nitrogen compound biosynthetic process	34	5.27E-18	ATPsyn-d, FBpp0305828, Rack1, Rbp2, RpL12, RpL13, RpL17, RpL19, RpL22, RpL26, RpL30, RpL34b, RpL36A, RpL37a, RpL4, RpL7, RpL7A, RpLP0, RpS11, RpS14a, RpS15Aa, RpS16, RpS19a, RpS2, RpS21, RpS25, RpS4, RpS5a, RpS6, RpS8, RpS9, blw, caz, l(1)G0230
Biological Process	organonitrogen compound metabolic process	34	2.43E-14	7B2, FBpp0305828, Rack1, Rbp2, RpL12, RpL13, RpL17, RpL19, RpL22, RpL26, RpL30, RpL34b, RpL36A, RpL37a, RpL4, RpL7, RpL7A, RpLP0, RpS11, RpS14a, RpS15Aa, RpS16, RpS19a, RpS2, RpS21, RpS25, RpS4, RpS5a, RpS6, RpS8, RpS9, blw, cype, l(1)G0230
Biological Process	protein complex subunit organization	28	7.21E-14	CG10440, CG13298, Cct5, Cdc42, Nlp, Pp2A-29B, RpL11, RpL12, RpL13, RpL17, RpL19, RpL21, RpL22, RpL26, RpL30, RpL36A, RpL7, RpL7A, RpS11, RpS15Aa, RpS16, RpS4, RpS5a, RpS6, RpS9, Set, cib, sn
Biological Process	cellular macromolecule biosynthetic process	30	1.36E-13	Rack1, Rbp2, RpL12, RpL13, RpL17, RpL19, RpL22, RpL26, RpL30, RpL34b, RpL36A, RpL37a, RpL4, RpL7, RpL7A, RpLP0, RpS11, RpS14a, RpS15Aa, RpS16, RpS19a, RpS2, RpS21, RpS25, RpS4, RpS5a, RpS6, RpS8, RpS9, caz
Biological Process	microtubule cytoskeleton organization	24	1.61E-13	CG13298, Cct5, FBpp0081153, Pp2A-29B, RpL11, RpL12, RpL13, RpL17, RpL19, RpL21, RpL22, RpL26, RpL30, RpL36A, RpL4, RpL7, RpL7A, RpS11,

Term Category	GO Term	Gene #	FDR	Genes
				RpS15Aa, RpS16, RpS4, RpS5a, RpS6, RpS9
Biological Process	cellular biosynthetic process	35	3.66E-13	ATPsyn-d, FBpp0305828, Rack1, Rbp2, RpL12, RpL13, RpL17, RpL19, RpL22, RpL26, RpL30, RpL34b, RpL36A, RpL37a, RpL4, RpL7, RpL7A, RpLP0, RpS11, RpS14a, RpS15Aa, RpS16, RpS19a, RpS2, RpS21, RpS25, RpS4, RpS5a, RpS6, RpS8, RpS9, blw, caz, l(1)G0230, qm
Biological Process	cytoskeleton organization	28	4.10E-13	CG13298, Cct5, Cdc42, FBpp0081153, Pp2A-29B, Prosap, RpL11, RpL12, RpL13, RpL17, RpL19, RpL21, RpL22, RpL26, RpL30, RpL36A, RpL4, RpL7, RpL7A, RpS11, RpS15Aa, RpS16, RpS4, RpS5a, RpS6, RpS9, cib, sn
Biological Process	organic substance biosynthetic process	35	6.88E-13	ATPsyn-d, FBpp0305828, Rack1, Rbp2, RpL12, RpL13, RpL17, RpL19, RpL22, RpL26, RpL30, RpL34b, RpL36A, RpL37a, RpL4, RpL7, RpL7A, RpLP0, RpS11, RpS14a, RpS15Aa, RpS16, RpS19a, RpS2, RpS21, RpS25, RpS4, RpS5a, RpS6, RpS8, RpS9, blw, caz, l(1)G0230, qm
Biological Process	mitotic cell cycle process	25	7.59E-13	CG13298, Cct5, FBpp0081153, Pp2A-29B, RpL11, RpL12, RpL13, RpL17, RpL19, RpL21, RpL22, RpL26, RpL30, RpL36A, RpL7, RpL7A, RpS11, RpS15Aa, RpS16, RpS4, RpS5a, RpS6, RpS9, lwr, tsr
Biological Process	mitotic cell cycle	26	7.75E-13	CG13298, Cct5, FBpp0081153, PPP4R2r, Pp2A-29B, RpL11, RpL12, RpL13, RpL17, RpL19, RpL21, RpL22, RpL26, RpL30, RpL36A, RpL7, RpL7A, RpS11, RpS15Aa, RpS16, RpS4, RpS5a, RpS6, RpS9, lwr, tsr
Biological Process	gene expression	32	1.21E-12	7B2, CG13298, Rack1, Rbp2, RpL12, RpL13, RpL17, RpL19, RpL22, RpL26, RpL30, RpL34b, RpL36A, RpL37a, RpL4, RpL7, RpL7A, RpLP0, RpS11, RpS14a, RpS15Aa, RpS16, RpS19a, RpS2, RpS21, RpS25, RpS4, RpS5a, RpS6, RpS8, RpS9, caz
Biological Process	cell cycle	28	1.41E-11	CG13298, Cct5, FBpp0081153, PPP4R2r, Pp2A-29B, RpL11, RpL12, RpL13, RpL17, RpL19, RpL21, RpL22, RpL26, RpL30, RpL36A, RpL4, RpL7, RpL7A, RpS11, RpS15Aa, RpS16, RpS27A, RpS4, RpS5a, RpS6, RpS9, lwr, tsr
Biological Process	cell cycle process	27	1.63E-11	CG13298, Cct5, FBpp0081153, Pp2A-29B, RpL11, RpL12, RpL13, RpL17, RpL19, RpL21, RpL22, RpL26, RpL30, RpL36A, RpL4, RpL7, RpL7A, RpS11, RpS15Aa, RpS16, RpS27A, RpS4, RpS5a, RpS6, RpS9, lwr, tsr
Biological Process	centrosome duplication	12	1.42E-10	Pp2A-29B, RpL11, RpL13, RpL17, RpL19, RpL21, RpL30, RpL4, RpL7, RpL7A, RpS4, RpS6
Biological Process	cellular protein metabolic process	35	5.13E-10	Cct5, Cdc42, ERp60, Pp2A-29B, Rack1, Rbp2, RpL12, RpL13, RpL17, RpL19, RpL22, RpL26, RpL30, RpL34b, RpL36A, RpL37a, RpL4, RpL7, RpL7A, RpLP0, RpS11, RpS14a, RpS15Aa, RpS16, RpS19a, RpS2, RpS21, RpS25, RpS4, RpS5a, RpS6, RpS8, RpS9, Rpn11, lwr
Biological Process	cellular component organization or biogenesis	46	7.26E-10	CG10440, CG13298, CadN, Cct5, Cdc42, Nckx30C, NetB, Nlp, Pp2A-29B, Prosap, Rack1, RpL11, RpL12, RpL13, RpL17, RpL19, RpL21, RpL22, RpL26, RpL30, RpL36A, RpL4, RpL7, RpLP0, RpS11, RpS15Aa, RpS16, RpS21, RpS27A, RpS4, RpS5a, RpS6, RpS8, RpS9, Sec61alpha, Set, Ten-m, Tim17b, caz, cib, dock, fra, kuk, lwr, porin, sn
Biological	centrosome cycle	12	7.32E-10	Pp2A-29B, RpL11, RpL13, RpL17, RpL19, RpL21,

Term Category	GO Term	Gene #	FDR	Genes
Process				RpL30, RpL4, RpL7, RpL7A, RpS4, RpS6
Biological Process	cellular nitrogen compound metabolic process	36	7.32E-10	7B2, CG13298, FBpp0305828, Rack1, Rbp2, RpL12, RpL13, RpL17, RpL19, RpL22, RpL26, RpL30, RpL34b, RpL36A, RpL37a, RpL4, RpL7, RpL7A, RpLP0, RpS11, RpS14a, RpS15Aa, RpS16, RpS19a, RpS2, RpS21, RpS25, RpS4, RpS5a, RpS6, RpS8, RpS9, blw, caz, cype, l(1)G0230
Biological Process	protein metabolic process	36	3.96E-09	7B2, Cct5, Cdc42, ERp60, Pp2A-29B, Rack1, Rbp2, RpL12, RpL13, RpL17, RpL19, RpL22, RpL26, RpL30, RpL34b, RpL36A, RpL37a, RpL4, RpL7, RpL7A, RpLP0, RpS11, RpS14a, RpS15Aa, RpS16, RpS19a, RpS2, RpS21, RpS25, RpS4, RpS5a, RpS6, RpS8, RpS9, Rpn11, lwr
Biological Process	single-organism organelle organization	30	4.23E-09	CG13298, Cct5, Cdc42, FBpp0081153, Pp2A-29B, Prosap, RpL11, RpL12, RpL13, RpL17, RpL19, RpL21, RpL22, RpL26, RpL30, RpL36A, RpL4, RpL7, RpL7A, RpS11, RpS15Aa, RpS16, RpS27A, RpS4, RpS5a, RpS6, RpS9, cib, lwr, sn
Biological Process	cellular component organization	44	4.65E-09	CG10440, CG13298, CadN, Cct5, Cdc42, Nckx30C, NetB, Nlp, Pp2A-29B, Prosap, Rack1, RpL11, RpL12, RpL13, RpL17, RpL19, RpL21, RpL22, RpL26, RpL30, RpL36A, RpL4, RpL7, RpL7A, RpS11, RpS15Aa, RpS16, RpS27A, RpS4, RpS5a, RpS6, RpS9, Sec61alpha, Set, Ten-m, Tim17b, caz, cib, dock, fra, kuk, lwr, porin, sn
Biological Process	organelle organization	35	5.59E-09	CG13298, Cct5, Cdc42, FBpp0081153, Nlp, Pp2A-29B, Prosap, RpL11, RpL12, RpL13, RpL17, RpL19, RpL21, RpL22, RpL26, RpL30, RpL36A, RpL4, RpL7, RpL7A, RpS11, RpS15Aa, RpS16, RpS27A, RpS4, RpS5a, RpS6, RpS9, Set, Tim17b, cib, kuk, lwr, porin, sn
Biological Process	cellular macromolecule metabolic process	37	6.59E-06	CG13298, Cct5, Cdc42, ERp60, Pp2A-29B, Rack1, Rbp2, RpL12, RpL13, RpL17, RpL19, RpL22, RpL26, RpL30, RpL34b, RpL36A, RpL37a, RpL4, RpL7, RpL7A, RpLP0, RpS11, RpS14a, RpS15Aa, RpS16, RpS19a, RpS2, RpS21, RpS25, RpS4, RpS5a, RpS6, RpS8, RpS9, Rpn11, caz, lwr
Biological Process	cellular metabolic process	45	7.67E-06	7B2, CG13298, Cct5, Cdc42, ERp60, FBpp0305828, Idh, Jafrac1, Pp2A-29B, Rack1, Rbp2, RpL12, RpL13, RpL17, RpL19, RpL22, RpL26, RpL30, RpL34b, RpL36A, RpL37a, RpL4, RpL7, RpL7A, RpLP0, RpS11, RpS14a, RpS15Aa, RpS16, RpS19a, RpS2, RpS21, RpS25, RpS4, RpS5a, RpS6, RpS8, RpS9, Rpn11, blw, caz, cype, l(1)G0230, lwr, qm
Biological Process	single-organism cellular process	59	2.02E-05	7B2, CG13298, CadN, Cct5, Cdc42, Cyp1, ERp60, FBpp0081153, FBpp0085193, Gdi, Idh, Jafrac1, Lrch, Nckx30C, NetB, Ntf-2, PPP4R2r, Pp2A-29B, Prosap, Rack1, RpL11, RpL12, RpL13, RpL17, RpL19, RpL21, RpL22, RpL26, RpL30, RpL36A, RpL4, RpL7, RpL7A, RpLP0, RpS11, RpS15Aa, RpS16, RpS27A, RpS4, RpS5a, RpS6, RpS8, RpS9, Sec61alpha, Sod, Task6, Ten-m, blw, caz, cib, cype, dock, fas, fra, gfA, kuk, lwr, porin, sn
Biological Process	single-organism process	65	3.95E-05	7B2, CG10440, CG13298, CG13830, CadN, Cct5, Cdc42, Cyp1, ERp60, FBpp0081153, FBpp0085193, FKBP59, Gdi, Idh, Jafrac1, Lrch, Nckx30C, NetB, Nlp, Ntf-2, PPP4R2r, Pp2A-29B, Prosap, Rack1, RpL11, RpL12, RpL13, RpL17, RpL19, RpL21, RpL22, RpL26,

Term Category	GO Term	Gene #	FDR	Genes
				RpL30, RpL36A, RpL4, RpL7, RpL7A, RpLP0, RpS11, RpS15Aa, RpS16, RpS21, RpS27A, RpS4, RpS5a, RpS6, RpS8, RpS9, Sec61alpha, Task6, Ten-m, Tim17b, blw, caz, cype, dock, fabp, fas, fra, gfA, kuk, lwr, miple, porin, sn
Biological Process	primary metabolic process	44	4.24E-05	7B2, CG13298, Cct5, Cdc42, ERp60, FBpp0305828, Idh, Pp2A-29B, Rack1, Rbp2, RpL12, RpL13, RpL17, RpL19, RpL22, RpL26, RpL30, RpL34b, RpL36A, RpL37a, RpL4, RpL7, RpL7A, RpLP0, RpS11, RpS14a, RpS15Aa, RpS16, RpS19a, RpS2, RpS21, RpS25, RpS4, RpS5a, RpS6, RpS8, RpS9, Rpn11, blw, caz, cype, l(1)G0230, lwr, qm
Biological Process	macromolecule metabolic process	38	7.94E-05	7B2, CG13298, Cct5, Cdc42, ERp60, Pp2A-29B, Rack1, Rbp2, RpL12, RpL13, RpL17, RpL19, RpL22, RpL26, RpL30, RpL34b, RpL36A, RpL37a, RpL4, RpL7, RpL7A, RpLP0, RpS11, RpS14a, RpS15Aa, RpS16, RpS19a, RpS2, RpS21, RpS25, RpS4, RpS5a, RpS6, RpS8, RpS9, Rpn11, caz, lwr
Biological Process	cellular process	64	0.000133	CG10440, CG13298, CadN, Cct5, Cdc42, FBpp0081153, Gdi, Idh, Jafrac1, Lrch, Nckx30C, NetB, Nlp, Ntf-2, PPP4R2r, Pp2A-29B, Prosap, Rack1, Rbp2, RpL12, RpL13, RpL17, RpL19, RpL22, RpL26, RpL30, RpL34b, RpL36A, RpL37a, RpL4, RpL7, RpL7A, RpLP0, RpS11, RpS14a, RpS15Aa, RpS16, RpS19a, RpS2, RpS21, RpS25, RpS4, RpS5a, RpS6, RpS8, RpS9, Rpn11, Sec61alpha, Set, Task6, Ten-m, Tim17b, blw, caz, cib, cype, dock, fas, fra, gfA, kuk, lwr, porin, sn
Biological Process	organic substance metabolic process	44	0.000493	7B2, CG13298, Cct5, Cdc42, ERp60, FBpp0305828, Idh, Pp2A-29B, Rack1, Rbp2, RpL12, RpL13, RpL17, RpL19, RpL22, RpL26, RpL30, RpL34b, RpL36A, RpL37a, RpL4, RpL7, RpL7A, RpLP0, RpS11, RpS14a, RpS15Aa, RpS16, RpS19a, RpS2, RpS21, RpS25, RpS4, RpS5a, RpS6, RpS8, RpS9, Rpn11, blw, caz, cype, l(1)G0230, lwr, qm
Biological Process	ATP synthesis coupled proton transport	4	0.00177	ATPsyn-d, FBpp0305828, blw, l(1)G0230
Biological Process	ribosomal small subunit biogenesis	3	0.00358	RpS21, RpS6, RpS8
Biological Process	developmental process	41	0.00555	ATPsyn-d, CG10641, CG13298, CadN, Cct5, Cdc42, Cyp1, FBpp0085193, FBpp0305828, FKBP59, Jafrac1, Nckx30C, NetB, PPP4R2r, Pp2A-29B, Prosap, Rack1, RpL30, RpL7, RpS11, RpS21, RpS27A, RpS8, Sec61alpha, Sod, Ten-m, blw, caz, cib, dock, fas, fra, kuk, lwr, mam, miple, porin, qm, sn, spri, tsr
Biological Process	cellular component biogenesis	17	0.00651	CG10440, Cct5, Cdc42, FBpp0081153, Nlp, Pp2A-29B, Prosap, RpL7A, RpLP0, RpS21, RpS6, RpS8, Set, Ten-m, caz, sn, tsr
Biological Process	single-multicellular organism process	40	0.00739	ATPsyn-d, CG10440, CG13298, CadN, Cct5, Cdc42, FBpp0085193, FKBP59, Jafrac1, Nckx30C, NetB, PPP4R2r, Pp2A-29B, Prosap, Rack1, RpL30, RpL7, RpS11, RpS21, RpS27A, RpS8, Sec61alpha, Sod, Ten-m, caz, cib, dock, fabp, fas, fra, gfA, kuk, lwr, mam, miple, porin, qm, sn, spri, tsr
Biological Process	cell migration	9	0.00852	Cdc42, Jafrac1, NetB, fra, lwr, qm, sn, spri, tsr

Term Category	GO Term	Gene #	FDR	Genes
Biological Process	single-organism developmental process	40	0.0103	ATPsyn-d, CG13298, CadN, Cct5, Cdc42, Cyp1, FBpp0085193, FBpp0305828, FKBP59, Jafrac1, Nckx30C, NetB, PPP4R2r, Pp2A-29B, Prosap, Rack1, RpL30, RpL7, RpS11, RpS21, RpS27A, RpS8, Sec61alpha, Sod, Ten-m, blw, caz, cib, dock, fas, fra, kuk, lwr, mam, miple, porin, qm, sn, spri, tsr
Biological Process	localization of cell	9	0.0137	Cdc42, Jafrac1, NetB, fra, lwr, qm, sn, spri, tsr
Molecular Function	hydrogen-exporting ATPase activity, phosphorylative mechanism	4	0.014	ATPsyn-d, FBpp0305828, blw, l(1)G0230
Biological Process	multicellular organismal development	35	0.0144	ATPsyn-d, CG13298, CadN, Cct5, Cdc42, FBpp0085193, FKBP59, Jafrac1, Nckx30C, NetB, PPP4R2r, Pp2A-29B, Prosap, Rack1, RpL30, RpL7, RpS11, RpS21, RpS8, Sec61alpha, Sod, Ten-m, caz, cib, dock, fas, fra, kuk, lwr, mam, miple, porin, qm, sn, tsr
Biological Process	nervous system development	24	0.0144	CG13298, CadN, Cct5, Cdc42, FBpp0085193, FKBP59, Nckx30C, NetB, PPP4R2r, Pp2A-29B, Prosap, RpL30, RpS11, RpS8, Sec61alpha, Ten-m, caz, cib, dock, fra, mam, qm, sn, tsr
Biological Process	positive regulation of viral life cycle	2	0.0144	Rack1, Sec61alpha
Biological Process	anatomical structure development	37	0.0146	CG10641, CG13298, CadN, Cct5, Cdc42, Cyp1, FBpp0085193, FKBP59, Jafrac1, Nckx30C, NetB, PPP4R2r, Pp2A-29B, Prosap, Rack1, RpL30, RpS11, RpS21, RpS27A, RpS8, Sec61alpha, Ten-m, blw, caz, cib, dock, fas, fra, kuk, lwr, mam, miple, porin, qm, sn, spri, tsr
Biological Process	ribosome biogenesis	5	0.0193	RpL7A, RpLP0, RpS21, RpS6, RpS8
Biological Process	metabolic process	44	0.0234	7B2, CG13298, Cct5, Cdc42, ERp60, FBpp0081153, Idh, Jafrac1, Nlp, Pp2A-29B, Rack1, Rbp2, RpL12, RpL13, RpL17, RpL19, RpL22, RpL26, RpL30, RpL34b, RpL36A, RpL37a, RpL4, RpL7, RpL7A, RpLP0, RpS11, RpS14a, RpS15Aa, RpS16, RpS19a, RpS2, RpS21, RpS25, RpS4, RpS5a, RpS6, RpS8, RpS9, Rpn11, blw, caz, cype, lwr
Biological Process	maturation of SSU-rRNA from tricistronic rRNA transcript (SSU-rRNA, 5.8S rRNA, LSU-rRNA)	2	0.0251	RpS21, RpS8
Biological Process	synaptic target attraction	2	0.0395	NetB, Ten-m
Biological Process	regulation of cell projection organization	5	0.0401	CadN, Cdc42, NetB, fra, tsr
Biological Process	locomotion	12	0.0445	CadN, Cdc42, Jafrac1, NetB, Ten-m, dock, fra, lwr, qm, sn, spri, tsr
Biological Process	multicellular organismal process	41	0.0463	ATPsyn-d, CG10440, CG13298, CadN, Cct5, Cdc42, FBpp0085193, FKBP59, Jafrac1, Nckx30C, NetB, PPP4R2r, Pp2A-29B, Prosap, Rack1, RpL30, RpL7,

Term Category	GO Term	Gene #	FDR	Genes
				RpS11, RpS21, RpS27A, RpS8, Sec61alpha, Sod, Ten-m, blw, caz, cib, dock, fabp, fas, fra, gfA, kuk, lwr, mam, miple, porin, qm, sn, spri, tsr

Table 4.S15 | WT 120hr 12A enriched compared to 576hr ETI GSEA GO molecular function and biological process. Terms sorted by FDR.

Type	Term	FDR	#	Gene
KG	Ribosome	1.02E-47	42	RpL11, RpL12, RpL13, RpL13A, RpL15, RpL17, RpL18, RpL18A, RpL19, RpL21, RpL22, RpL23, RpL24, RpL26, RpL30, RpL34a, RpL34b, RpL35, RpL36A, RpL37a, RpL4, RpL5, RpL7, RpL7A, RpL8, RpLP1, RpLP2, RpS10b, RpS11, RpS14b, RpS16, RpS17, RpS19a, RpS21, RpS25, RpS27A, RpS30, RpS4, RpS5a, RpS6, RpS8, RpS9
MF	structural constituent of ribosome	1.08E-40	42	RpL11, RpL12, RpL13, RpL13A, RpL15, RpL17, RpL18, RpL18A, RpL19, RpL21, RpL22, RpL23, RpL24, RpL26, RpL30, RpL34a, RpL34b, RpL35, RpL36A, RpL37a, RpL4, RpL5, RpL7, RpL7A, RpL8, RpLP1, RpLP2, RpS10b, RpS11, RpS14a, RpS14b, RpS16, RpS17, RpS19a, RpS21, RpS25, RpS30, RpS4, RpS5a, RpS6, RpS8, RpS9
BP	translation	7.98E-28	39	Rack1, Rbp2, RpL12, RpL13, RpL13A, RpL15, RpL17, RpL18, RpL18A, RpL19, RpL22, RpL23, RpL24, RpL26, RpL30, RpL34b, RpL35, RpL36A, RpL37a, RpL4, RpL7, RpL7A, RpL8, RpS10b, RpS11, RpS14a, RpS14b, RpS16, RpS17, RpS19a, RpS21, RpS25, RpS30, RpS4, RpS5a, RpS6, RpS8, RpS9, eIF-3p40
BP	mitotic spindle organization	7.98E-28	36	CG1240, CG13298, CG5525, CG8258, Cam, Cct5, FBpp0081153, Hsp83, Pp2A-29B, RpL11, RpL12, RpL13, RpL17, RpL18, RpL18A, RpL19, RpL21, RpL22, RpL23, RpL24, RpL26, RpL30, RpL35, RpL36A, RpL7, RpL7A, RpL8, RpS11, RpS16, RpS30, RpS4, RpS5a, RpS6, RpS9, eIF-1A, mgr
BP	mitotic spindle elongation	1.79E-27	26	RpL11, RpL12, RpL13, RpL17, RpL18, RpL18A, RpL19, RpL21, RpL22, RpL23, RpL24, RpL26, RpL30, RpL35, RpL36A, RpL7, RpL7A, RpL8, RpS11, RpS16, RpS30, RpS4, RpS5a, RpS6, RpS9, eIF-1A
BP	peptide metabolic process	1.15E-26	40	7B2, Rack1, Rbp2, RpL12, RpL13, RpL13A, RpL15, RpL17, RpL18, RpL18A, RpL19, RpL22, RpL23, RpL24, RpL26, RpL30, RpL34b, RpL35, RpL36A, RpL37a, RpL4, RpL7, RpL7A, RpL8, RpS10b, RpS11, RpS14a, RpS14b, RpS16, RpS17, RpS19a, RpS21, RpS25, RpS30, RpS4, RpS5a, RpS6, RpS8, RpS9, eIF-3p40
MF	structural molecule activity	2.57E-24	45	Act42A, Act5C, Prosap, RpL11, RpL12, RpL13, RpL13A, RpL15, RpL17, RpL18, RpL18A, RpL19, RpL21, RpL22, RpL23, RpL24, RpL26, RpL30, RpL34a, RpL34b, RpL35, RpL36A, RpL37a, RpL4, RpL5, RpL7, RpL7A, RpL8, RpLP1, RpLP2, RpS10b, RpS11, RpS14a, RpS14b, RpS16, RpS17, RpS19a, RpS21, RpS25, RpS30, RpS4, RpS5a, RpS6, RpS8, RpS9
BP	organonitrogen compound biosynthetic process	2.49E-23	43	ATPsyn-d, FBpp0305828, Rack1, Rbp2, RpL12, RpL13, RpL13A, RpL15, RpL17, RpL18, RpL18A, RpL19, RpL22, RpL23, RpL24, RpL26, RpL30, RpL34b, RpL35, RpL36A, RpL37a, RpL4, RpL7, RpL7A, RpL8, RpS10b, RpS11, RpS14a, RpS14b, RpS16, RpS17, RpS19a, RpS21, RpS25, RpS30, RpS4, RpS5a, RpS6, RpS8, RpS9, blw, eIF-3p40, l(1)G0230
BP	microtubule cytoskeleton organization	3.32E-22	39	CG1240, CG13298, CG5525, CG8258, Cam, Cct5, FBpp0081153, Hsp83, Pp2A-29B, Rab6, RpL11, RpL12, RpL13, RpL13A, RpL17, RpL18, RpL18A, RpL19, RpL21, RpL22, RpL23, RpL24, RpL26, RpL30, RpL35, RpL36A, RpL4, RpL7, RpL7A, RpL8, RpS11, RpS16, RpS30, RpS4, RpS5a, RpS6, RpS9, eIF-1A, mgr
BP	mitotic cell cycle process	2.87E-20	40	Act42A, Act5C, CG1240, CG13298, CG5525, CG8258, Cam, Cct5, FBpp0081153, Hsp83, Pp2A-29B, RpL11,

Type	Term	FDR	#	Gene
				RpL12, RpL13, RpL17, RpL18, RpL18A, RpL19, RpL21, RpL22, RpL23, RpL24, RpL26, RpL30, RpL35, RpL36A, RpL7, RpL7A, RpL8, RpS11, RpS16, RpS30, RpS4, RpS5a, RpS6, RpS9, eIF-1A, lwr, mgr, tsr
BP	cytoskeleton organization	6.14E-20	44	Act42A, Act5C, CG1240, CG13298, CG5525, CG8258, Cam, Cct5, Cdc42, FBpp0081153, Hsp83, Pp2A-29B, Prosap, Rab6, RpL11, RpL12, RpL13, RpL13A, RpL17, RpL18, RpL18A, RpL19, RpL21, RpL22, RpL23, RpL24, RpL26, RpL30, RpL35, RpL36A, RpL4, RpL7, RpL7A, RpL8, RpS11, RpS16, RpS30, RpS4, RpS5a, RpS6, RpS9, eIF-1A, mgr, sn
BP	mitotic cell cycle	1.09E-19	41	Act42A, Act5C, CG1240, CG13298, CG5525, CG8258, Cam, Cct5, FBpp0081153, Hsp83, PPP4R2r, Pp2A-29B, RpL11, RpL12, RpL13, RpL17, RpL18, RpL18A, RpL19, RpL21, RpL22, RpL23, RpL24, RpL26, RpL30, RpL35, RpL36A, RpL7, RpL7A, RpL8, RpS11, RpS16, RpS30, RpS4, RpS5a, RpS6, RpS9, eIF-1A, lwr, mgr, tsr
BP	cellular nitrogen compound biosynthetic process	1.09E-19	45	ATPsyn-d, FBpp0305828, Rack1, Rbp2, RpL12, RpL13, RpL13A, RpL15, RpL17, RpL18, RpL18A, RpL19, RpL22, RpL23, RpL24, RpL26, RpL30, RpL34b, RpL35, RpL36A, RpL37a, RpL4, RpL7, RpL7A, RpL8, RpS10b, RpS11, RpS14a, RpS14b, RpS16, RpS17, RpS19a, RpS21, RpS25, RpS30, RpS4, RpS5a, RpS6, RpS8, RpS9, blw, caz, crc, eIF-3p40, l(1)G0230
BP	cellular protein metabolic process	6.55E-19	61	CG5525, CG5830, CG7048, CG8258, Cam, CanB, Cct5, Cdc42, ERp60, HIP-R, Hsp22, Hsp27, Hsp67Bc, Hsp68, Hsp83, IA-2, Pp2A-29B, Prosalpha6, Rack1, Rbp2, RpL12, RpL13, RpL13A, RpL15, RpL17, RpL18, RpL18A, RpL19, RpL22, RpL23, RpL24, RpL26, RpL30, RpL34b, RpL35, RpL36A, RpL37a, RpL4, RpL7, RpL7A, RpL8, RpS10b, RpS11, RpS14a, RpS14b, RpS16, RpS17, RpS19a, RpS21, RpS25, RpS30, RpS4, RpS5a, RpS6, RpS8, RpS9, Rpn11, Uch, eIF-3p40, lwr, mgr
BP	cell cycle process	7.35E-18	43	Act42A, Act5C, CG1240, CG13298, CG5525, CG8258, Cam, Cct5, FBpp0081153, Hsp83, Pp2A-29B, RpL11, RpL12, RpL13, RpL13A, RpL17, RpL18, RpL18A, RpL19, RpL21, RpL22, RpL23, RpL24, RpL26, RpL30, RpL35, RpL36A, RpL4, RpL7, RpL7A, RpL8, RpS11, RpS16, RpS27A, RpS30, RpS4, RpS5a, RpS6, RpS9, eIF-1A, lwr, mgr, tsr
BP	protein complex subunit organization	8.92E-18	40	CG10440, CG1240, CG13298, CG5525, CG8258, Cam, Cct5, Cdc42, Hsp83, Nlp, Pp2A-29B, RpL11, RpL12, RpL13, RpL17, RpL18, RpL18A, RpL19, RpL21, RpL22, RpL23, RpL24, RpL26, RpL30, RpL35, RpL36A, RpL7, RpL7A, RpL8, RpS11, RpS16, RpS30, RpS4, RpS5a, RpS6, RpS9, Set, eIF-1A, mgr, sn
BP	cell cycle	1.65E-17	44	Act42A, Act5C, CG1240, CG13298, CG5525, CG8258, Cam, Cct5, FBpp0081153, Hsp83, PPP4R2r, Pp2A-29B, RpL11, RpL12, RpL13, RpL13A, RpL17, RpL18, RpL18A, RpL19, RpL21, RpL22, RpL23, RpL24, RpL26, RpL30, RpL35, RpL36A, RpL4, RpL7, RpL7A, RpL8, RpS11, RpS16, RpS27A, RpS30, RpS4, RpS5a, RpS6, RpS9, eIF-1A, lwr, mgr, tsr
BP	protein metabolic process	1.65E-17	63	7B2, CG5525, CG5830, CG7048, CG8258, Cam, CanB, Cct5, Cdc42, ERp60, HIP-R, Hsp22, Hsp27, Hsp67Bc, Hsp68, Hsp83, IA-2, Pp2A-29B, Prosalpha6, Rack1, Rbp2, RpL12, RpL13, RpL13A, RpL15, RpL17, RpL18, RpL18A, RpL19, RpL22, RpL23, RpL24, RpL26, RpL30,

Type	Term	FDR	#	Gene
				RpL34b, RpL35, RpL36A, RpL37a, RpL4, RpL7, RpL7A, RpL8, RpS10b, RpS11, RpS14a, RpS14b, RpS16, RpS17, RpS19a, RpS21, RpS25, RpS30, RpS4, RpS5a, RpS6, RpS8, RpS9, Rpn11, Uch, eIF-3p40, lwr, mgr, mmd
BP	cellular macromolecule biosynthetic process	1.76E-16	42	Hsp67Bc, Rack1, Rbp2, RpL12, RpL13, RpL13A, RpL15, RpL17, RpL18, RpL18A, RpL19, RpL22, RpL23, RpL24, RpL26, RpL30, RpL34b, RpL35, RpL36A, RpL37a, RpL4, RpL7, RpL7A, RpL8, RpS10b, RpS11, RpS14a, RpS14b, RpS16, RpS17, RpS19a, RpS21, RpS25, RpS30, RpS4, RpS5a, RpS6, RpS8, RpS9, caz, crc, eIF-3p40
BP	organonitrogen compound metabolic process	6.45E-16	46	7B2, CG32230, CG9603, FBpp0305828, Rack1, Rbp2, RpL12, RpL13, RpL13A, RpL15, RpL17, RpL18, RpL18A, RpL19, RpL22, RpL23, RpL24, RpL26, RpL30, RpL34b, RpL35, RpL36A, RpL37a, RpL4, RpL7, RpL7A, RpL8, RpS10b, RpS11, RpS14a, RpS14b, RpS16, RpS17, RpS19a, RpS21, RpS25, RpS30, RpS4, RpS5a, RpS6, RpS8, RpS9, blw, cype, eIF-3p40, l(1)G0230
BP	centrosome cycle	7.96E-16	19	Cam, Hsp83, Pp2A-29B, RpL11, RpL13, RpL13A, RpL17, RpL18A, RpL19, RpL21, RpL24, RpL30, RpL35, RpL4, RpL7, RpL7A, RpL8, RpS4, RpS6
BP	centrosome duplication	1.07E-15	18	Cam, Pp2A-29B, RpL11, RpL13, RpL13A, RpL17, RpL18A, RpL19, RpL21, RpL24, RpL30, RpL35, RpL4, RpL7, RpL7A, RpL8, RpS4, RpS6
BP	centrosome organization	6.43E-15	20	Cam, Hsp83, Pp2A-29B, RpL11, RpL13, RpL13A, RpL17, RpL18A, RpL19, RpL21, RpL24, RpL30, RpL35, RpL4, RpL7, RpL7A, RpL8, RpS4, RpS6, mgr
BP	cellular biosynthetic process	1.22E-14	48	ATPsyn-d, FBpp0305828, Hsp67Bc, Lpin, Rack1, Rbp2, RpL12, RpL13, RpL13A, RpL15, RpL17, RpL18, RpL18A, RpL19, RpL22, RpL23, RpL24, RpL26, RpL30, RpL34b, RpL35, RpL36A, RpL37a, RpL4, RpL7, RpL7A, RpL8, RpS10b, RpS11, RpS14a, RpS14b, RpS16, RpS17, RpS19a, RpS21, RpS25, RpS30, RpS4, RpS5a, RpS6, RpS8, RpS9, blw, caz, crc, eIF-3p40, l(1)G0230, qm
BP	gene expression	2.99E-14	44	7B2, CG13298, Rack1, Rbp2, RpL12, RpL13, RpL13A, RpL15, RpL17, RpL18, RpL18A, RpL19, RpL22, RpL23, RpL24, RpL26, RpL30, RpL34b, RpL35, RpL36A, RpL37a, RpL4, RpL7, RpL7A, RpL8, RpS10b, RpS11, RpS14a, RpS14b, RpS16, RpS17, RpS19a, RpS21, RpS25, RpS30, RpS4, RpS5a, RpS6, RpS8, RpS9, caz, crc, eIF-3p40, snf
BP	organic substance biosynthetic process	3.01E-14	48	ATPsyn-d, FBpp0305828, Hsp67Bc, Lpin, Rack1, Rbp2, RpL12, RpL13, RpL13A, RpL15, RpL17, RpL18, RpL18A, RpL19, RpL22, RpL23, RpL24, RpL26, RpL30, RpL34b, RpL35, RpL36A, RpL37a, RpL4, RpL7, RpL7A, RpL8, RpS10b, RpS11, RpS14a, RpS14b, RpS16, RpS17, RpS19a, RpS21, RpS25, RpS30, RpS4, RpS5a, RpS6, RpS8, RpS9, blw, caz, crc, eIF-3p40, l(1)G0230, qm
BP	macromolecular complex subunit organization	5.21E-14	42	CG10440, CG1240, CG13298, CG5525, CG8258, Cam, Cct5, Cdc42, Hsp83, Nlp, Pp2A-29B, RpL11, RpL12, RpL13, RpL17, RpL18, RpL18A, RpL19, RpL21, RpL22, RpL23, RpL24, RpL26, RpL30, RpL35, RpL36A, RpL5, RpL7, RpL7A, RpL8, RpS11, RpS16, RpS17, RpS30, RpS4, RpS5a, RpS6, RpS9, Set, eIF-1A, mgr, sn
BP	single-organism organelle organization	1.82E-13	47	CG1240, CG13298, CG5525, CG8258, Cam, Cct5, Cdc42, FBpp0081153, Hsp70Aa, Hsp70Ab, Hsp70Ba, Hsp83, Pp2A-29B, Prosap, Rab6, RpL11, RpL12, RpL13, RpL13A, RpL17, RpL18, RpL18A, RpL19, RpL21, RpL22, RpL23, RpL24, RpL26, RpL30, RpL35, RpL36A,

Type	Term	FDR	#	Gene
				RpL4, RpL7, RpL7A, RpL8, RpS11, RpS16, RpS27A, RpS30, RpS4, RpS5a, RpS6, RpS9, eIF-1A, lwr, mgr, sn
BP	organelle organization	3.79E-13	55	Act42A, Act5C, CG1240, CG13298, CG5525, CG8258, Cam, Cct5, Cdc42, FBpp0081153, Hsp70Aa, Hsp70Ab, Hsp70Ba, Hsp83, Nlp, Pp2A-29B, Prosap, Rab6, RpL11, RpL12, RpL13, RpL13A, RpL17, RpL18, RpL18A, RpL19, RpL21, RpL22, RpL23, RpL24, RpL26, RpL30, RpL35, RpL36A, RpL4, RpL5, RpL7, RpL7A, RpL8, RpS11, RpS16, RpS17, RpS27A, RpS30, RpS4, RpS5a, RpS6, RpS9, Set, Tim17b, eIF-1A, kuk, lwr, mgr, sn
BP	cellular component organization	7.65E-13	69	Act42A, Act5C, CG10440, CG1240, CG13298, CG5525, CG8258, CadN, Cam, Cct5, Cdc42, Cip4, Dscam, Fas2, Frq1, Hsp70Aa, Hsp70Ab, Hsp70Ba, Hsp83, NetB, Nlp, Pp2A-29B, Prosap, Rab6, Rack1, RpL11, RpL12, RpL13, RpL13A, RpL17, RpL18, RpL18A, RpL19, RpL21, RpL22, RpL23, RpL24, RpL26, RpL30, RpL35, RpL36A, RpL4, RpL5, RpL7, RpL7A, RpL8, RpS11, RpS16, RpS17, RpS27A, RpS30, RpS4, RpS5a, RpS6, RpS9, Sec61alpha, Set, Ten-m, Tim17b, caz, chn, dock, eIF-1A, fax, fra, kuk, lwr, mgr, sn
BP	cellular component organization or biogenesis	7.84E-13	70	Act42A, Act5C, CG10440, CG1240, CG13298, CG5525, CG8258, CadN, Cam, Cct5, Cdc42, Cip4, Dscam, Fas2, Frq1, Hsp70Aa, Hsp70Ab, Hsp70Ba, Hsp83, NetB, Nlp, Pp2A-29B, Prosap, Rab6, Rack1, RpL11, RpL12, RpL13, RpL13A, RpL17, RpL18, RpL18A, RpL19, RpL21, RpL22, RpL23, RpL24, RpL26, RpL30, RpL35, RpL36A, RpL4, RpL5, RpL7, RpL8, RpS11, RpS16, RpS17, RpS21, RpS27A, RpS30, RpS4, RpS5a, RpS6, RpS8, RpS9, Sec61alpha, Set, Ten-m, Tim17b, caz, chn, dock, eIF-1A, fax, fra, kuk, lwr, mgr, sn
BP	cellular macromolecule metabolic process	4.99E-12	65	CG13298, CG5525, CG5830, CG7048, CG8258, Cam, CanB, Cct5, Cdc42, ERp60, HIP-R, Hsp22, Hsp27, Hsp67Bc, Hsp68, Hsp83, IA-2, Pp2A-29B, Prosalpha6, Rack1, Rbp2, RpL12, RpL13, RpL13A, RpL15, RpL17, RpL18, RpL18A, RpL19, RpL22, RpL23, RpL24, RpL26, RpL30, RpL34b, RpL35, RpL36A, RpL37a, RpL4, RpL7, RpL7A, RpL8, RpS10b, RpS11, RpS14a, RpS14b, RpS16, RpS17, RpS19a, RpS21, RpS25, RpS30, RpS4, RpS5a, RpS6, RpS8, RpS9, Rpn11, Uch, caz, crc, eIF-3p40, lwr, mgr, snf
BP	cellular metabolic process	4.84E-11	77	7B2, CG13298, CG32230, CG5525, CG5830, CG7048, CG8258, CG9603, Cam, CanB, Cct5, Cdc42, ERp60, FBpp0305828, HIP-R, Hsp22, Hsp27, Hsp67Bc, Hsp68, Hsp83, IA-2, Idh, Jafrac1, Lpin, Pal2, Pp2A-29B, Prosalpha6, Rack1, Rbp2, RpL12, RpL13, RpL13A, RpL15, RpL17, RpL18, RpL18A, RpL19, RpL22, RpL23, RpL24, RpL26, RpL30, RpL34b, RpL35, RpL36A, RpL37a, RpL4, RpL7, RpL7A, RpL8, RpS10b, RpS11, RpS14a, RpS14b, RpS16, RpS17, RpS19a, RpS21, RpS25, RpS30, RpS4, RpS5a, RpS6, RpS8, RpS9, Rpn11, Uch, blw, caz, crc, cype, eIF-3p40, l(1)G0230, lwr, mgr, qm, snf
BP	cellular nitrogen compound metabolic process	1.88E-10	50	7B2, CG13298, CG32230, CG9603, FBpp0305828, Rack1, Rbp2, RpL12, RpL13, RpL13A, RpL15, RpL17, RpL18, RpL18A, RpL19, RpL22, RpL23, RpL24, RpL26, RpL30, RpL34b, RpL35, RpL36A, RpL37a, RpL4, RpL7, RpL7A, RpL8, RpS10b, RpS11, RpS14a, RpS14b, RpS16, RpS17, RpS19a, RpS21, RpS25, RpS30, RpS4, RpS5a, RpS6, RpS8, RpS9, blw, caz, crc, cype, eIF-3p40, l(1)G0230, snf

Type	Term	FDR	#	Gene
BP	macromolecule metabolic process	3.67E-10	67	7B2, CG13298, CG5525, CG5830, CG7048, CG8258, Cam, CanB, Cct5, Cdc42, ERp60, HIP-R, Hsp22, Hsp27, Hsp67Bc, Hsp68, Hsp83, IA-2, Pp2A-29B, Prosalpha6, Rack1, Rbp2, RpL12, RpL13, RpL13A, RpL15, RpL17, RpL18, RpL18A, RpL19, RpL22, RpL23, RpL24, RpL26, RpL30, RpL34b, RpL35, RpL36A, RpL37a, RpL4, RpL7, RpL7A, RpL8, RpS10b, RpS11, RpS14a, RpS14b, RpS16, RpS17, RpS19a, RpS21, RpS25, RpS30, RpS4, RpS5a, RpS6, RpS8, RpS9, Rpn11, Uch, caz, crc, eIF-3p40, lwr, mgr, mmd, snf
BP	primary metabolic process	4.54E-10	76	7B2, CG13298, CG32230, CG5525, CG5830, CG7048, CG8258, CG9603, Cam, CanB, Cct5, Cdc42, ERp60, FBpp0305828, HIP-R, Hsp22, Hsp27, Hsp67Bc, Hsp68, Hsp83, IA-2, Idh, Lpin, Pp2A-29B, Prosalpha6, Rack1, Rbp2, RpL12, RpL13, RpL13A, RpL15, RpL17, RpL18, RpL18A, RpL19, RpL22, RpL23, RpL24, RpL26, RpL30, RpL34b, RpL35, RpL36A, RpL37a, RpL4, RpL7, RpL7A, RpL8, RpS10b, RpS11, RpS14a, RpS14b, RpS16, RpS17, RpS19a, RpS21, RpS25, RpS30, RpS4, RpS5a, RpS6, RpS8, RpS9, Rpn11, Uch, blw, caz, crc, cype, eIF-3p40, l(1)G0230, lwr, mgr, mmd, qm, snf
BP	single-organism process	4.67E-09	109	2mit, 7B2, Act42A, Act5C, CG10440, CG1240, CG13298, CG13830, CG1943, CG2993, CG32230, CG32975, CG5525, CG8258, CG9603, CadN, Cam, CanB, Cct5, Cdc42, Cip4, Cyp1, Dscam, ERp60, Eaat2, Evi5, FBpp0081153, FBpp0085193, FKBP59, Fas2, Frq1, Gdi, Hsp22, Hsp27, Hsp67Bc, Hsp68, Hsp70Aa, Hsp70Ab, Hsp70Ba, Hsp83, IA-2, Idh, Jafrac1, Lpin, Lrch, NetB, Nlp, PPP4R2r, Pp2A-29B, Prosalpha6, Prosap, Pvf3, Rab10, Rab6, Rack1, RpL11, RpL12, RpL13, RpL13A, RpL17, RpL18, RpL18A, RpL19, RpL21, RpL22, RpL23, RpL24, RpL26, RpL30, RpL35, RpL36A, RpL4, RpL7, RpL7A, RpL8, RpS11, RpS16, RpS21, RpS27A, RpS30, RpS4, RpS5a, RpS6, RpS8, RpS9, Sec61alpha, Task6, Ten-m, Tim17b, blw, caz, chn, crc, cype, dock, eIF-1A, eIF-3p40, fabp, fax, fra, kuk, lwr, mgr, miple, nrm, shep, sn, snf, tinc
BP	cellular process	1.96E-08	108	Act42A, Act5C, CG10440, CG1240, CG13298, CG32230, CG32975, CG5830, CG7048, CG8258, CG9603, CadN, Cam, CanB, Cct5, Cdc42, Cip4, Dscam, Eaat2, Evi5, FBpp0081153, Fas2, Frq1, Gdi, HIP-R, Hsp22, Hsp27, Hsp67Bc, Hsp68, Hsp70Aa, Hsp70Ab, Hsp70Ba, Hsp83, IA-2, Idh, Jafrac1, Lpin, Lrch, NetB, Nlp, PPP4R2r, Pal2, Pp2A-29B, Prosalpha6, Prosap, Pvf3, Rab10, Rab6, Rack1, Rbp2, RpL12, RpL13, RpL13A, RpL15, RpL17, RpL18, RpL18A, RpL19, RpL22, RpL23, RpL24, RpL26, RpL30, RpL34b, RpL35, RpL36A, RpL37a, RpL4, RpL7, RpL7A, RpL8, RpS10b, RpS11, RpS14a, RpS14b, RpS16, RpS17, RpS19a, RpS21, RpS25, RpS4, RpS5a, RpS6, RpS8, RpS9, Rpn11, Sec61alpha, Set, Task6, Ten-m, Tim17b, Uch, blw, caz, chn, crc, cype, dock, eIF-3p40, fax, fra, kuk, lwr, nrm, shep, sn, snf, tinc
BP	single-organism cellular process	2.93E-08	96	7B2, Act42A, Act5C, CG1240, CG13298, CG32230, CG32975, CG5525, CG8258, CG9603, CadN, Cam, CanB, Cct5, Cdc42, Cip4, Cyp1, Dscam, ERp60, Eaat2, Evi5, FBpp0081153, FBpp0085193, Fas2, Frq1, Gdi, Hsp67Bc, Hsp68, Hsp70Aa, Hsp70Ab, Hsp70Ba, Hsp83, IA-2, Idh, Jafrac1, Lpin, Lrch, NetB, PPP4R2r, Pp2A-29B, Prosap, Pvf3, Rab10, Rab6, Rack1, RpL11, RpL12, RpL13,

Type	Term	FDR	#	Gene
				RpL13A, RpL17, RpL18, RpL18A, RpL19, RpL21, RpL22, RpL23, RpL24, RpL26, RpL30, RpL35, RpL36A, RpL4, RpL7, RpL7A, RpL8, RpS11, RpS16, RpS27A, RpS30, RpS4, RpS5a, RpS6, RpS8, RpS9, Sec61alpha, Sod, Task6, Ten-m, blw, caz, chn, crc, cype, dock, eIF-1A, eIF-3p40, fax, fra, kuk, lwr, mgr, nrm, shep, sn, snf, tinc
BP	organic substance metabolic process	3.56E-08	76	7B2, CG13298, CG32230, CG5525, CG5830, CG7048, CG8258, CG9603, Cam, CanB, Cct5, Cdc42, ERp60, FBpp0305828, HIP-R, Hsp22, Hsp27, Hsp67Bc, Hsp68, Hsp83, IA-2, Idh, Lpin, Pp2A-29B, Prosalpha6, Rack1, Rbp2, RpL12, RpL13, RpL13A, RpL15, RpL17, RpL18, RpL18A, RpL19, RpL22, RpL23, RpL24, RpL26, RpL30, RpL34b, RpL35, RpL36A, RpL37a, RpL4, RpL7, RpL7A, RpL8, RpS10b, RpS11, RpS14a, RpS14b, RpS16, RpS17, RpS19a, RpS21, RpS25, RpS30, RpS4, RpS5a, RpS6, RpS8, RpS9, Rpn11, Uch, blw, caz, crc, cype, eIF-3p40, l(1)G0230, lwr, mgr, mmd, qm, snf
BP	protein folding	1.71E-07	12	CG5525, CG7048, CG8258, Cct5, ERp60, FKBP59, HIP-R, Hsp22, Hsp27, Hsp68, Hsp83, mgr
BP	metabolic process	5.73E-06	79	7B2, CG13298, CG32230, CG5830, CG7048, CG8258, CG9603, Cam, CanB, Cct5, Cdc42, ERp60, FBpp0081153, HIP-R, Hsp22, Hsp27, Hsp67Bc, Hsp68, Hsp83, IA-2, Idh, Jafrac1, Lpin, Mgstl, Nlp, Pal2, Pp2A-29B, Prosalpha6, Rab10, Rab6, Rack1, Rbp2, RpL12, RpL13, RpL13A, RpL15, RpL17, RpL18, RpL18A, RpL19, RpL22, RpL23, RpL24, RpL26, RpL30, RpL34b, RpL35, RpL36A, RpL37a, RpL4, RpL7, RpL7A, RpL8, RpS10b, RpS11, RpS14a, RpS14b, RpS16, RpS17, RpS19a, RpS21, RpS25, RpS30, RpS4, RpS5a, RpS6, RpS8, RpS9, Rpn11, Uch, blw, caz, crc, cype, eIF-3p40, lwr, mgr, mmd, snf
BP	response to heat	9.07E-06	10	Hsp22, Hsp23, Hsp27, Hsp67Ba, Hsp67Bc, Hsp68, Hsp70Aa, Hsp70Ab, Hsp70Ba, Hsp83
BP	single-multicellular organism process	0.000212	65	2mit, ATPsyn-d, Act5C, CG10440, CG13298, CG1943, CG5525, CadN, Cam, CanB, Cct5, Cdc42, Cip4, Dscam, Evi5, FBpp0085193, FKBP59, Fas2, Hsp22, Hsp27, Hsp68, Hsp83, IA-2, Jafrac1, Lpin, NetB, PPP4R2r, Pp2A-29B, Prosalpha6, Prosap, Pvf3, Rab6, Rack1, RpL13A, RpL23, RpL30, RpL7, RpL8, RpS11, RpS21, RpS27A, RpS8, Sec61alpha, Sod, Ten-m, caz, chn, crc, dock, eIF-3p40, fabp, fax, fra, kuk, lwr, mam, miple, nrm, qm, shep, sn, snf, spri, tinc, tsr
BP	developmental process	0.000216	66	ATPsyn-d, Act5C, CG10641, CG13298, CG1943, CG5525, CadN, Cam, Cct5, Cdc42, Cip4, Cyp1, Dscam, Evi5, FBpp0085193, FBpp0305828, FKBP59, Fas2, Hsp22, Hsp27, Hsp68, Hsp83, IA-2, Jafrac1, Lpin, NetB, PPP4R2r, Pp2A-29B, Prosalpha6, Prosap, Pvf3, Rab10, Rab6, Rack1, RpL13A, RpL23, RpL30, RpL7, RpL8, RpS11, RpS21, RpS27A, RpS8, Sec61alpha, Sod, Ten-m, blw, caz, chn, crc, dock, eIF-3p40, fax, fra, kuk, lwr, mam, miple, nrm, qm, shep, sn, snf, spri, tinc, tsr
BP	multicellular organismal development	0.000253	58	ATPsyn-d, Act5C, CG13298, CG1943, CG5525, CadN, Cam, Cct5, Cdc42, Cip4, Dscam, FBpp0085193, FKBP59, Fas2, Hsp22, Hsp27, Hsp68, Hsp83, IA-2, Jafrac1, Lpin, NetB, PPP4R2r, Pp2A-29B, Prosalpha6, Prosap, Pvf3, Rab6, Rack1, RpL13A, RpL23, RpL30, RpL7, RpL8, RpS11, RpS21, RpS8, Sec61alpha, Sod, Ten-m, caz, chn, crc, dock, eIF-3p40, fax, fra, kuk, lwr, mam, miple, nrm, qm, shep, sn, snf, tinc, tsr

Type	Term	FDR	#	Gene
BP	ribosomal small subunit biogenesis	0.000289	4	RpS17, RpS21, RpS6, RpS8
BP	anatomical structure development	0.00033	61	Act5C, CG10641, CG13298, CG1943, CG5525, CadN, Cam, Cct5, Cdc42, Cip4, Cyp1, Dscam, Evi5, FBpp0085193, FKBP59, Fas2, Hsp27, Hsp68, Hsp83, IA-2, Jafrac1, Lpin, NetB, PPP4R2r, Pp2A-29B, Prosalpha6, Prosap, Pvf3, Rab10, Rab6, Rack1, RpL13A, RpL23, RpL30, RpL8, RpS11, RpS21, RpS27A, RpS8, Sec61alpha, Ten-m, blw, caz, chn, crc, dock, eIF-3p40, fax, fra, kuk, lwr, mam, miple, nrm, qm, shep, sn, snf, spri, tinc, tsr
BP	single-organism developmental process	0.000336	65	ATPsyn-d, Act5C, CG13298, CG1943, CG5525, CadN, Cam, Cct5, Cdc42, Cip4, Cyp1, Dscam, Evi5, FBpp0085193, FBpp0305828, FKBP59, Fas2, Hsp22, Hsp27, Hsp68, Hsp83, IA-2, Jafrac1, Lpin, NetB, PPP4R2r, Pp2A-29B, Prosalpha6, Prosap, Pvf3, Rab10, Rab6, Rack1, RpL13A, RpL23, RpL30, RpL7, RpL8, RpS11, RpS21, RpS27A, RpS8, Sec61alpha, Sod, Ten-m, blw, caz, chn, crc, dock, eIF-3p40, fax, fra, kuk, lwr, mam, miple, nrm, qm, shep, sn, snf, spri, tinc, tsr
BP	nervous system development	0.000387	39	Act5C, CG13298, CG5525, CadN, Cam, Cct5, Cdc42, Cip4, Dscam, FBpp0085193, FKBP59, Fas2, Hsp68, Hsp83, NetB, PPP4R2r, Pp2A-29B, Prosap, Pvf3, Rab6, RpL23, RpL30, RpS11, RpS8, Sec61alpha, Ten-m, caz, chn, dock, eIF-3p40, fax, fra, mam, nrm, qm, shep, sn, tinc, tsr
BP	system development	0.00205	47	Act5C, CG13298, CG1943, CG5525, CadN, Cam, Cct5, Cdc42, Cip4, Dscam, FBpp0085193, FKBP59, Fas2, Hsp27, Hsp68, Hsp83, IA-2, Lpin, NetB, PPP4R2r, Pp2A-29B, Prosap, Pvf3, Rab6, Rack1, RpL13A, RpL23, RpL30, RpL8, RpS11, RpS21, RpS8, Sec61alpha, Ten-m, caz, chn, dock, eIF-3p40, fax, fra, mam, nrm, qm, shep, sn, tinc, tsr
BP	multicellular organismal process	0.00213	68	2mit, ATPsyn-d, Act5C, CG10440, CG13298, CG1943, CG5525, CadN, Cam, CanB, Cct5, Cdc42, Cip4, Dscam, Evi5, FBpp0085193, FKBP59, Fas2, Hsp22, Hsp27, Hsp68, Hsp83, IA-2, Jafrac1, Lpin, NetB, PPP4R2r, Pp2A-29B, Prosalpha6, Prosap, Pvf3, Rab10, Rab6, Rack1, RpL13A, RpL23, RpL30, RpL7, RpL8, RpS11, RpS21, RpS27A, RpS8, Sec61alpha, Sod, Ten-m, blw, caz, chn, crc, dock, eIF-3p40, fabp, fax, fne, fra, kuk, lwr, mam, miple, nrm, qm, shep, sn, snf, spri, tinc, tsr
BP	macromolecular complex assembly	0.00233	15	CG10440, CG1240, CG5525, Cam, Cct5, Cdc42, FBpp0081153, Hsp83, Nlp, Pp2A-29B, RpL5, RpS17, Set, mgr, tsr
BP	mitotic spindle assembly	0.00233	6	CG1240, CG5525, Cam, Cct5, Pp2A-29B, mgr
BP	response to abiotic stimulus	0.00333	15	Cam, Dscam, FKBP59, Hsp22, Hsp23, Hsp27, Hsp67Ba, Hsp67Bc, Hsp68, Hsp70Aa, Hsp70Ab, Hsp70Ba, Hsp83, chn, shep
BP	locomotion	0.00367	19	CadN, Cam, Cdc42, Dscam, Evi5, Fas2, Jafrac1, NetB, Pvf3, Rab6, Ten-m, dock, fra, lwr, qm, shep, sn, spri, tsr
BP	cellular component biogenesis	0.00378	24	CG10440, CG1240, CG5525, Cam, Cct5, Cdc42, FBpp0081153, Hsp83, Nlp, Pp2A-29B, Prosap, Rab6, RpL5, RpL7A, RpS17, RpS21, RpS6, RpS8, Set, Ten-m, caz, mgr, sn, tsr
MF	protein binding	0.00412	41	CG13830, CG5036, CG5525, CG7048, CG8258, CadN, Cam, CanB, Cct5, Cdc42, Cip4, Dscam, Evi5, FKBP59,

Type	Term	FDR	#	Gene
				Fas2, HIP-R, Hsp23, Hsp27, Hsp68, Hsp83, Nlp, Prosap, Rab6, Rack1, RpL11, RpL23, RpL34a, RpL5, Set, Sod, Task6, Ten-m, chn, crc, dock, lwr, mgr, miple, snf, spri, tsr
BP	neuron recognition	0.00454	8	CadN, Dscam, Fas2, NetB, Pvf3, Ten-m, fra, nrm
BP	heat shock-mediated polytene chromosome puffing	0.00522	3	Hsp70Aa, Hsp70Ab, Hsp70Ba
BP	protein refolding	0.00522	3	HIP-R, Hsp22, Hsp27
BP	neurogenesis	0.00754	33	CG13298, CG5525, CadN, Cam, Cct5, Cdc42, Cip4, Dscam, FBpp0085193, Fas2, Hsp68, Hsp83, NetB, PPP4R2r, Pp2A-29B, Pvf3, Rab6, RpL23, RpS11, RpS8, Sec61alpha, Ten-m, chn, dock, eIF-3p40, fax, fra, nrm, qm, shep, sn, tinc, tsr
BP	biological_process	0.00826	128	2mit, 7B2, Act42A, Act5C, CG10098, CG10641, CG1240, CG13298, CG13830, CG1943, CG2269, CG2993, CG31051, CG32230, CG32975, CG34362, CG4341, CG43759, CG5036, CG5830, CG7048, CG8223, CG8258, CG9603, CadN, Cam, CanB, Cct5, Cdc42, Cip4, Dscam, Eaat2, Evi5, FBpp0081153, FKBP59, Fas2, Frq1, Gdi, HIP-R, Hsp22, Hsp23, Hsp27, Hsp67Ba, Hsp67Bc, Hsp68, Hsp70Aa, Hsp70Ab, Hsp70Ba, Hsp83, IA-2, Idh, Jafrac1, Lpin, Lrch, Mgstl, NetB, Nlp, PPP4R2r, Pal2, Pp2A-29B, Prosalpha6, Prosap, Pvf3, Rab6, Rack1, Rbp2, RpL12, RpL13, RpL13A, RpL15, RpL17, RpL18, RpL18A, RpL19, RpL22, RpL23, RpL24, RpL26, RpL30, RpL34b, RpL35, RpL36A, RpL37a, RpL4, RpL7, RpL8, RpS10b, RpS11, RpS14a, RpS14b, RpS16, RpS17, RpS19a, RpS21, RpS25, RpS27A, RpS4, RpS5a, RpS6, RpS8, RpS9, Rpn11, Sec61alpha, Set, Task6, Ten-m, Tim17b, Uch, beat-Vb, blw, caz, chn, crc, cype, dock, eIF-3p40, fax, fne, fra, kuk, lwr, miple, mmd, nrm, shep, sn, snf, tinc
BP	ATP synthesis coupled proton transport	0.00883	4	ATPsyn-d, FBpp0305828, blw, l(1)G0230
BP	cell differentiation	0.0107	45	Act5C, CG13298, CG5525, CadN, Cam, Cct5, Cdc42, Cip4, Cyp1, Dscam, Evi5, FBpp0085193, FBpp0305828, Fas2, Hsp68, Hsp83, Jafrac1, NetB, PPP4R2r, Pp2A-29B, Pvf3, Rab10, Rab6, Rack1, RpL23, RpS11, RpS27A, RpS8, Sec61alpha, Ten-m, blw, chn, dock, eIF-3p40, fax, fra, mam, nrm, qm, shep, sn, snf, spri, tinc, tsr
BP	protein complex assembly	0.011	12	CG10440, CG1240, CG5525, Cam, Cct5, Cdc42, FBpp0081153, Hsp83, Pp2A-29B, Set, mgr, tsr
BP	protein complex biogenesis	0.012	12	CG10440, CG1240, CG5525, Cam, Cct5, Cdc42, FBpp0081153, Hsp83, Pp2A-29B, Set, mgr, tsr
BP	axonogenesis	0.0131	12	CadN, Cam, Cdc42, Dscam, Fas2, NetB, Rab6, Ten-m, dock, fax, fra, tsr
BP	movement of cell or subcellular component	0.0144	18	CadN, Cam, Cdc42, Dscam, Evi5, Fas2, Jafrac1, NetB, Pvf3, Rab6, Ten-m, dock, fra, lwr, qm, sn, spri, tsr
KG	Phototransduction - fly	0.0163	4	Act42A, Act5C, Cam, Ggamma30A

Type	Term	FDR	#	Gene
BP	cell development	0.0167	32	Act5C, CG13298, CadN, Cam, Cdc42, Cyp1, Dscam, Evi5, Fas2, Hsp83, Jafrac1, NetB, Pvf3, Rab10, Rab6, Rack1, RpS27A, Sec61alpha, Ten-m, blw, chn, dock, fax, fra, mam, nrm, qm, shep, sn, snf, spri, tsr
BP	axon development	0.0167	12	CadN, Cam, Cdc42, Dscam, Fas2, NetB, Rab6, Ten-m, dock, fax, fra, tsr
BP	cell migration	0.0175	11	Cdc42, Evi5, Jafrac1, NetB, Pvf3, fra, lwr, qm, sn, spri, tsr
BP	neuron differentiation	0.018	21	CG13298, CadN, Cam, Cdc42, Cip4, Dscam, Fas2, Hsp83, NetB, Pvf3, Rab6, Sec61alpha, Ten-m, chn, dock, fax, fra, nrm, shep, sn, tsr
BP	neuron development	0.0201	19	CG13298, CadN, Cam, Cdc42, Dscam, Fas2, NetB, Pvf3, Rab6, Sec61alpha, Ten-m, chn, dock, fax, fra, nrm, shep, sn, tsr
BP	ribosome biogenesis	0.0212	6	RpL5, RpL7A, RpS17, RpS21, RpS6, RpS8
BP	response to stimulus	0.0223	45	7B2, ATPsyn-d, CadN, Cam, Cdc42, Cip4, Dscam, FBpp0081153, FKBP59, Fas2, Hsp22, Hsp23, Hsp27, Hsp67Ba, Hsp67Bc, Hsp68, Hsp70Aa, Hsp70Ab, Hsp70Ba, Hsp83, IA-2, Jafrac1, Lpin, Lrch, NetB, Pvf3, Rab10, Rab6, Rack1, RpL13A, RpL8, RpS27A, RpS6, Sec61alpha, Sod, Ten-m, chn, crc, dock, eIF-1A, fra, lwr, shep, sn, spri
BP	localization of cell	0.0282	11	Cdc42, Evi5, Jafrac1, NetB, Pvf3, fra, lwr, qm, sn, spri, tsr
BP	positive regulation of viral life cycle	0.0282	2	Rack1, Sec61alpha
BP	neuron projection morphogenesis	0.0313	16	CG13298, CadN, Cam, Cdc42, Dscam, Fas2, NetB, Rab6, Sec61alpha, Ten-m, chn, dock, fax, fra, sn, tsr
BP	cellular component assembly	0.0355	20	CG10440, CG1240, CG5525, Cam, Cct5, Cdc42, FBpp0081153, Hsp83, Nlp, Pp2A-29B, Prosap, Rab6, RpL5, RpS17, Set, Ten-m, caz, mgr, sn, tsr
BP	regulation of axonogenesis	0.0355	4	CadN, Cdc42, Dscam, NetB
BP	axon guidance	0.0399	10	CadN, Cam, Cdc42, Dscam, Fas2, NetB, Rab6, Ten-m, dock, fra
BP	neuron projection development	0.0399	16	CG13298, CadN, Cam, Cdc42, Dscam, Fas2, NetB, Rab6, Sec61alpha, Ten-m, chn, dock, fax, fra, sn, tsr
BP	generation of neurons	0.0399	22	CG13298, CadN, Cam, Cdc42, Cip4, Dscam, Fas2, Hsp83, NetB, Pvf3, Rab6, Sec61alpha, Ten-m, chn, dock, fax, fra, nrm, shep, sn, tinc, tsr
BP	motor neuron axon guidance	0.0465	5	Cdc42, Fas2, NetB, Ten-m, fra
BP	maturation of SSU-rRNA from tricistronic rRNA transcript (SSU-rRNA, 5.8S rRNA, LSU-rRNA)	0.0499	2	RpS21, RpS8
BP	regulation of cell projection organization	0.0499	6	CadN, Cdc42, Dscam, NetB, fra, tsr

Table 4.S16 | GSEA term enrichments for hierarchical clustering of differentially expressed genes - cluster 3, highest expression in WT 120hr 12A. Terms sorted by FDR. Terms for biological process (BP), Molecular function (MF), and KEGG pathway (KG) terms were included and are categorized in the Type column. The number of genes associated with each term is indicated in the # column.

Type	Term	#	FDR	Genes
CC	nuclear part	34	4.03E-07	Bacc, CG18316, CG6340, CG8801, Dp, Fas3, Hrb27C, Lk6, MED31, Mapmodulin, Pabp2, Pc, Prp3, Rbp1-like, Rm62, S6k, SF2, Taf4, Tif-IA, YT521-B, akirin, lark, lola, lost, nudE, pUf68, pho, rap, sbr, sec31, seq, sqd, vfl, yps
MF	protein binding	48	1.30E-06	AGO1, Aac11, CG11486, CG13624, CG14408, CG18619, CG2950, Dcp2, Df31, Dp, FBpp0091066, FBpp0091081, FBpp0091148, FBpp0091152, His2Av, Hrb27C, Lk6, Mapmodulin, Msi, NKAIN, Paip2, Pc, Rab7, RhoGAP68F, Rm62, S6k, SF2, Slip1, Thor, Unr, Xrp1, akirin, crc, csw, dlg1, drpr, ens, fd68A, futsch, lea, lola, nudE, pUf68, pk, stan, stau, vfl, wech
CC	nucleus	52	1.40E-06	AGO1, Aac11, Aps, Bacc, CG18316, CG5059, CG6340, CG8801, Df31, Dp, FBpp0091066, FBpp0091081, FBpp0091148, FBpp0091152, Fas3, His2Av, Hrb27C, Lk6, MED31, Mapmodulin, Pabp2, Pc, Prp3, Rbp1-like, Rm62, S6k, SF2, Taf4, Tif-IA, YT521-B, akirin, crc, fd68A, fru, jigr1, jim, lark, lola, lost, nerfin-1, nudE, pUf68, pho, rap, sbr, scrt, sec31, seq, spen, sqd, vfl, yps
BP	regulation of gene expression	35	8.34E-06	AGO1, CG13624, CG18316, CG18619, CG2950, Dcp2, Hrb27C, MED31, Paip2, Pc, Prp3, Rm62, Taf4, Thor, Tif-IA, Unr, akirin, crc, csw, fd68A, fru, hdc, jigr1, jim, lola, nerfin-1, pUf68, pho, scrt, seq, spen, sqd, stau, vfl, yps
BP	cell development	42	8.34E-06	AGO1, CG11448, CG2950, Dp, Fas3, His2Av, Hrb27C, Lin29, Msi, Pc, Pdcd4, Rab7, S6k, Sh, Taf4, cora, csw, drpr, ens, fru, futsch, galectin, hdc, hig, jim, lark, larp, lea, lola, lost, nerfin-1, nudE, pUf68, pho, puc, scrt, seq, spen, sqd, stan, stau, yps
BP	regulation of biological process	70	8.34E-06	AGO1, Aac11, Alg-2, CG13624, CG18316, CG18619, CG2950, CG5059, CycG, Dcp2, His2Av, Hrb27C, Lk6, MED31, Mapmodulin, NKAIN, NaCP60E, Paip2, Pc, Pdcd4, Prp3, Rab7, Rdl, RhoGAP68F, Rm62, SF2, Sh, Taf4, Teh4, Thor, Tif-IA, Unr, Xrp1, akirin, crc, csw, dlg1, drpr, eIF-4B, ens, fd68A, fru, futsch, hdc, jigr1, jim, lark, lea, lola, mtt, nerfin-1, pUf68, pho, pk, pog, puc, qvr, rap, scrt, sec31, seq, spen, sqd, stan, stau, stj, vfl, viaf, wech, yps
BP	regulation of cellular process	66	8.36E-06	AGO1, Aac11, Alg-2, CG13624, CG18316, CG18619, CG2950, CG5059, CycG, Dcp2, His2Av, Hrb27C, Lk6, MED31, NaCP60E, Paip2, Pc, Pdcd4, Prp3, Rab7, Rdl, RhoGAP68F, Rm62, SF2, Sh, Taf4, Thor, Tif-IA, Unr, Xrp1, akirin, chrb, crc, csw, dlg1, drpr, eIF-4B, ens, fd68A, fru, futsch, hdc, jim, lea, lola, mtt, nerfin-1, pUf68, pho, pk, pog, puc, qvr, rap, scrt, scyl, seq, spen, sqd, stan, stau, stj, vfl, viaf, wech, yps
BP	cell differentiation	54	9.02E-06	AGO1, Aac11, CG11448, CG2950, Dp, Fas3, His2Av, Hrb27C, Lin29, MED31, Msi, Pabp2, Pc, Pdcd4, Rab7, Rm62, S6k, SF2, Sh, Taf4, Thor, Unr, cora, csw, dlg1, drpr, ens, foi, fru, futsch, galectin, hdc, hig, jim, lark, larp, lea, lola, lost, nerfin-1, nudE, pUf68, pho, pk, puc, qtc, rap, scrt, seq, spen, sqd, stan, stau, yps
MF	nucleic acid binding	41	1.12E-05	AGO1, CG10077, CG11486, CG12054, CG13624, CG18619, CG2950, CG32767, CG43444, CG4404, Dcp2, Dp, FBpp0091066, FBpp0091081, FBpp0091148, FBpp0091152, Hrb27C, Lin29, Pabp2, Pc, Rbp1-like, Taf4, Xrp1, YT521-B, crc, eIF-4B, fru, jigr1, jim, lola, lost, mus210, nerfin-1, pUf68, pho, sbr, scrt, seq, spen,

Type	Term	#	FDR	Genes
				stau, vfl
BP	biological regulation	72	1.25E-05	AGO1, Aac11, Alg-2, CG13624, CG18316, CG18619, CG2950, CG5059, CycG, Dcp2, His2Av, Hrb27C, Lin29, Lk6, MED31, Mapmodulin, NKAIN, NaCP60E, Paip2, Pc, Pdcd4, Prp3, Rab7, Rdl, RhoGAP68F, Rm62, SF2, Sh, Taf4, Teh4, Thor, Tif-IA, Unr, Xrp1, akirin, cora, crc, csw, dlg1, drpr, eIF-4B, ens, fd68A, fru, futsch, hdc, jigr1, jim, lark, lea, lola, mtt, nerfin-1, pUf68, pho, pk, pog, puc, qvr, rap, scrt, sec31, seq, spen, sqd, stan, stau, stj, vfl, viaf, wech, yps
BP	negative regulation of biological process	37	1.41E-05	AGO1, Aac11, CG2950, CycG, Dcp2, His2Av, Hrb27C, Lk6, MED31, Mapmodulin, Paip2, Pc, Rab7, Rdl, RhoGAP68F, Rm62, SF2, Thor, Unr, Xrp1, crc, csw, dlg1, fd68A, futsch, hdc, lark, pho, pk, puc, qvr, rap, scrt, seq, sqd, stan, stj
BP	anatomical structure development	64	1.47E-05	AGO1, Aac11, CG11448, CG2950, CG6767, CycG, Dp, Fas3, His2Av, Hrb27C, Lin29, MED31, Msi, Pabp2, Pc, Pdcd4, Rab7, RhoGAP68F, Rm62, S6k, SF2, Sh, Taf4, Thor, Xrp1, akirin, chrb, cora, crc, csw, dlg1, drpr, ens, fd68A, foi, fru, futsch, galectin, hdc, hig, jim, lark, larp, lea, lola, lost, nerfin-1, nudE, pUf68, pho, pk, pog, puc, rap, scrt, scyl, seq, spen, sqd, stan, stau, vfl, wech, yps
BP	negative regulation of cellular process	34	1.68E-05	AGO1, Aac11, CG2950, CycG, His2Av, Hrb27C, Lk6, MED31, Paip2, Pc, Rdl, RhoGAP68F, SF2, Thor, Unr, Xrp1, chrb, crc, csw, dlg1, fd68A, futsch, hdc, pho, pk, puc, qvr, rap, scrt, scyl, seq, sqd, stan, stj
BP	regulation of metabolic process	45	3.27E-05	AGO1, Alg-2, CG13624, CG18316, CG18619, CG2950, CycG, Dcp2, Hrb27C, MED31, Mapmodulin, Paip2, Pc, Prp3, RhoGAP68F, Rm62, S6k, Taf4, Thor, Tif-IA, Unr, akirin, crc, csw, ens, fd68A, fru, hdc, jigr1, jim, lola, nerfin-1, pUf68, pho, pog, puc, rap, scrt, seq, spen, sqd, stau, vfl, viaf, yps
BP	single-multicellular organism process	66	3.27E-05	AGO1, Aac11, Bacc, CG11448, CG2950, CG6767, Dp, Fas3, His2Av, Hrb27C, Lin29, MED31, Pabp2, Pc, Rab7, Rdl, RhoGAP68F, Rm62, S6k, SF2, Sh, Taf4, Thor, Xrp1, akirin, chrb, cora, crc, csw, dlg1, drpr, ens, fd68A, foi, fru, futsch, galectin, hdc, hig, jim, lark, larp, lea, lola, lost, mtt, nerfin-1, nudE, pUf68, pho, pk, pog, puc, qvr, rap, sbr, scrt, scyl, seq, spen, sqd, stan, stau, stj, vfl, wech
BP	regulation of nitrogen compound metabolic process	33	3.27E-05	AGO1, CG13624, CG18316, CG18619, CG2950, Hrb27C, MED31, Paip2, Pc, Prp3, Rm62, Taf4, Thor, Tif-IA, Unr, akirin, crc, csw, fd68A, fru, jim, lola, nerfin-1, pUf68, pho, pog, scrt, seq, spen, sqd, stau, vfl, yps
BP	regulation of macromolecule metabolic process	40	3.73E-05	AGO1, Alg-2, CG13624, CG18316, CG18619, CG2950, CycG, Dcp2, Hrb27C, MED31, Paip2, Pc, Prp3, Rm62, Taf4, Thor, Tif-IA, Unr, akirin, crc, csw, fd68A, fru, hdc, jigr1, jim, lola, nerfin-1, pUf68, pho, puc, rap, scrt, seq, spen, sqd, stau, vfl, viaf, yps
BP	regulation of cellular macromolecule biosynthetic process	30	4.13E-05	AGO1, CG13624, CG18316, CG18619, CG2950, Hrb27C, MED31, Paip2, Pc, Prp3, Taf4, Thor, Tif-IA, Unr, akirin, crc, csw, fd68A, fru, jim, lola, nerfin-1, pho, scrt, seq, spen, sqd, stau, vfl, yps
BP	regulation of cellular biosynthetic process	31	4.18E-05	AGO1, CG13624, CG18316, CG18619, CG2950, Hrb27C, MED31, Paip2, Pc, Prp3, Taf4, Thor, Tif-IA, Unr, akirin, crc, csw, fd68A, fru, jim, lola, nerfin-1, pho, pog, scrt, seq, spen, sqd, stau, vfl, yps

Type	Term	#	FDR	Genes
BP	generation of neurons	29	4.18E-05	CG11448, Fas3, Hrb27C, Lin29, MED31, Pc, S6k, Sh, Taf4, cora, csw, dlg1, drpr, fru, futsch, galectin, hdc, hig, jim, lea, lola, nerfin-1, pho, pk, scrt, seq, spen, stan, stau
BP	developmental process	66	5.30E-05	AGO1, Aac11, CG11448, CG2950, CG6767, CycG, Dp, Fas3, His2Av, Hrb27C, Lin29, MED31, Msi, Pabp2, Pc, Pdcd4, Rab7, RhoGAP68F, Rm62, S6k, SF2, Sh, Taf4, Thor, Unr, Xrp1, akirin, chrb, cora, crc, csw, dlg1, drpr, ens, fd68A, foi, fru, futsch, galectin, hdc, hig, jim, lark, larp, lea, lola, lost, nerfin-1, nudE, pUf68, pho, pk, pog, puc, qtc, rap, scrt, scyl, seq, spen, sqd, stan, stau, vfl, wech, yps
BP	neuron differentiation	26	9.23E-05	CG11448, Fas3, Hrb27C, Lin29, Pc, S6k, Sh, Taf4, cora, csw, drpr, fru, futsch, galectin, hdc, hig, jim, lea, lola, nerfin-1, pho, pk, scrt, seq, spen, stan
BP	single-organism developmental process	65	9.23E-05	AGO1, Aac11, CG11448, CG2950, CG6767, Dp, Fas3, His2Av, Hrb27C, Lin29, MED31, Msi, Pabp2, Pc, Pdcd4, Rab7, RhoGAP68F, Rm62, S6k, SF2, Sh, Taf4, Thor, Unr, Xrp1, akirin, chrb, cora, crc, csw, dlg1, drpr, ens, fd68A, foi, fru, futsch, galectin, hdc, hig, jim, lark, larp, lea, lola, lost, nerfin-1, nudE, pUf68, pho, pk, pog, puc, qtc, rap, scrt, scyl, seq, spen, sqd, stan, stau, vfl, wech, yps
BP	multicellular organismal process	70	0.000114	AGO1, Aac11, Bacc, CG11448, CG2950, CG6767, Dp, Fas3, His2Av, Hrb27C, Lin29, MED31, Msi, Pabp2, Pc, Pdcd4, Rab7, Rdl, RhoGAP68F, Rm62, S6k, SF2, Sh, Taf4, Thor, Xrp1, akirin, chrb, cora, crc, csw, dlg1, drpr, ens, fd68A, foi, fru, futsch, galectin, hdc, hig, jim, lark, larp, lea, lola, lost, mtt, nerfin-1, nudE, pUf68, pho, pk, pog, puc, qtc, qvr, rap, sbr, scrt, scyl, seq, spen, sqd, stan, stau, stj, vfl, wech, yps
BP	posttranscriptional regulation of gene expression	11	0.000123	AGO1, CG2950, Dcp2, Hrb27C, Paip2, Rm62, Thor, Unr, hdc, sqd, stau
BP	mRNA metabolic process	15	0.00013	AGO1, CG11486, Dcp2, Hrb27C, Pabp2, Prp3, Rbp1-like, Rm62, SF2, lark, lost, pUf68, sbr, sqd, yps
CC	cell	94	0.000152	AGO1, Aac11, Aldh-III, Aps, Bacc, CG10077, CG11486, CG11658, CG18316, CG2950, CG32549, CG42258, CG42389, CG43066, CG4729, CG5059, CG6340, CG6439, CG8801, CG9281, CycG, Dcp2, Df31, Dp, Edc3, Fas3, His2Av, Hrb27C, Lk6, MED31, MSBP, Mapmodulin, Pabp2, Pc, Pdcd4, Prp3, Rab7, Rbp1-like, Rdl, RhoGAP68F, Rm62, S6k, SF2, Sh, Taf4, Tif-IA, Tsp42Ee, Unr, YT521-B, akirin, chrb, cora, crc, csw, dlg1, eIF-4B, ens, fd68A, foi, fru, futsch, galectin, hdc, hig, jigr1, jim, lark, larp, lea, lola, lost, mtt, nerfin-1, nudE, pUf68, pho, pk, pog, puc, qvr, rap, sbr, scrt, scyl, sec31, seq, spen, sqd, stau, stj, vfl, viaf, wech, yps
CC	cell part	94	0.000152	AGO1, Aac11, Aldh-III, Aps, Bacc, CG10077, CG11486, CG11658, CG18316, CG2950, CG32549, CG42258, CG42389, CG43066, CG4729, CG5059, CG6340, CG6439, CG8801, CG9281, CycG, Dcp2, Df31, Dp, Edc3, Fas3, His2Av, Hrb27C, Lk6, MED31, MSBP, Mapmodulin, Pabp2, Pc, Pdcd4, Prp3, Rab7, Rbp1-like, Rdl, RhoGAP68F, Rm62, S6k, SF2, Sh, Taf4, Tif-IA, Tsp42Ee, Unr, YT521-B, akirin, chrb, cora, crc, csw, dlg1, eIF-4B, ens, fd68A, foi, fru, futsch, galectin, hdc,

Type	Term	#	FDR	Genes
				hig, jigr1, jim, lark, larp, lea, lola, lost, mtt, nerfin-1, nudE, pUf68, pho, pk, pog, puc, qvr, rap, sbr, scrt, scyl, sec31, seq, spen, sqd, stau, stj, vfl, viaf, wech, yps
BP	multicellular organismal development	57	0.000158	AGO1, Aac11, CG11448, CG6767, Dp, Fas3, Hrb27C, Lin29, MED31, Pabp2, Pc, Rab7, RhoGAP68F, Rm62, S6k, SF2, Sh, Taf4, Thor, Xrp1, akirin, chrb, cora, crc, csw, dlg1, drpr, ens, fd68A, foi, fru, futsch, galectin, hdc, hig, jim, lark, larp, lea, lola, lost, nerfin-1, pUf68, pho, pk, pog, puc, rap, scrt, scyl, seq, spen, sqd, stan, stau, vfl, wech
BP	regulation of RNA metabolic process	28	0.000162	AGO1, CG13624, CG18316, CG18619, Hrb27C, MED31, Pc, Prp3, Rm62, Taf4, Tif-IA, Unr, akirin, crc, csw, fd68A, fru, jim, lola, nerfin-1, pUf68, pho, scrt, seq, spen, sqd, vfl, yps
BP	cellular process	94	0.000167	AGO1, Aac11, Aldh-III, Alg-2, Aps, CG11448, CG11486, CG11658, CG2950, CG32000, CG32549, CG6364, CG6439, CG6767, CG8801, CG9281, CG9836, CycG, Dcp2, Df31, Dp, Drat, FBpp0091066, FBpp0091081, Fas3, His2Av, Hrb27C, Lin29, Lk6, MED31, Mapmodulin, Msi, NaCP60E, Pabp2, Pc, Pdcd4, Prp3, Rab7, Rbp1-like, Rdl, RhoGAP68F, Rm62, S6k, SF2, Sh, Taf4, Thor, Unr, Xrp1, YT521-B, chrb, cora, crc, csw, dlg1, drpr, eIF-4B, ens, fd68A, foi, fru, futsch, galectin, hdc, hig, jim, lark, larp, lea, lola, lost, mtt, mus210, nerfin-1, nudE, pUf68, pho, pk, pog, puc, qtc, rap, sbr, scrt, scyl, seq, spen, sqd, stan, stau, stj, vfl, viaf, yps
BP	regulation of cellular metabolic process	38	0.000176	AGO1, Alg-2, CG13624, CG18316, CG18619, CG2950, CycG, Hrb27C, MED31, Paip2, Pc, Prp3, Rm62, S6k, Taf4, Thor, Tif-IA, Unr, akirin, crc, csw, fd68A, fru, jim, lola, nerfin-1, pUf68, pho, pog, puc, rap, scrt, seq, spen, sqd, stau, vfl, yps
BP	regulation of primary metabolic process	37	0.000229	AGO1, Alg-2, CG13624, CG18316, CG18619, CG2950, CycG, Hrb27C, MED31, Paip2, Pc, Prp3, Rm62, Taf4, Thor, Tif-IA, Unr, akirin, crc, csw, fd68A, fru, jim, lola, nerfin-1, pUf68, pho, puc, rap, scrt, seq, spen, sqd, stau, vfl, viaf, yps
BP	neuron development	23	0.000231	CG11448, Fas3, Hrb27C, Lin29, Pc, S6k, Sh, Taf4, drpr, fru, futsch, galectin, hdc, hig, jim, lea, lola, nerfin-1, pho, scrt, seq, spen, stan
BP	neurogenesis	36	0.000288	Aac11, CG11448, Fas3, Hrb27C, Lin29, MED31, Pabp2, Pc, Rm62, S6k, SF2, Sh, Taf4, cora, csw, dlg1, drpr, foi, fru, futsch, galectin, hdc, hig, jim, lea, lola, nerfin-1, pUf68, pho, pk, rap, scrt, seq, spen, stan, stau
BP	cellular component organization or biogenesis	50	0.00033	AGO1, CG11448, CG8801, CG9836, CycG, Df31, Dp, FBpp0091066, FBpp0091081, Fas3, His2Av, Hrb27C, Lin29, Rbp1-like, S6k, SF2, Taf4, Thor, Tif-IA, Unr, Xrp1, cora, csw, dlg1, drpr, ens, fru, futsch, hdc, jim, lark, larp, lea, lola, lost, mus210, nerfin-1, nudE, pUf68, pho, pk, puc, scrt, sec31, seq, spen, sqd, stan, stau, stj
BP	cellular component organization	49	0.000355	AGO1, CG11448, CG8801, CG9836, CycG, Df31, Dp, FBpp0091066, FBpp0091081, Fas3, His2Av, Hrb27C, Lin29, Rbp1-like, S6k, SF2, Taf4, Thor, Unr, Xrp1, cora, csw, dlg1, drpr, ens, fru, futsch, hdc, jim, lark, larp, lea, lola, lost, mus210, nerfin-1, nudE, pUf68, pho, pk, puc, scrt, sec31, seq, spen, sqd, stan, stau, stj
BP	nervous system development	38	0.000393	AGO1, Aac11, CG11448, Fas3, Hrb27C, Lin29, MED31, Pabp2, Pc, Rm62, S6k, SF2, Sh, Taf4, cora, csw, dlg1,

Type	Term	#	FDR	Genes
				drpr, foi, fru, futsch, galectin, hdc, hig, jim, lea, lola, nerfin-1, pUf68, pho, pk, puc, rap, scrt, seq, spen, stan, stau
BP	anatomical structure morphogenesis	39	0.000453	AGO1, CG11448, CG6767, Dp, Fas3, Hrb27C, Pdcd4, RhoGAP68F, S6k, Sh, Taf4, Thor, Xrp1, chrb, cora, crc, csw, dlg1, foi, fru, futsch, hdc, jim, lea, lola, nerfin-1, nudE, pho, pk, pog, puc, rap, scrt, scyl, seq, spen, sqd, stan, vfl
BP	mRNA processing	13	0.000514	CG11486, Hrb27C, Pabp2, Prp3, Rbp1-like, Rm62, SF2, lark, lost, pUf68, sbr, sqd, yps
BP	behavior	20	0.000558	AGO1, Bacc, Fas3, Lin29, NaCP60E, Rdl, S6k, Sh, Xrp1, dlg1, drpr, ens, fru, futsch, lark, lola, mtt, qtc, sbr, stau
MF	RNA binding	18	0.000559	AGO1, CG11486, CG2950, Dcp2, Hrb27C, Pabp2, Rm62, SF2, Unr, YT521-B, eIF-4B, lark, lost, pUf68, sbr, sqd, stau, yps
BP	system development	47	0.000602	AGO1, Aac11, CG11448, CG6767, Fas3, Hrb27C, Lin29, MED31, Pabp2, Pc, Rab7, RhoGAP68F, Rm62, S6k, SF2, Sh, Taf4, Xrp1, akirin, cora, csw, dlg1, drpr, ens, fd68A, foi, fru, futsch, galectin, hdc, hig, jim, lea, lola, nerfin-1, pUf68, pho, pk, puc, rap, scrt, seq, spen, stan, stau, vfl, wech
BP	nucleobase-containing compound metabolic process	30	0.000766	AGO1, Aps, CG11486, CG32549, CG6364, CG6767, CycG, Dcp2, Dp, Hrb27C, MED31, Msi, Pabp2, Prp3, Rbp1-like, Rm62, SF2, Taf4, YT521-B, crc, dlg1, lark, lost, mus210, pUf68, pho, sbr, sec31, sqd, yps
BP	regulation of growth	13	0.000766	Lk6, Paip2, Rab7, RhoGAP68F, S6k, Thor, chrb, dlg1, drpr, futsch, pUf68, scyl, stj
CC	spliceosomal complex	11	0.00102	Pabp2, Prp3, Rbp1-like, Rm62, SF2, lark, lost, pUf68, sec31, sqd, yps
CC	precatalytic spliceosome	10	0.00102	Pabp2, Prp3, Rbp1-like, Rm62, SF2, lark, lost, pUf68, sqd, yps
BP	cell morphogenesis involved in neuron differentiation	17	0.00103	Fas3, Hrb27C, S6k, Sh, Taf4, fru, futsch, hdc, jim, lea, lola, nerfin-1, pho, scrt, seq, spen, stan
BP	single-organism cellular process	80	0.00109	AGO1, Aac11, Aldh-III, Alg-2, Aps, CG11448, CG2950, CG32000, CG6364, CG6439, CG6767, CG8801, CG9281, CycG, Dcp2, Dp, Fas3, His2Av, Hrb27C, Lin29, Lk6, MED31, Mapmodulin, Msi, NaCP60E, Pabp2, Pc, Pdcd4, Rab7, Rdl, RhoGAP68F, Rm62, SF2, Sh, Taf4, Thor, Unr, chrb, cora, crc, csw, dlg1, drpr, ens, fd68A, foi, fru, futsch, galectin, hdc, hig, jim, lark, larp, lea, lola, lost, mtt, mus210, nerfin-1, nudE, pUf68, pho, pk, pog, puc, qtc, rap, scrt, scyl, sec31, seq, spen, sqd, stan, stau, stj, vfl, viaf, yps
BP	neuron projection development	19	0.00131	CG11448, Fas3, Hrb27C, Lin29, S6k, Sh, Taf4, fru, futsch, hdc, jim, lea, lola, nerfin-1, pho, scrt, seq, spen, stan
BP	RNA processing	15	0.00137	AGO1, CG11486, Hrb27C, Pabp2, Prp3, Rbp1-like, Rm62, SF2, lark, lost, pUf68, sbr, sec31, sqd, yps
MF	poly(A) RNA binding	12	0.00159	CG11486, Hrb27C, Pabp2, Rm62, SF2, Unr, eIF-4B, lark, pUf68, sqd, stau, yps
BP	embryo development	18	0.00162	AGO1, Hrb27C, MED31, Pc, RhoGAP68F, chrb, cora, csw, dlg1, larp, lea, lost, pog, puc, scyl, sqd, stan, stau
BP	cell projection organization	21	0.00162	CG11448, Fas3, Hrb27C, Lin29, S6k, Sh, Taf4, cora, fru, futsch, hdc, jim, lea, lola, nerfin-1, pho, pk, scrt, seq,

Type	Term	#	FDR	Genes
				spen, stan
BP	regulation of transcription, DNA-templated	24	0.00164	AGO1, CG13624, CG18316, CG18619, MED31, Pc, Prp3, Taf4, Tif-IA, Unr, akirin, crc, csw, fd68A, fru, jim, lola, nerfin-1, pho, scrt, seq, spen, vfl, yps
BP	dendrite morphogenesis	11	0.00167	S6k, Taf4, fru, futsch, jim, lola, nerfin-1, pho, scrt, seq, stan
BP	dendrite development	11	0.00191	S6k, Taf4, fru, futsch, jim, lola, nerfin-1, pho, scrt, seq, stan
BP	negative regulation of translation	6	0.00195	AGO1, Hrb27C, Paip2, Thor, Unr, sqd
BP	regulation of translation	8	0.00213	AGO1, CG2950, Hrb27C, Paip2, Thor, Unr, sqd, stau
BP	pattern specification process	18	0.00222	AGO1, Dp, Hrb27C, MED31, Pc, Rab7, cora, csw, drpr, fd68A, lea, lost, pk, puc, spen, sqd, stan, stau
BP	RNA splicing	11	0.00231	Pabp2, Prp3, Rbp1-like, Rm62, SF2, lark, lost, pUf68, sec31, sqd, yps
BP	axonogenesis	13	0.00234	Fas3, Hrb27C, S6k, Sh, fru, futsch, hdc, lea, lola, nerfin-1, seq, spen, stan
BP	neuron projection morphogenesis	18	0.00246	CG11448, Fas3, Hrb27C, S6k, Sh, Taf4, fru, futsch, hdc, jim, lea, lola, nerfin-1, pho, scrt, seq, spen, stan
BP	morphogenesis of an epithelium	20	0.00283	CG6767, Dp, Fas3, RhoGAP68F, Xrp1, cora, csw, dlg1, foi, fru, hdc, lola, pk, puc, rap, seq, spen, sqd, stan, vfl
BP	multi-organism process	31	0.00283	AGO1, Bacc, Dp, Fas3, Hrb27C, Lin29, Msi, Pdcd4, Rdl, Rm62, S6k, Sh, Thor, akirin, csw, dlg1, drpr, foi, fru, lark, lola, lost, nudE, pUf68, puc, qtc, sec31, spen, sqd, stau, yps
BP	axon development	13	0.00291	Fas3, Hrb27C, S6k, Sh, fru, futsch, hdc, lea, lola, nerfin-1, seq, spen, stan
BP	nucleic acid metabolic process	24	0.00291	AGO1, CG11486, CycG, Dcp2, Dp, Hrb27C, MED31, Pabp2, Prp3, Rbp1-like, Rm62, SF2, Taf4, YT521-B, crc, lark, lost, mus210, pUf68, pho, sbr, sec31, sqd, yps
BP	cellular component assembly	22	0.00304	AGO1, CG8801, CG9836, Df31, Dp, FBpp0091148, FBpp0091152, Hrb27C, Rbp1-like, S6k, SF2, Sh, Unr, cora, dlg1, ens, larp, lost, pUf68, puc, sqd, stau
CC	nuclear lumen	19	0.00325	Bacc, CG18316, CG6340, CG8801, Hrb27C, MED31, Mapmodulin, Pc, S6k, Taf4, Tif-IA, YT521-B, akirin, lola, pho, sbr, seq, sqd, vfl
CC	smooth septate junction	3	0.00345	Fas3, cora, dlg1
CC	intracellular organelle part	47	0.00345	Bacc, CG10077, CG18316, CG5059, CG6340, CG6439, CG8801, Df31, Dp, Edc3, FBpp0091066, FBpp0091081, FBpp0091148, FBpp0091152, Fas3, His2Av, Hrb27C, Lk6, MED31, Mapmodulin, Pabp2, Pc, Prp3, Rab7, Rbp1-like, Rm62, S6k, SF2, Taf4, Tif-IA, YT521-B, akirin, futsch, lark, lola, lost, nudE, pUf68, pho, rap, sbr, sec31, seq, sqd, stau, vfl, yps
CC	intracellular	79	0.00356	AGO1, Aac11, Aldh-III, Aps, Bacc, CG10077, CG11486, CG11658, CG18316, CG2950, CG32549, CG5059, CG6340, CG6439, CG8801, CycG, Dcp2, Df31, Dp, Edc3, Fas3, His2Av, Hrb27C, Lk6, MED31, Mapmodulin, Pabp2, Pc, Pdcd4, Prp3, Rab7, Rbp1-like, RhoGAP68F, Rm62, S6k, SF2, Taf4, Tif-IA, Tsp42Ee, Unr, YT521-B, akirin, chrb, cora, crc, csw, dlg1, eIF-4B, ens, fd68A, fru, futsch, galectin, hdc, jigr1, jim, lark, larp,

Type	Term	#	FDR	Genes
				lola, lost, nerfin-1, nudE, pUf68, pho, pk, puc, rap, sbr, scrt, scyl, sec31, seq, spen, sqd, stau, vfl, viaf, wech, yps
BP	tissue development	28	0.00364	CG6767, CycG, Dp, Fas3, Hrb27C, Rab7, RhoGAP68F, Xrp1, cora, csw, dlg1, drpr, ens, fd68A, foi, fru, hdc, lea, lola, nudE, pk, puc, rap, seq, spen, sqd, stan, vfl
BP	regulation of cellular amide metabolic process	9	0.00378	AGO1, CG2950, Hrb27C, Paip2, Thor, Unr, pog, sqd, stau
BP	tube morphogenesis	18	0.00383	CG6767, Fas3, RhoGAP68F, Xrp1, cora, csw, dlg1, foi, fru, hdc, lea, lola, pk, puc, rap, seq, spen, vfl
BP	epithelium development	26	0.00388	CG6767, CycG, Dp, Fas3, Hrb27C, Rab7, RhoGAP68F, Xrp1, cora, csw, dlg1, drpr, foi, fru, hdc, lea, lola, nudE, pk, puc, rap, seq, spen, sqd, stan, vfl
CC	intracellular part	78	0.00394	AGO1, Aac11, Aldh-III, Aps, Bacc, CG10077, CG11486, CG11658, CG18316, CG2950, CG32549, CG5059, CG6340, CG6439, CG8801, CycG, Dcp2, Df31, Dp, Edc3, Fas3, His2Av, Hrb27C, Lk6, MED31, Mapmodulin, Pabp2, Pc, Pdcd4, Prp3, Rab7, Rbp1-like, RhoGAP68F, Rm62, S6k, SF2, Taf4, Tif-IA, Tsp42Ee, Unr, YT521-B, akirin, chrb, cora, crc, csw, dlg1, eIF-4B, ens, fd68A, fru, futsch, galectin, hdc, jigr1, jim, lark, larp, lola, lost, nerfin-1, nudE, pUf68, pho, pk, puc, rap, sbr, scrt, scyl, sec31, seq, spen, sqd, stau, vfl, viaf, yps
BP	cellular component biogenesis	23	0.00398	AGO1, CG8801, CG9836, Df31, Dp, FBpp0091148, FBpp0091152, Hrb27C, Rbp1-like, S6k, SF2, Sh, Tif-IA, Unr, cora, dlg1, ens, larp, lost, pUf68, puc, sqd, stau
BP	RNA metabolic process	20	0.00402	AGO1, CG11486, Dcp2, Hrb27C, MED31, Pabp2, Prp3, Rbp1-like, Rm62, SF2, Taf4, YT521-B, crc, lark, lost, pUf68, sbr, sec31, sqd, yps
BP	single-organism behavior	15	0.00475	AGO1, Bacc, Fas3, Lin29, NaCP60E, S6k, Sh, Xrp1, dlg1, drpr, futsch, lark, mtt, sbr, stau
BP	locomotion	18	0.00487	Fas3, Hrb27C, S6k, csw, dlg1, ens, foi, fru, lea, lola, nerfin-1, nudE, puc, rap, seq, spen, sqd, stan
MF	mRNA binding	11	0.00495	Hrb27C, Pabp2, Rm62, SF2, Unr, eIF-4B, lark, pUf68, sqd, stau, yps
BP	mRNA splicing, via spliceosome	10	0.00497	Pabp2, Prp3, Rbp1-like, Rm62, SF2, lark, lost, pUf68, sqd, yps
BP	negative regulation of gene expression	15	0.00504	AGO1, Dcp2, Hrb27C, Paip2, Pc, Rm62, Thor, Unr, crc, fd68A, hdc, pho, scrt, seq, sqd
CC	ribonucleoprote in complex	16	0.00511	AGO1, Dcp2, Edc3, Hrb27C, Pabp2, Prp3, Rbp1-like, Rm62, SF2, lark, lost, pUf68, sec31, sqd, stau, yps
CC	catalytic step 2 spliceosome	8	0.00511	Pabp2, Rm62, SF2, lark, lost, pUf68, sqd, yps
BP	epithelial tube morphogenesis	17	0.00568	CG6767, Fas3, RhoGAP68F, Xrp1, cora, csw, dlg1, foi, fru, hdc, lola, pk, puc, rap, seq, spen, vfl
BP	segmentation	11	0.0057	AGO1, Hrb27C, MED31, Pc, csw, lost, pk, spen, sqd, stan, stau
BP	regionalization	16	0.00578	AGO1, Dp, Hrb27C, MED31, Pc, Rab7, cora, csw, drpr, lea, lost, pk, spen, sqd, stan, stau
BP	mRNA catabolic process	5	0.00578	AGO1, CG11486, Dcp2, Pabp2, sqd
BP	mating behavior, sex discrimination	3	0.0058	Sh, fru, qtc

Type	Term	#	FDR	Genes
BP	regulation of ion transport	6	0.00584	NKAIN, NaCP60E, Sh, Teh4, qvr, stj
BP	cell death	10	0.007	Alg-2, Dp, Rab7, chrb, drpr, hdc, larp, lola, scyl, viaf
MF	organic cyclic compound binding	47	0.00734	AGO1, CG10077, CG11486, CG12054, CG13624, CG18619, CG2950, CG32000, CG32767, CG43444, CG4404, CG6364, CG6439, CG8801, CG9281, Dcp2, Dp, FBpp0091066, FBpp0091081, FBpp0091148, FBpp0091152, Hrb27C, Lin29, Lk6, MSBP, Pc, Rab7, Rbp1-like, S6k, Taf4, Xrp1, YT521-B, crc, fru, jigr1, jim, lola, lost, mus210, nerfin-1, pho, sbr, scrt, seq, spen, stau, vfl
BP	tube development	21	0.00804	CG6767, Fas3, Rab7, RhoGAP68F, Xrp1, cora, csw, dlg1, drpr, fd68A, foi, fru, hdc, lea, lola, pk, puc, rap, seq, spen, vfl
BP	cellular nitrogen compound metabolic process	32	0.00834	AGO1, Aps, CG11486, CG2950, CG32549, CG6364, CG6767, CycG, Dcp2, Dp, Hrb27C, MED31, Msi, Pabp2, Prp3, Rbp1-like, Rm62, SF2, Taf4, YT521-B, crc, dlg1, eIF-4B, lark, lost, mus210, pUf68, pho, sbr, sec31, sqd, yps
CC	intracellular non-membrane-bounded organelle	32	0.00844	Aldh-III, CG10077, CG18316, CG6439, CG8801, CycG, Dcp2, Df31, Dp, Edc3, FBpp0091066, FBpp0091081, FBpp0091148, FBpp0091152, His2Av, Hrb27C, Lk6, Mapmodulin, Pc, Rab7, Rm62, Tif-IA, akirin, cora, dlg1, ens, futsch, nudE, pho, rap, sqd, stau
MF	heterocyclic compound binding	46	0.0114	AGO1, CG10077, CG11486, CG12054, CG13624, CG18619, CG2950, CG32000, CG32767, CG43444, CG4404, CG6364, CG6439, CG8801, CG9281, Dcp2, Dp, FBpp0091066, FBpp0091081, FBpp0091148, FBpp0091152, Hrb27C, Lin29, Lk6, Pc, Rab7, Rbp1-like, S6k, Taf4, Xrp1, YT521-B, crc, fru, jigr1, jim, lola, lost, mus210, nerfin-1, pho, sbr, scrt, seq, spen, stau, vfl
BP	regulation of multicellular organismal process	18	0.0122	AGO1, Dp, Hrb27C, MED31, Rdl, RhoGAP68F, S6k, Sh, csw, dlg1, futsch, hdc, lark, lea, qvr, stan, stau, stj
BP	regulation of developmental process	19	0.0136	AGO1, CG2950, Dp, His2Av, Hrb27C, MED31, Pdcd4, RhoGAP68F, S6k, csw, dlg1, futsch, hdc, lark, lea, puc, stan, stau, stj
BP	nucleobase-containing compound catabolic process	6	0.0137	AGO1, CG11486, Dcp2, Msi, Pabp2, sqd
BP	mRNA splice site selection	3	0.0145	Rbp1-like, SF2, pUf68
BP	neuron recognition	7	0.0149	Fas3, fru, galectin, hig, lea, lola, stan
BP	establishment or maintenance of polarity of follicular epithelium	4	0.0169	Dp, csw, dlg1, sqd
BP	regulation of cellular component organization	18	0.0172	CG2950, Dcp2, Hrb27C, Paip2, Prp3, RhoGAP68F, S6k, Thor, dlg1, drpr, futsch, jim, pUf68, puc, rap, stan, stau, stj
BP	movement of cell or	17	0.0173	Fas3, Hrb27C, S6k, csw, foi, fru, futsch, lea, lola, nerfin-1, nudE, puc, rap, seq, spen, sqd, stan

Type	Term	#	FDR	Genes
	subcellular component			
BP	single-organism process	85	0.0178	AGO1, Aac11, Alg-2, Aps, Bacc, CG11448, CG2950, CG32000, CG6364, CG6439, CG8801, CG9281, CycG, Dcp2, Dp, Drat, Fas3, His2Av, Hrb27C, Lin29, Lk6, MED31, Mapmodulin, Msi, NaCP60E, Pabp2, Pc, Pdcd4, Rab7, Rdl, RhoGAP68F, Rm62, SF2, Sh, Taf4, Thor, Unr, Xrp1, akirin, chrb, cora, crc, csw, dlg1, drpr, eIF-4B, ens, fd68A, foi, fru, futsch, galectin, hdc, hig, jim, lark, larp, lea, lola, lost, mtt, mus210, nerfin-1, nudE, pUf68, pho, pk, pog, puc, qvr, rap, sbr, scrt, scyl, sec31, seq, spen, sqd, stan, stau, stj, vfl, viaf, wech, yps
BP	nuclear-transcribed mRNA catabolic process, deadenylation-dependent decay	3	0.0179	CG11486, Dcp2, Pabp2
BP	cell fate commitment	15	0.0192	AGO1, CG2950, Hrb27C, Unr, csw, dlg1, lea, lola, nerfin-1, nudE, qtc, seq, spen, stan, stau
BP	establishment or maintenance of cell polarity	9	0.0195	Dp, cora, csw, dlg1, lola, pk, puc, sqd, stan
BP	regulation of cell differentiation	12	0.02	AGO1, CG2950, Dp, His2Av, Hrb27C, MED31, Pdcd4, csw, dlg1, hdc, stan, stau
BP	nuclear-transcribed mRNA catabolic process	4	0.0204	CG11486, Dcp2, Pabp2, sqd
BP	cellular localization	19	0.0204	His2Av, Hrb27C, Mapmodulin, Rab7, cora, dlg1, ens, futsch, lark, larp, lost, nudE, puc, qtc, sbr, sec31, sqd, stau, stj
BP	blastoderm segmentation	9	0.0211	AGO1, Hrb27C, MED31, Pc, csw, lost, sqd, stan, stau
BP	maintenance of imaginal disc-derived wing hair orientation	2	0.0213	cora, spen
BP	localization	34	0.0213	CG32000, CG6364, CG9281, His2Av, Hrb27C, Mapmodulin, NaCP60E, Rab7, Rdl, S6k, Sh, cora, csw, dlg1, drpr, ens, foi, futsch, galectin, lark, larp, lea, lost, nudE, pk, puc, qtc, rap, sbr, sec31, spen, sqd, stau, stj
BP	negative regulation of cellular macromolecule biosynthetic process	12	0.0213	AGO1, Hrb27C, Paip2, Pc, Thor, Unr, crc, fd68A, pho, scrt, seq, sqd
BP	axon guidance	10	0.0224	Fas3, Hrb27C, S6k, fru, lea, lola, nerfin-1, seq, spen, stan
BP	regulation of localization	12	0.0224	Hrb27C, NKAIN, NaCP60E, RhoGAP68F, Sh, Teh4, drpr, ens, lea, qvr, stau, stj
BP	regulation of synapse structure or	8	0.0232	RhoGAP68F, S6k, Sh, Thor, dlg1, futsch, stan, stj

Type	Term	#	FDR	Genes
	activity			
BP	regulation of synapse organization	7	0.0235	RhoGAP68F, S6k, Thor, dlg1, futsch, stan, stj
BP	negative regulation of metabolic process	18	0.0237	AGO1, Dcp2, Hrb27C, Mapmodulin, Paip2, Pc, Rm62, Thor, Unr, crc, fd68A, hdc, pho, puc, rap, scrt, seq, sqd
CC	intracellular membrane-bounded organelle	57	0.0242	AGO1, Aac11, Aps, Bacc, CG18316, CG5059, CG6340, CG6439, CG8801, Df31, Dp, FBpp0091066, FBpp0091081, FBpp0091148, FBpp0091152, Fas3, His2Av, Hrb27C, Lk6, MED31, Mapmodulin, Pabp2, Pc, Prp3, Rab7, Rbp1-like, RhoGAP68F, Rm62, S6k, SF2, Taf4, Tif-IA, YT521-B, akirin, crc, fd68A, fru, jigr1, jim, lark, larp, lola, lost, nerfin-1, nudE, pUf68, pho, puc, rap, sbr, scrt, sec31, seq, spen, sqd, vfl, yps
BP	organ development	27	0.0243	CG6767, Fas3, Lin29, Rab7, RhoGAP68F, Taf4, Xrp1, akirin, cora, csw, dlg1, drpr, ens, foi, fru, futsch, hdc, lea, lola, pk, puc, rap, seq, spen, stan, vfl, wech
CC	nucleoplasm	13	0.0243	Bacc, CG6340, Hrb27C, MED31, Mapmodulin, S6k, Taf4, YT521-B, lola, sbr, seq, sqd, vfl
BP	sexual reproduction	23	0.0247	AGO1, Dp, Fas3, Hrb27C, Lin29, Msi, Pdcd4, S6k, Sh, csw, dlg1, foi, fru, lark, lola, lost, nudE, pUf68, puc, qtc, sqd, stau, yps
BP	regulation of gene expression, epigenetic	7	0.0247	AGO1, Dcp2, Pc, Rm62, Unr, hdc, pho
BP	metamorphosis	15	0.0248	CG6767, Fas3, RhoGAP68F, Xrp1, cora, crc, dlg1, fru, hdc, lola, pk, puc, rap, spen, vfl
BP	pole plasm oskar mRNA localization	4	0.0255	Hrb27C, lost, sqd, stau
CC	cytoplasmic mRNA processing body	3	0.0255	Dcp2, Edc3, stau
BP	negative regulation of macromolecule metabolic process	17	0.0256	AGO1, Dcp2, Hrb27C, Paip2, Pc, Rm62, Thor, Unr, crc, fd68A, hdc, pho, puc, rap, scrt, seq, sqd
BP	reproductive process	24	0.0258	AGO1, Dp, Fas3, Hrb27C, Lin29, Msi, Pdcd4, S6k, Sh, csw, dlg1, foi, fru, lark, lea, lola, lost, nudE, pUf68, puc, qtc, sqd, stau, yps
BP	cell morphogenesis	18	0.0267	CG11448, Fas3, Hrb27C, S6k, Sh, Taf4, fru, futsch, hdc, jim, lea, lola, nerfin-1, pho, scrt, seq, spen, stan
CC	chromatin	10	0.0275	Df31, FBpp0091066, FBpp0091081, FBpp0091148, FBpp0091152, His2Av, Pc, akirin, pho, sqd
CC	neuron part	11	0.0275	Rab7, Rdl, S6k, dlg1, futsch, hig, lea, mtt, rap, sec31, stj
BP	dorsal/ventral axis specification, ovarian follicular epithelium	3	0.0277	Dp, csw, sqd
BP	cellular component morphogenesis	20	0.0277	CG11448, Dp, Fas3, Hrb27C, S6k, Sh, Taf4, fru, futsch, hdc, jim, lea, lola, nerfin-1, pho, puc, scrt, seq, spen, stan

Type	Term	#	FDR	Genes
BP	imaginal disc morphogenesis	14	0.0297	CG6767, Fas3, RhoGAP68F, Xrp1, cora, dlg1, fru, hdc, lola, pk, puc, rap, spen, vfl
CC	chromosomal part	13	0.0299	Df31, Dp, FBpp0091066, FBpp0091081, FBpp0091148, FBpp0091152, His2Av, Pc, Rm62, akirin, nudE, pho, sqd
BP	post-embryonic organ development	15	0.0309	CG6767, Fas3, RhoGAP68F, Xrp1, akirin, cora, dlg1, fru, hdc, lola, pk, puc, rap, spen, vfl
BP	macromolecular complex assembly	12	0.0309	AGO1, CG8801, Df31, FBpp0091148, FBpp0091152, Rbp1-like, SF2, Sh, Unr, ens, larp, pUf68
CC	basolateral plasma membrane	4	0.0312	Fas3, dlg1, foi, stau
CC	macromolecular complex	44	0.0312	AGO1, CG10077, CG11486, CG11658, CG18316, CG2950, CG6439, CG9281, Dcp2, Df31, Dp, Edc3, FBpp0091066, FBpp0091081, FBpp0091148, FBpp0091152, His2Av, Hrb27C, Lk6, MED31, Mapmodulin, NaCP60E, Pabp2, Pc, Prp3, Rbp1-like, Rm62, SF2, Sh, Taf4, Tif-IA, akirin, fd68A, futsch, lark, lost, nudE, pUf68, pho, rap, sqd, stau, stj, yps
BP	spliceosomal complex assembly	3	0.0321	Rbp1-like, SF2, pUf68
BP	organ morphogenesis	19	0.0331	CG6767, Fas3, RhoGAP68F, Xrp1, cora, csw, dlg1, foi, fru, hdc, lea, lola, pk, puc, rap, seq, spen, stan, vfl
BP	regulation of cytoplasmic mRNA processing body assembly	2	0.0331	Dcp2, stau
BP	chemotaxis	10	0.0336	Fas3, Hrb27C, S6k, fru, lea, lola, nerfin-1, seq, spen, stan
CC	intracellular organelle	63	0.0341	AGO1, Aac11, Aldh-III, Aps, Bacc, CG10077, CG18316, CG5059, CG6340, CG6439, CG8801, CycG, Dcp2, Df31, Dp, Edc3, Fas3, His2Av, Hrb27C, Lk6, MED31, Mapmodulin, Pabp2, Pc, Prp3, Rab7, Rbp1-like, RhoGAP68F, Rm62, S6k, SF2, Taf4, Tif-IA, YT521-B, akirin, cora, crc, dlg1, ens, fd68A, fru, futsch, jigr1, jim, lark, larp, lola, lost, nerfin-1, nudE, pUf68, pho, puc, rap, sbr, scrt, sec31, seq, spen, sqd, stau, vfl, yps
BP	developmental process involved in reproduction	20	0.0342	AGO1, Dp, Fas3, Hrb27C, Msi, Pdcd4, S6k, csw, foi, fru, lark, lea, lola, lost, nudE, pUf68, puc, sqd, stau, yps
BP	imaginal disc development	17	0.0342	CG6767, Fas3, Rab7, RhoGAP68F, Xrp1, cora, csw, dlg1, drpr, fru, hdc, lola, pk, puc, rap, spen, vfl
BP	regulation of cellular component biogenesis	9	0.0364	CG2950, Dcp2, Hrb27C, RhoGAP68F, dlg1, futsch, stan, stau, stj
BP	posttranscriptional gene silencing by RNA	4	0.0366	AGO1, Dcp2, Rm62, hdc
BP	multicellular organismal reproductive process	22	0.0366	AGO1, Dp, Fas3, Hrb27C, Lin29, Msi, Pdcd4, S6k, csw, dlg1, foi, fru, lark, lola, lost, nudE, pUf68, puc, qtc, sqd, stau, yps
BP	instar larval or	14	0.0366	CG6767, Fas3, RhoGAP68F, Xrp1, cora, dlg1, fru, hdc,

Type	Term	#	FDR	Genes
	pupal morphogenesis			lola, pk, puc, rap, spen, vfl
BP	taxis	11	0.038	Fas3, Hrb27C, S6k, dlg1, fru, lea, lola, nerfin-1, seq, spen, stan
CC	cytoplasmic ribonucleoprote in granule	4	0.0381	Dcp2, Edc3, Hrb27C, stau
BP	reproduction	27	0.0398	AGO1, CycG, Dp, Fas3, Hrb27C, Lin29, Msi, Pdcd4, S6k, Sh, csw, dlg1, foi, fru, lark, larp, lola, lost, mus210, nudE, pUf68, puc, qtc, scyl, sqd, stau, yps
BP	gene silencing	6	0.0399	AGO1, Dcp2, Pc, Rm62, hdc, pho
BP	negative regulation of nitrogen compound metabolic process	12	0.0412	AGO1, Hrb27C, Paip2, Pc, Thor, Unr, crc, fd68A, pho, scrt, seq, sqd
BP	positive regulation of translation	3	0.0417	CG2950, Hrb27C, stau
BP	regulation of multi-organism process	7	0.0433	Dp, Hrb27C, Rab7, Rm62, dlg1, pog, stau
BP	morphogenesis of a polarized epithelium	6	0.0446	dlg1, lola, pk, puc, spen, stan
MF	mRNA 3 -UTR binding	4	0.046	Hrb27C, Unr, sqd, stau
BP	multi-organism behavior	8	0.0471	Bacc, Lin29, Rdl, Sh, dlg1, fru, lola, qtc
BP	single-organism cellular localization	11	0.0479	Hrb27C, cora, dlg1, larp, lost, nudE, qtc, sec31, sqd, stau, stj

Table 4.S17 | GSEA term enrichments for hierarchical clustering of differentially expressed genes - cluster 10, genes with expression that increase over the course of the time series. Terms sorted by FDR. Terms for biological process (BP), Molecular function (MF), and cellular component (CC) terms were included and described in the Type column. The number of genes associated with each term is indicated in the # column.

gene	12A	120hr ETI	12A/120hr ETI
CG9973	22	163	0.1
noe	3578	16517	0.2
Edc3	30	129	0.2
CG1600	61	252	0.2
CG11267	139	569	0.2
His2A:CG33820	226	897	0.3
CG15098	27	103	0.3
Ef1alpha48D	672	2546	0.3
TfIIA-S	211	741	0.3
CG42510	81	283	0.3
Lac	78	266	0.3
CG8801	62	208	0.3
scyl	193	624	0.3
YT521-B	89	288	0.3
CG18619	64	204	0.3
His2A:CG33835	762	2415	0.3
CG5059	51	160	0.3
CG4068	156	488	0.3
rn	65	203	0.3
CG10990	169	524	0.3
CG42240	78	226	0.3
CG32486	68	193	0.4
CG9413	43	119	0.4
lola	758	2114	0.4
Teh4	43	117	0.4
CG9894	1248	3391	0.4
Rm62	615	1669	0.4
CG31530	59	155	0.4
Xrp1	74	195	0.4
CG18316	46	119	0.4
His2Av	347	888	0.4
CG6041	39	101	0.4
pUf68	82	209	0.4
vfl	64	164	0.4
MED31	81	203	0.4
CG17765	53	132	0.4
kn	48	119	0.4
yps	306	755	0.4
Lk6	285	700	0.4
hdc	1054	2582	0.4
roX2	368	872	0.4
CG2950	47	110	0.4
CG17233	58	135	0.4
pAbp	814	1896	0.4
Hsromega	658	1526	0.4
unk	61	141	0.4
Wnt4	64	148	0.4
CG9821	720	1655	0.4
rap	78	175	0.4
Aats-thr	58	125	0.5
fd68A	110	234	0.5
HmgD	746	1581	0.5

gene	12A	120hr ETI	12A/120hr ETI
Paip2	114	241	0.5
phyl	83	174	0.5
CG15628	154	316	0.5
TfAP-2	163	333	0.5
smt3	1200	2440	0.5
CG6765	55	110	0.5
Fer2LCH	311	627	0.5
Jupiter	391	786	0.5
sbr	54	108	0.5
Mapmodulin	551	1105	0.5
shep	775	384	2.0
RpL18	448	222	2.0
CG2993	209	103	2.0
chn	223	110	2.0
alphagamma-element:CR32865	193	95	2.0
CG5830	218	107	2.0
fne	786	383	2.1
Eaat2	138	66	2.1
2mit	130	62	2.1
tinc	174	79	2.2
mbf1	161	73	2.2
CG8223	133	59	2.3
RpL23	883	371	2.4
Hsp67Ba	517	204	2.5
CG9603	217	85	2.6
CG1240	348	135	2.6
Hsp23	4188	1564	2.7
nAcRalpha-34E	152	55	2.8
Act42A	704	248	2.8
CG5151	174	60	2.9
Fas2	196	68	2.9
mmd	151	50	3.0
Hsp68	457	140	3.3
Hsp70Ab	222	68	3.3
Hsp27	2752	832	3.3
Pvf3	112	33	3.4
Hsp70Aa, Hsp70Ab	238	63	3.8
CG32230	278	68	4.1
CG14989	137	30	4.5
CG1943	306	64	4.7
CG2269	154	29	5.4
ia2	141	25	5.6
CG32521	167	27	6.1
Hsp22	279	43	6.6
Hsp70Ba	244	29	8.3
Frq1	233	27	8.5
Hsp67Bc	199	19	10.7
CG14459	152	11	13.8
CG32458	109	3	32.7

Table 4.S18 | WT 120hr 12A vs 120hr ETI, >100 FPKM, 2-fold change, q<0.1. Genes with greater expression in 120hr ETI neurons are shown in green, while genes with greater expression in WT 120hr 12A neurons are shown in blue. Numbers are expression values in FPKM.

Top 20 genes - positive PC1	Correlation coefficient
hdc	0.352127455
jim	0.350008335
CR42862	0.264871393
Df31	0.234705117
CG9894	0.226317744
lola	0.212213412
His2A:CG33835	0.208091687
CG9821	0.190954357
Hsromega	0.187308664
pAbp	0.131489153
CG42622	0.124865344
Lk6	0.098416974
scyl	0.075936801
l(3)neo38	0.074477013
Rm62	0.073594059
His2A:CG33820	0.069714818
CG33229	0.062637842
roX1	0.062127938
snoRNA:Me28S-A2589a	0.061656863
CG2052	0.058451661
Top 20 genes - negative PC1	**Correlation coefficient**
Hsp23	-0.189605366
RpL41	-0.15450222
Act5C	-0.13838154
Hsp27	-0.133585298
14-3-3epsilon	-0.10901842
miple	-0.088615758
Ef1alpha100E	-0.088303897
snmRNA:331	-0.084986658
Qm	-0.08031502
CG13928	-0.0771229
fax	-0.074586433
Cam	-0.072664874
tsr	-0.066249799
RpS27A	-0.061351796
RpS15	-0.058373619
RpS7	-0.057931599
cib	-0.054467786
alphaTub84B	-0.053123545
pros	-0.050819368
RpS11	-0.048993339
Top 20 genes - positive PC2	**Correlation coefficient**
Hsp23	0.165819849
Hsp27	0.122935141
l(3)neo38	0.091667777
jim	0.071077085
snoRNA:Me28S-A2589c	0.063489818
snoRNA:Or-aca4	0.04566598
tsr	0.042122193
Qm	0.04210967
kis	0.039772896
14-3-3zeta	0.037749736
Obp44a	0.0371018
CG42644	0.03677846
sm	0.035526187
Hsp68	0.032958386

shep	0.031611633
Jupiter	0.030979413
roX1	0.028567365
CG34360	0.02804981
pUf68	0.027941521
betaTub56D	0.027449049
Top 20 genes - negative PC2	**Correlation coefficient**
snmRNA:331	-0.437956909
His4r	-0.355308096
RpL41	-0.297745862
CG42622	-0.21465545
Ef1alpha48D	-0.201594547
pros	-0.195311578
snRNA:U6:96Aa	-0.17564838
snoRNA:Me28S-A2589a	-0.172924419
His3.3B	-0.16627797
CG13928	-0.149381091
smt3	-0.144290979
Df31	-0.134372106
RpS3	-0.12641891
14-3-3epsilon	-0.123733868
CG9894	-0.113533351
RpS7	-0.110479481
Rm62	-0.109222558
RpL40	-0.089814269
cib	-0.087082908
chic	-0.086236481
Top 20 genes - positive PC3	**Correlation coefficient**
roX1	0.268955769
l(3)neo38	0.26075789
RpS3	0.183424649
Ef1alpha48D	0.182912465
snoRNA:Me28S-A2589a	0.16790409
Jupiter	0.140893754
His2A:CG33835	0.132704254
CR42862	0.099720489
snoRNA:Or-aca4	0.097196143
Obp44a	0.092298154
roX2	0.087713729
HmgD	0.086426148
RpL31	0.067717395
RpS7	0.06601724
snmRNA:331	0.057821809
kis	0.055691134
CG14654	0.05387731
smt3	0.053372494
vsg	0.053205148
His2Av	0.048309633
Top 20 genes - negative PC3	**Correlation coefficient**
pros	-0.365086621
Df31	-0.309833176
jim	-0.21352876
snRNA:U6:96Aa	-0.186607929
hth	-0.155706384
Hsp23	-0.151762796
hdc	-0.138028015
Hsp27	-0.11645462

Act5C	-0.10976541
pAbp	-0.080700895
cib	-0.068445394
RpL39	-0.067932015
Tctp	-0.067313613
snoRNA:Psi18S-1377d	-0.066081344
CG3800	-0.063946683
ctp	-0.055091434
snoRNA:Me28S-A2589c	-0.053648981
Rm62	-0.053571083
Hsromega	-0.049581219
CG1746	-0.048843831

Table 4.S19 | Summary of largest contributions to PCA of ETI and WT 120hr 12A neurons. Top 20 positive and negative gene contributions to each of the first 3 principal components from PCA of ETI 12A and WT 120hr 12A neurons excluding *noe* expression.

Chapter 5

Discussion

RNA-Seq of larval postembryonic hemilineage neurons purified with FACS using double fluorescent protein reporter expression

I showed in this thesis that a sufficiently pure sample of postembryonic hemilineage neurons can be isolated from *Drosophila* ventral nervous systems (VNSs) for RNA-seq. I achieved this through flow cytometry of neurons using GAL4 lines with nSyb-GAL80 to remove mature neuron expression and labeling the neurons with two reporters with translational enhancers: tdTomato with a nuclear localization signal to label nuclei in the red excitation channel and myristoylated green fluorescent protein to label membranes in the green excitation channel. This has distinct advantages over manual sorting of neurons, including the amount of time and resources required to perform the experiment. The cells are not only subjected to being isolated from the surrounding tissue for a shorter period of time, but the cells are also kept cold during most of the process, which should minimize the expression changes over the course of cell isolation.

Hemilineages

Hemilineages are a developmental and structural unit of the *Drosophila* nervous system. The neurons in each hemilineage express patterns of genes that distinguish them from neurons of other hemilineages as a downstream consequence of neuroblast identity and Notch activity at the time of their birth. In order to better understand how similar gene expression is between hemilineages and the relative contribution of neuroblast identity and Notch activity, I performed RNA-seq on neurons from 11 of the 33 hemilineages. Treating the hemilineage neurons from all thoracic segments collectively as a single class of neurons proved to be a valid approach. Despite some segmental and temporal differences between the neurons in the samples, each hemilineage sample showed a unique combination of gene expression relative to other hemilineages. Despite some known heterogeneity, based at least partially on birth order, the neurons within a hemilineage form discrete anatomical and computational

units that perform distinct behaviors upon activation. This is reflected by a degree of transcriptional homogeneity: gene expression is similar enough between the neurons within the hemilineage to distinguish hemilineages from one another.

Comparing highly expressed genes in two pairs of sibling hemilineages strongly suggested that hemilineages have been free to evolve independently. Neither shared neuroblast identity nor shared Notch activity increased the percentage of shared highly expressed genes. While there are certainly genes with low or moderate expression that are known to be important for these neurons, I restricted this analysis to highly expressed genes in order to exclude genes that were not unambiguously expressed and expressed at a high enough level that expression differences should be meaningful. The idea that Notch does not cause expression of the same genes in each "A" ("Notch-on") hemilineage is supported by finding exceptionally few differences in a comparison of all postembryonic neurons to only A hemilineage postembryonic neurons.

I showed that immature postembryonic neurons do not express many of the genes associated with mature neurons including neuropeptides, genes required for synapse formation, and genes required for loading of synaptic vesicles. Intriguingly, neurotransmitter type is predicted in these developmentally arrested neurons. Most of the individual hemilineages that were assayed expressed genes for neurotransmitter biosynthesis enzymes and/or transporters for an individual neurotransmitter. For those arrested hemilineage neurons that express genes for either neurotransmitter biosynthetic enzymes or transporters, neurotransmitter type predicted by the expression of these genes correlated to the neurotransmitter type of these neurons in the adult after maturation in all cases. Neurotransmitter type must therefore be fated and committed in these neurons long before they form synapses.

Despite being able to successfully treat an entire hemilineage as being composed of identical neurons, there were differentially expressed genes between younger and older immature neurons that suggested that older immature neurons were more mature than younger neurons. Older neurons expressed fewer transcription factors and a greater number of genes associated with synapse formation. Presumably, most of these differences are not due to a temporal switch associated with birth order and are

instead due to a transition from newly-born neurons to ones that have already undergone pathfinding and interactions with their immature axon targets.

Most of the gene expression that distinguishes hemilineages from each other is combinatorial, but there are examples of genes that do not appear to be expressed by other hemilineages in the VNS based on expression level relative to other hemilineage samples and relative to the sum of immature postembryonic neurons. *TfAP-2* expressed in hemilineage 12A neurons is one such example. I showed both that *TfAP-2* expression is unique to hemilineage 12A neurons in the larval VNS and that it is required for wildtype axon projection. I confirmed the expression pattern with antibody staining and performed experiments using two null mutants. Trans-heterozygote animals and mutant clones both showed an in inability to generate distal arbors. Dorsal arbors were severely reduced or missing in trans-heterozygote animals while both dorsal and medial arbors were missing in mutant clones using both alleles.

I expect that many of the other genes that I showed to be highly enriched in a single hemilineage are also important to their wildtype morphology and function. Some examples are *Ptx1* and *Ets21C* in hemilineage 21A and *exex* in hemilineage 4B. A disproportionate percentage of these genes are transcription factors. These genes are likely important for establishing many downstream expression differences as the cells mature. Finding these early differences in gene expression that are important during the identity specification and fate commitment of the neurons was precisely the intended aim of this thesis. I showed that there are many transcription factors with similar expression levels in all hemilineages that are likely important for postembryonic neurons generally. By determining which highly expressed transcription factors are the most variable between hemilineages, I also describe a number of genes with combinatorial expression that provide a transcription factor "code" for each hemilineage.

Extended Third Instar

Hemilineage 12A neuron morphology changes over the course of the extended third instar. A number of different hypotheses about why this may occur can be considered. The neurons could be losing their identity. Alternatively, the neurons could be

undergoing some of the processes of maturation proper ecdysone signaling due to an inability to maintain the arrested neuronal state. Important transcription factor, neurotransmitter synthesis, and neurotransmitter transport gene expression related to the identity of the hemilineage 12A neurons is not lost, which suggests that the neurons have not lost their identity. There are many differentially expressed genes between the wildtype 12A neurons and the extended third instar neurons. Some known ecdysone response genes are differentially expressed as expected. Many genes are differentially expressed over the course of the time series as well, including some genes associated with neuronal maturation, but no obvious pattern emerges from these genes. They are involved in many disparate processes. The neurons do not appear to have lost their neuronal identity nor do they appear to be undergoing general maturation processes. I propose, instead, that the primary cause of this phenotype is due to loss of TfAP-2 function.

The expression of two genes for proteins that have been previously shown to be required for TfAP-2 function are decreased in ETI neurons compared to WT neurons and decreases over the course of the ETI time series: *lwr* and *twz*. The pruning of hemilineage 12A neuron axons observed at 360hrs into the ETI time series is similar to the TfAP-2 mutant clone phenotype. In both cases, the neurons are missing their wildtype dorsal and medial branch and instead are arrested at or pruned to the choice point between the two paths. Ectopic branching is observed after pruning in the ETI neurons and was also observed on one occasion in the TfAP-2 mutant clones.

Chapter 6

References

Allen Institute for Brain Science. 2008. "Allen Spinal Cord Atlas." Allen Institute for Brain Science. Accessed November 6, 2017. http://mousespinal.brain-map.org.

Amcheslavsky A, Nie Y, Li Q. Gene expression profiling identifies the zinc-finger protein Charlatan as a regulator of intestinal stem cells in Drosophila. Development (Cambridge, England). 141(13):2621-32. 2014.

Amin J, Mestril R, Voellmy R. Genes for Drosophila small heat shock proteins are regulated differently by ecdysterone. Molecular and cellular biology. 11(12):5937-44. 1991.

Ashraf SI, Hu X, Roote J, Ip YT. The mesoderm determinant snail collaborates with related zinc-finger proteins to control Drosophila neurogenesis. The EMBO journal. 18(22):6426-38. 1999.

Ashraf SI, Ip YT. The Snail protein family regulates neuroblast expression of inscuteable and string, genes involved in asymmetry and cell division in Drosophila. Development (Cambridge, England). 128(23):4757-67. 2001.

Attrill H, Falls K, Goodman JL. FlyBase: establishing a Gene Group resource for Drosophila melanogaster. Nucleic acids research. 44(D1):D786-92. 2016.

Bailey AM, Posakony JW. Suppressor of hairless directly activates transcription of enhancer of split complex genes in response to Notch receptor activity. Genes & development. 9(21):2609-22. 1995.

Baines RA, Bate M. Electrophysiological development of central neurons in the Drosophila embryo. The Journal of neuroscience : the official journal of the Society for Neuroscience. 18(12):4673-83. 1998.

Bakken TE, Miller JA, Ding SL, et al. A comprehensive transcriptional map of primate brain development. Nature. 2016;535(7612):367-75.

Bauer R, McGuffin ME, Mattox W, Tainsky MA. Cloning and characterization of the Drosophila homologue of the AP-2 transcription factor. Oncogene. 17(15):1911-22. 1998.

Bayer, S.A., and Altman, J. Neocortical Development. Raven Press, New York, 1991.

Beck ES, Gasque G, Imlach WL. Regulation of Fasciclin II and synaptic terminal development by the splicing factor beag. The Journal of neuroscience : the official journal of the Society for Neuroscience. 32(20):7058-73. 2012.

Bello BC, Hirth F, Gould AP. A pulse of the Drosophila Hox protein Abdominal-A schedules the end of neural proliferation via neuroblast apoptosis. Neuron. 37(2):209-19. 2003.

Berdnik D, Favaloro V, Luo L. The SUMO protease Verloren regulates dendrite and axon targeting in olfactory projection neurons. The Journal of neuroscience : the official journal of the Society for Neuroscience. 32(24):8331-40. 2012.

Berdnik D, Török T, González-gaitán M, Knoblich JA. The endocytic protein alpha-Adaptin is required for numb-mediated asymmetric cell division in Drosophila. Dev Cell. 2002;3(2):221-31.

Bhaskar V, Valentine SA, Courey AJ. A functional interaction between dorsal and components of the Smt3 conjugation machinery. The Journal of biological chemistry. 275(6):4033-40. 2000.

Bhat KM. The patched signaling pathway mediates repression of gooseberry allowing neuroblast specification by wingless during Drosophila neurogenesis. Development (Cambridge, England). 122(9):2921-32. 1996.

Bivik C, Bahrampour S, Ulvklo C. Novel Genes Involved in Controlling Specification of Drosophila FMRFamide Neuropeptide Cells. Genetics. 200(4):1229-44. 2015.

Booker R, Truman JW. Postembryonic neurogenesis in the CNS of the tobacco hornworm, Manduca sexta. II. Hormonal control of imaginal nest cell degeneration

and differentiation during metamorphosis. The Journal of neuroscience : the official journal of the Society for Neuroscience. 7(12):4107-14. 1987.

Boquet I, Boujemaa R, Carlier MF, Préat T. Ciboulot regulates actin assembly during Drosophila brain metamorphosis. Cell. 102(6):797-808. 2000.

Borgmann-winter KE, Rawson NE, Wang HY, et al. Human olfactory epithelial cells generated in vitro express diverse neuronal characteristics. Neuroscience. 2009;158(2):642-53.

Brand AH, Perrimon N. Targeted gene expression as a means of altering cell fates and generating dominant phenotypes. Development (Cambridge, England). 118(2):401-15. 1993.

Buescher M, Yeo SL, Udolph G, et al. Binary sibling neuronal cell fate decisions in the Drosophila embryonic central nervous system are nonstochastic and require inscuteable-mediated asymmetry of ganglion mother cells. Genes Dev. 1998;12(12):1858-70.

Buescher M, Yeo SL, Udolph G. Binary sibling neuronal cell fate decisions in the Drosophila embryonic central nervous system are nonstochastic and require inscuteable-mediated asymmetry of ganglion mother cells. Genes & development. 12(12):1858-70. 1998.

Burtis KC, Thummel CS, Jones CW, Karim FD, Hogness DS. The Drosophila 74EF early puff contains E74, a complex ecdysone-inducible gene that encodes two ets-related proteins. Cell. 61(1):85-99. 1990.

Cai T, Krause MW, Odenwald WF, Toyama R, Notkins AL. The IA-2 gene family: homologs in Caenorhabditis elegans, Drosophila and zebrafish. Diabetologia. 44(1):81-8. 2001.

Cai Y, Chia W, Yang X. A family of snail-related zinc finger proteins regulates two distinct and parallel mechanisms that mediate Drosophila neuroblast asymmetric divisions. The EMBO journal. 20(7):1704-14. 2001.

Cardona A, Saalfeld S, Arganda I, Pereanu W, Schindelin J, Hartenstein V. Identifying neuronal lineages of Drosophila by sequence analysis of axon tracts. The Journal of neuroscience : the official journal of the Society for Neuroscience. 30(22):7538-53. 2010.

Caviness VS, Takahashi T, Nowakowski RS. Numbers, time and neocortical neuronogenesis: a general developmental and evolutionary model. Trends Neurosci. 1995;18(9):379-83.

Cenci C, Gould AP. Drosophila Grainyhead specifies late programmes of neural proliferation by regulating the mitotic activity and Hox-dependent apoptosis of neuroblasts. Development (Cambridge, England). 132(17):3835-45. 2005.

Centanin L, Wittbrodt J. Retinal neurogenesis. Development. 2014;141(2):241-4.

Cepko CL, Austin CP, Yang X, Alexiades M, Ezzeddine D. Cell fate determination in the vertebrate retina. Proc Natl Acad Sci USA. 1996;93(2):589-95.

Chang HC, Solomon NM, Wassarman DA. phyllopod functions in the fate determination of a subset of photoreceptors in Drosophila. Cell. 80(3):463-72. 1995.

Chell JM, Brand AH. Nutrition-responsive glia control exit of neural stem cells from quiescence. Cell. 143(7):1161-73. 2010.

Chen P, Nordstrom W, Gish B, Abrams JM. grim, a novel cell death gene in Drosophila. Genes & development. 10(14):1773-82. 1996.

Chu-LaGraff Q, Doe CQ. Neuroblast specification and formation regulated by wingless in the Drosophila CNS. Science (New York, N.Y.). 261(5128):1594-7. 1993.

Clendening B, Hume RI. Expression of multiple neurotransmitter receptors by sympathetic preganglionic neurons in vitro. J Neurosci. 1990;10(12):3977-91.

Colinet H, Lee SF, Hoffmann A. Temporal expression of heat shock genes during cold stress and recovery from chill coma in adult Drosophila melanogaster. The FEBS journal. 277(1):174-85. 2010.

Del barrio MG, Bourane S, Grossmann K, et al. A transcription factor code defines nine sensory interneuron subtypes in the mechanosensory area of the spinal cord. PLoS ONE. 2013;8(11):e77928.

Del Fabbro C, Scalabrin S, Morgante M, Giorgi FM. An extensive evaluation of read trimming effects on Illumina NGS data analysis. PloS one. 8(12):e85024. 2013.

Demarque M, Represa A, Becq H, Khalilov I, Ben-ari Y, Aniksztejn L. Paracrine intercellular communication by a Ca2+- and SNARE-independent release of GABA and glutamate prior to synapse formation. Neuron. 2002;36(6):1051-61.

Doe CQ. Molecular markers for identified neuroblasts and ganglion mother cells in the Drosophila central nervous system. Development. 1992;116(4):855-63.

Dominick OS, Truman JW. The physiology of wandering behaviour in Manduca sexta. III. Organization of wandering behaviour in the larval nervous system. The Journal of experimental biology. 121:115-32. 1986.

Eloranta JJ, Hurst HC. Transcription factor AP-2 interacts with the SUMO-conjugating enzyme UBC9 and is sumolated in vivo. The Journal of biological chemistry. 277(34):30798-804. 2002.

Emery IF, Bedian V, Guild GM. Differential expression of Broad-Complex transcription factors may forecast tissue-specific developmental fates during Drosophila metamorphosis. Development. 1994;120(11):3275-87.

Fernlund P, Josefsson L. Crustacean color-change hormone: amino acid sequence and chemical synthesis. Science (New York, N.Y.). 177(4044):173-5. 1972.

Gabilondo H, Losada-Pérez M, del Saz D. A targeted genetic screen identifies crucial players in the specification of the Drosophila abdominal Capaergic neurons. Mechanisms of development. 128(3-4):208-21. 2011.

Gage FH, Temple S. Neural stem cells: generating and regenerating the brain. Neuron. 2013;80(3):588-601.

Gellon G, Harding KW, McGinnis N, Martin MM, McGinnis W. A genetic screen for modifiers of Deformed homeotic function identifies novel genes required for head development. Development (Cambridge, England). 124(17):3321-31. 1997.

Genzen JR, Van cleve W, Mcgehee DS. Dorsal root ganglion neurons express multiple nicotinic acetylcholine receptor subtypes. J Neurophysiol. 2001;86(4):1773-82.

Georgiou M, Tear G. Commissureless is required both in commissural neurones and midline cells for axon guidance across the midline. Development (Cambridge, England). 129(12):2947-56. 2002.

Gibbens YY, Warren JT, Gilbert LI, O'Connor MB. Neuroendocrine regulation of Drosophila metamorphosis requires TGFbeta/Activin signaling. Development (Cambridge, England). 138(13):2693-703. 2011.

Gilbert LI, Rybczynski R, Warren JT. Control and biochemical nature of the ecdysteroidogenic pathway. Annual review of entomology. 47:883-916. 2002.

Giot L, Bader JS, Brouwer C. A protein interaction map of Drosophila melanogaster. Science (New York, N.Y.). 302(5651):1727-36. 2003.

Gomes FL, Zhang G, Carbonell F, et al. Reconstruction of rat retinal progenitor cell lineages in vitro reveals a surprising degree of stochasticity in cell fate decisions. Development. 2011;138(2):227-35.

Graveley BR, Kaur A, Gunning D, Zipursky SL, Rowen L, Clemens JC. The organization and evolution of the dipteran and hymenopteran Down syndrome cell adhesion molecule (Dscam) genes. RNA (New York, N.Y.). 10(10):1499-506. 2004.

Grosskortenhaus R, Robinson KJ, Doe CQ. Pdm and Castor specify younger motor neuron identity in the NB7-1 lineage. Genes & development. 20(18):2618-27. 2006.

Hafler BP, Surzenko N, Beier KT, et al. Transcription factor Olig2 defines subpopulations of retinal progenitor cells biased toward specific cell fates. Proc Natl Acad Sci USA. 2012;109(20):7882-7.

Hagel KR, Beriont J, Tessier CR. Drosophila Cbp53E Regulates Axon Growth at the Neuromuscular Junction. PloS one. 10(7):e0132636. 2015.

Harris RM, Pfeiffer BD, Rubin GM, Truman JW. Neuron hemilineages provide the functional ground plan for the Drosophila ventral nervous system. eLife. 4:. 2015.

Hasegawa E, Truman JW, Nose A. Identification of excitatory premotor interneurons which regulate local muscle contraction during Drosophila larval locomotion. Scientific reports. 6:30806. 2016.

Hatzihristidis T, Desai N, Hutchins AP, Meng TC, Tremblay ML, Miranda-Saavedra D. A Drosophila-centric view of protein tyrosine phosphatases. FEBS letters. 589(9):951-66. 2015.

Hawrylycz MJ, Lein ES, Guillozet-bongaarts AL, et al. An anatomically comprehensive atlas of the adult human brain transcriptome. Nature. 2012;489(7416):391-399.

He J, Zhang G, Almeida AD, Cayouette M, Simons BD, Harris WA. How variable clones build an invariant retina. Neuron. 2012;75(5):786-98.

Hekmat-Scafe DS, Mercado A, Fajilan AA. Seizure sensitivity is ameliorated by targeted expression of K+-Cl- cotransporter function in the mushroom body of the Drosophila brain. Genetics. 184(1):171-83. 2010.

Hemler ME. Tetraspanin functions and associated microdomains. Nature reviews. Molecular cell biology. 6(10):801-11. 2005.

Henry GL, Davis FP, Picard S, Eddy SR. Cell type-specific genomics of Drosophila neurons. Nucleic acids research. 40(19):9691-704. 2012.

Hiesinger PR, Fayyazuddin A, Mehta SQ. The v-ATPase V0 subunit a1 is required for a late step in synaptic vesicle exocytosis in Drosophila. Cell. 121(4):607-20. 2005.

Homem CC, Reichardt I, Berger C, Lendl T, Knoblich JA. Long-term live cell imaging and automated 4D analysis of drosophila neuroblast lineages. PloS one. 8(11):e79588. 2013.

Honarpour N, Du C, Richardson JA, Hammer RE, Wang X, Herz J. Adult Apaf-1-deficient mice exhibit male infertility. Developmental biology. 218(2):248-58. 2000.

Honjo K, Mauthner SE, Wang Y, Skene JH, Tracey WD. Nociceptor-Enriched Genes Required for Normal Thermal Nociception. Cell reports. 16(2):295-303. 2016.

Hortsch M, Bieber AJ, Patel NH, Goodman CS. Differential splicing generates a nervous system-specific form of Drosophila neuroglian. Neuron. 4(5):697-709. 1990.

Hoskins RA, Carlson JW, Wan KH. The Release 6 reference sequence of the Drosophila melanogaster genome. Genome research. 25(3):445-58. 2015.

Huang da W, Sherman BT, Lempicki RA. Bioinformatics enrichment tools: paths toward the comprehensive functional analysis of large gene lists. Nucleic acids research. 37(1):1-13. 2009.

Huang da W, Sherman BT, Lempicki RA. Systematic and integrative analysis of large gene lists using DAVID bioinformatics resources. Nature protocols. 4(1):44-57. 2009.

Huang S, Yuan S, Dong M. The phylogenetic analysis of tetraspanins projects the evolution of cell-cell interactions from unicellular to multicellular organisms. Genomics. 86(6):674-84. 2005.

Inaki M, Yoshikawa S, Thomas JB, Aburatani H, Nose A. Wnt4 is a local repulsive cue that determines synaptic target specificity. Current biology : CB. 17(18):1574-9. 2007.

Isshiki T, Pearson B, Holbrook S, Doe CQ. Drosophila neuroblasts sequentially express transcription factors which specify the temporal identity of their neuronal progeny. Cell. 106(4):511-21. 2001.

Iyer EP, Iyer SC, Sulkowski MJ, Cox DN. Isolation and purification of Drosophil peripheral neurons by magnetic bead sorting. Journal of visualized experiments : JoVE. 2009.

Jiménez F, Martin-Morris LE, Velasco L. vnd, a gene required for early neurogenesis of Drosophila, encodes a homeodomain protein. The EMBO journal. 14(14):3487-95. 1995.

Jinushi-Nakao S, Arvind R, Amikura R, Kinameri E, Liu AW, Moore AW. Knot/Collier and cut control different aspects of dendrite cytoskeleton and synergize to define final arbor shape. Neuron. 56(6):963-78. 2007.

Kambadur R, Koizumi K, Stivers C, Nagle J, Poole SJ, Odenwald WF. Regulation of POU genes by castor and hunchback establishes layered compartments in the Drosophila CNS. Genes & development. 12(2):246-60. 1998.

Kanai MI, Okabe M, Hiromi Y. seven-up Controls switching of transcription factors that specify temporal identities of Drosophila neuroblasts. Developmental cell. 8(2):203-13. 2005.

Kim B, Shortridge RD, Seong C, Oh Y, Baek K, Yoon J. Molecular characterization of a novel Drosophila gene which is expressed in the central nervous system. Molecules and cells. 8(6):750-7. 1998.

King-Jones K, Charles JP, Lam G, Thummel CS. The ecdysone-induced DHR4 orphan nuclear receptor coordinates growth and maturation in Drosophila. Cell. 121(5):773-84. 2005.

Kirilly D, Gu Y, Huang Y. A genetic pathway composed of Sox14 and Mical governs severing of dendrites during pruning. Nature neuroscience. 12(12):1497-505. 2009.

Knust E, Tietze K, Campos-Ortega JA. Molecular analysis of the neurogenic locus Enhancer of split of Drosophila melanogaster. The EMBO journal. 6(13):4113-23. 1987.

Kohler SJ, Williams NI, Stanton GB, Cameron JL, Greenough WT. Maturation time of new granule cells in the dentate gyrus of adult macaque monkeys exceeds six months. Proc Natl Acad Sci USA. 2011;108(25):10326-31.

Kohwi M, Doe CQ. Temporal fate specification and neural progenitor competence during development. Nat Rev Neurosci. 2013;14(12):823-38.

Kokubo H, Lun Y, Johnson RL. Identification and expression of a novel family of bHLH cDNAs related to Drosophila hairy and enhancer of split. Biochemical and biophysical research communications. 260(2):459-65. 1999.

Kuan CY, Roth KA, Flavell RA, Rakic P. Mechanisms of programmed cell death in the developing brain. Trends in neurosciences. 23(7):291-7. 2000.

Kumar A, Bello B, Reichert H. Lineage-specific cell death in postembryonic brain development of Drosophila. Development (Cambridge, England). 136(20):3433-42. 2009.

Kuzin A, Brody T, Moore AW, Odenwald WF. Nerfin-1 is required for early axon guidance decisions in the developing Drosophila CNS. Developmental biology. 277(2):347-65. 2005.

Kvon EZ, Kazmar T, Stampfel G. Genome-scale functional characterization of Drosophila developmental enhancers in vivo. Nature. 512(7512):91-5. 2014.

Lacin H, Rusch J, Yeh RT, et al. Genome-wide identification of Drosophila Hb9 targets reveals a pivotal role in directing the transcriptome within eight neuronal lineages, including activation of nitric oxide synthase and Fd59a/Fox-D. Developmental biology. 388(1):117-33. 2014.

Lacin H, Truman JW. Lineage mapping identifies molecular and architectural similarities between the larval and adult Drosophila central nervous system. eLife. 5:e13399. 2016.

Lacin H, Zhu Y, Wilson BA, Skeath JB. Transcription factor expression uniquely identifies most postembryonic neuronal lineages in the Drosophila thoracic central nervous system. Development (Cambridge, England). 141(5):1011-21. 2014.

Lai SL, Lee T. Genetic mosaic with dual binary transcriptional systems in Drosophila. Nature neuroscience. 9(5):703-9. 2006.

Lai ZC, Fortini ME, Rubin GM. The embryonic expression patterns of zfh-1 and zfh-2, two Drosophila genes encoding novel zinc-finger homeodomain proteins. Mechanisms of development. 34(2-3):123-34. 1991.

Langmead B, Trapnell C, Pop M, Salzberg SL. Ultrafast and memory-efficient alignment of short DNA sequences to the human genome. Genome biology. 10(3):R25. 2009.

Lee, T; Luo, L. "Mosaic analysis with a repressible cell marker (MARCM) for Drosophila neural development". Trends in Neurosciences 24 (5): 251–4. 2001.

Lein ES, Hawrylycz MJ, Ao N, et al. Genome-wide atlas of gene expression in the adult mouse brain. Nature. 2007;445(7124):168-76.

Levine RB, Truman JW. Dendritic reorganization of abdominal motoneurons during metamorphosis of the moth, Manduca sexta. The Journal of neuroscience : the official journal of the Society for Neuroscience. 5(9):2424-31. 1985.

Li HH, Kroll JR, Lennox SM. A GAL4 driver resource for developmental and behavioral studies on the larval CNS of Drosophila. Cell reports. 8(3):897-908. 2014.

Littleton JT, Ganetzky B. Ion channels and synaptic organization: analysis of the Drosophila genome. Neuron. 26(1):35-43. 2000.

Liu WW, Wilson RI. Glutamate is an inhibitory neurotransmitter in the Drosophila olfactory system. Proceedings of the National Academy of Sciences of the United States of America. 110(25):10294-9. 2013.

Liu Z, Yang CP, Sugino K. Opposing intrinsic temporal gradients guide neural stem cell production of varied neuronal fates. Science (New York, N.Y.). 350(6258):317-20. 2015.

Livesey FJ, Cepko CL. Vertebrate neural cell-fate determination: lessons from the retina. Nat Rev Neurosci. 2001;2(2):109-18.

Livesey FJ, Young TL, Cepko CL. An analysis of the gene expression program of mammalian neural progenitor cells. Proc Natl Acad Sci USA. 2004;101(5):1374-9.

Lodato S, Arlotta P. Generating neuronal diversity in the mammalian cerebral cortex. Annu Rev Cell Dev Biol. 2015;31:699-720.

Loncle N, Williams DW. An interaction screen identifies headcase as a regulator of large-scale pruning. The Journal of neuroscience : the official journal of the Society for Neuroscience. 32(48):17086-96. 2012.

Losick R, Desplan C. Stochasticity and cell fate. Science. 2008;320(5872):65-8.

Lovick JK, Ngo KT, Omoto JJ, Wong DC, Nguyen JD, Hartenstein V. Postembryonic lineages of the Drosophila brain: I. Development of the lineage-associated fiber tracts. Developmental biology. 384(2):228-57. 2013.

Marin EC, Dry KE, Alaimo DR. Ultrabithorax confers spatial identity in a context-specific manner in the Drosophila postembryonic ventral nervous system. Neural development. 7:31. 2012.

Maurange C, Cheng L, Gould AP. Temporal transcription factors and their targets schedule the end of neural proliferation in Drosophila. Cell. 133(5):891-902. 2008.

McBrayer Z, Ono H, Shimell M. Prothoracicotropic hormone regulates developmental timing and body size in Drosophila. Developmental cell. 13(6):857-71. 2007.

McDonald JA, Holbrook S, Isshiki T, Weiss J, Doe CQ, Mellerick DM. Dorsoventral patterning in the Drosophila central nervous system: the vnd homeobox gene specifies ventral column identity. Genes & development. 12(22):3603-12. 1998.

Mellerick DM, Kassis JA, Zhang SD, Odenwald WF. castor encodes a novel zinc finger protein required for the development of a subset of CNS neurons in Drosophila. Neuron. 9(5):789-803. 1992.

Mellerick DM, Nirenberg M. Dorsal-ventral patterning genes restrict NK-2 homeobox gene expression to the ventral half of the central nervous system of Drosophila embryos. Developmental biology. 171(2):306-16. 1995.

Mellert DJ, Williamson WR, Shirangi TR, Card GM, Truman JW. Genetic and Environmental Control of Neurodevelopmental Robustness in Drosophila. PLoS ONE. 2016;11(5):e0155957.

Mi H, Lazareva-Ulitsky B, Loo R. The PANTHER database of protein families, subfamilies, functions and pathways. Nucleic acids research. 33(Database issue):D284-8. 2005.

Miguel-Aliaga I, Thor S, Gould AP. Postmitotic specification of Drosophila insulinergic neurons from pioneer neurons. PLoS biology. 6(3):e58. 2008.

Miller DL, Ballard SL, Ganetzky B. Analysis of synaptic growth and function in Drosophila with an extended larval stage. The Journal of neuroscience : the official journal of the Society for Neuroscience. 32(40):13776-86. 2012.

Mirth CK, Truman JW, Riddiford LM. The ecdysone receptor controls the post-critical weight switch to nutrition-independent differentiation in Drosophila wing imaginal discs. Development (Cambridge, England). 136(14):2345-53. 2009.

Miura SK, Martins A, Zhang KX, Graveley BR, Zipursky SL. Probabilistic splicing of Dscam1 establishes identity at the level of single neurons. Cell. 155(5):1166-77. 2013.

Mizeracka K, Demaso CR, Cepko CL. Notch1 is required in newly postmitotic cells to inhibit the rod photoreceptor fate. Development. 2013;140(15):3188-97.

Monastirioti M, Giagtzoglou N, Koumbanakis KA, et al. Drosophila Hey is a target of Notch in asymmetric divisions during embryonic and larval neurogenesis. Development (Cambridge, England). 137(2):191-201. 2010.

Monastirioti M, Giagtzoglou N, Koumbanakis KA, et al. Drosophila Hey is a target of Notch in asymmetric divisions during embryonic and larval neurogenesis. Development (Cambridge, England). 137(2):191-201. 2010.

Monge I, Krishnamurthy R, Sims D. Drosophila transcription factor AP-2 in proboscis, leg and brain central complex development. Development (Cambridge, England). 128(8):1239-52. 2001.

Nagaraj R, Banerjee U. Regulation of Notch and Wingless signalling by phyllopod, a transcriptional target of the EGFR pathway. The EMBO journal. 28(4):337-46. 2009.

Nakayama M, Suzuki E, Tsunoda S, Hama C. The Matrix Proteins Hasp and Hig Exhibit Segregated Distribution within Synaptic Clefts and Play Distinct Roles in Synaptogenesis. The Journal of neuroscience : the official journal of the Society for Neuroscience. 36(2):590-606. 2016.

Neumüller RA, Richter C, Fischer A, Novatchkova M, Neumüller KG, Knoblich JA. Genome-wide analysis of self-renewal in Drosophila neural stem cells by transgenic RNAi. Cell stem cell. 8(5):580-93. 2011.

Nijhout HF, Williams CM. Control of moulting and metamorphosis in the tobacco hornworm, Manduca sexta (L.): cessation of juvenile hormone secretion as a trigger for pupation. The Journal of experimental biology. 61(2):493-501. 1974b.

Nijhout HF, Williams CM. Control of moulting and metamorphosis in the tobacco hornworm, Manduca sexta (L.): growth of the last-instar larva and the decision to pupate. The Journal of experimental biology. 61(2):481-91. 1974a.

Novotny T, Eiselt R, Urban J. Hunchback is required for the specification of the early sublineage of neuroblast 7-3 in the Drosophila central nervous system. Development (Cambridge, England). 129(4):1027-36. 2002.

Nusslein-Volhard C., Wieschaus, E., Kluding, H. Mutations affecting the pattern of the larval cuticule in Drosophila melanogaster: I. Zygotic loci on the second chromosome. Wilhelm Roux's Arch. Dev. Biol. 193:267–282. 1984.

Oyler GA, Higgins GA, Hart RA. The identification of a novel synaptosomal-associated protein, SNAP-25, differentially expressed by neuronal subpopulations. The Journal of cell biology. 109(6 Pt 1):3039-52. 1989.

Parrish JZ, Kim MD, Jan LY, Jan YN. Genome-wide analyses identify transcription factors required for proper morphogenesis of Drosophila sensory neuron dendrites. Genes & development. 20(7):820-35. 2006.

Pearson BJ, Doe CQ. Regulation of neuroblast competence in Drosophila. Nature. 425(6958):624-8. 2003.

Pearson JC, Lemons D, Mcginnis W. Modulating Hox gene functions during animal body patterning. Nat Rev Genet. 2005;6(12):893-904.

Pereanu W, Hartenstein V. Neural lineages of the Drosophila brain: a three-dimensional digital atlas of the pattern of lineage location and projection at the late

larval stage. The Journal of neuroscience : the official journal of the Society for Neuroscience. 26(20):5534-53. 2006.

Pfeiffer BD, Jenett A, Hammonds AS. Tools for neuroanatomy and neurogenetics in Drosophila. Proceedings of the National Academy of Sciences of the United States of America. 105(28):9715-20. 2008.

Pfeiffer BD, Truman JW, Rubin GM. Using translational enhancers to increase transgene expression in Drosophila. Proceedings of the National Academy of Sciences of the United States of America. 109(17):6626-31. 2012.

Pi H, Wu HJ, Chien CT. A dual function of phyllopod in Drosophila external sensory organ development: cell fate specification of sensory organ precursor and its progeny. Development (Cambridge, England). 128(14):2699-710. 2001.

Pompeiano M, Blaschke AJ, Flavell RA, Srinivasan A, Chun J. Decreased apoptosis in proliferative and postmitotic regions of the Caspase 3-deficient embryonic central nervous system. The Journal of comparative neurology. 423(1):1-12. 2000.

Prasher DC, Eckenrode VK, Ward WW, Prendergast FG, Cormier MJ. Primary structure of the Aequorea victoria green-fluorescent protein. Gene. 111(2):229-33. 1992.

Prokop A, Technau GM. The origin of postembryonic neuroblasts in the ventral nerve cord of Drosophila melanogaster. Development (Cambridge, England). 111(1):79-88. 1991.

Ramat A, Audibert A, Louvet-Vallée S, Simon F, Fichelson P, Gho M. Escargot and Scratch regulate neural commitment by antagonizing Notch activity in Drosophila sensory organs. Development (Cambridge, England). 143(16):3024-34. 2016.

Rewitz KF, Yamanaka N, Gilbert LI, O'Connor MB. The insect neuropeptide PTTH activates receptor tyrosine kinase torso to initiate metamorphosis. Science (New York, N.Y.). 326(5958):1403-5. 2009.

Rewitz KF, Yamanaka N, O'Connor MB. Developmental checkpoints and feedback circuits time insect maturation. Current topics in developmental biology. 103:1-33. 2013.

Riddiford LM, Truman JW, Mirth CK, Shen YC. A role for juvenile hormone in the prepupal development of Drosophila melanogaster. Development (Cambridge, England). 137(7):1117-26. 2010.

Ritter AR, Beckstead RB. Sox14 is required for transcriptional and developmental responses to 20-hydroxyecdysone at the onset of drosophila metamorphosis. Developmental dynamics : an official publication of the American Association of Anatomists. 239(10):2685-94. 2010.

Rohrbough J, Broadie K. Electrophysiological analysis of synaptic transmission in central neurons of Drosophila larvae. Journal of neurophysiology. 88(2):847-60. 2002.

Ross SE, Greenberg ME, Stiles CD. Basic helix-loop-helix factors in cortical development. Neuron. 2003;39(1):13-25.

Rowitch DH, Kriegstein AR. Developmental genetics of vertebrate glial-cell specification. Nature. 2010;468(7321):214-22.

Schaffer MH, Noyes BE, Slaughter CA, Thorne GC, Gaskell SJ. The fruitfly Drosophila melanogaster contains a novel charged adipokinetic-hormone-family peptide. The Biochemical journal. 269(2):315-20. 1990.

Schmid A, Chiba A, Doe CQ. Clonal analysis of Drosophila embryonic neuroblasts: neural cell types, axon projections and muscle targets. Development. 1999;126(21):4653-89.

Schmucker D, Clemens JC, Shu H. Drosophila Dscam is an axon guidance receptor exhibiting extraordinary molecular diversity. Cell. 101(6):671-84. 2000.

Schubiger M, Wade AA, Carney GE, Truman JW, Bender M. Drosophila EcR-B ecdysone receptor isoforms are required for larval molting and for neuron remodeling during metamorphosis. Development (Cambridge, England). 125(11):2053-62. 1998.

Scott JA, Williams DW, Truman JW. The BTB/POZ zinc finger protein Broad-Z3 promotes dendritic outgrowth during metamorphic remodeling of the peripheral stretch receptor dbd. Neural development. 6:39. 2011.

Sen S, Cao D, Choudhary R. Genetic transformation of structural and functional circuitry rewires the Drosophila brain. eLife. 3:. 2014.

Shaner NC, Campbell RE, Steinbach PA, Giepmans BN, Palmer AE, Tsien RY. Improved monomeric red, orange and yellow fluorescent proteins derived from Discosoma sp. red fluorescent protein. Nature biotechnology. 22(12):1567-72. 2004.

Shen EH, Overly CC, Jones AR. The Allen Human Brain Atlas: comprehensive gene expression mapping of the human brain. Trends Neurosci. 2012;35(12):711-4.

Shepherd JC, Walldorf U, Hug P, Gehring WJ. Fruit flies with additional expression of the elongation factor EF-1 alpha live longer. Proceedings of the National Academy of Sciences of the United States of America. 86(19):7520-1. 1989.

Shih HP, Hales KG, Pringle JR, Peifer M. Identification of septin-interacting proteins and characterization of the Smt3/SUMO-conjugation system in Drosophila. Journal of cell science. 115(Pt 6):1259-71. 2002.

Shikama N, Ackermann R, Brack C. Protein synthesis elongation factor EF-1 alpha expression and longevity in Drosophila melanogaster. Proceedings of the National Academy of Sciences of the United States of America. 91(10):4199-203. 1994.

Shimomura O, Johnson FH, Saiga Y. Extraction, purification and properties of aequorin, a bioluminescent protein from the luminous hydromedusan, Aequorea. Journal of cellular and comparative physiology. 59:223-39. 1962.

Sidman RL. 1961. Histogenesis of the mouse retina studied with thymidine 3-H. In: Smelser GK, editor. The structure of the eye. New York: Academic Press. p 487–506.

Siebert M, Banovic D, Goellner B, Aberle H. Drosophila motor axons recognize and follow a Sidestep-labeled substrate pathway to reach their target fields. Genes & development. 23(9):1052-62. 2009.

Skeath JB, Doe CQ. Sanpodo and Notch act in opposition to Numb to distinguish sibling neuron fates in the Drosophila CNS. Development (Cambridge, England). 125(10):1857-65. 1998.

Skeath JB, Doe CQ. Sanpodo and Notch act in opposition to Numb to distinguish sibling neuron fates in the Drosophila CNS. Development. 1998;125(10):1857-65.

Skeath JB, Zhang Y, Holmgren R, Carroll SB, Doe CQ. Specification of neuroblast identity in the Drosophila embryonic central nervous system by gooseberry-distal. Nature. 1995;376(6539):427-30.

Skeath JB, Zhang Y, Holmgren R, Carroll SB, Doe CQ. Specification of neuroblast identity in the Drosophila embryonic central nervous system by gooseberry-distal. Nature. 376(6539):427-30. 1995.

Skeath JB. At the nexus between pattern formation and cell-type specification: the generation of individual neuroblast fates in the Drosophila embryonic central nervous system. BioEssays : news and reviews in molecular, cellular and developmental biology. 21(11):922-31. 1999.

Skeath JB. At the nexus between pattern formation and cell-type specification: the generation of individual neuroblast fates in the Drosophila embryonic central nervous system. BioEssays : news and reviews in molecular, cellular and developmental biology. 21(11):922-31. 1999.

Slater JL, Landman KA, Hughes BD, Shen Q, Temple S. Cell lineage tree models of neurogenesis. J Theor Biol. 2009;256(2):164-79.

Söllner T, Whiteheart SW, Brunner M. SNAP receptors implicated in vesicle targeting and fusion. Nature. 362(6418):318-24. 1993.

Song HJ, Stevens CF, Gage FH. Neural stem cells from adult hippocampus develop essential properties of functional CNS neurons. Nat Neurosci. 2002;5(5):438-45.

Spana EP, Doe CQ. Numb antagonizes Notch signaling to specify sibling neuron cell fates. Neuron. 1996;17(1):21-6.

Spana EP, Doe CQ. The prospero transcription factor is asymmetrically localized to the cell cortex during neuroblast mitosis in Drosophila. Development (Cambridge, England). 121(10):3187-95. 1995.

Spokony RF, Restifo LL. Anciently duplicated Broad Complex exons have distinct temporal functions during tissue morphogenesis. Development genes and evolution. 217(7):499-513. 2007.

Spokony RF, Restifo LL. Broad Complex isoforms have unique distributions during central nervous system metamorphosis in Drosophila melanogaster. The Journal of comparative neurology. 517(1):15-36. 2009.

Stolt CC, Lommes P, Sock E, Chaboissier MC, Schedl A, Wegner M. The Sox9 transcription factor determines glial fate choice in the developing spinal cord. Genes Dev. 2003;17(13):1677-89.

Stone JV, Mordue W, Batley KE, Morris HR. Structure of locust adipokinetic hormone, a neurohormone that regulates lipid utilisation during flight. Nature. 263(5574):207-11. 1976.

Su MT, Venkatesh TV, Wu X, Golden K, Bodmer R. The pioneer gene, apontic, is required for morphogenesis and function of the Drosophila heart. Mechanisms of development. 80(2):125-32. 1999.

Syed MH, Mark B, Doe CQ. Steroid hormone induction of temporal gene expression in Drosophila brain neuroblasts generates neuronal and glial diversity. Elife. 2017;6

Szklarczyk D, Franceschini A, Wyder S. STRING v10: protein-protein interaction networks, integrated over the tree of life. Nucleic acids research. 43(D1):D447-52. 2015.

Thomas A, Lee PJ, Dalton JE. A versatile method for cell-specific profiling of translated mRNAs in Drosophila. PloS one. 7(7):e40276. 2012.

Thompson CL, Ng L, Menon V, et al. A high-resolution spatiotemporal atlas of gene expression of the developing mouse brain. Neuron. 2014;83(2):309-323.

Thummel CS, Burtis KC, Hogness DS. Spatial and temporal patterns of E74 transcription during Drosophila development. Cell. 61(1):101-11. 1990.

Tomer R, Denes AS, Tessmar-raible K, Arendt D. Profiling by image registration reveals common origin of annelid mushroom bodies and vertebrate pallium. Cell. 2010;142(5):800-9.

Trapnell C, Pachter L, Salzberg SL. TopHat: discovering splice junctions with RNA-Seq. Bioinformatics (Oxford, England). 25(9):1105-11. 2009.

Trapnell C, Williams BA, Pertea G. Transcript assembly and quantification by RNA-Seq reveals unannotated transcripts and isoform switching during cell differentiation. Nature biotechnology. 28(5):511-5. 2010.

Truman JW, Ball EE. Patterns of embryonic neurogenesis in a primitive wingless insect, the silverfish, Ctenolepisma longicaudata: comparison with those seen in flying insects. Development genes and evolution. 208(7):357-68. 1998.

Truman JW, Bate M. Spatial and temporal patterns of neurogenesis in the central nervous system of Drosophila melanogaster. Developmental biology. 125(1):145-57. 1988.

Truman JW, Booker R. Adult-specific neurons in the nervous system of the moth, Manduca sexta: selective chemical ablation using hydroxyurea. Journal of neurobiology. 17(6):613-25. 1986.

Truman JW, Moats W, Altman J, Marin EC, Williams DW. Role of Notch signaling in establishing the hemilineages of secondary neurons in Drosophila melanogaster. Development (Cambridge, England). 137(1):53-61. 2010.

Truman JW, Reiss SE. Dendritic reorganization of an identified motoneuron during metamorphosis of the tobacco hornworm moth. Science (New York, N.Y.). 192(4238):477-9. 1976.

Truman JW, Reiss SE. Hormonal regulation of the shape of identified motoneurons in the moth Manduca sexta. The Journal of neuroscience : the official journal of the Society for Neuroscience. 8(3):765-75. 1988.

Truman JW, Reiss SE. Neuromuscular metamorphosis in the moth Manduca sexta: hormonal regulation of synapses loss and remodeling. The Journal of neuroscience : the official journal of the Society for Neuroscience. 15(7 Pt 1):4815-26. 1995.

Truman JW, Riddiford LM. Physiology of insect rhythms. 3. The temporal organization of the endocrine events underlying pupation of the tobacco hornworm. The Journal of experimental biology. 60(2):371-82. 1974.

Truman JW, Schuppe H, Shepherd D, Williams DW. Developmental architecture of adult-specific lineages in the ventral CNS of Drosophila. Development (Cambridge, England). 131(20):5167-84. 2004.

Truman JW, Talbot WS, Fahrbach SE, Hogness DS. Ecdysone receptor expression in the CNS correlates with stage-specific responses to ecdysteroids during Drosophila and Manduca development. Development (Cambridge, England). 120(1):219-34. 1994.

Tsuji T, Hasegawa E, Isshiki T. Neuroblast entry into quiescence is regulated intrinsically by the combined action of spatial Hox proteins and temporal identity factors. Development (Cambridge, England). 135(23):3859-69. 2008.

Tuthill JC. Lessons from a compartmental model of a Drosophila neuron. The Journal of neuroscience : the official journal of the Society for Neuroscience. 29(39):12033-4. 2009.

Udolph G, Lüer K, Bossing T, Technau GM. Commitment of CNS progenitors along the dorsoventral axis of Drosophila neuroectoderm. Science (New York, N.Y.). 269(5228):1278-81. 1995.

Usui-Ishihara A, Simpson P, Usui K. Larval multidendrite neurons survive metamorphosis and participate in the formation of imaginal sensory axonal pathways in the notum of Drosophila. Developmental biology. 225(2):357-69. 2000.

Vähäsöyrinki M, Niven JE, Hardie RC, Weckström M, Juusola M. Robustness of neural coding in Drosophila photoreceptors in the absence of slow delayed rectifier K+ channels. The Journal of neuroscience : the official journal of the Society for Neuroscience. 26(10):2652-60. 2006.

Warren JT, Petryk A, Marqués G. Phantom encodes the 25-hydroxylase of Drosophila melanogaster and Bombyx mori: a P450 enzyme critical in ecdysone biosynthesis. Insect biochemistry and molecular biology. 34(9):991-1010. 2004.

Weeks JC, Truman JW. Independent steroid control of the fates of motoneurons and their muscles during insect metamorphosis. The Journal of neuroscience : the official journal of the Society for Neuroscience. 5(8):2290-300. 1985.

Wellik DM. Hox patterning of the vertebrate axial skeleton. Dev Dyn. 2007;236(9):2454-63.

Whiteley M, Noguchi PD, Sensabaugh SM, Odenwald WF, Kassis JA. The Drosophila gene escargot encodes a zinc finger motif found in snail-related genes. Mechanisms of development. 36(3):117-27. 1992.

Williams DW, Shepherd D. Persistent larval sensory neurones are required for the normal development of the adult sensory afferent projections in Drosophila. Development (Cambridge, England). 129(3):617-24. 2002.

Williams DW, Shepherd D. Persistent larval sensory neurons in adult Drosophila melanogaster. Journal of neurobiology. 39(2):275-86. 1999.

Williams MJ, Goergen P, Rajendran J. Obesity-linked homologues TfAP-2 and Twz establish meal frequency in Drosophila melanogaster. PLoS genetics. 10(9):e1004499. 2014.

Wong DC, Lovick JK, Ngo KT, Borisuthirattana W, Omoto JJ, Hartenstein V. Postembryonic lineages of the Drosophila brain: II. Identification of lineage projection patterns based on MARCM clones. Developmental biology. 384(2):258-89. 2013.

Wong JJ, Li S, Lim EK. A Cullin1-based SCF E3 ubiquitin ligase targets the InR/PI3K/TOR pathway to regulate neuronal pruning. PLoS biology. 11(9):e1001657. 2013.

Wong LL, Rapaport DH. Defining retinal progenitor cell competence in Xenopus laevis by clonal analysis. Development. 2009;136(10):1707-15.

Yamakawa K, Huot YK, Haendelt MA. DSCAM: a novel member of the immunoglobulin superfamily maps in a Down syndrome region and is involved in the development of the nervous system. Human molecular genetics. 7(2):227-37. 1998.

Yoav Benjamini, Yosef Hochberg. Controlling the False Discovery Rate: A Practical and Powerful Approach to Multiple Testing. Journal of the Royal Statistical Society. Series B (Methodological). 57(1):289-300. 1995.

Young RW. Cell differentiation in the retina of the mouse. Anat Rec. 1985;212(2):199-205.

Yuan L, Hu S, Okray Z. The Drosophila neurogenin Tap functionally interacts with the Wnt-PCP pathway to regulate neuronal extension and guidance. Development (Cambridge, England). 143(15):2760-6. 2016.

Zernicka-goetz M, Huang S. Stochasticity versus determinism in development: a false dichotomy?. Nat Rev Genet. 2010;11(11):743-4.

Zhao C, Teng EM, Summers RG, Ming GL, Gage FH. Distinct morphological stages of dentate granule neuron maturation in the adult mouse hippocampus. J Neurosci. 2006;26(1):3-11.

Zheng X, Wang J, Haerry TE. TGF-beta signaling activates steroid hormone receptor expression during neuronal remodeling in the Drosophila brain. Cell. 112(3):303-15. 2003.

Zhou B, Williams DW, Altman J, Riddiford LM, Truman JW. Temporal patterns of broad isoform expression during the development of neuronal lineages in Drosophila. Neural Dev. 2009;4:39.

Zhou X, Riddiford LM. Broad specifies pupal development and mediates the 'status quo' action of juvenile hormone on the pupal-adult transformation in Drosophila and Manduca. Development (Cambridge, England). 129(9):2259-69. 2002.

Zhu S, Lin S, Kao CF, Awasaki T, Chiang AS, Lee T. Gradients of the Drosophila Chinmo BTB-zinc finger protein govern neuronal temporal identity. Cell. 127(2):409-22. 2006.

Zou, Y., Stoeckli, E., Chen, H. and Tessier-Lavigne, M. (2000). Squeezing axons out of the gray matter: a role for slit and semaphorin proteins from midline and ventral spinal cord. Cell 102, 363-375.